Identification of molecular characteristics of CNS-seeking cancer cells

Dissertation

zur Erlangung des Doktorgrades

der Biomedizinischen Wissenschaften (Dr. rer. physiol.)

der

Fakultät für Medizin

der Universität Regensburg

Cäcilia Anita Rosa Köstler

Neualbenreuth, 8. April 2024

Identification of molecular characteristics of CNS-seeking cancer cells

Dissertation

zur Erlangung des Doktorgrades

der Biomedizinischen Wissenschaften (Dr. rer. physiol.)

der

Fakultät für Medizin

der Universität Regensburg

Cäcilia Anita Rosa Köstler

Neualbenreuth, 8. April 2024

Dekan	Prof. Dr. med. Dirk Hellwig
Mentorat	Prof. Dr. med. Christoph A. Klein – **Supervisor**
	Prof. Dr. med. Tobias Pukrop
	Prof. Dr. rer. nat. Michael Rehli
	Prof. Dr. med. Markus J. Riemenschneider
Practical advisor	Dr. med. habil. Bernhard Polzer

Oral examination

„Niad nougebm zwingt all`s“

(Übersetzung: Nie aufgeben, dann ist alles machbar!)

Zitat aus dem „Böllnhaus von Haislan“

Table of contents

Table of figures

Table of tables

Table of abbreviations

Abbreviation	Meaning
AB	Antibody
AF	AlexFluor
AP	Alkaline Phosphatase
APC	Allophycocyanin
AR	Antigen Retrieval
ATP	Adenosine triphosphate
bp	Basepairs
BSA	Bovine serum albumin
CD45	Cluster of Differentiation 45
cfDNA	Zellfreie zirkulierende DNA / cell free circulating DNA
CK	Cytokeratin
CNA	Copy number alteration
CNS	Central nervous system
CNV	Copy number variation
CSF	Cerebrospinal fluid
CTC	Circulating tumor cell
cfDNA	zellfreie DNA / circulating DNA
ctDNA	Zellfreie zirkulierende TumorDNA / circulating tumor DNA
CUP	Unbekannter Primärtumor / Cancer of unknown primary
D5S2117	DNA-Locus on Chromosom 5 (D5S2117)
DAB	Diaminobenzidin-Tetrahydrochlorid
DAPI	4',6-Diamidin-2-phenylindol
dATP	Deoxy Adenosine triphosphate
DCC	Disseminierte Krebszelle / disseminated cancer cell
dCTP	Deoxy cytosin triphosphate
DEPArray	DiElectroPhoresis Array
dGTP	Deoxy guanosine triphosphate
DNA	Deoxyribonucleic acid
DNA	Deoxyribonucleic acid
dNTP	Deoxynucleotide triphosphate
ds	Doublestrand
dsDNA	Doublestrand DNA
dTTP	Deoxy thymidin triphosphate
EANO	European Association of Neuro-Oncology
ESMO	European Society for Medical Oncology
e.g.	Example given
EGFR	Epidermal Growth Factor Receptor
EpCAM	Epithelial Cell Adhesion Molecule, epitheliales Zelladhäsionsmolekül
ERBB2/Her2	Human epidermal growth factor receptor 2
EtBr	Ethidium bromide
FCS	Fetal calf serum
FDA	Food and drug administration
FFPE	Formalinfixiertes, in Paraffin eingebettet / Formalin Fixed Paraffin Embedded
FU	Fluorescent units
GII	Genomic integrity index

h	Hours
H2O Water	Water
HE	Hematoxylin and Eosin
HMB45	Human Melanoma Black 45
HS	High sensitivity
IgG	Immunoglobulin G
kbp	Kilobasepairs
KRAS	Kirsten rat sarcoma viral oncogene homolog
LM	Leptomeningeale Metastasen / leptomeningeal metastases
MCSP	Melanoma-associated chondroitin sulfate proteoglycan
min	Minutes
mL	Milliliter
MRI	Magnetic resonance imaging
MRT	Magnetresonanztherapie
MSB	Menarini Silicon Biosystems
µg	Microgram
µL	Microliter
NaCl	Natriumchloride
ng	Nanogram
NGS	Next generation sequencing
NIH	National Institute of Health
PBMCs	Peripheral blood mononuclear cells
PBS	Phosphate-buffered saline
PCR	Polymerase chain reaction
PEG	Polyethylenglycol
pg	Picogram
pH	Potential of Hydrogen
PK	Proteinase K
PT	Primary tumor
QC	Quality control
qPCR	Quantitative PCR
RNA	Ribonucleic acid
rpm	Rounds per minute
RPMI	Roswell Park Memorial Institute
RT	Room temperature
SC	Single cell
SCP-L	Systemic cancer progression laboratory
sec	Seconds
TP53	TumorProtein
V	Volt
Vim	Vimentin
WGA	Whole genome amplification
WMA	World Medical Association
ZNS	Zentrales Nervensystem

Zusammenfassung

Tumorzellen, welche im Liquor oder den Membranen, die Gehirn und Rückenmark (Meningen) umgeben, oder in beidem detektiert werden, werden als leptomeningeale Metastasen (LM) bezeichnet (1–4). Sie sind als schwerwiegende Komplikation einer fortgeschrittenen Krebserkrankungen charakterisiert, können zu einschneidenden neurologischen Symptomen führen und treten bei 5-10 % der Patientinnen und Patienten mit soliden Tumoren auf. Brustkrebs, Lungenkrebs und Melanome (5) sind die häufigsten damit verbundenen Erkrankungen, jedoch können auch Fälle mit unbekanntem Primärtumor (Cancer of unknown primary (CUP)-Syndrom) betroffen sein (6). LM treten eher selten auf, sind aber von aggressiver Natur und weisen begrenzte Behandlungsmöglichkeiten und eine ungünstige Lage im zentralen Nervensystem (ZNS) auf, was mit einer ungünstigen Prognose und einer erschwerten therapeutischen Entscheidungsfindung einhergeht. Die Diagnose von LM stützt sich hauptsächlich auf die Zytologie des Liquors sowie die Auswertung der Magnetresonanztherapie (MRT), beides der aktuelle Goldstandard in der Diagnostik, (7) und, soweit vorhanden, Informationen zum Primärtumor. Da Letztere nicht immer zugänglich sind und Liquorzytologie und Magnetresonanztherapie (MRT) eine geringe Sensitivität aufweisen, derer Aussagen rein quantitativer Natur sind, wurde in dieser Arbeit ein molekularer Ansatz für die Liquorflüssigkeitsbiopsie entwickelt, welcher in Zukunft die Therapievorhersage für betroffene Patientinnen und Patienten erleichtern soll.

In einer monozentrischen Machbarkeitsstudie wurde dahingehend ein qualitativer Vergleich zwischen Liquorzytologie, MRT-Daten und molekularen Flüssigbiopsie-Ergebnissen erwachsener Betroffener mit Verdacht auf LM und unterschiedlichen Primärtumoren durchgeführt. Dafür wurden disseminierte Krebszellen (DCCs), zellfreie Tumor-DNA (ctDNA) und Formalin fixiertes in Paraffin eingebettetes (FFPE) Gewebe, molekular charakterisiert. Mit Hilfe der Ergebnisse sollten folgende drei Fragen beantwortet werden:

i) Liefert die molekulare Flüssigkeitsbiopsie von Liquor vergleichbare Ergebnisse zum aktuellen klinischen Goldstandard, derzeit Liquorzytologie und MRT, für Patientinnen und Patienten mit Verdacht auf LM?
ii) Ist die Isolierung einzelner Zellen aus dem Liquor eine wertvolle Option zur Bereitstellung relevanter molekularer Daten und wie zuverlässig sind diese Ergebnisse im Vergleich zur Analyse zirkulierender zellfreier Tumor-DNA aus Liquor hinsichtlich Qualität, Aussagekraft und Anwendbarkeit?
iii) Gibt die heterogene Landschaft von Tumor- und Metastasengewebe einen Hinweis auf die Sedimentation spezifischer Subklone, welche das ZNS besiedeln?

Im ersten, technischen Teil, dieser Arbeit wurde ein molekularer diagnostischer Workflow etabliert und optimiert, der darauf abzielte, DCCs im Liquor zu detektieren, anzureichern und zu isolieren. In Abhängigkeit des zugrundeliegenden Primärtumors und dessen assoziierten Expressionsmarkern wurde evaluiert, ob Zellen entweder mit der von der FDA (U.S. Food and Drug Administration) zugelassenen CellSearch®-Technologie, auf Basis des EpCAM-Expressionsmusters (Epitheliales Zelladhäsions Molekül) und der Cytokeratin-Färbung von Karzinomzellen, oder mittels einer Dichtegradientenzentrifugation, gefolgt von spezifischer Fluoreszenzfärbung für Melanomzellen, detektiert werden können. Diese Ergebnisse dienten im Vergleich zu simultan durchgeführten zytologischen Analysen und zugehörigen MRT-Daten dazu, die CellSearch® Methode für Liquor in diesem Kollektiv zu validieren. Der große Vorteil dieser Detektionsmethode ist es, einzelne Zellen nach der Zellanreicherung anhand ihrer spezifischen Färbung zu erkennen und zu isolieren. Diese Möglichkeit wurde genutzt, um ein aus dem Liquor gewonnenes Einzelzellkollektiv für die anschließende Molekularanalyse aufzubauen. Hierbei konnten zwei unterschiedliche Isolationsmethoden evaluiert und die Unterschiede in der DNA-Qualität abhängig von der Herkunft der Zelle und der technischen Wiederaufbereitung bewertet werden: Die manuelle Methode der Fluoreszenzmikroskopie und die automatisierte Isolierung mit der DEPArray™-Technologie. Die Kategorisierung der DNA-Qualität diente dabei als zusätzliches Instrument zur Unterscheidung von Proben geringer und hoher Qualität, wobei Letztere für weiterführende molekulare Analysen eingesetzt wurden. Durch die

Sequenzierung des gesamten Genoms wurden die Allelfrequenzen ermittelt, die es ermöglichten, den Ursprung der Probe zu bestimmen und die subklonale Diversität innerhalb verschiedener isolierter Liquor Einzelzellen zu untersuchen. Darüber hinaus wurde neben den Tumorzellen zusätzlich zirkulierende Tumor-DNA aus dem Liquor isoliert. Anhand dieser Proben wurde der Workflow für die Extraktion von zellfreier DNA optimiert, eine neue Amplifikationsstrategie getestet und diese validiert. Die molekularen Daten dieser Proben wurden anschließend genutzt, um nachzuweisen, ob es sich bei der angereicherten DNA um Tumor-DNA handelt oder nicht und ob die molekularen Daten mit den Daten der isolierten DCCs übereinstimmen. Hier konnten die Vor- und Nachteile der beiden Biomarker im ZNS bezüglich Qualität, Aussagekraft, Anwendbarkeit und Zuverlässigkeit gegenübergestellt werden. Die Analyse des Tumorgewebes der in der Studie inkludierten Patientinnen und Patienten ermöglichte die Untersuchung der intratumoralen Heterogenität. Hierfür wurden Tumor- und Stromazellpopulationen aus Formalin fixiertem in Paraffin eingebettetem (FFPE) Gewebe isoliert, um zum einen die technische Machbarkeit der DEPArray^{TM}-Technologie zu validieren und zum anderen das Extraktionsprotokoll für verschiedene Tumorarten und -materialien zu optimieren. Nach dem Isolationsprozess wurden die Zellpopulationen auf molekularer Ebene analysiert und die aus nicht-ZNS- oder ZNS-Gewebe isolierten Daten mit Daten aus Liquor isolierter DNA verglichen.

Mit dieser Arbeit konnte gezeigt werden, dass der Ansatz der Liquor-Einzelzellanalyse vergleichbare Ergebnisse zur konventionellen Liquorzytologie liefert und damit gemeinsam mit dem MRT eine sensitivere Alternative zum aktuellen klinischen Goldstandard darstellen kann. Ein wesentlicher Vorteil ist die Möglichkeit, qualitativ hochwertige Zellen zu isolieren und anschließend auf molekularer Ebene zu charakterisieren. Damit könnte Liquor auch eine wertvolle Quelle für die Kultivierung und funktionelle Analyse vitaler Zellen sein anhand derer klinisch relevante, tumorspezifische Informationen detektiert werden können, die perspektivisch zur Entscheidungsfindung einer geeigneten Therapie beitragen können. Eine schnelle und kostengünstige Methode der Analyse von Tumor-DNA ist die Isolierung von ctDNA aus Liquor. Die Zuverlässigkeit und Aussagekraft dieses Biomarkers ist gegenüber der Einzelzellanalyse innerhalb dieses Kollektivs jedoch deutlich geringer. Eine Analyse

beider Liquor Biomarker kann eine praktikable Lösung sein, schnell erste Informationen aus ctDNA zu erhalten und darauf basierend eine tiefergehende molekulare Analyse der Einzelzellen anzuschließen. Die Tatsache, dass sich das genetische Profil von Zellen, die in das ZNS sedimentieren, eindeutig von Zellen unterscheiden, die aus dem viszeralen Bereich der Betroffenen isoliert wurden, macht die Wichtigkeit der molekularen Analyse von Liquor-DNA deutlich. Damit können mögliche ZNS spezifische Marker für individuelle Therapieansätze detektiert werden, die ohne die Analyse von Liquor unentdeckt bleiben würden.

Summary

In patients diagnosed with leptomeningeal metastases (LM), cancer cells have disseminated to the brain and colonized the meninges, leading to a dismal prognosis (2–4,6). However, the sensitivities of currently available diagnostic methods to detect LM, such as cerebrospinal fluid (CSF) cytology and magnet resonance imaging (MRI), are known to be very low (8). To address these limitations, we tested a cellular and a molecular liquid biopsy approach using CSF, and explored whether either of them or both could provide advantages for diagnosis and clinical decision-making, including the choice of brain-specific cancer targeting.

In total, 38 patients with suspected LM were included into analysis of CSF (n = 41). Epithelial cells from CSF were enriched using the FDA-approved EpCAM-ferrofluid based CellSearch® technology if they represent single disseminated cancer cells (DCCs). In parallel, circulating tumor DNA (ctDNA) was extracted from CSF (n = 29), and cellular and cell-free DNA samples underwent molecular copy number variation (CNV) analysis. Moreover, the molecular analysis of these biomarker derived from the central nervous system (CNS) were compared to available visceral tissue (n = 22) of the patients.

The CellSearch® enrichment workflow for circulating tumor cells could be adapted from blood to cerebrospinal fluid (CSF) on patients with suspected leptomeningeal metastases (LM). It is a higher sensitive alternative for DCC detection (38 %) compared to conventional cytology (32 % DCC detection rate). The quality of isolated single cells from CSF is very high for both CD45 positive cells (78 %) and DCCs (76 %, Pearson Chi Square ~ 1). This is contradictory to findings for isolated single cells from blood in which the quality of circulating tumor cells is significantly lower (35 %) than the quality of CD45 positive cells (65 %, $p<0.0001$, Pearson Chi Square; quality measured by the genomic integrity index (GII)). The molecular downstream analysis of CSF-DCCs confirmed 92 % (12 of 13) of positive CellSearch® samples as tumor derived. A new amplification protocol yielded in a significantly higher ($p<0.001$, paired two-tailed t-test) ctDNA amount (median 24,6 ng/µl; range: 2,56 – 82,4 ng/µl) than before amplification

(median 0.304 ng/µl; range: 0,13 – 1,83 ng/µl), but a high dropout rate (27 %) proved this biomarker as less reliable than the DCC analysis. Furthermore, comparing molecular data from DCC and ctDNA to formalin-fixed-paraffin-embedded (FFPE) tissue derived from visceral compartments confirms the presence of specific subclones in DNA isolated from the CNS.

The CSF analysis of patients with suspected LM could be improved by a molecular downstream analysis of CSF-DCCs automatic enriched with tumor specific marker. They serve as reliable and informative biomarker, providing molecular insights into cancer pathology which might be an additional benefit for patients diagnosed with cancer of unknown primary. While ctDNA analysis offers rapid results that complement those obtained from DCCs, the high dropout rate suggests that this approach serves as a supplementary rather than an alternative method. The identification of CNS specific subclones confirms CSF as a valuable source for high quality single cells offering the option for functional analysis and the detection of new drug targets.

Our data suggest exploration of an alternative, stepwise clinical approach. First, MRI should be applied to clarify if the symptoms of patients are caused by LM. Then, molecular, and subsequently cellular CSF analysis should be performed enabling high sensitive detection and molecular characterization of LM cells. Implementing the serial CSF analysis would offer the opportunity to monitor tumor burden during therapy, particularly during innovative therapy trials.

1. Introduction

1.1 Different strategies of cancer care

Over the past few decades, significant advancements in oncology have revolutionized cancer care, leading to improved outcomes and quality of life for patients. However, with almost 20 Mio new cancer cases per year worldwide (9) and a rising trend observed – there is urgent demand for new constructive and applicable therapeutic strategies. Surgery, radiation therapy, chemotherapy, and combined therapies are some of the current strategies in cancer care and the decision for a specific treatment is dependent on various factors including the type and stage of cancer but also the patient's overall health. Over the last years, the emphasis was increasingly placed on precision medicine which includes personalized treatment plans based on specific characteristics of an individual´s cancer. In this field of modern oncology, advanced approaches to treatment such as targeted therapies, immunotherapy and genetic testing are indispensable to provide patients with the most effective and least invasive treatment possibilities. Here, the molecular characterization of tumors can be a fundamental pillar in selecting the optimal conditions for cancer patients towards a personalized approach which integrates various treatment modalities to maximize efficacy and patient outcomes while minimizing side effects. Although these already seem to be implemented in the daily clinical routine, challenges arise if tumors are difficult to biopsy due to their anatomical location, multiple tissue samples are needed over time or patients present with diffuse systemic metastasis.

1.2 Leptomeningeal metastases

1.2.1 Epidemiology

All these aspects are particularly important for patients affected with Central Nervous System (CNS) tumors, which leads to the current setting in which treatment decisions still are mainly based on imaging instead of molecular analysis. This is especially obvious in patients with leptomeningeal spread. Leptomeningeal metastases (LM) are

characterized as a devastating complication of advanced cancer by dissemination of cancer cells to the subarachnoid space (1–4). It occurs in 5-10 % of patients with solid cancer, with breast cancer, lung cancer, and melanoma (5) being the most frequent underlying diseases, but also patients with unknown primary (CUP) syndrome are affected (6). Despite being relatively rare, LM is associated with significant morbidity and poor prognosis with a median overall survival of approximately four months due to its aggressive nature and limited treatment options.

1.2.2 Diagnosis

The diagnosis of LM is mainly based on information on the primary tumor, cytology and clinical chemistry of cerebrospinal fluid (CSF) as well as the evaluation of magnetic resonance imaging (MRI) (7). While being the gold standard in clinic diagnosis, both MRI and standard cytology, are known as low sensitive diagnostic methods (8) resulting in qualitative statements with limited options for further molecular downstream analysis. Early treatment by pharmacotherapy, radiation, and chemotherapy can help to treat the debilitating symptoms (5,10–15) but prognosis for patients with leptomeningeal spread remains still very poor. This leads to the following question: Can DNA analysis methods, including sequencing technologies and protocols which allow the characterization and molecularly analysis of rare cells even down to a single-cell level, be an option to improve this situation?

1.3 Liquid biopsy as minimally invasive analysis option

These advancements significantly improved the field of liquid biopsy (16–19) by extracting molecular information from peripheral blood. Circulating tumor cells (CTCs) from blood were first described by the Australian physician Thomas Ashworth. In his article published 1869 in the *Australian Medical Journal*, he argued that “cells identical with those of the cancer itself being seen in the blood may tend to throw some light upon the mode of origin of multiple tumors existing in the same person”. After an extended phase of inviolacy, mainly due to the rarity of tumor cells in the blood of most patients but also the lack of efficient enrichment and isolation technologies, the interest

in this topic only grew in the latter part of the 20th and the early 21st century. Then, minimally invasive diagnostic approaches helped to detect and analyze biomarkers associated with cancer not only in blood but also in other body fluids such as urine (20), malignant effusions (21), and leukapheresis (22). These approaches offered a great potential of getting important information about the indication or the status of the disease. Also, those biomolecular features generated great interest in the past decade and are expected to increase in the next years (23).

1.4 Liquid biopsy of cerebrospinal fluid

For patients affected with CNS tumors, this analysis can be challenging as the associated circulating tumor cells are often difficult to detect in the blood due to the blood brain barrier and because predictive biomarkers are missing. So biomarkers derived directly from CSF can be an auspicious alternative to provide important molecular information for clinical decision-making (23–26) in patients. Generally, CSF is a clear, colorless fluid surrounding the brain and the spinal cord between the arachnoid mater and the pia mater layers of the meninges. It fulfills several important functions in the CNS such as protection, buoyancy, nutrient transport, waste removal, and regulation of the cranial pressure (27). The potential of CSF analysis for patients with LM is enormous. The direct contact of tumor cells with the cerebrospinal fluid and its low cell number (28) favors the probability that tumor DNA can be detected in CNS affected patients. Several tumor capturing methods exist and are being employed in cancer research. Many, however, are not approved for diagnostic purposes. The CellSearch® System is the first FDA cleared tests for capturing and counting CTCs from blood and provides insights into disease progression, prognosis, and treatment response in cancer patients. CellSearch® was initially approved for breast, and later on also for prostate and colorectal cancer patients (29–32). It is based on an immunomagnetic separation and fluorescent labeling technique for tagging CTCs in blood samples with specific antibodies that recognize proteins expressed on the surface of tumor cells.

1.4.1 Disseminated cancer cells from cerebrospinal fluid

By adapting the CellSearch® technology, it was shown in many studies that disseminated cancer cells (DCCs) can be enriched from CSF of cancer patients (10,33). Furthermore, the additionally exported quantification of DCCs provides the possibility to longitudinally monitor the progress e.g. especially under therapy conditions (34). In a recent study from on breast cancer patients with suspected leptomeningeal metastasis, it was demonstrated that quantifying DCCs from CSF correlates with overall survival (35). Besides the enrichment and number of DCCs this technology offers the opportunity to subsequently isolate and molecularly characterize them down to the single-cell level. This approach has shown that tumor cells from the CNS exhibit significant clonal differences compared to the primary tumor (36) and allows the detection of therapy-relevant molecular biomarkers, such as EGFR mutations or ERBB2/Her2 amplifications (37).

1.4.2 Circulating tumor DNA from cerebrospinal fluid

Moreover, CSF cannot only be a valuable source to deliver important information in terms of DCCs but also of circulating tumorDNA (ctDNA). ctDNA is detected in the blood of around 75 % of patients with metastatic cancer and described as DNA shed from tumor and blood cells derived via apoptosis or necrosis. Circulating Tumor DNA has been widely studied as a potential biomarker for cancer diagnosis, prognosis, treatment monitoring, and detection of minimal residual disease (38–40) and can deliver reliable measurements of clinically relevant genetic changes (41–45) even with high sensitivity and specificity through minimal invasion. Since circulating cell-free DNA is a mixture of DNA from non-malignant and malignant cells, an early detection of tumor cell subclones might be challenging even more for patients with brain or leptomeningeal metastases. However, one advantage of this approach lies in the significantly lower technological effort in pre-analytical processing and can be adapted to CSF for this patient cohort.

1.4.3 Additional benefits of cerebrospinal fluid biomarker

The examination of ctDNA and DCCs in CSF presents valuable avenues for enhancing the molecular understanding of leptomeningeal metastases. Specifically, the insights gleaned from liquid biopsy techniques can complement traditional diagnostic modalities like cytopathology and imaging, offering a more comprehensive grasp of tumor heterogeneity and treatment response dynamics. Despite its promise, it is imperative to recognize the limitations of liquid biopsy, including the risk of false positives and negatives, along with the technical hurdles associated with isolating and characterizing rare tumor cells or low ctDNA concentrations. Moreover, extensive clinical investigations are necessary to confirm the clinical significance and efficacy of liquid biopsy strategies in guiding therapeutic decisions and improving patient outcomes. The incorporation of liquid biopsy into routine clinical practice for individuals with leptomeningeal metastases demands further optimization and standardization of methodologies, alongside robust collaboration among researchers, healthcare practitioners, and industry stakeholders. Ultimately, the effective utilization of liquid biopsy in managing leptomeningeal metastases has the potential to transform personalized cancer care, furnishing real-time, minimally invasive molecular insights crucial for treatment planning.

1.5 Objective of this PhD thesis

The challenges for patients diagnosed with LM are manifold. Amongst other things, metastatic diseases in general come with a poor prognosis. Additionally, the adverse location of those metastasis in the central nervous system often complicates analysis limitations followed by missing concrete therapeutic decisions.

To overcome these limitations, I will answer three important questions with my thesis.

i) Can our liquid biopsy CSF approach deliver results comparable to the gold standard in the clinic, currently the CSF cytology and MRI, for patients with suspected LM?

ii) Is the isolation of CSF single cells a valuable option for delivering important molecular data and how reliable are those results compared to the analysis of CSF derived circulating tumor DNA regarding their quality, expressiveness, and applicability?

iii) Does the heterogeneous landscape of tumor and metastatic tissue give a hint as to the sedimentation of specific CNS seeking subclones?

In the first, more technical, part of this thesis, a molecular diagnostic workflow, with the intention to detect, enrich and isolate DCCs in CSF, was established and optimized for obtaining tumor DNA from cerebrospinal fluid. Depending on the site of origin of the underlying primary tumor and its associated expression marker, it was evaluated, if cells can be detected either with the purchasable FDA cleared CellSearch® technology based on the Epithelial Cell Adhesion Molecule (EpCAM) expression and Cytokeratin (CK) staining of carcinoma cells or via a density gradient centrifugation followed by specific fluorescence staining for melanoma cells. These results were compared with those obtained from parallel analyses of cytology and dedicated MRI data and the CellSearch® approach could be validated as it delivered approximately equivalent and reliable results.

One big advantage of our CSF detection method was the ability to isolate single cells after the cell enrichment. I used this option to establish a CSF derived single cell collective for a molecular downstream analysis. Within this part of the process the two different isolation methods, on the one hand the manual pipetting on the fluorescent microscope and/or the automated isolation with the DEPArray™ technology, could be evaluated and the differences in the DNA quality depending on the cell source and the technical reprocessing were validated. Using DNA quality classification was used as an instrument to distinguish between DNA samples of low quality and samples worth to continue for further downstream analysis. The copy number variation analysis allowed defining the origin of the sample and to prove sub clonal diversity within several isolated CSF single cells. Using not only the cell compartment of CSF allowed me to isolate additional circulating DNA and which in turn enabled the comparison of different biomarkers. An existing cfDNA extraction protocol was optimized, and on the isolated samples a new amplification strategy was tested and validated. The molecular data

derived from those samples was subsequently utilized to assess which type of circulating DNA is present, whether the tumor derived or not and if a similar copy number variation profile exists in the isolated DCCs. A comparison between both, the DCC and the ctDNA approach should show benefits and drawbacks concerning quality, expressiveness, applicability, and reliability of both methods.

By analyzing the available tumor tissue of patients who entered this collective I wanted to go explore what the tumor landscape looks like. Therefore, tumor and stromal cell populations from formalin-fixed paraffin-embedded (FFPE) tumor tissue were isolated. The technical feasibility of the DEPArray™ technology was established and the protocol optimized for different tumor types and material. After the isolation process different cell populations were analyzed on a molecular level and data derived from non-CNS or CNS-tissue material were compared to the CSF isolated DNA data. Subsequently, a conclusion could be drawn whether specific subclones seeking different locations for metastatic spread exist could be made.

To summarize, the work for my PhD thesis was performed, on the one hand, to explore whether the CellSearch® technology used for enrichment of tumor cells in CSF can be a viable alternative to the current gold standard in the clinic diagnosis. And on the other hand, my thesis assessed the advantage of this technology as being an option for molecular downstream possibilities delivering valuable decision-making information.

2. Materials and Methods

2.1 Cerebrospinal fluid sampling

Samples of consenting patients were withdrawn at the University hospital and the Bezirksklinikum of Regensburg. The native cerebrospinal fluid (CSF) was transported in a sterile 10 mL polystyrol tube at room temperature (RT) to the incoming registration lab of the pathology department at the university hospital of Regensburg. There the volume was splitted into two parts while one part was given to the neuropathology for cytological CSF standard analysis and the other part entered the “systemic cancer progression laboratory” (SCP-L) at the chair “Experimental medicine” (University of Regensburg, Prof. CA Klein), where the experiments described in this thesis were performed. The written informed consent for DNA isolation, characterization and comparative molecular analyses and the signed privacy policy was obtained for all patients before sample analysis. All experiments conformed to the principles set out in the WMA Declaration of Helsinki and were approved by the ethical committee (Vote numbers: 18-948-101, 17-672-101) responsible for the corresponding partner.

2.2 Cerebrospinal fluid preprocessing and storage of samples

Before starting with analysis, the volume of the CSF was defined and the cell compartment was separated from the supernatant, by centrifuging the tube at 500g, 5 min, break = 0, at RT in a swinging bucket centrifuge. The supernatant was removed careful and slowly down to 500 µL without touching or disturbing the pellet by a 1 mL pipet. It was collected in 1.5- or 2-mL sterile reaction tube and stored at -80 °C until its analysis of the cell-free DNA. In order not to harm the quality of the sample we used the Mr. Frosty (Nalgene™) freezing system where tubes are stored in a rack covered with foamed material in a lockable bin filled with isopropanol. This makes a slow cooling temperature of 1 °C/min possible which is required to save the quality of the DNA within the sample.

The residual 500 µL cell compartment was used for cell enrichment. Depending on tumor entity this was performed automatically with the CellSearch® system

(Carcinoma) or manually (Melanoma) by centrifugation, collection and staining on adhesive object slides. For a proof-of-concept trial parts of the cell compartments were cultivated under special 3D conditions to try if this could be an option of generating organoid models for further molecular testing.

2.3 Reagents

2.3.1 Chemicals and commercial solutions

Table 1 List of Chemicals and commercial solutions

Name	Producer	Order Number
1 kb Plus DNA Ladder + Dye	New England Biolabs	N3200L
AB serum, human	BioRad	805135
Agarose LE	Anprotec	AC-GN-00009
AMPure XP purification beads	Beckman Coulter	A63882
BCIP/NBT solution, AP conjugate substrate Kit	ThermoFisher	34042
Bio-Clear	Bio-Optica	06-1782D
Bovine serum albumin (BSA) (20 mg/ml)	Roche Diagnostics	10711454001
BSA (for picking and cell culture)	Sigma Aldrich	B8667-5ml
dNTP Set ;100 mM each A, C, G, T; 4x 24 µM	GE Healthcare	28-4065-51
Dulbecco's Modified Eagle Medium (DMEM)	PAN Biotech	P04-05551
Ehtanol absolute Mol. Bio.Grade 250 ml	VWR Chemicals	437443T
Ethidium Bromide Solution (10 mg/ml)	Sigma-Aldrich	E1510-10ML
Ethylenediaminetetraacetic acid (EDTA)	J.T. Baker	B-1073.1000
Expand Long Template Buffer 1	Roche Diagnostics	11759060001
FastStart dNTP mix	Roche Diagnostics	4738420001
FastStart PCR buffer with MgCl2	Roche Diagnostics	4738420001
Fetal bovine serum (FBS) sera Plus	PAN Biotech	P30-3702
Formaaldehyd	VWR	97.131.000
Gel loading dye 6x, purple, no SDS	New England Biolabs	B7025S
Igepal CA-630 viscous liquid	Sigma-Aldrich	I3021-50ml
iQ™ SYBR® Green Supermix	BioRad	1708885
Low molecular weight ladder	New England Biolabs	N3233L
Magnesium chloride (MgCl2) solution 1 M	Sigma Aldrich	M1028-100ml
Natriumhypochloritlösung	CarlRoth	7681-52-9
Penicillin (10.000 U/ml) / Streptomycin (10 mg/ml)	PAN Biotech	P06-07100
RPMI 1640	PAN Biotech	P04-17500
SPRI Select beads	Beckman Coulter	B23317
Trypan blue	Sigma Aldrich	T8154-20ml

Trypsin/ EDTA (10x) (0.05% Trypsin/ 0.02% EDTA)	PAN Biotech	P10-024100
TWEEN® 20, for molecular biology	Sigma-Aldrich	P9416-50ml
Water for chromatography, LiChrosolv®, LC-MS grade (PCR-water)	Merck	1.153.331.000
Water, aqua ad iniectabilia (NGS-water)	Braun	2351744
Water, demineralized	Taken from tap	n.a.
Xylol 3	VWR Chemicals	28973.36

2.3.2 Custom buffers, media, and solutions

Table 2 List of Custom buffers, media, and solutions

Name	**Components**
dNTPs 10 mM	10 µl dATP 100 mM 10 µl dCTP 100 mM 10 µl dGTP 100 mM 10 µl dTTP 100 mM 60 µl DEPC-water
Igepal 10 %	2 ml 100 % Igepal CA-630 18 ml DEPC-Water
One Phor All (OPA) buffer	5 ml 1 M Tris acetate 5 ml 1 M Magnesium acetate 1 ml 5 M Potassium acetate PCR-Water ad 1 L Sterile filtrate
PBS pH 7.4 10x	450 g Sodium chloride 71.65 g Disodium phosphate (Na2HPO4) 13.35 g Monopotassium phosphate (KH2PO4) Distilled water ad 5 L
Tris/Borate/EDTA (TBE) buffer	10x 539 g Tris 275 g Boric acid 37 g EDTA 5 l Demineralized water
Tween 10 %	2 ml 100 % TWEEN® 20 18 ml DEPC-Water

2.3.3 Antibodies

Table 3 List of Antibodies

Antibodies	Producer	Order Number
Alkaline Phosphatase-Polymer anti-mouse antibody	Zytomed systems	n.a.
Hoechst 33342, Trihydrochloride Trihydrate 10mg/ml	Life Technologies	H3570
isotype control, melanoma/lung carcinoma samples: IgG1, Kappa **from murine myeloma, Clone MOPC 21**	SigmaAldrich	n.a.
Monoclonal Mouse Anti-Human **Melanosome, Clone HMB45**	Agilent	n.a.
Monoclonal Mouse Anti-Human **Cytokeratin 8,18,19, Clone A45 B/B3**	AS Diagnostic	n.a.

2.3.4 Enzymes

Table 4 List of Enzymes

Enzyme	Producer	Order Number
FastStart Taq Polymerase	Roche Diagnostics	4738420001
Mse I, recombinant, conc., 2500U 50000U/ml	New England Biolabs	R0525M
Pol Mix 5 U/µl (Expand Long Template enzyme mix)	Roche Diagnostics	11759060001
Proteinase K, recombinant	Roche	3115828001
T4 DNA Ligase 500U 5U/µl	Roche	10799009001

2.3.5 Primer and Oligonucleotides

Table 5 List of Primer and Oligonucleotides.
* These primers amplify a polymorphic DNA section on human chromosome 5. Precisely, this is a length polymorphism, i.e., the length may vary for each individual and between the two alleles of one individual.

Primer and oligonucleotides	Base sequence (5'->3')	T_A [°C]	Amplicon Size
cf-Lib1 adapter - long oligo	AGTGGGATTCCTGCTGTCAGT	68	-
cf-Lib1 adapter - short oligo	CTGACAGddC	68	-
ddMSE11	TAA CTG ACAG ddC	65	-

hD5S2117 for	CCA GGT GAG AAC CTA GTC AG	58	140bp*
hD5S2117 rev	ACT GTG TCC TCC AAC CAT GG	58	140bp*
hKRAS for	ATA AGG CCT GCT GAA AAT GAC	58	91bp
hKRAS rev	CTG AAT TAG CTG TAT CGT CAA GG	58	91bp
hKRT19 for	GAA GAT CCG CGA CTG GTA C	58	621bp
hKRT19 rev	TTC ATG CTC AGC TGT GAC TG	58	621bp
hTP53 Exon2/3 for	GAA GCG TCT CAT GCT GGA TC	58	301bp
hTP53 Exon2/3 rev	CAG CCC AAC CCT TGT CCT TA	58	301bp
Lib1	AGT GGG ATT CCT GCT GTC AGT	65	-

2.3.6 Commercial kits

Table 6 List of Commercial kits

Kit	**Producer**	**Order Number**
Ampli1™ LowPass Kit for Illumina - PEG	Menarini Silicon Biosystems	KI0112
Ampli1™ LowPass Kit ILLUMINA (Set A)	Menarini Silicon Biosystems	KI0041
Ampli1™ LowPass Kit ILLUMINA (Set B)	Menarini Silicon Biosystems	KI0040
Ampli1™ QC Kit	Menarini Silicon Biosystems	KI0027
Ampli1™ WGA Plus Kit	Menarini Silicon Biosystems	KI0143
Bioanalyzer DNA High Sensitivity Kit	Agilent Technologies	5067-4626
CellSave® Preservative Tubes 100	Menarini Silicon Biosystems	CS0018
CELLSEARCH® Circulating Tumor Cell Control Kit - IVD	Menarini Silicon Biosystems	CS0011
CELLSEARCH® Circulating Tumor Cell Kit - IVD	Menarini Silicon Biosystems	CS0009
CellTracks® AutoPrep Instrument Buffer	Menarini Silicon Biosystems	CS0005
DEPArray™ Buffer	Menarini Silicon Biosystems	KI0066
DEPArray™ SamplePrep Kit BOX1	Menarini Silicon Biosystems	KI0114
DEPArray™ SamplePrep Kit BOX2	Menarini Silicon Biosystems	KI0115
Expand Long Template PCR System	Roche Diagnostics (Sigma Aldrich)	11759060001
KAPA Library Quantification Kit	Roche Diagnostics	7960298001
MiSeq® Reagent Kit v3 (150 cycles)	Illumina	MS-102-3001
QIAamp® circulating nucleic acid kit	Qiagen	55114
QiaQuick PCR purification kit	Qiagen	28106
Qubit® dsDNA HS Assay Kit	Thermo Fisher Scientific	Q32845

2.3.7 Celllines

Table 7 List of Celllines

Celllines	
MCF7	Human breast cancer cellline
MelHo	Human melanoma cellline

2.3.8 Consumables

Table 8 List of Consumables

Consumables	Producer	Order Number
1,5ml Eppendorf® protein LoBind tube	Eppendorf	30.108.116
BD Luer-Lok™ Syringe 50 ml	BD Plastipak™	300865
Cell culture flask T175	Greiner Bio-One	660175
Cell culture flask T25	Greiner Bio-One	690160
Cell culture flask T75	Greiner Bio-One	658175
Cell Strainer 40µm	Becton Dickinson	352340
Cellstar® serological pipette 10 ml	Greiner Bio-One	607180
Cellstar® serological pipette 2 ml	Greiner Bio-One	710180
Cellstar® serological pipette 25 ml	Greiner Bio-One	760180
Cellstar® serological pipette 5 ml	Greiner Bio-One	606180
Centrifuge tube 15 ml	Greiner Bio-One	188271
Centrifuge tube 50 ml	Greiner Bio-One	227261
Corning® 1-200µl Round 0,5 mm Thick Gel Loading Pipet Tip	Corning	4853
Countess Chamber Slides	Thermo Fisher Scientific	C10228
Countess® Cell Counting Chamber Slides	Thermo Fisher Scientific	C10228
DEPArray™ PLUS Cartridge	Menarini Silicon Biosystems	DA0752
epT.I.P.S® LoRetention dualfilter 0,1-10µl	Eppendorf	30.077.610
epT.I.P.S® LoRetention dualfilter 0,5-20µl	Eppendorf	30.077.628
epT.I.P.S® LoRetention dualfilter 20-300µl	Eppendorf	30.077.636
epT.I.P.S® LoRetention dualfilter 50-1000µl	Eppendorf	30.077.652
Injekt® 10 ml B	Braun	4606108V
MicroAmp reaction tube with cap 0,2ml	Applied Biosystems	N801-0612
Microscope slides, ground edges 90°, frosted end	ROTH	H870.1
Nitril BestGen® Powederfree gloves	Meditrade	1286
Nunc™ Lab-Tek™ Chamber Slides; 8 fields	Thermo Fisher Scientific	11367764
Parafilm "M"	Bemis Company, Inc., Fisher Scientific	11772644
Pasteur pipettes, long	Brand	747720
PCR tube 0.2 ml, single tube	4titude Deutschland	4ti-0795
PipetBoy	Integra	n.a.

Protein LoBind Tube 2 ml	Eppendorf	22431102
Protein LoBind Tube 5 ml	Eppendorf	30108302
QiaxCel High resolution Cartridge	Qiagen	n.a.
Rotilabo® syringe filter, PVDF, sterile, 22 µm	ROTH	P666.1
Transparent 96-well PCR plate	Biozym	710884

2.3.9 Devices

Table 9 List of Devices

Devices	Producer
Research plus pipette 20-200µl	Eppendorf
Research plus pipette 100-1000µl	Eppendorf
Countess® II FL Automated Cell Counter equipped with EVOS® Light Cube, DAPI	Thermo Fisher Scientific
EVOS® Light Cube, DAPI	Thermo Fisher Scientific
Autoclave 3150 EL	Systec
Bioanalyzer 2100	Agilent Technologies
Centrifuge 5424	Eppendorf
Centrifuge 5424R	Eppendorf
Centrifuge 5810R	Eppendorf
Centrifuge Plate Fuge	Benchmark Scientific
Centrifuge Rotina 380R	Hettich
DNA Engine Tetrad2 Peltier Thermal Cycler	BioRad
Electrophoresis chamber 40-1214	Peqlab
Genetouch thermal cycler	Bioer
Incubator Heraeus BB15	Thermo Fisher Scientific
Laminar flow bench Her Safe KS18	Thermo Fisher Scientific
LightCyler 480	Roche Diagnostics
Microscope CX23	Olympus
Automatic image-based cell sorter DEPArray™	Menarini Silicon Biosystems
CellSearch® AutoPrep System	Menarini Silicon Biosystems
CellTracks™ Analyzer II	Menarini Silicon Biosystems
Microscope IB inverted	Optech
MiSeq	Illumina
Nanodrop 2000c c	Thermo Fisher Scientifi
Patchman NP2 micromanipulator	Eppendorf
Power Supply MP-250N	Kisker Biotech
Qubit3 fluorometer	Thermo Fisher Scientific
Roller Mixer SRT1	Stuart Scientific
Thermomixer C	Eppendorf
UV-Illuminator	Intas
Vortex/centrifuge PCV-2400	Grant-bio
Vortexer	VELP Scientifica

QIAxcel® Advanced System	Qiagen
PCR bench UVT-S-AR	Thermo Fisher Scientific
pH-meter PB-11	Sartorius
Erlenmeyer flask 250 ml DURAN	Schott
Research plus pipette 2-20µl	Eppendorf
Research plus pipette 0,5-10µl	Eppendorf

2.3.10 Software

Table 10 List of Software used in this thesis

Software	Provider	Application
Microsoft Office 2013/2016	Microsoft	Data management
PubMed	https://www.ncbi.nlm.nih.gov/pubmed	Literature search
VassarStats	http://vassarstats.net/	Statistics
ImageJ	W. Rusband, NIH	Countess - Cell counting
CellSearch Autoprep Software Version 2.7.0	Menarini Silicon Biosystems	CellSearch Navigation
CellTracks Analyzer II Software 2.8.0	Menarini Silicon Biosystems	CellDetection CellSearch
CellBrowser™ Software 3.5.1	Menarini Silicon Biosystems	DEPArray Nxt
CellBrowser™ Software 4.0.1	Menarini Silicon Biosystems	DEPArray Plus
LightCycler 480 Software 1.5	Roche	qPCR
Chat GPT Version 3.5		Sprachkorrektur
2100 Expert Software Version B.02.09SIO725 (SR1)	Agilent Technologies	Bionalyzer

2.4 Disseminated cancer cell enrichment from CSF with the CellSearch® system

The CellSearch™ System (developed by Janssen Diagnostics, inherited by Menarini Silicon Biosystems, MSB; Figure 1) is an American “Food and Drug Administration (FDA)” approved technology developed for the detection and enumeration of circulating tumor cells (CTCs) in the blood of cancer patients (46). It is providing a non-

invasive method for monitoring and analyzing the presence of cancer cells in the blood stream in the diagnostics but can also be applied to other body fluids shown in different publications (8,10,47,48). It consists of the CellTracks® AutoPrep® System utilizes immunomagnetic separation and fluorescent labeling techniques to enrich target cells in liquid biopsy samples and the CellTracks® Analyzer II to select those cells. For DCC enrichment from CSF the CellSearch® Circulating Tumor Cell Kit (49) with the primarily target *Epithelial Cell Adhesion Molecule (*EpCAM*)* and an included fluorescent dye for labeling the cells with DAPI, Cytokeratin (tumor cells) and CD45 (immune cells) was used. The captured and labeled cells are collected in cartridges fixed in a magnetic holder and identified under the fluorescence microscope included in the CellTracks® Analyzer II. They are selected by their staining and morphological characteristics but also controlled by experienced users and confirmed by clinicians. Prior to run a sample it must be incubated at least two hours in a CellSave Preservative Tube. This obligatory integral component of the system is a special sample collection tube containing a mild fixative to keep the viability and morphology of fresh samples and thereby cells stable. Furthermore, it offers the possibility to transport samples up to 96 hours from the clinic site to the analysis lab.

Sample processing (50):

The residual CSF cell pellet from all carcinoma samples were transferred to a CellSave Preservative Tube, filled up to 7.5 mL with the CellSearch™ dilution buffer (MSB, included in the kit) and incubated at RT at least 2 hours before processing. The complete sample was transferred to a conical tube (included in the CTC kit) filled up to 14 mL with the dilution buffer and centrifuged in a swinging bucket centrifuge at 1000g, 10 min, break = 0 at RT. The samples were analyzed in the sample mode, for breast cancer samples an additional Her2/neu marker was used, following the instructions of the user manual of the CellSearch® system (49,51,52). Since the CellSearch™ system was developed for analysis of blood the erythrocyte level after the centrifugation step is a crucial sign for starting the enrichment workflow. Because CSF is a cell rare and clear solution, the system had to be passed over by marking the tube wall for darkening and so imitating the erythrocyte level needed to start the process (53). After the enrichment of the samples the target cell solution was stored automatically in a sample cartridge fixed by a magnetic holder (MagNest®) and scanned within the next 24 hours by the CellTracks® Analyzer II to define the cell number. Samples which could not be scanned automatically by the system, also a side effect of the low cell number in CSF,

Figure 1 The CellSearch™ System with its compartments. The CellTracks® Autoprep (A) and the CellTrack® Analyzer II (B). For analyzing the samples the CellSave Tubes (C) and an appropriate Kit, in this case the CellSearch™ Circulating Tumor Cell Kit (D) are required. https://www.cellsearchctc.com

which is necessary for correct focusing, were screened manually at the fluorescent microscope prior to cell isolation (Olympus, methods described in the following).

2.5 Isolating cells of enriched cell suspension from CellSearch™ cartridge

For the isolation of single cells, the enriched sample had to be removed from the CellSearch™ cartridge by following a detailed protocol for the extraction of fixed enriched cells (54) provided by the manufacturer (MSB). If the sample was prepared for an automatic isolation of cells with the DEPArray™ system (see 2.11) the sample volume was reduced to 12 µL as described in the last step of the protocol (step 6). If the sample was screened and isolated manually at the fluorescent microscope (see 2.6), the volume reduction step 6 in the protocol was not performed to 12 µL but to a final volume of ~80 µL.

2.6 Fluorescence microscopy and cell isolation by micromanipulation

Two fields of an eight-chamber microscope slide (Nunc, Thermofisher) were coated with bovine serum albumin (BSA) by pipetting up and down all over the bottom several times to avoid sticking of sedimented cells. A final volume of 200 µL, containing the cell suspension (~ 80 µL) filled up with phosphate-buffered saline (PBS), was transferred into the first field (sample field) and 200 µL PBS was pipetted in the second field (cell free picking field). The slide was set under an inverted fluorescence microscope (Olympus, Figure 2) and the cells got some minutes time to settle to the bottom. The sample field was screened for Cytokeratin positive cells in the PE (phycoerythrin, emission maximum 578 nm) channel and for the CD45 positive cells in the APC (Allophycocyanin, emission maximum 660 nm). The DAPI (4,6-Diamidino-2-phenylindole, emission maximum 457 nm) and the brightfield channels were used as a control to confirm the individual staining as an intact cell by the nuclear staining and the morphology. During the screening step the DCC (disseminated cancer cell) number was determined. For isolating a cell of interest, a glass capillary coated with fetal calf serum (FCS) was fixed in the micromanipulator (Patchman NP2 including a pump, CellTram, both Eppendorf) and the cell was aspirated. It was released to the picking

field and transferred within 1 µL in a P2 micropipette to a 200 µL reaction tube, prepared with 2 µL of reaction buffer (Proteinase K digestion) necessary for initializing the amplification of the whole genome (see 2.12). A negative control, only reagents from the picking field prior to isolating cells, was taken to validate the assay.

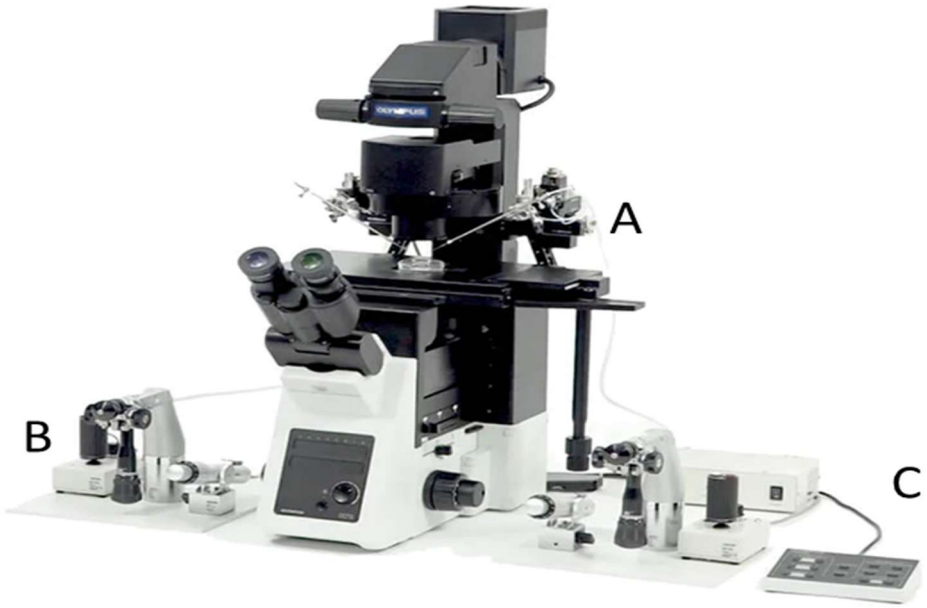

Figure 2 Inverted fluorescent microscope.
The Olympus microscope with a fixed micromanipulator (A), the pump (B) and the filter changing board (C). https://us.ivfstore.com

2.7 Manual DCC enrichment and storage on glass adhesion slides

The CSF sample was transferred to a 5 mL LoBind tube and centrifuged for 500g, 5 min at RT. The cell-free supernatant was removed down to ~150 µL and stored in Cryo Vials at -80 °C (see 2.2) for further analysis. 10 µL of the cell pellet were used to count peripheral blood mononuclear cells (PBMCs) by adding 10 µL of Trypanblau under the microscope. Depending on the cell number the cell suspension is diluted and transferred to the appropriate number of glass adhesion slides. After settling down (one hour) and drying overnight, the slides were frozen at -20 °C for long term storage or used for immunocytological staining directly.

2.8 Immunocytological staining of samples on glass adhesion slides

Frozen HOTs were thawn and dried at RT before processing. The spots of interest are blocked by a BSA/PBS solution for 25 min. After removing the blocking solution, the marker antibody (for melanoma samples: Monoclonal Mouse Anti-Human Melanosome, Clone HMB45, Agilent, 1:50; for lung carcinoma samples: Monoclonal Mouse Anti-Human Cytokeratin 8,18,19, Clone A45 B/B3, AS Diagnostic, 1:100) was added in the suggested concentration (user manual) and incubated for 45 min, RT. In the next step the Alkaline Phosphatase-Polymer anti-mouse antibody (Zytomed systems) was added, incubated for 30 min and the developing was activated by adding the BCIP/NBT solution (AP conjugate substrate Kit) for 10 – 15 min. After fixation with Formaldehyde (37 % buffered, VWR) and a washing step the HOTs could be analyzed directly under the microscope for cell isolation or stored covered with PBS in the fridge. As a negative control one slide was stained with an isotype control for each marker (melanoma/lung carcinoma samples: IgG1, Kappa from murine myeloma, Clone MOPC 21 (lung: 2 µg/mL; melanoma: 0.4 µg/mL), Sigma Aldrich). As a positive control a cell mixture consisting of a marker specific cell line (melanoma: MelHo; lung carcinoma: MCF7) and as a negative control immune cells (peripheral blood lymphocytes from voluntary healthy test donors) were stained.

2.9 Isolation of cells from glass adhesion slides

The adhesion slide was washed and coated with PBS and mounted under the microscope. The spot is screened for cells of interest and pictures are made with the connected camera. The glass capillary is lowered close to the cell which should be isolated and by scratching with the capillary detached from the slide. After aspiration the cell is released in a clean pick field (filled with sterile PBS), collected by a 2 µL pipette and transferred into a 200 µL PCR reaction tube with 2 µL Proteinase K buffer for going on with the first step of the whole genome amplification (WGA) (see 2.12).

2.10 Dissociation of Formalin Fixed Paraffin Embedded Tissue slices

FFPE slices (20 – 50 µm) were dissociated and stained using the DEPArray™ SamplePrep Kit (55). It includes two boxes with different reagents (Table 11) stored at 4 °C (Box 1) and -20 °C (Box2). Slices up to 50 µm are collected separately in nylon biopsy bags (included in the kit) and closed by melting the aperture with a lighter. By incubating the bag in Xylene in a 50 mL centrifugation tube 3 times for 10 minutes the tissue was deparaffinized. The rehydration war performed by an ethanol row (incubation in 100 %, 3 x in 70 % and 3 x in 50 % ethanol 3 x 5 min each step) followed by a washing step in PCR grade water. The antigens were made accessible by a heat induced antigen retrieval buffer incubation in an 80 °C water bath for one hour and subsequent washing steps with RPMI1640 (Roswell Park Memorial Institute) medium. The enzyme-based digestion was performed in a 37 °C water bath by controlling every ten minutes the progress in order not to over digest the sample. After a filtration step (30 µm nylon mesh strainer Miltenyi – not included in the kit) the cell solution was stained with the Hoechst dye to determine the cell number with an automated counter (Countess™, Lifetechnologies). The evaluation was performed by the ImageJ (56,57) and an appropriate cell number (up to 500.000 cells) was stained. The first step was an incubation of Cytokeratin A/B (putative tumor cells) and Vimentin (stromal cells) which were conjugated in a second step with the fluorochromes Alexa®488 (Cytokeratin) and Alexa®647 (Vimentin) in addition to the DAPI staining. After counting again with the Countess™ the sample was ready to isolate cells with the DEPArray™ FFPE application.

Table 11 Components of the DEPArray™ SamplePrep Kit (MSB)
for dissociating Formalin Fixed Paraffin Embedded Tissue into a single cell suspension.

Box	Storage	Reagent	Color	#Vials/Content
1	+2°C ...+8°C	Antigen Retrieval Buffer 10x (AR Buffer 10x)		1 x 55ml
		Enzyme 1 (lyophilized)		4 x 50mg
		Perm Reagent		1 x 20ml
		Blocking Reagent		1 x 9ml
		Anti-Cytokeratin A (CK Ab1 A)		1 x 60µl
		Anti-Cytokeratin B (CK Ab1 B)		1 x 60µl
		Secondary Ab-Alexa Fluor®488 (AF488)		1 x 20µl
		Secondary Ab-Alexa Fluor®647 (AF647)		1 x 20µl
		Tissue Bags	-	20 Units
2	-25°C...-15°C	Enzyme 2 (lyophilized)		4 x 50mg
		DAPI nuclear stain		8 x 10µl
		Anti-Vimentin (Vim Ab1)		8 x 10µl

2.11 Isolation of cells with the DEPArray™ system

To isolate pure single cells or pools automatically DCCs the automatic image based cell sorter DEPArray™ (MSB, (58)) was used. If cells from CellSearch® enriched samples were isolated the DEPArray™ CTC application was used based on the actual version of the protocol (50). Single cells or pools from dissociated FFPE slices could be isolated with the DEPArray™ FFPE application (59). For both applications 12 µL of a stained cell suspension are pipetted into the DEPArray™ cartridge (57), a single use consumable with microfluidic channels and electrodes to allow controlled movement and sorting of individual cells. By inserting the cartridge into the DEPArray™ system the system uses the electrical properties of particles within a microfluidic environment and based on dielectrophoresis, in which non uniform electric fields exert forces on particles, single cells can be isolated moving along the field gradient (Figure 3). The CellBrowser™ software helps to select cells of interest and calculates possible ways to exit the cartridge as single cell or in cell pools. After isolation the cells are rebuffered by different centrifugation steps and after volume reduction to 1 µL ready for whole genome amplification.

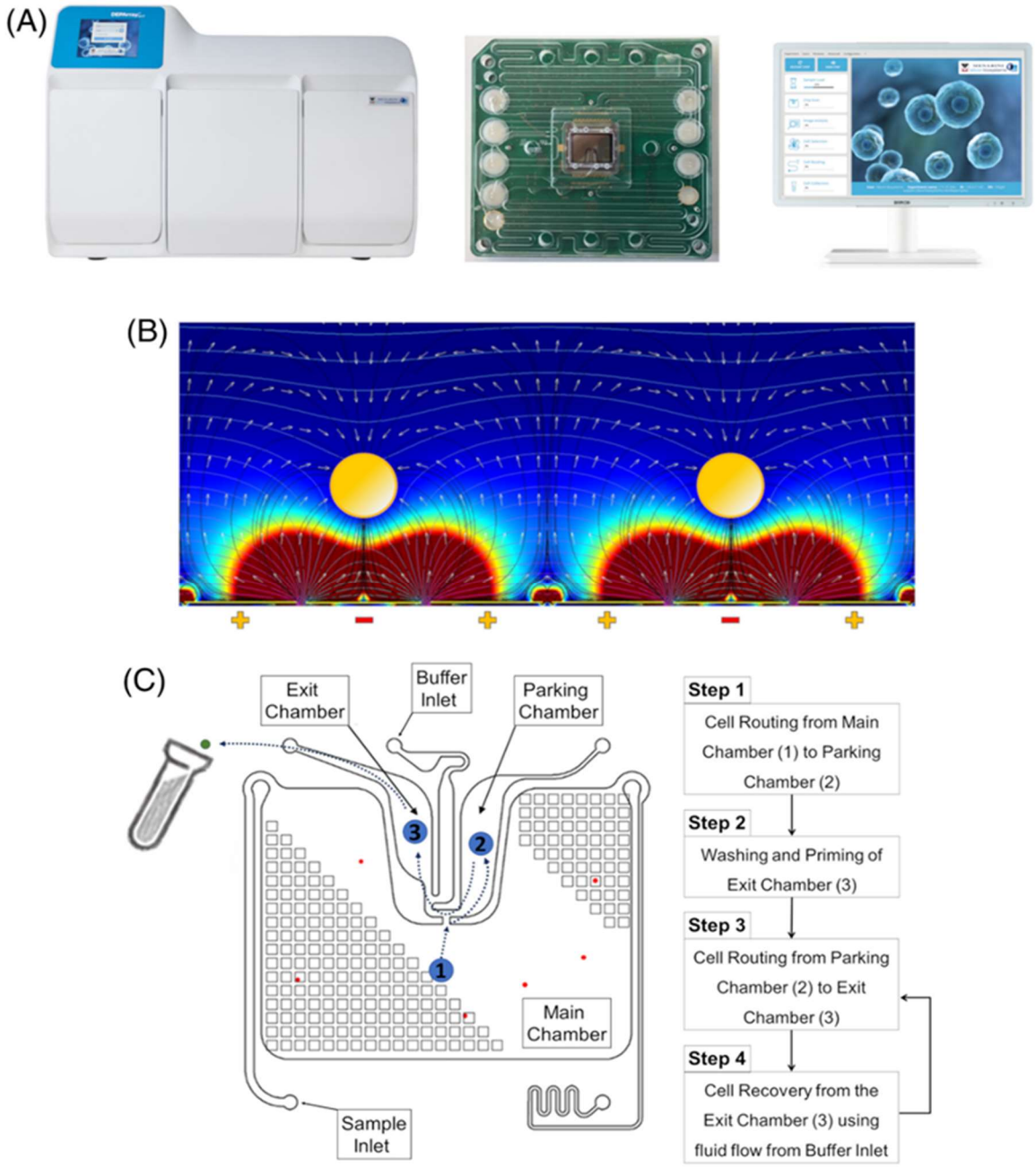

Figure 3 Main components of DEPArray™ NxT system.
(**A**) The benchtop instrument (left), the cartridge (middle) that combines microfluidics and microelectronics, and the CellBrowser™ software (right) to elaborate fluorescence and bright field images for automatic or operator-assisted cell selection. Schematic representation of dielectrophoresis showing the nonuniform electric field generated in the silicon chip that induces a polarization of cells, which are trapped in stable levitation (**B**) Schematic representation of DEPArray™ chip (**C**) After the phases of sample and buffer loading, the cells are randomly distributed into the Main chamber (1). Then, the selected cells are simultaneously moved toward the parking chamber (2). After a washing and priming phase of exit chamber (3), the cells are moved from the parking chamber (2) to exit chamber (3) for the cell recovery (4). Source (28). www.siliconbiosystems.com

2.12 Whole Genome Amplification of isolated cells

The genome of isolated cells was amplified by the whole genome amplification (WGA) (Table 12) an adaptor-ligation mediated method initially developed in our lab (60) but meanwhile commercially available as a kit (Ampli1^{TM} WGA Kit, MSB). An initial Proteinase K digestion overnight is followed by an incubation of the genomic DNA with the restriction enzyme MseI resulting in fragments of different lengths. By annealing linker sequences the binding of the primers essential for global amplification is ensured. In the amplification PCR fragments with a length of 200bp to 2000bp are enriched with an amount of 15 – 20 ng/µL in a total volume of 50 µL.

Table 12: Pipetting scheme and cycler programs
of the different steps of the Whole Genome Amplification (WGA) method

Proteinase K digestion

OPA plus	2.0 µL
Tween 10%	1.3 µL
Igepal 10%	1.3 µL
Proteinase K (10mg/mL)	2.6 µL
PCR-H_2O	12.7 µL
Total per Tube:	**2 µL**

Cycler program	Temperature	Time
Step 1	42.0°C	15 h
Step 2	80.0°C	10 min
Step 3	8.0°C	forever

MseI digestion

OPA plus	0.2 µL
MSE I (50.000 U/mL)	0.2 µL
PCR-H_2O	1.6 µL
Total per Tube:	**2 µL**

Cycler program	Temperature	Time
Step 1	37.0°C	3 h
Step 2	65.0°C	5 min
Step 3	8.0°C	forever

Preannealing

OPA plus	0.5 µL
Lib1 100µM	0.5 µL
ddMse11 100µM	0.5 µL
PCR-H_2O	1.5 µL

Cycler program	Temperature	Time
Step 1	65.0°C	1 min
Step 2*		
Step 3	15.0°C	forever

*Decrease 1.0°C/cycle50times

Ligation: add 1 µL ATP (10mM) and 1 µL T4-Ligase (high concentrated) per sample – Incubation over night

Cycler program	Temperature	Time
Step 1	15.0°C	forever

Primary PCR

BM Buffer 1	3 µL
dNTPs (10 mM)	2 µL
PolMix	1 µL
PCR-H_2O	35 µL
Total per Tube:	**40 µL**

Cycler program	Temperature	Time	
Step 1	68.0°C	3 min	
Step 2	94.0°C	40 s	14 cycles
Step 3	57.0°C	30 s	
Step 4	68.0°C	1:30 min	(2-4)
Step 5	94.0°C	40 s	8 cycles
Step 6	57.0°C	30 s	
Step 7	68.0°C	1:45 min	(5-7) Increase 1.0°C/cycle
Step 8	94.0°C	40 s	
Step 9	65.0°C	30 s	22 cycles
Step 10	68.0°C	1:53 min	(8-10)
Step 10	65.0°C	3:40 min	
Step 11	8.0°C	forever	

2.13 WGA Quality Control Assay – Genomic Integrity Index

As quality control of the isolated, amplified samples a multiplex PCR assay was performed initially developed in our lab (61) meanwhile available as Ampli1™ QC Kit (MSB). From 1 µL of each WGA product (except of FFPE derived material) four DNA fragments (KRAS, D5S2117, CK19 and TP53 Exon 2/3) of different sizes were amplified (Table 13 Pipetting scheme and cycler program of the multiplex quality control PCR) and analyzed by electrophoresis (*QIAxcel® Advanced System,* 2.14*).* Depending on the presence and the combination of the bands the “genome integrity index” (GII) is determined and can be connected directly to DNA quality and further molecular downstream success (61). If three of the long fragments (D5S2117, CK19, TP53 Exon 2/3) and optional KRAS are present, the highest GII = 4 is achieved, which mirrors, that the genome has largely been amplified.

For GII of 2 one long fragment, for the GII 3, two long fragments must be detected (KRAS optional), which reflects still a good DNA quality sufficient for molecular downstream analysis. The KRAS fragment only is connected to a poor amplification and therefore low DNA quality and receives the GII of 1. No bands in the electrophoresis resulted in a GII of 0 and defined samples which dropped out for further downstream analysis. As a control a defined positive (pool of diploid immune cells of voluntary healthy donor) and negative (PCR-grade water) sample are implemented in the analysis.

Table 13 Pipetting scheme and cycler program of the multiplex quality control PCR

dNTPs (10mM)	0.3 µL
Primer-Mix (4 Primer Pairs)	1.5 µL
BSA (20mg/mL)	0.3 µL
PCR-H_2O	10.25 µL
FastStart Taq-Polymerase (5U/µL)	0.15 µL
Total per sample:	**14µL**

Cycler program	Temperature	Time	
Step 1	95.0°C	4 min	
Step 2	95.0°C	30 s	32 cycles (2-4)
Step 3	58.0°C	30 s	
Step 4	72.0°C	90 s	
Step 5	72.0°C	7 min	
Step 6	8.0°C	forever	

2.14 Automated Capillary Gel Electrophoresis – the QIAxcel System

The QIAxcel Advanced system (QIAGEN) is a fully automated gel loading system used for the qualitative and quantitative assessment of DNA (and RNA) samples. It utilizes microcapillary electrophoresis technology to separate and analyze nucleic acid fragments based on size. It provides automated sizing and quantification of DNA and RNA fragments and is a fast and less dangerous method compared to former ethidium

bromide manual gel preparation and electrophoresis. 15 µL of each PCR product is pipetted in a separate well (max. runs in parallel n = 96) and two alignment markers (15bp and 5000bp) and a size marker are included to define the areas where the bands of interests should appear. The high-resolution cartridge aspirated a small amount of the samples via a glass capillary by electrokinetic injection into the analysis core of the cartridge. The included software offers an evaluation of the intercalation results of DNA and ethidium bromide in terms of a gel picture with visible bands (e.g., Figure 4) but also as calculated values of the detected DNA amount.

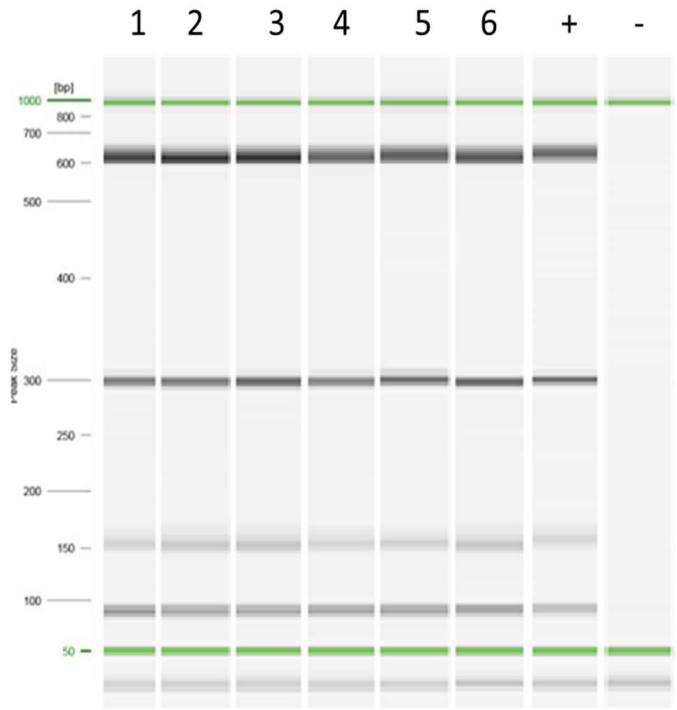

Figure 4 Digital Analysis of a quality control PCR.
Measured with the QIAxcel and the high-resolution cartridge, green lines = upper and lower alignment marker (50bp and 1000bp), left scale = size marker to determine the peak size [bp], 1 – 6 = PCR result of single cell 1 to 6, + = positive control (pool of peripheral blood mononuclear cells (PBMCs)), - = negative control

2.15 Agarose gel electrophoresis

Agarose gel electrophoresis is a widely used technique in molecular biology for the separation and analysis of nucleic acids. A 2 % agarose gel solution was prepared using Tris-Borate-EDTA 1x buffer (ThermoScientific) and Agarose powder LE (Anprotec) in a glass flask with a wide opening (e.g., 5 g Agarose powder, 250 mL

buffer). After heating in the microwave, the solution is mixed carefully, cooled down (approx. 2, ~60 °C) min and Ethidium bromide (EtBr, 0,5 µg/mL) is added. A prepared gel slide including a comb for the appropriate sample number is filled with the liquid gel. Once the gel is hardened the slide is inserted in the gel chamber system and filled with TBE buffer until the gel is covered. The PCR samples (2 µL plus 3 µL loading dye, BioRad) are pipetted in the wells and for defining the size of the DNA fragments a DNA ladder (1kb plus DNA ladder, NEB) was added. To verify the method a positive (pool of PBMCs) and negative control (water) was included. By applying low voltage (100 V) the negative loaded DNA follows the way to the anode and the positive loaded EtBr the other way around. Depending on size and charge the fragments are migrating in a different velocity. After 45 minutes the DNA can be visualized by imaging under the UV lamp (e.g., **Figure 17** in Part 3, Results).

2.16 cfDNA isolation and amplification method*

* Based on information from Dr. G. Feliciello – Biotechnological scientist and developer of this method

The frozen CSF supernatants (-80 °C) were thawn slowly on ice. Independent of the volume the cfDNA was isolated by using the QIAamp® circulating nucleic acid kit (QIAGEN) and following the steps of the user manual. For a better yield an in-house ligation and amplification step was included after the isolation. Therefore 1 - 3 ng of CSF-cfDNA were diluted in 10 mM Tris-HCl (pH 8.5) to total volume of 50 µL into a 0.2 mL tube. Seven µL of KAPA End Repair & A-Tailing Buffer and 3 µL of KAPA End Repair & A-Tailing Enzyme Mix (KAPA Biosystems) were added. The reaction was incubated in a thermocycler using the following program with heated lid (105 °C).

Table 14 Cycler program of the End Repair and A-Tailing reaction

Cycler program	Temperature	Time
Step 1	20 °C	30 min
Step 2	65 °C	30 min
Step 3	4 °C	forever

After this step, the adapter ligation was performed by adding 5 µL of pre-annealed cf-Lib1 adapter (16.6 µM), 5 µL of PCR-grade water, 30 µL of KAPA Ligation Buffer and 10 µL of KAPA DNA Ligase (KAPA Biosystems) to each sample containing 60 µL of End Repair and A-Tailing mix/DNA. The ligation mix was incubated for 3 h (or over-night to increase the amount of ligated product) at 15 °C. To each ligation product 132 µL (1.2x) of SPRIselect beads (Beckman Coulter) were added following the instruction of the manufacturer up to the last washing step with 80 % ethanol. Within this the CSF-cfDNA was not eluted from the beads enabling a “with bead” library preparation. The PCR master mix, 1x conc. Expand Long Template Buffer 1, 1 µM of the Lib1 primer, 1.75 µL dNTPs (10 mM), 1.25 µL BSA (Roche Diagnostic), 5 U of Expand-Long-Template DNA Polymerase (Roche Diagnostic) in 50 µl of water solution was added to the beads. The fill-up of the primer binding site program was performed in a thermal cycler:

Table 15 Cycler program of the circulating tumor DNA amplification step

Cycler program	Temperature	Time	Cycles
Step 1	68 °C	5 min	
Step 2	95 °C	45 sec	
Step 3	95 °C	15 sec	17 x
	60 °C	30 sec	
	68 °C	30 sec	
Step 4	68 °C	3 min	
Step 5	4 °C	forever	

After the PCR, 125 µL of PEG-NaCl have been added to the reaction and incubated for 5 min at room temperature. The beads-DNA reaction was placed on the magnetic rack and allowed to separate for 5 min at room temperature. The supernatant was removed, and the bead pellet was washed two times with 200 µL of 80 % ethanol for 30 sec at room temperature. The complete ethanol was removed, and beads were allowed to dry about 1 min at room temperature. The final amplified CSF-cfDNA was eluted in 20 µL of Tris-HCl, pH 8.5. DNA concentration was quantified with the

Invitrogen™ Qubit dsDNA High sensitivity assay (see 2.17) and fragment size distribution was analyzed with the Bioanalyzer High Sensitivity Assay from Agilent (see 2.19). Libraries for LowPass sequencing were prepared with Ampli1™ LowPass kit for Illumina® platforms (MSB) (see 0).

2.17 Fluorometric DNA Quantification by Qubit 2.0 Measurement

The Qubit assay is a fluorometric assay used for the quantification of double stranded nucleic acids using a fluorochrome dye that specifically bind to nucleic acids. When these dyes bind to the target nucleic acids, they emit fluorescence that is proportional to the concentration of the nucleic acid in the sample. The measurement of the samples was performed with the Qubit ds DNA High sensitivity assay (range 0.2 – 100 ng; 10 pg/µL – 100 ng/µL) and the Qubit 2.0 system mixing 2 µL of sample together with 198 µL of working solution included in the kit. After a short incubation time (2 min) in the dark the samples were measured in the system after reading the two standards (10 µL plus 190 µL working solution). The amounts were used for calculating the sufficient input of DNA for further molecular methods.

2.18 Quantitative Polymerase Chain Reaction Analysis

For optimal utilization of the sequencing capacity of the next generation sequencing (NGS) Illumina® platform a precise quantification of the DNA library is necessary. This ensures that comparable amounts of raw sequencing data are generated from each sample included in the library pool and excessive DNA as well as insufficient DNA concentrations are avoided. The KAPA Library Quantification Kit Illumina (Roche) includes six DNA Standards (80 µL each), a Primer Mix (1 mL) and the KAPA SYBR® FAST qPCR Master Mix (5 mL). A reaction mix is prepared for the number of samples analyzed (Table 16, left) and dispensed in the wells of a 96 well plate. Each library sample is measured in two different dilutions 1:10 000 and 10:20 000, pipetted in triplets and a negative control (blank water) and the standard curve (1-6) are included, for calculating the absolute DNA amount within the primer defined regions.

The amplification program (Table 16, right) was used as suggested from manufacturer within the incorporation of the SYBR fluorescent dye and is measured continuously as an indicator of PCR product amplification in the LightCycler®480 detection system. By implementing the mean concentration values (Cp) of the samples in a predefined excel sheet (delivered by manufacturer) the output is an average DNA concentration [nM] which can be used for calculating the optimal DNA amount for an efficient NGS run.

Table 16 Mastermix pipetting scheme for qPCR reaction
with the KAPA Library Quantification Kit Illumina® (Roche, left) and LightCycler®480 (Roche) program for quantification reaction (right)

For ABI Prism™, Bio-Rad iCycler™, LightCycler 480 or ROX Low qPCR Master Mix	
KAPA SYBR FAST qPCR Master Mix (2X) + Primer Premix (10X)	12.0 µL
PCR-grade water	4.0 µL
Total volume:	16.0 µL

Step	Temp.	Duration	Cycles
Initial denaturation	95°C	5 min	1
Denaturation	95°C	30 sec	35
Annealing/Extension/ Data acquisition	60°C	45 sec	
Melt curve analysis	65 – 95°C		

2.19 Fragment size distribution with the Bioanalyzer

Before determining the fragment size with the Bioanalyzer (Agilent) High Sensitivity Kit the WGA samples had to undergo a double strand synthesis. To 10 µL of WGA product 2 µL of the reaction mix (Table 17) were added and incubated at 68 °C for 2 hours followed by an inactivation step at 12 °C forever. The DNA amount after the synthesis was quantified with the Qubit assay (see 2.17) and the samples were diluted to a final concentration of 1.5 – 2 ng/µL prior to loading the Bioanalyzer chip. The chip preparation is obligatory before 1 µL of each sample can be loaded.

Table 17 Pipetting scheme for double strand synthesis
reaction per 10 µl of WGA sample prior to fragment size determination with the Bioanalyzer.

Reagents	Volumes
Expand Buffer 2	0.2 µl
dNTPs (10 mM)	0.2 µl
Lib1 (100 µM)	0.2 µl
PolMix	0.1 µl
PCR H2O	1.3 µl
Total Volume	2 µl

Therefore, the gel dye was prepared following the user manual and 9 µL of the dye was pipetted in the appropriate well and incubated for 1 min at the chip priming station. The residual gel dye (3 x 9 µL), 5 µL of the High Sensitivity DNA marker and 1 µL of the High Sensitivity Ladder were pipetted in the dedicated wells. In each sample well (n = 11) 1 µL of double stranded DNA product were loaded and the chip, after vortexing (2400 rpm, 1 min, on chip adapter) inserted in the machine. The program dsDNA-high sensitivity DNA was started, and the results were evaluated by the instrument internal software.

DCCs (whole genome amplified) show typically a single broad peak at around 700bp (e.g., **Figure 5** A,B) within the two markers, low at 35 and high at 10380bp (x-Axis) and the measured tension in fluorescent units (FU, y-Axis) which represent the concentration of the fragments (the higher the peak the higher the concentration). Also peaks at lower or higher fragmentation size can be detected (~500 – 800bp) and are correlated to the amplification quality, the higher the better.

Cell-Free DNA refers to free-circulating DNA fragments outside the cell and typically consists of shorter fragments, including DNA wrapped around nucleosomes and DNA of differing lengths linking nucleosomes. Thus, electrophoretic separations of cfDNA often display three types of fragments: mononucleosome (~165bp), dinucleosome (~350bp), and trinucleosome (~565bp) (https://www.agilent.com/en/product/automated-electrophoresis/cfdna-analysis). For assessment of the CSF sample integrity a heterogenous combination of two peaks (~200bp and 400bp (e.g., see Figure 5 C)) are expected. Also, more peaks or less defined ones (see Figure 5 D) can be detected but reveal that this sample contains a lot of fragments with different sizes and might make the analysis even more challenging.

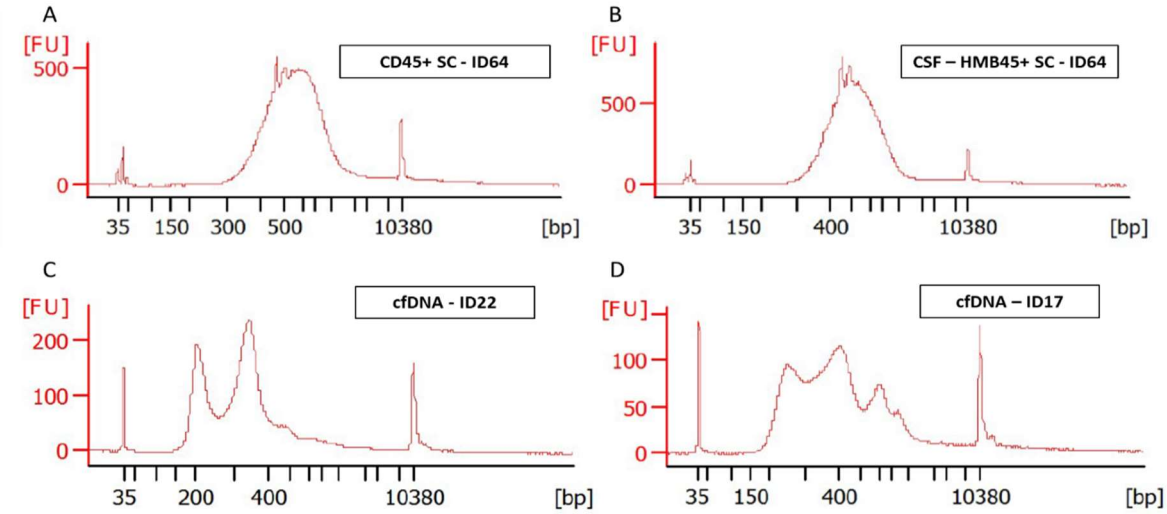

Figure 5 Fragmentation profiles of amplified DNA from cerebrospinal fluid (CSF).
Amplified DNA samples from single cells (A,B) and cell-free DNA (C,D) analyzed with the Bioanalyzer High Sensitivity kit (Agilent). X-Axis: fragment length in base pairs (bp) defined by a low marker (35bp) and a high marker (10380bp). Y-Axis: tension measured in fluorescent units (FU). A,B: Fragment distribution of amplified DNA derived from a CSF melanoma single CD45 positive (A) and HMB45 positive (B) cell from patient ID65. Both show one main peak (500 - 700bp) typically for WGA amplified DNA of single cells with high quality. C: fragment distribution of the CSF-cfDNA sample from breast cancer patient ID22 which shows a main peak at 200bp and a second slightly higher peak at 400bp and represents a typically expected profile. D: fragment distribution of the CSF-cfDNA sample from breast cancer patient ID17 which shows a broad range of different fragment sizes contained in this sample.

2.20 Ampli1 LowPass library for sequencing on the Illumina® platform

Low pass whole genome sequencing is proportionally a cost-efficient DNA sequencing method, which allows to discover genetic variation (gains and losses) within the whole genome by low depth of coverage in a high throughput assay. In this thesis selected DNA samples were processed with the Ampli1™ LowPass Kit for Illumina (MSB, Table 18 (62)) and sequenced on the Illumina® MiSeq (Figure 6).

Five µL of high-quality WGA product were purified before by using magnetic SPRIselect beads (Beckmann Coulter). 8 µL of the first barcoding reaction mix was added per sample and incubated in the thermocycler. The ligated samples were washed using the SPRIselect beads and eluted afterwards, by adding the second

barcoding mix. After the incubation in the thermocycler the double labelled samples were purified using the magnetic beads, eluted in the amplification reaction mix and processed in the intended thermocycler program.

Table 18 Components of the Ampli1 LowPass Kit.

Box 1 contains *Ampli*1 LowPass kit reagents	
This Hand Book	HB
Reagent Name	**Content**
*Ampli*1 PCR Reaction Buffer	1 x 1100 µl
*Ampli*1 PCR Taq Polymerase	1 x 20 µl
*Ampli*1 PCR Water	2 x 1100 µl
*Ampli*1 PCR dNTPs	1 x 200 µl
*Ampli*1 PCR BSA	1 x 250 µl
*Ampli*1 D7xx *	6 x 30 µl
*Ampli*1 D5xx *	8 x 24 µl
*Ampli*1 P5 primer	1 x 60 µl
*Ampli*1 P7 primer	1 x 60 µl
*Ampli*1 SEQ primer [60 µM]	1 x 30 µl

* *Ampli*1 LowPass Kit **Set A** provides 48 unique dual-index combinations from D701 to D706 and *Ampli*1 index from D501 to D508.
* *Ampli*1 LowPass Kit **Set B** provides 48 unique dual-index combinations from D707 to D712 and *Ampli*1 index from D501 to D508.

Box 2 contains PEG NaCl solution:	
Reagent Name	**Content**
PEG NaCl solution	1 x 5000 µl

The amplified samples (15 µL) had to be cleaned up in a last washing step and the DNA amount was quantified using the Bioanalyzer (2.19) technology or the Qubit assay (see 2.17). In case samples were used directly a final library pool (up to 32 samples, each labelled with a unique barcode for correlating in later statistical evaluation) was created with a final concentration of 4 nM (calculation 1 ng/µL = 2 nM) and pipetted to the sequencing cartridge following the instruction of the user manual. In case samples were used not directly after amplification, they were stored at -20 °C.

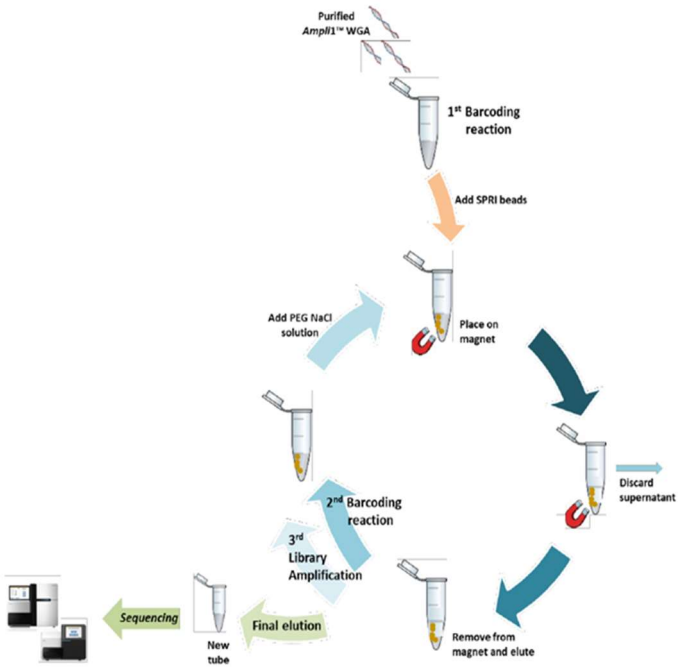

Figure 6 Schematic overview about the working steps of the Ampli1 LowPass method. Including a first and a second barcoding and an amplification step prior to sequencing. www.siliconbiosystems.com

2.21 Statistical Analyses for LowPass sequencing data*

* Based on information from Dr. J. Warfsmann – Bioinformatic specialist at ITEM Regensburg

LowPass is a sequencing approach targeting the whole genome with low coverage of approximately 1 %. The bioinformatics CNV-profile analysis started, after demultiplexing, with raw FASTQ files, which were submitted to an in-house single cell lowpass analysis pipeline. The raw sequences were trimmed with BBDuk 38.84 (63), removing adapter sequences and poor-quality bases at the end of each read.

Non-human reads originating from microbial and/or fungal fresh water and or reagents contaminations might interfere with downstream analysis, therefore, read decontamination was performed using BioBloom Tools 2.0.13 (64) with filters for the genomes of *Homo sapiens* (hg38), *Mus musculus* (mm38), *Escherichia coli* (BL21), *Mycoplasma pneumonia* (M129), *Sphingobium sp.* (SYK-6), *Bradyrhizobium japonicum* (USDA 110), *Pichia pastoris* (GS115), *Malassezia globosa* (CBS 7966), *Aspergillus fumigatus* (AF293), and a set of viral genomes (RefSeq, 5k+ genomes).

All reads that did not map exclusively to hg19 were defined as likely contamination and discarded from downstream processing. Sequence quality per sample was evaluated before as well as after trimming and decontamination using FastQC 0.11.9 (65) and, in addition, all samples were analyzed as a collective with MultiQC 1.9 (66).

Next, the cleaned sample reads were aligned to the reference genome hg19 with bwa mem 0.7.17 (67) and duplicates removed using picard 2.21.8 (68). Samples having an alignment with less than 100 000 unique reads were rejected from the CNV-analysis. For the following LowPass CNV-profile analysis the human genome was divided into non-overlapping bins, each with a size of 500 kbp. Mapped reads of the remaining samples were counted per bin, corrected, filtered, normalized and segmented with the bioconductor package QDNAseq 1.26.0 (69). The same package was used to create the $log_2(ratio)$ CNV-profiles.

The bioconductor packages ACE 1.8.0 (70) and standard rounding is used to convert $log_2(ratio)$ into integer copy numbers.

Further quality characteristics were assessed with QualiMap 2.2.2d (71) and circos plots were made by an in-house software using circos 0.69.810 (72) as back-end.

2.22 How to interpret a copy number variation profile?

The processing of raw data, generated in the sequencing run, by using the bioinformatic pipeline resulted in copy number variation (CNV) profiles, expected to be aberrant (**Figure 7**) for cancer cells and balanced (**Figure 8**) for peripheral blood lymphocytes. The profile shows different information which can be interpreted the following:

A: The bins (4k x 500 kbp) typically refer to individual genomic regions that are defined for the purpose of analyzing and quantifying read depth across the genome. The genome is divided into non-overlapping segments and assessed by the number of sequencing reads that align to each bin (á 500 kbp). The bin size is chosen empirically and a critical parameter responsible for a successful analysis and resolution.

B: The segments are fragmented parts of the chromosomes which are analyzed. They generally refer to coherent genomic regions with similar or consistent copy number alterations.

C: The expected deviation value “Eσ” is context-dependent and generated by considering different values including the coefficient of variation, signal-to-noise ratio, and the ability to detect known copy number variations. It is an important measurement for assessing the quality of sequencing data.

D: $\hat{\sigma}_{\Delta}$ describes the spread of individual data points from central tendency and associated the variability in the dataset. Empirically it is best lower than 0.1, good between 0.1 and 0.2 and worse higher than 0.2.

E: The log2 ratio provides a linear scale for representing fold changes in copy number. A log2 ratio of 0 indicates no change (**Figure 8**), positive values represent gains (F, **Figure 7**), and negative values represent losses (G, Figure 7).

F: The red dot areas represent copy number gains and a log value of 0.63 means a gain of one copy.

G: The blue dot areas represent a copy number loss and a log value of – 1 means a loss of one copy, a value of – 2 a loss of two copies.

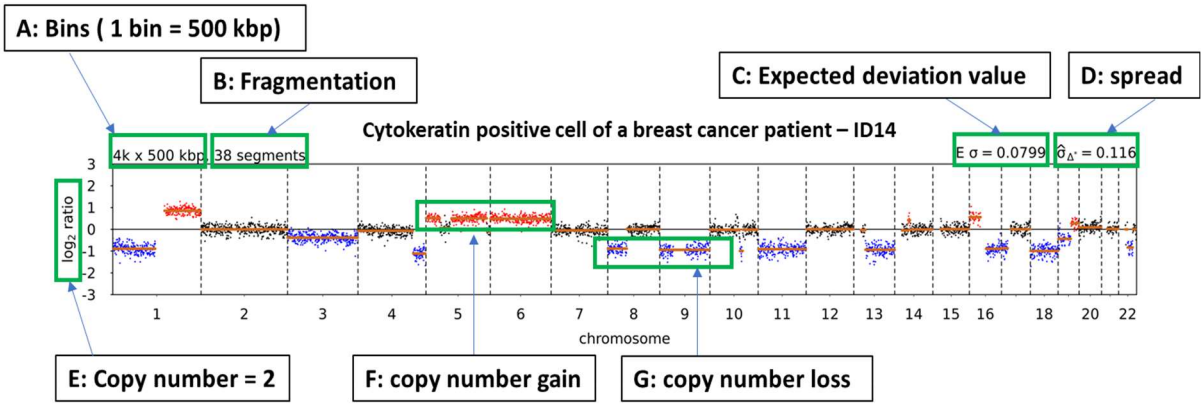

Figure 7 Aberrant CNV profile of a CSF isolated disseminated cancer cell.
This aberrant copy number variation (CNV) profile is derived from breast cancer patient ID14 including explanation fields more detailed written in the text (2.22).

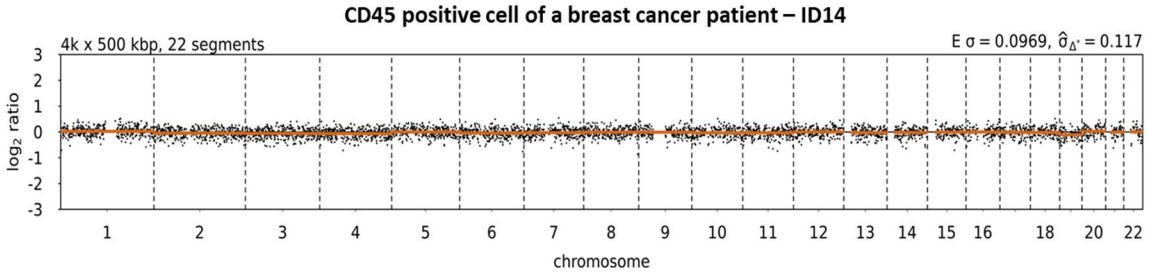

Figure 8 Balanced CNV profile of a CSF isolated CD45 positive cell.
This balanced copy number variation (CNV) profile is derived from breast cancer patient ID14 showing the Chromosomes 1 to 22 and a log2 ratio of 0 which means that no losses or gains were detected in this sample.

2.23 3D cultivation of CSF derived cells for generating organoid models

In a proof-of-concept trial the cell part of CSF was divided prior to enrichment with the CellSearch® or the manual approach for generating organoid models and further molecular downstream possibilities, supported by the cell cultivating specialists in our group. The cell pellet was cultivated in DMEM medium (added growth factors, HEPES 5mM, penicillin/streptavidin 0,5 x) in a CO2 incubator and cells were controlled in regular intervals and rendered after achievement of appropriate cell clusters. They were isolated under the microscope manually from suspension (2.6), amplified (2.12, 0) and CNV analysis (0) was performed.

2.24 Slide preparation of cerebrospinal fluid for cytohistological examination*

* Based on information from Dr. Saida Zoubaa – Chair of Neuropathology Uni Regensburg

This method was not performed by myself within this thesis but processed in parallel to my analysis by Dr. Saida Zoubaa, at the chair of Neuropathology of the University hospital Regensburg, Prof. Dr. M.J. Riemenschneider. Nevertheless, the comparison between the results generated with the methods used in this project and the results of their method, which is up to now the gold standard for CSF analysis of patients with suspected leptomeningeal metastases, was one of the main tasks in this thesis why the method they used is described here:

For cell stabilization, 22 % albumin was added to liquor samples. Samples were centrifuged for 5 min at 125 g. The cell-free supernatant was removed except for a small remainder. The cell pellet was re-suspended, and the liquid distributed to the number of slides required for diagnosis. 100 – 200 µL were applied to each funnel chamber. The cytospin inserts were assembled with a filter card. The cytospin chambers were instantly centrifuged for 10 min at 275 g, during which cells sediment onto the slides. Slides were drained for 5 – 10 min and then stained with May-Grünwald's and Giemsa's solutions (Pappenheim´s stain). In addition, Immunocytochemistry was performed (Table 19). The standardized protocol included epitope retrieval for 24 – 48 min at 110 °C in citrate pH 6.0. Endogen peroxidase activity was blocked by 1X Dako Peroxidase-Blocking Solution® (S2023; Dako GmbH, Jena, Germany) for 10 min. The sections were then incubated with the primary antibody (Table 19). The antigen–antibody complex was detected with 3,3'-Diaminobenzidin-Tetrahydrochlorid (DAB). Slides were counterstained with Hematoxylin and Bluing reagent.

Table 19 Marker used for the Cytospin Analysis of CSF
from patients with suspected leptomeningeal metastases in the Institute of Neuropathology of the University hospital of Regensburg, Prof. Dr. MJ Riemenschneider

Marker	Clone	Order Number	Company
CK5/6	clone D5/16 B4	M 7237	Dako
CK7	clone OV-TL 12/30	M 7018	Dako
CKpan	clone AE1/AE3	M 3515	Dako
Gata3	L50-823	CM 405 A, C	Biocare Medical
gp100/Pmel17	clone HMB45	M 0634	Dako
Her2 (c-erbB2)	polyclonal	A0485	Dako
Melan A	A103	NCL-L-MelanA	Leica

2.25 MRI

The MRI data of the brain (e.g. Figure 9 (73)) were performed at the Bezirksklinikum at Regensburg, Prof. Dr. C. Wendl and results were delivered as “leptomeningeal seed detected/not detected” via imaging at the timepoint of CSF withdrawal.

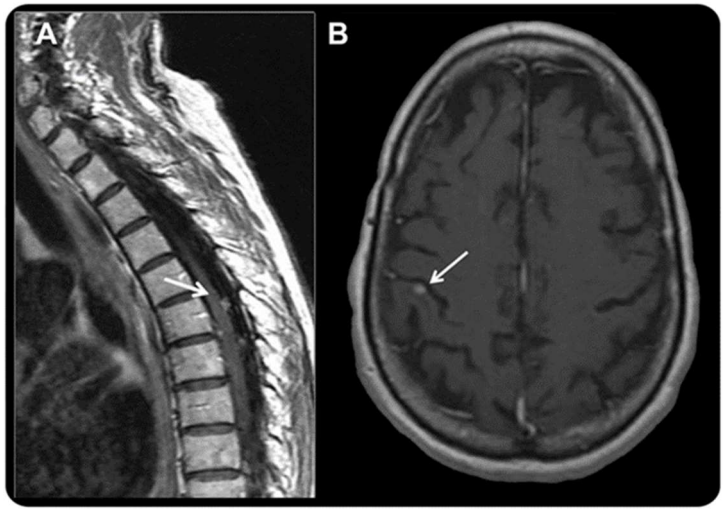

Figure 9 Imaging of a diagnosed leptomeningeal metastases.
A: Arrow shows a leptomeningeal metastasis in the spinal cord, (B) a leptomeningeal metastasis in the brain of a patient with a solid tumor.
https://www.neurology.org/doi/10.1212/WNL.0b013e31828f183f

3. Results

3.1 Structure of the work

This thesis explores the applicability and reliability of a workflow for molecular analysis of DNA derived from cerebrospinal fluid samples withdrawn from patients with different primary tumors but suspected leptomeningeal metastases (Figure 10). The so called "molecular CSF Liquid Biopsy" approach includes the enrichment of disseminated cancer cells (DCCs) with the automated ferromagnetic based CellSearch® technology in carcinoma patients or a manual workflow for melanoma patients.

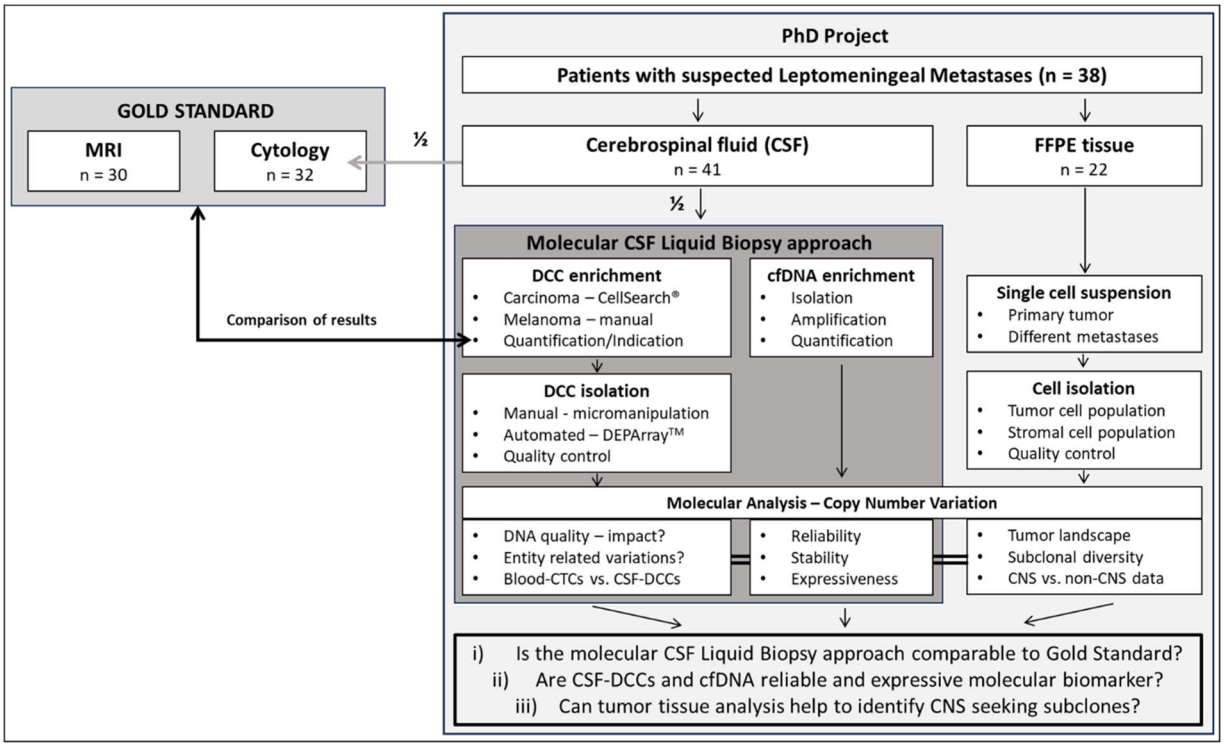

Figure 10 PhD project design.
Cerebrospinal fluid (CSF) of patients with suspicion of leptomeningeal metastases (LM) were analyzed within the molecular CSF liquid biopsy approach. This consists of a disseminated cancer cell (DCC) and a cell free DNA (cfDNA) enrichment, isolation, and subsequent molecular downstream analysis. In parallel data from CSF cytology and magnetic resonance imaging (MRI), both the actual gold standard methods for LM examination, were collected and compared to results derived from the liquid biopsy approach. Formalin fixed paraffin embedded (FFPE) tissue of dedicated patients was dissociated and pure cell populations were isolated and characterized molecularly. With this the three pressing questions i) Delivers the molecular CSF liquid biopsy approach comparable results to the Gold Standard methods – cytology and MRI? II) Are CSF-DCCs and cfDNA reliable and expressive biomarker for valuable molecular data? Iii) Can tumor tissue analysis help to identify CNS seeking subclones?

Cytological data derived from the same sample and dedicated MRI data enabled us to assess the CellSearch® method in terms of technology, reliability, sensitivity, and applicability.

The additional isolation of circulating cell free tumor DNA (ctDNA) opened the possibility to evaluate different CSF biomarker on a molecular level from the same sample with low volume. Furthermore, data from patient related formalin fixed paraffin embedded (FFPE) tissue offered the chance to detect specific central nervous system (CNS) seeking subclones by copy number variation analysis and thereby allowed us to build a more complete picture about the tumor landscape in selected patients.

Native CSF was withdrawn and for reliability tests split for parallel cytological (neuropathology) and immunohistochemical (CellSearch®) analysis. The DCCs enriched from the cellular part of the CSF, either automatically or manually, were quantified and subsequently isolated with different methods (manual or DEPArray™ technology). The quality of the DNA was determined prior to molecular downstream analysis. The cell-free compartment of the CSF was used for isolating circulating tumor DNA (ctDNA). After an adapted amplification protocol, the copy number variation analysis was performed and compared to variation profiles of CSF derived DCCs. Both CSF biomarkers were evaluated in terms of their utility, quality, reliability, expressiveness, and applicability. Tumor tissue from different sites, primary, non-CNS and brain metastases were selected and the single cell suspension was used for isolating pure cell populations with the DEPArray™ system. The results of the subsequent molecular analysis were compared to data derived from CSF or blood DCCs and CSF-cfDNA.

3.2 Patients – samples and characteristics

Patients with suspected leptomeningeal metastases (LM) from the University Clinic of Regensburg and the Bezirksklinikum of Regensburg build the collective analyzed in this thesis. Written informed consent for tumor DNA isolation, characterization and comparative molecular analyses was obtained for all patients included and the requirements of the DSGVO were complied. All experiments conformed to the

principles set out in the WMA Declaration of Helsinki and were approved by the ethical committees responsible for the corresponding partner (vote numbers 18-948-101, 17-672-101).

Fourty-one CSF samples (Figure 11) from 38 adult patients (28 females, 10 males; median age 65 years – range 21-81 years) from the University Clinic of Regensburg and the Bezirksklinikum of Regensburg with clinical and/or radiological suspicion (MRI performed for n = 30) of LM were included in this analysis. The patients have been diagnosed with breast cancer (n = 17), melanoma (n = 8), lung cancer (n = 8), cancer of unknown primary (CUP, n = 4, at the time point of lumbar puncture), larynx (n = 2), gastric and colon cancer (each n = 1). CSF was collected for all patients at the first lumbar punction but could be collected over a period of six months for one breast cancer patient at three different time points (ID 14, 16, 18). The two samples derived from the same larynx cancer patient (ID44, 45; more details on sampling in Table 1A, Appendix) were collected within one week and not counted as two different timepoints from the perspective of therapy or progress. Out of this collective 32 CSF samples of carcinoma patients could be analyzed in parallel to the cytological analysis from the institute of pathology (Prof. Dr. MJ Riemenschneider, Dr. Saida Zoubaa, University

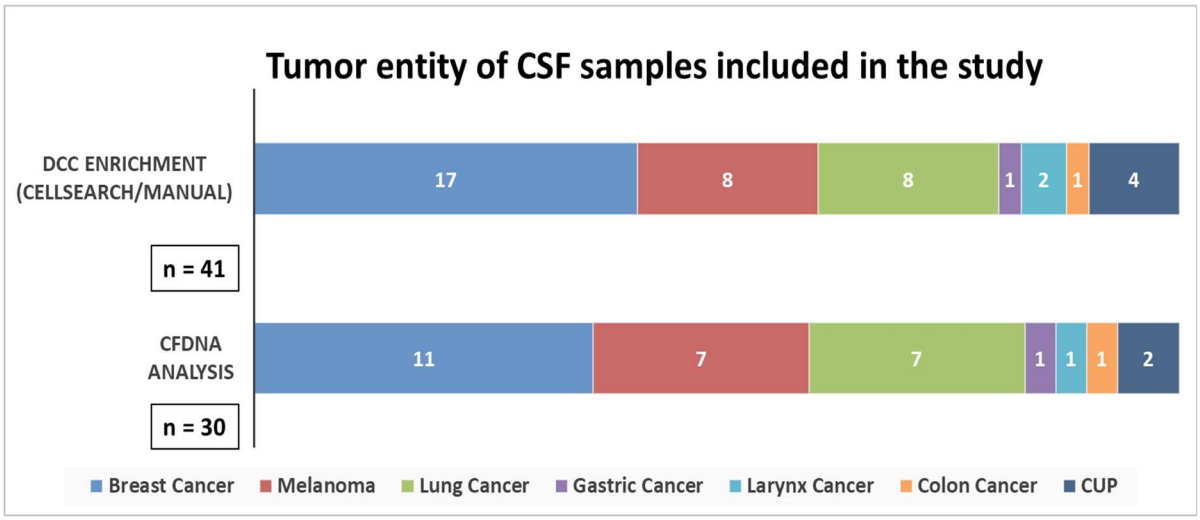

Figure 11 Tumor entity of study included Cerebrospinal Fluid (CSF) samples.
In total the cell-compartments of 41 CSF samples of patients with leptomeningeal metastases were enriched either by the automated CellSearch® system (carcinomas: breast = 17, lung = 8, Cancer of unknown primary (CUP) = 4, larynx = 2, gastric/colon = 1 each) or a manual procedure (melanoma = 8). The cell-free compartment of 30 CSF samples was analyzed in parallel as the supernatant of the cell compartment after centrifugation (breast = 11, melanoma = 7, lung = 7, Cancer of unknown primary (CUP) = 2, larynx/gastric/colon = 1 each).

Hospital Regensburg) and entered a proof-of-concept study described more in detail in 0. Within this the automated cell enrichment CellSearch® technology and the cytological approach were compared and evaluated regarding specificity, sensitivity, subsequent molecular downstream analysis, and implementation possibilities in the daily clinical routine. Parts of these data are included in the publication "*Molecular analysis of single tumor cells from cerebrospinal fluid as a diagnostic tool for patients with leptomeningeal metastasis*" (Koestler et al., unpublished) which will be submitted in the Journal *Clinical Chemistry*.

From twelve patients (breast n = 7, melanoma/lung n = 2 each, gastric cancer n = 1) 22 FFPE tissue samples were available for analysis (Figure 12). The samples were selected due to availability but also preferably analyzed if a CSF analysis of this patient could be performed successfully. Considering the frequency of entities, it is not surprising, that most FFPE sample variability (n = 13) exists for breast cancer patients. In total, six primary tumors and four brain metastases but also variant distant metastases from lymph Node (n = 5), bone (n = 2), pleura (n = 2), peritoneum, bladder, and liver (n = 1, each) were analyzed.

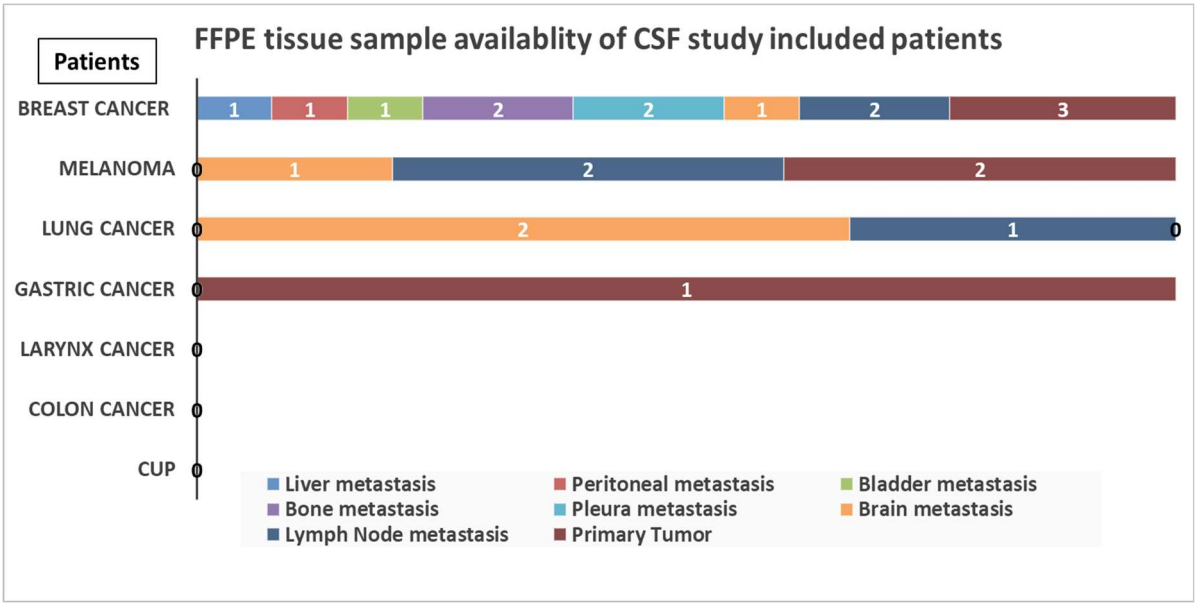

Figure 12 Available Formalin fixed Paraffin Embedded (FFPE) tissue samples.
In total 22 FFPE tissue samples were available in the collective of patients with different primary tumor entities (left) but suspected leptomeningeal metastases (LM). Greatest sample variability exists for breast cancer (n = 13), melanoma (n = 5) and lung cancer (n = 3) patients including different metastatic sites but also primary tumor tissue. For four cancer types (gastric, larynx, colon, unknown primary-CUP) no samples could be analyzed.

3.3 Cell enrichment of CSF samples

In total, 41 CSF samples were analyzed, 33 samples from patients diagnosed with carcinoma and eight with melanoma. 31 of the 33 carcinoma samples (94 %) were enriched with the automated CellSearch® Circulating Tumor Cell (CTC) Kit via an EpCAM ferrofluid capturing and stained with fluorescent markers for DAPI, Cytokeratin (CK) and CD45. Two carcinoma samples had to be enriched and stained (A45 antibody) manually due to technical issues. The eight melanoma samples were enriched manually a priori and underwent an immunocytological staining against the gp100 antigen. In total, 15 of 41 (37 %) samples were evaluated positive for putative tumor cells via a fluorescence or immunocytological staining.

3.3.1 Carcinoma samples successfully enriched by the CellSearch® technology

Native CSF volumes between 0.4 and 7 mL (median 2.5 mL) from 33 carcinoma patients (26 female, 7 male) arrived at the lab for processing. All CellSearch® analyzed samples were filled up to 7 mL with sample buffer and incubated for two hours in the CellSave fixation tube prior to the enrichment, which was performed on the same day. The two lung carcinoma samples (ID3, ID57) not enriched with the CellSearch® system (median 4.5 mL) were processed and stained directly using a non-automated workflow (see 522.24) directly after arrival.

For defining the tumor cell number, the automated scan with the CellTracks Analyzer II® was used for all enriched cartridges but was only successful in half of the samples (20/41, 49 %). Nine of those samples (breast = 6, CUP = 2, Lung = 1) resulted in a Cytokeratin positive CellSearch® gallery report (e.g., **Figure 13**) and eleven samples were defined negative for DCCs (all available reports/galleries in Appendix).

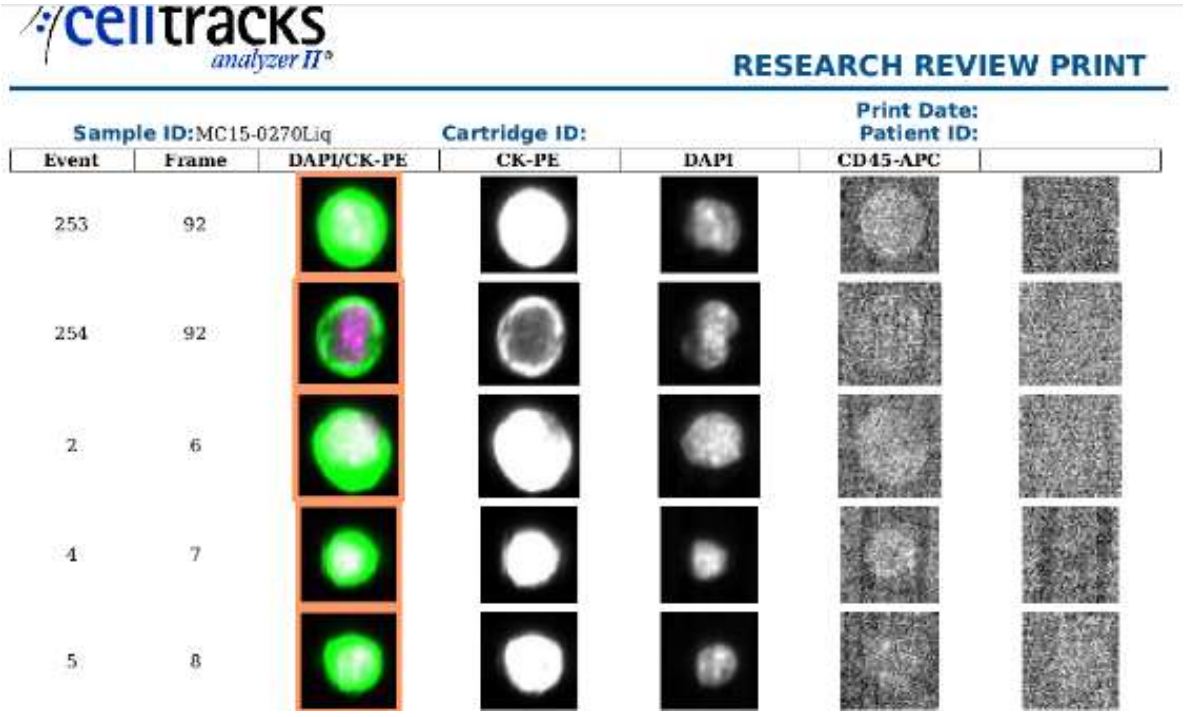

Figure 13 Excerpt of a CellSearch Gallery.
DAPI/Cytokeratin positive disseminated cancer cells (DCC) enriched from cerebrospinal fluid (CSF) of breast cancer patient ID5. Corresponding to a frame number each cell/event is shown per row and can be assigned by three fluorescent channels Phycoerythrin (PE, conjugated to Cytokeratin - CK) DAPI signal merge which represent the putative disseminated cancer cells (DCCs) and the single channels of CK-PE, 4′,6-Diamidino-2-phenylindole (DAPI) and Allophycocyanin (APC, conjugated to Tyrosin Proteinphosphatase C - CD45) as well as an overlap. 334 DAPI/CK+ events were detected

For finding a proper level the CellTracks Analyzer II® needs to detect a signal to ensure the finding of putative tumor cells on the correct focus. In blood, the CellSearch® system originally approved for, this focus is set on the DAPI signal of CD45 positive blood cells, still available in a sufficient number after the enrichment. If the analyzed solution, in this case CSF, lacks a sufficient number of those cells, the system does not find the correct focus and is not able to scan the cartridge. For samples (n = 21) affected by those detection difficulties the automated system could be balanced by manual screening and counting at the fluorescence microscope (e.g. **Figure 14**) so that four additional carcinoma samples (breast = 2, lung = 1, gastric = 1) could be defined Cytokeratin positive, which resulted in 40 % (13/33) DCC positive carcinoma samples in total.

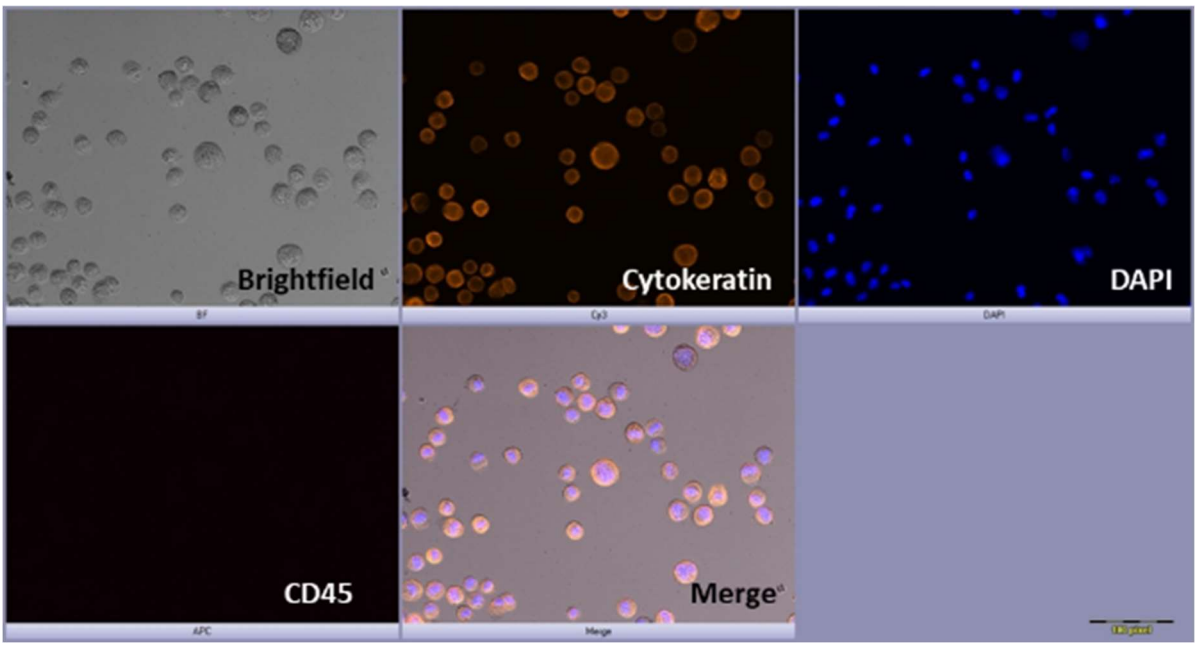

Figure 14 Fluorescent microscope pictures of disseminated cancer cells (DCCs).
DCCs derived from cerebrospinal fluid (CSF) of gastric cancer patient ID56 enriched with the CellSearch® Circulating Tumor Cell Kit. Represented are the different channels of the fluorescent microscope: Brightfield (BF; left up), Cyanine3 (Cy3) which represents the Cytokeratin positive cells (middle up), 4′,6-Diamidino-2-phenylindole (DAPI; right up), Allophycocyanin (APC) which represents the CD45+ cells (left down), a merge of all four channels (BF, Cy3, DAPI, APC; middle down) and the enlargement scale (right down). In total 100000 DAPI/CK+ events were counted in this sample.

3.3.2 Two gp100 positive CSF melanoma samples with manual workflow

The native CSF samples derived from the eight melanoma patients (5 female, 3 male) were processed directly after arrival by the manual enrichment workflow (see chapter 2.7). The median volume was 2.75 mL (range 1.3 – 6.5 mL) and up to two adhesion slides, depending on the cell number, were prepared for the staining. Via the gp100 (HMB45 antibody clone) staining, two (25 %) melanoma samples were defined positive after manual scanning at the microscope (e.g., Figure 15).

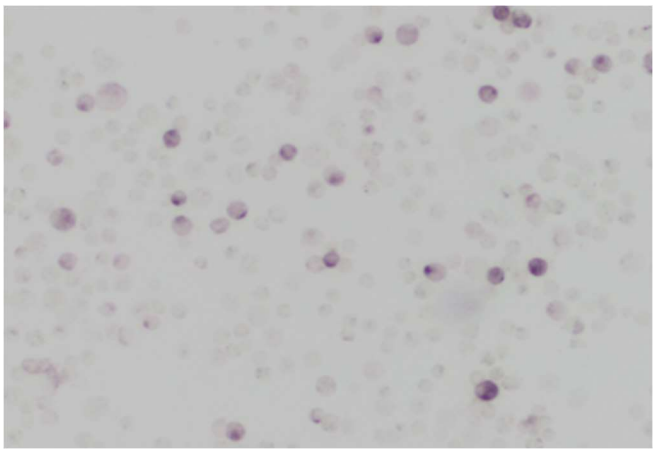

Figure 15 Brightfield picture of HMB45 stained cells.
Manually enriched cells from cerebrospinal fluid (CSF) of melanoma patient ID65 and stained with immunohistochemical antibody HMB45. Cells were settled down on a glass adhesion slide before staining and cells of interest, putative disseminated cancer cells (DCCs), are visible in dark purple. Imagination 20 x.

3.4 Selection criteria for successful downstream analysis

3.4.1 Cell quantification

Within the 15 positive CSF samples both, high and low cell numbers with a median of 70 (range 1 – 100.000, Table 1A, Appendix), were detected. Samples with a low (1 – 12) or high cell number (> 20 000) had to be quantified manually due to detection difficulties. Nevertheless, for both, the EpCAM/CK positive cell enrichment with the CellSearch® system and the manual staining followed by tumor specific immunohistochemistry and quantitative results could be achieved, independently of a high or low cell number.

3.4.2 Cell morphology

Although not systematically analyzed in this thesis, it is worth mentioning, that assessing the cell morphology might be an additional factor to predict sample quality prior to isolation and DNA amplification. Therefore, the size, the shape, and the staining quality are characteristics that demand attention during the scanning process of the sample prior to isolation under the microscope (Figure 16). We realized that even if the

staining looks intense, a more disrupted or granular appearance in brightfield could be a hint that the quality of the cell might impaired. As a result of this close attention, chances increase for selecting cells most successful in molecular downstream analysis what must be evaluated in a separate high scale approach.

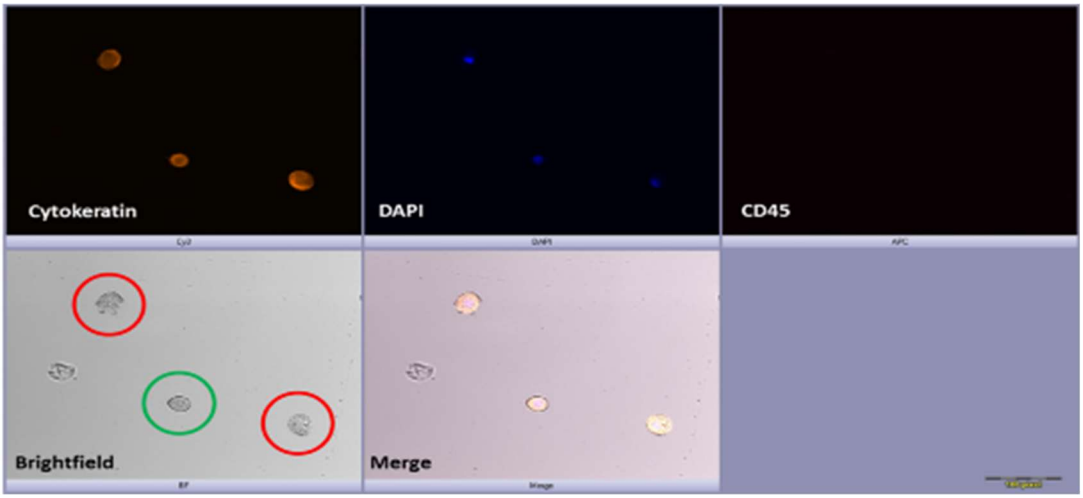

Figure 16 Fluorescence microscope picture of disseminated cancer cells (DCCs).
The cells are derived from cerebrospinal fluid (CSF) of breast cancer patient ID14 enriched with the CellSearch® Circulating Tumor Cell Kit. The green highlighted DAPI/Cytokeratin positive cell (Cell ID20) with a round, healthy shape has a Genomic Integrity Index (GII) of 4, corresponding to a high DNA quality. Aside two DAPI/Cytokeratin positive cells (red, ID21 up left, ID22 down right) with a more disrupted, granular appearance and a GII of 0, corresponding to a low DNA quality. Represented are the different channels of the fluorescent microscope: Cyanine3 (Cy3) which represents the Cytokeratin positive cells (left up); 4′,6-Diamidino-2-phenylindole (DAPI; middle up); Allophycocyanin (APC) which represents the CD45+ cells (left up)Brightfield (BF; (left down), a merge of all four channels (BF, Cy3, DAPI, APC; middle down) and the enlargement scale (right down).

3.5 High-quality single cells from enriched CSF samples

In total, 15 CSF samples were defined positive by fluorescent or immunohistochemical staining with a total putative DCC number of n = 121276 (Table 20). For further molecular downstream analysis 273 stained single cells were isolated using the micromanipulator (14 samples, Table 20) or/and the DEPArray^{TM} system (2 samples, ID 14 and 39) of 14 patient samples in total. From sample patient ID 48 (lung carcinoma) the only single cell detected by fluorescence microscopy could not be isolated due to technical issues, consequently cells from 14 cartridges (12 patients) could be amplified.

Table 20 Sample list of detected and isolated DCCs from cerebrospinal fluid (CSF) samples.

ID	Primary tumor	Sex	Age at withdrawal	Number of CK+/HMB45+ cells detected	Cells isolated	Number of CK+/HMB45+ cells isolated	Number of cells isolated GII >= 2
3	**Lung**	**f**	**65**	10	yes	10	9
4	**Breast**	f	56	9	yes	9	8
5	**Breast**	f	65	334	yes	15	14
10	**CUP**	f	44	363	yes	20	20
14	**Breast**	f	71	20000	yes	93	49
16	**Breast**	f	71	114	yes	20	19
17	**Breast**	f	81	190	yes	20	20
18	**Breast**	f	71	145	yes	20	20
21	**Breast**	f	47	5	yes	5	5
38	**Melanoma**	f	59	10	yes	10	0
39	**CUP**	m	70	70	yes	19	13
48	**Lung**	f	67	1	no	0	0
56	**Gastric**	f	62	100000	yes	12	12
64	**Breast**	f	68	5	yes	4	3
65	**Melanoma**	m	52	20	yes	16	16
Total	-	-	-	**121276**	**n = 15**	**273**	**208**

3.5.1 Isolation by micromanipulation delivers high quality single cells from CSF

Micromanipulation (Chapter 2.6) helped to isolate 181 single putative DCCs (Cytokeratin or HMB45 positivity confirmed by microscopy), 31 single CD45+ cells and 16 CD45+ pools (á 5 single cells). After the whole genome amplification (WGA, 2.12) 92 % (166/181) of DCCs were identified as high DNA quality samples on the basis of the genomic integrity index (GII >=2;(61)) via gel electrophoresis (e.g. Figure 17).

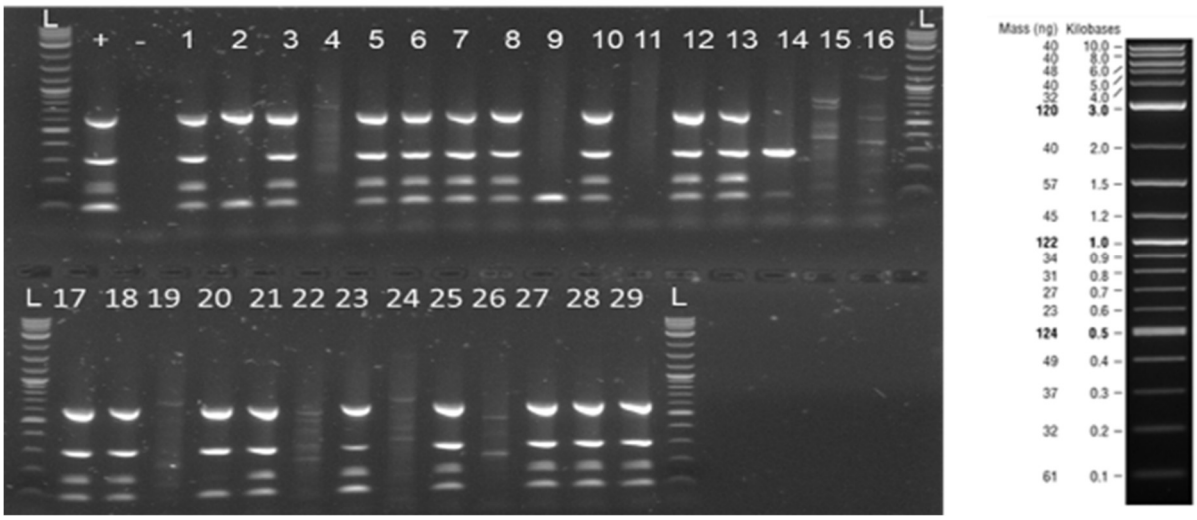

Figure 17 2 % Agarose Gel with multiplex QC PCR analysis.
Quality control assay of CSF isolated single cells from the cancer of unknown primary (CUP) patient ID 39 for defining the genomic integrity index (GII). L = DNA Ladder (1 kb plus DNA ladder, NEB; compare scale on the right side), + = positive control made from a pool of peripheral blood mononuclear cells (PBMCs), - = negative control (water), 1 – 29: Mulitplex PCR reactions of CSF isolated single cells with a different genomic integrity index (GII) as a grade of DNA quality (e.g. 4 = GII 0, 8 = GII1, 2/14 = GII2, 20 = GII3, 5 = GII4).

Considering absolute cell numbers (Table 21) the quality of cells isolated from carcinoma (cytokeratin positive) is much higher (97 %) than the quality of melanoma (HMB45 positive cells, 62 %).

Table 21 Manually isolated high- and low-quality DNA cells
isolated manually from CSF of patients with leptomeningeal metastases categorized by the genomic integrity index (GII).

Manually Isolated cells	high DNA quality (GII 4 - 2)	low DNA quality (GII 1 - 0)	total number of cells	high quality [%]
Single cells CK+	150	5	155	97
Single cells HMB45+	16	10	26	62
Single DCCs in total (CK & HMB45 pos.)	166	15	181	92
Single cells CD45+	26	5	31	84
Pools CD45+	14	2	16	88

Interestingly, the ratio for isolated high-quality CD45 positive cells (84 %) is lower than the ratio for DCCs (92 %, Table 21) isolated from CSF. Nevertheless, many cells, both DCCs and CD45 positive cells, with a promising quality for a successful downstream analysis could be isolated by the manual procedure for 12 cartridges.

3.5.2 DEPArray™ isolation procedure might harm DNA quality of single cells

For two samples the DEPArray™ system was tested as an automated single cell isolator. Samples with high cell numbers were selected (ID14, ID39), because this workflow requires a single use cartridge with a sample dead volume of 23 % and using samples with low cell numbers (experience from former projects > 25 cells) would risk losing valuable cells. 92 single Cytokeratin positive (CK+) cells, two CK+ pools, nine CD45+ single cells and four CD45+ pools were isolated automatically and amplified (see 2.12). Around half of automatic isolated single cells show a DNA quality sufficient

Table 22 Automatic isolated high- and low-quality DNA cells
with the DEPArray™ device categorized by the genomic integrity index (GII).

Automatic Isolated cells	high DNA quality (GII 4 - 2)	low DNA quality (GII 1 - 0)	total number of cells	high quality [%]
Single cells CK+	42	50	92	46
Pools CK+	2	0	2	100
Single cells CD45+	5	4	9	56
Pools CD45+	3	1	4	75

for molecular analysis, although on the lowest level (GII = 2), independently if DCCs (46 %) or CD45 positive cells (56 %) (Table 22). For the isolated cell pools the quality was much better (100 % cytokeratin positive, 75 % CD45 positive) than for the single cells, which obviously results from the higher amount of DNA (5 single cells per pool) in these samples. Nevertheless, for one additional sample (ID39) cells with high DNA quality could be isolated for further downstream analysis.

3.5.3 Direct comparison of isolation methods

Comparing the quality of the manually isolated DCCs (92 %) to cytokeratin positive cells (46 %) isolated with the automated system a large quality loss appeared. This raised up the question if the automated workflow per se might be responsible for this effect. Luckily a direct comparison between single cells isolated manually and with the automated system could be performed for the breast cancer sample ID 14. While 100 % (20/20) of the manually isolated single cells showed a high DNA quality only 40 % (29/73) of automatic isolated cells had a GII>=2 (Table 23). Even if the quality of automatic isolated single DCCs for CUP sample ID 39 was indeed higher (68 %) there is still a big quality difference to manually isolated single cells from CSF.

Table 23 Above: Quality of manually or automatically isolated single cells from CSF of breast cancer patient ID14 and cancer of unknown primary (CUP) patient ID39.

Sample ID 14	Isolated cells in total	GII 4	GII 3	GII 2	GII 1	GII 0	high quality single cells [%]
Manually isolated single DCCs	20	20	0	0	0	0	100
Automatic isolated single DCCs	73	18	1	10	18	26	40
Sample ID 39	Isolated cells in total	GII 4	GII 3	GII 2	GII 1	GII 0	high quality single cells [%]
Automatic isolated single DCCs	19	11	1	1	1	5	68

Comparing the quality of automatically isolated DCCs derived from both samples it seems that the isolation method has a great impact on the quality of the DNA because not even half of the cells (46 %) reached a quality possible or rather worth to analyze on a molecular level (Table 24).

Table 24 Quality of automatically (DEPArray™) isolated single cells from CSF combined from a breast cancer patient (ID14) and a cancer of unknown primary patient (ID39).

Combined IDs 14 & 39	Isolated cells in total	GII 4	GII 3	GII 2	GII 1	GII 0	high quality single cells [%]
Automatic isolated single DCCs	92	29	2	11	19	31	46

3.6 DNA quality dependent of isolation source – blood vs. CSF

Circulating tumor cells (CTCs) are a prognostic marker for metastatic tumor patients and can provide important molecular data about the progression of disease. Prior to this CSF project, blood samples from metastatic breast cancer patients belonging to the multicentral German DETECT study (74), enriched with the FDA-approved CellSearch® technology, were isolated and analyzed in our lab. I processed those samples in my PhD project (“Molecular and functional analysis of CTCs under therapy selection in M1 breast cancer patients”) announced in 2014 in the BIOMEDIGS Graduate School. The project paused from 2016 to 2019 and was then converted to this PhD, this is why they rank among preliminary work of the actual work.

In total, 3164 single CTCs and 923 single CD45 positive cells were isolated between 2012 and 2020 (including patients from DIII, DIV and DV) using the DEPArray™ technology. By determining the quality of DNA using the genomic integrity index (GII, Chapter 2.13), isolated tumor cells were significantly worse ($p < 0.0001$, Pearson Chi Square) than isolated CD45 positive cells (Figure 18). Only 36 % of blood tumor cells had a realistic chance to deliver successful results by further molecular downstream analysis.

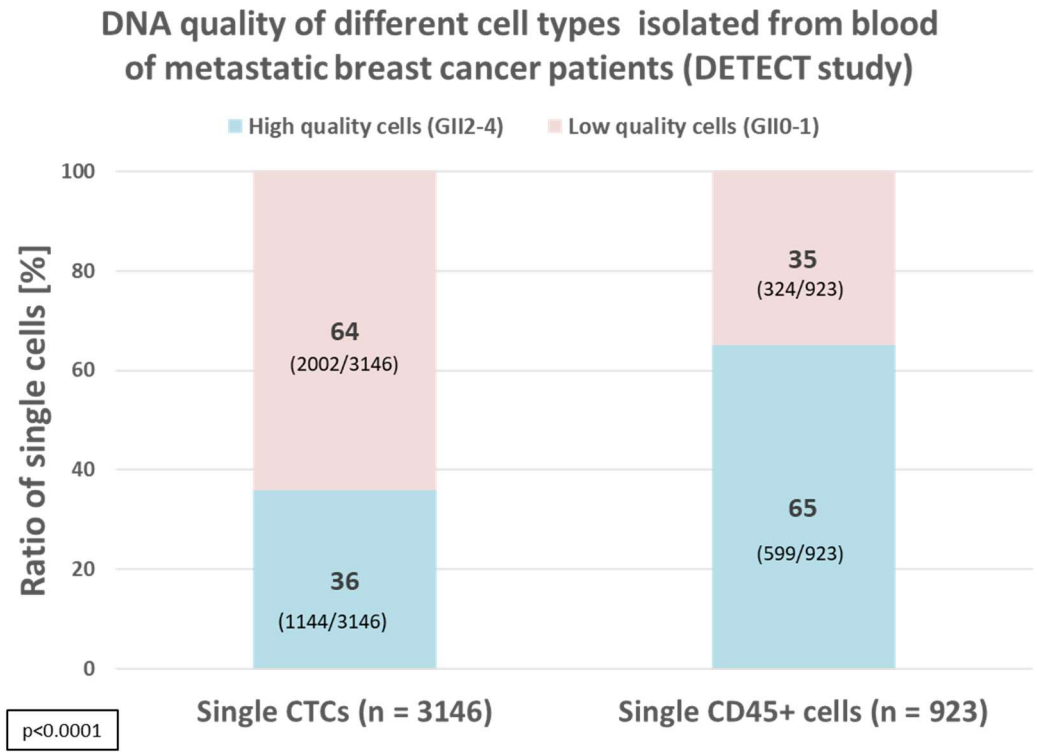

Figure 18 DNA quality of different cell types isolated from blood.
Single circulating tumor (CTCs) and CD45 positive cells, isolated from blood of breast cancer patients included in the multicentral German DETECT study. p<0.0001 (Pearson Chi Square).

Interestingly this could not be confirmed by findings in single cells isolated from CSF. These show a very high quality ~77 % independent of the cell type (Figure 19) with no significant difference (p~1, Pearson Chi Square). This could mean that the sample source, either blood or CSF, might have had an influence on the quality of the cells. The method itself detects in principle the same no matter if from blood of CSF because also in blood the DNA quality of single CD45 positive cells was very high (65 %, $p < 0.1$, Pearson Chi Square) while the derived tumor cells differ significantly ($p < 0.0001$, Pearson Chi Square).

It appears that, beside their proximity to LM, DCCs derived from CSF may draw a more precise picture about CNS spreading tumors compared to cells derived from blood. This increases the chance for generating clinically relevant molecular data out of their high-quality DNA and seems that CSF is a more convenient or protective environment for tumor cells than blood.

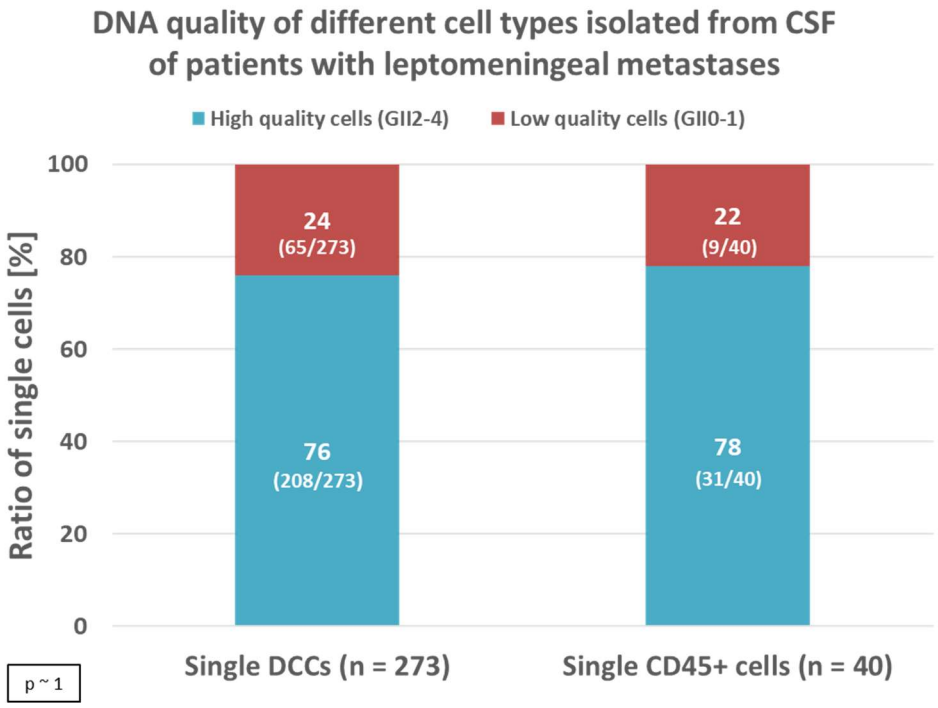

Figure 19 DNA quality of different cell types isolated from cerebrospinal fluid (CSF). Single disseminated cancer (DCCs) and CD45 positive cells, isolated from CSF of patients with different primary tumors but suspicion of leptomeningeal metastases (LM). P-value ~ 1 (Chi Square).

3.7 Fragment size distribution of DNA is not correlated to CNV success

As described in chapter 2.19, the determination of the fragment size distribution as well as the concentration of amplified DNA (see Chapter 2.18) is important for preparing the most efficient DNA approach prior to sequencing. All CSF derived high quality cells which showed a definite peak around 700 base pair (bp) fragment length were selected for CNV analysis. A correlation between the fragmentation of single cells and the evaluability of resulting CNV profiles was not detected. All single cell CNV profiles

which were not evaluable (n = 23) showed also the typically expected fragment distribution (Figure 5) and enough DNA.

3.8 Evidence of origin for single cells by Copy Number variation analysis

For validating the origin of the cells, the low pass whole genome sequencing for copy number variation (CNV) calling with the *Ampli*1^{TM} Low Pass Kit (Menarini Silicon Biosystems) was performed. 208 high quality DCCs and 19 CD45 positive single cells from 13 cartridges underwent the CNV process (Table 25).

Table 25 Number of isolated high-quality cells from CSF of cancer patients used for copy number variation (CNV) analysis. 204 single disseminated cancer cells (DCCs) and 19 single CD45 positive cells (* ID5: only a CD45 positive cell pool was available) were analyzed. In one case the CNV profile of putative DCCs were balanced (ID21) and in two cases (ID5, ID65) the CD45 positive profiles were aberrant (all highlighted by red frames).

ID	Primary tumor	Number of DCCs isolated GII >= 2	CNV profile DCCs available	CNV profile aberrant	Number of CD45+ cells isolated GII>=2	CNV profile CD45+ available	CNV profile balanced
3	Lung	9	8	yes	2	1	yes
4	Breast	8	7	yes	2	2	yes
5	Breast	14	14	yes	2*	1	no
10	CUP	20	19	yes	4	1	yes
14	Breast	49	48	yes	2	3	yes
16	Breast	19	19	yes	2	1	yes
17	Breast	20	20	yes	2	1	yes
18	Breast	20	20	yes	2	1	yes
21	Breast	5	5	no	2	2	yes
39	CUP	13	13	yes	3	2	yes
56	Gastric	12	12	yes	2	1	yes
64	Breast	3	3	yes	2	1	yes
65	Melanoma	16	16	yes	2	2	no
Total	-	208	204	-	27	19	-

3.8.1 Proof of tumor origin of DCCs by CNV analysis

98 % (n = 199) of analyzed cytokeratin positive single cells showed aberrant CNV profiles (e.g., Figure 20; interpretation see Chapter 2.22). Thus twelve (of thirteen) samples selected as DCC positive by fluorescent markers could be confirmed positive for leptomeningeal spread also on a molecular level.

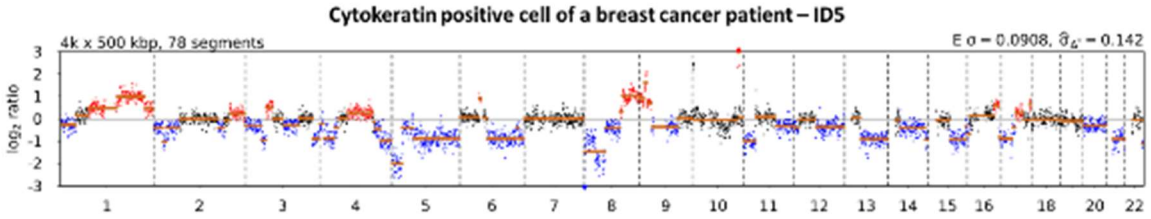

Figure 20 Copy number variation (CNV) profile of a Cytokeratin positive cell.
Aberrant CNV profile of a manually isolated disseminated cancer cell (DCC) from CSF of breast cancer patient ID5 with gains (red) and losses (blue) of. For detailed explanation refer to 2.22.

The five putative tumor cells of ID21 could not be confirmed on a molecular level as tumor derived. Going back to the fluorescent microscope pictures (representative DCC 2, Figure 21) the cells of these patients were selected due to verified signals in DAPI

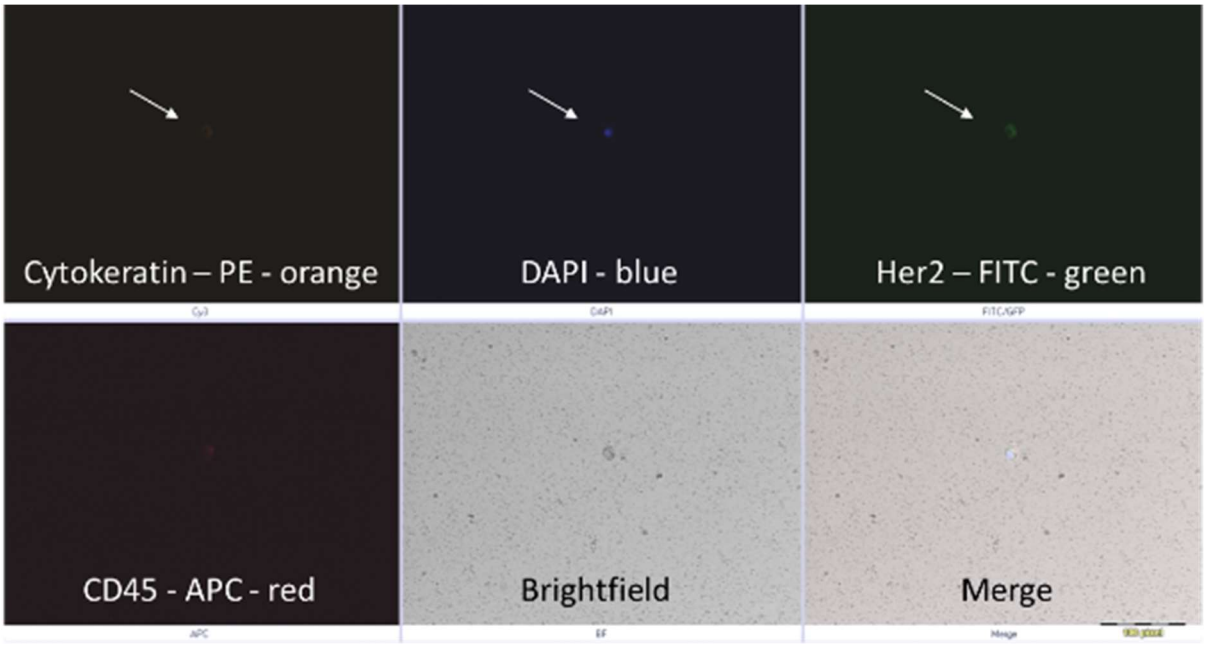

Figure 21 Fluorescent microscope picture of disseminated cancer cell (DCC).
Cancer cell number 2 from breast cancer patient ID21 with Cytokeratin, DAPI, Her2 and CD45 staining, brightfield and a merge. The arrows point on the single cell in the different channels.

and FITC, whereat the latter represents the Her2 expression pattern of the cells. As this was a convincing sign for a tumor cell, the weak cytokeratin signal was defined as acceptable, and five cells were isolated and selected for molecular downstream analysis. On closer inspection, the profiles of four (from five isolated) cells showed a balances profile (see Figure 22 above) and one a slightly aberrant profile (see Figure 22 middle). The two CD45 positive cells of this sample were also balanced in CNV profiling (see Figure 22 below). This sample was evaluated as LM negative because the profiles of the five DCCs were not convincing to define them as tumor derived.

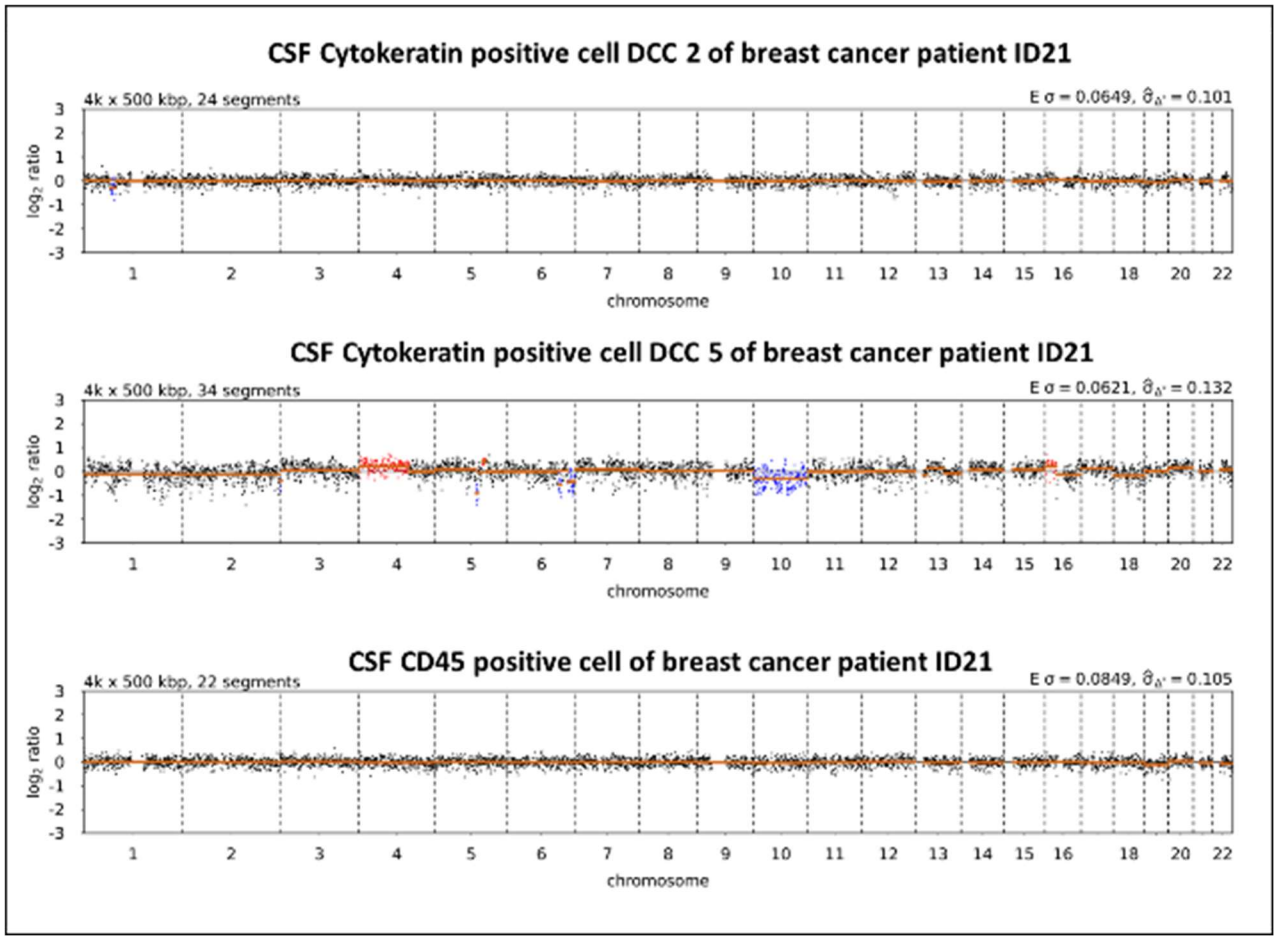

Figure 22 CNV profiles of CSF isolated single cells.
Three copy number variation (CNV) profiles of isolated single cells from breast cancer patient ID21. Above the balanced CNV profile of cytokeratin (CK) positive disseminated cancer cell (DCC) number 2, in the middle the slightly aberrant CNV profile of the CK positive DCC number 5 and below the balanced profile of a CD45 positive cell derived from the same cerebrospinal fluid (CSF) sample.

3.8.2 CNV profiles of dedicated CD45 positive cells

For each DCC isolated sample CD45 positive cells were isolated to have a comparison whose alterations might be a germline mutation, and which are tumor related. Having a closer look at the selected CD45 positive cells, all CNV profiles were balanced (e.g., Figure 22 below) except of patients ID5 and 65. The challenging point for isolating CD45 positive cells from CSF of breast cancer patient ID5 was a missing APC channel signal. At the timepoint when this sample was isolated the microscope was not yet equipped with this further channel.

The cells were assessed by a positive DAPI signal and an absent CK-PE signal. Furthermore, for this ID it was impossible to isolate single cells because the CD45 cell number in the picking field was very high, therefore only pools could be selected. Comparing the CNV profiles of the CD45 positive cells pool and a CK positive DCC isolated from the same sample the assumption that the CD45 cell pool was most likely contaminated with tumor cells floating around in the dense cell suspension. It can be observed that the aberrancies in the single DCC 12 are more distinct than those in the

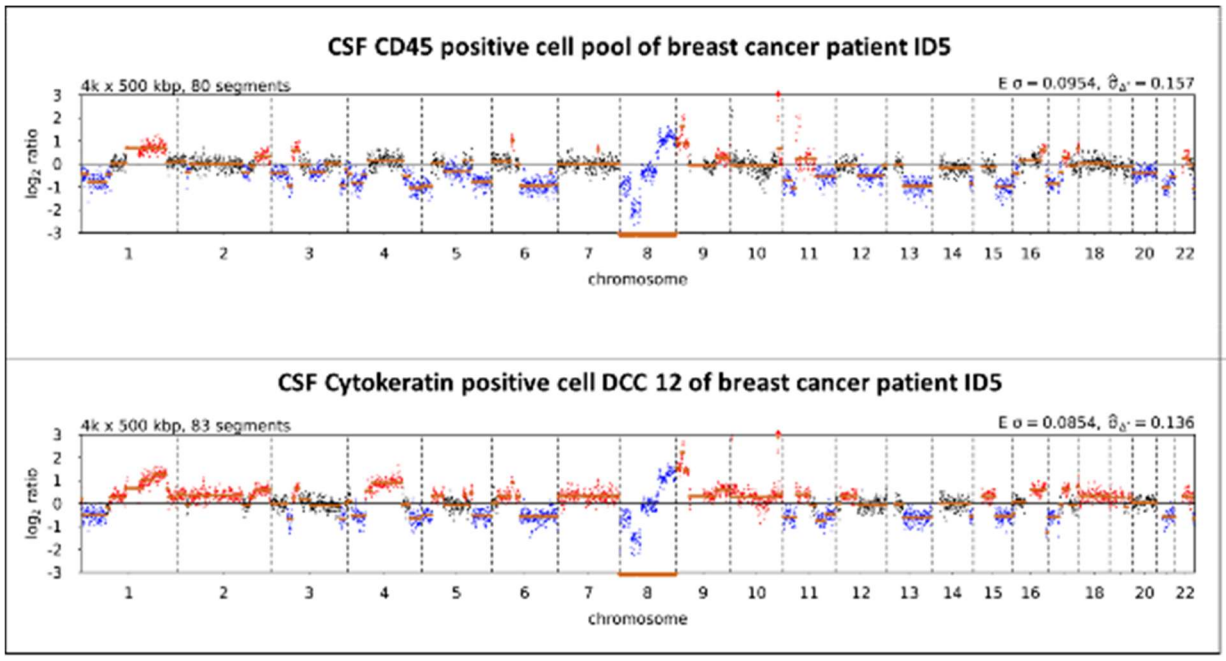

Figure 23 CNV profiles of CSF isolated single cells.
Two aberrant copy number variation (CNV) profiles of single cells isolated from cerebrospinal fluid (CSF) of breast cancer patient ID5. Above the aberrant CNV profile of the CD45 positive cell pool and below an aberrant CNV profile of CK positive DCC 12.

CD45 positive cell pool. This might be an effect that the CD45 ratio in the pool is high enough to equilibrate the aberrancies derived from the contaminating DCCs and cluster the signals close to the log2 ratio = 0 (e.g., Chromosome 2, 7, 18 in Figure 23 below).

For ID 65 (melanoma patient) the two CD45 single cells isolated from the CSF the CNV profile were, contrary to expectations, also aberrant. Going back to the microscopy pictures the sample seemed not as dense for difficulties in isolating pure single cells (Figure 24).

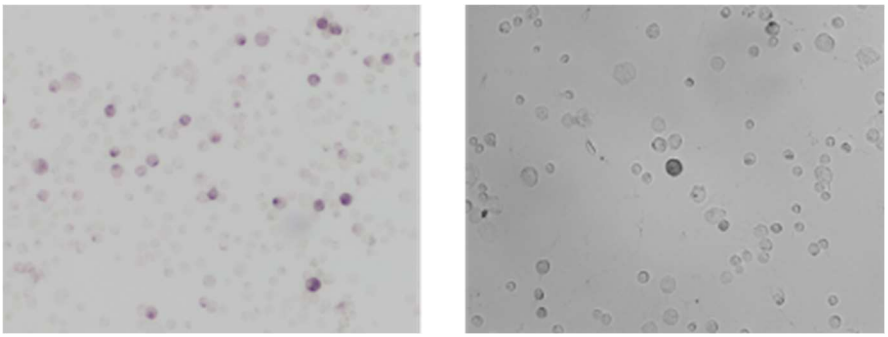

Figure 24 Brightfield picture of a HMB45 staining from a CSF melanoma sample (ID65).
Left: HMB45 staining of enriched, stained, and screened sample on a glass adhesion slide manually at the microscope, imagination 20 x. Cells of interest are visible in dark purple, which mirrors the putative HMB45 expressed melanoma cells. Right: Brightfield picture of single HMB45 positive cell 6 isolated from the same CSF melanoma sample.

For melanoma samples the isolation process from glass adhesion slides is slightly more complex compared to the isolation from suspension. Because the cells must be detached by mechanical scratching of the capillary along the glass slide it might happen that not only the favored cell is moving. Also, nearby cells from a different cell type or at least parts of their DNA material could have entered the glass capillary. It might also be that the detached tumor cells became soluble due to the surface coating during the isolation process, but as the CD45 cells are selected before the tumor cells this is very unlikely. A mixture of sample tubes can be excluded because the similarity of the CNV profiles between the CD45 and the HMB cells (Figure 25) is very high, that a contamination with tumor DNA due to technical issues is most likely.

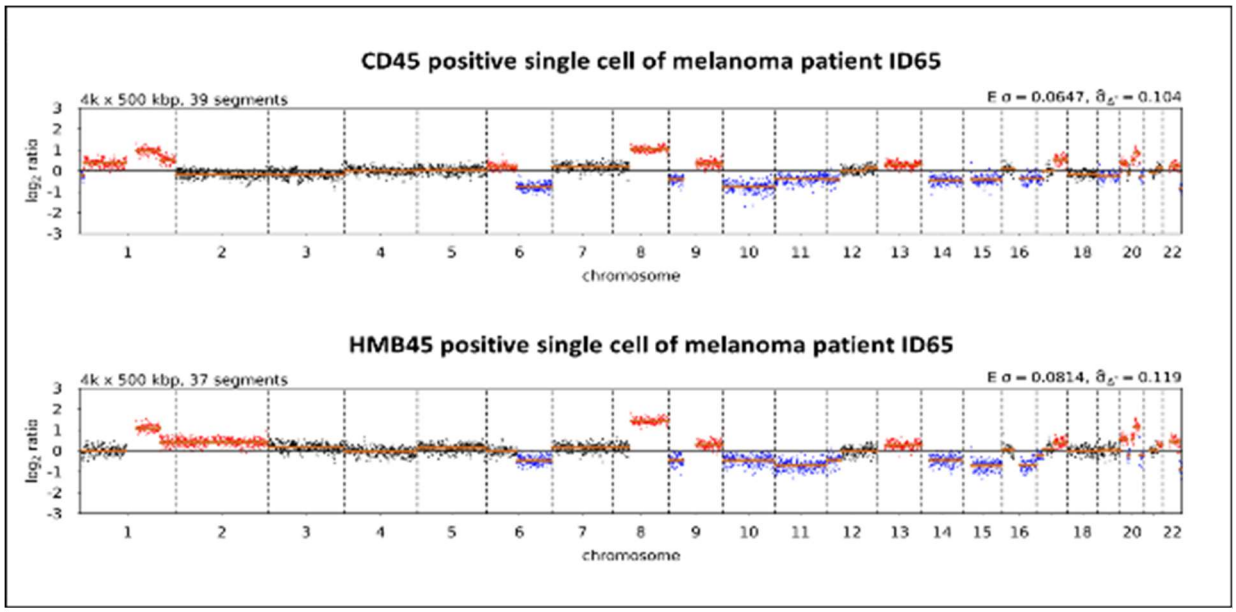

Figure 25 Copy number variation (CNV) profiles of CSF isolated melanoma single cells.
Above the aberrant CNV profile of a CD45 positive single cell, below the aberrant profile of a HMB45 positive single cell. Both cells are isolated from melanoma patient ID65.

3.8.3 Clonality of CSF DCCs

A comparison of molecular CNV data from DCCs should determine whether the isolated CSF cells were derived from one or more subclones. Therefore, the CNV profiles were represented in so-called patient specific circosplots which made it possible to realize immediately the accordance or discordance of gains and losses. Most of the samples revealed clonal relationships with some divergence (Figure 26, e.g., Chr 3, 19) but led to the assumption that they are most likely derived from the same subclone. Only DCCs from the cancer of an unknown primary sample ID39 (Figure 27) showed a more dissimilar pattern. But here as well a relationship between different cells can be observed which could mean that also those cells were derived most likely from one subclone. Interestingly the gain on the short arm of Chromosome 5 unifies all DCCs but is not a germline mutation.

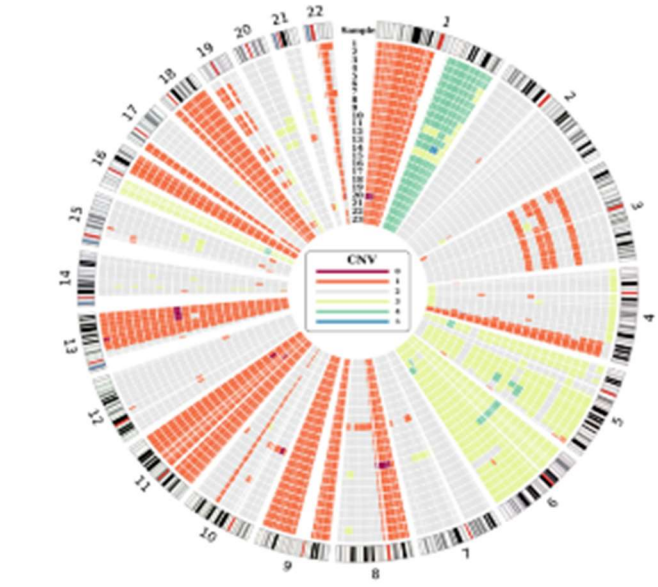

Patient ID 14 Breast Cancer	ID of isolated cell
1	CSF-DCC25-D1
2	CSF-DCC26-D1
3	CSF-DCC27-D2
4	CSF-DCC29-D2
5	CSF-DCC2
6	CSF-DCC31-D2
7	CSF-DCC33-D2
8	CSF-DCC35-D2
9	CSF-DCC39-D2
10	CSF-DCC3
11	CSF-DCC41-D1
12	CSF-DCC44-D2
13	CSF-DCC46-D2
14	CSF-DCC47-D2
15	CSF-DCC4
16	CSF-DCC5-D1
17	CSF-DCC5
18	CSF-DCC6-D1
19	CSF-DCC7
20	CSF-DCC8-D1
21	CSF-DCC8
22	CSF-DCC9-D1
23	CSF-DCC9

Figure 26 Circosplot with copy number variation (CNV) profiles patient ID 14.
CNV profiles of cerebrospinal fluid (CSF) isolated disseminated cancer cells (DCCs) from breast cancer patient ID14 arranged in a circosplot. Colours in the middle of the plot explain the ploidy of colored regions in the profiles. The samples (1-23) in the plot are described in the table and represent Cytokeratin positive cells only.

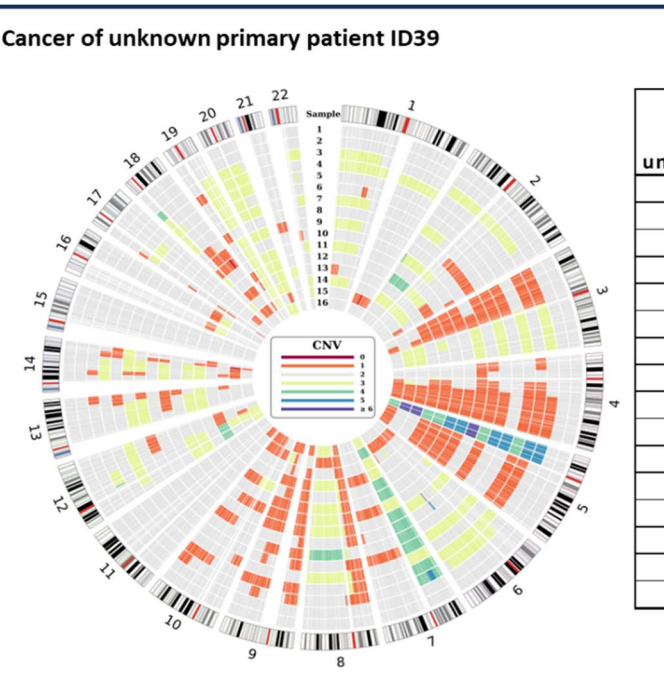

Patient ID 39 Cancer of unknown primary	ID of isolated cell
1	CSF-CD45p-1
2	CSF-CD45sc-3
3	CSF-DCC10
4	CSF-DCC12
5	CSF-DCC13
6	CSF-DCC14
7	CSF-DCC17
8	CSF-DCC18
9	CSF-DCC1
10	CSF-DCC2
11	CSF-DCC3
12	CSF-DCC5
13	CSF-DCC6
14	CSF-DCC7
15	CSF-DCC8
16	CSF-DCCP-1

Figure 27 Circosplot with copy number variation (CNV) profiles patient ID 39.
CNV profiles of cerebrospinal fluid (CSF) isolated disseminated cancer cells (DCCs) from cancer of unknown primary patient ID39 arranged in a circosplot. Colors in the middle of the plot explain the ploidy of colored regions in the profiles. The samples (1-16) in the plot are described in the table: 1 and 2 CD45 positive cells, 3 – 15 Cytokeratin positive single cells, 16 Cytokeratin positive cell pool.

3.8.4 Detection of cancer related CNV mutations

In two of eight positive breast cancer samples an *ERBB2* signal was detected by the CellSearch® system (e.g., Figure 28 A, ID16) but could neither be confirmed by the CNV plot (Figure 28 B) nor by screening the gene specific locus in the sequencing statistics (ploidy on coding region of ERBB2 = 2).

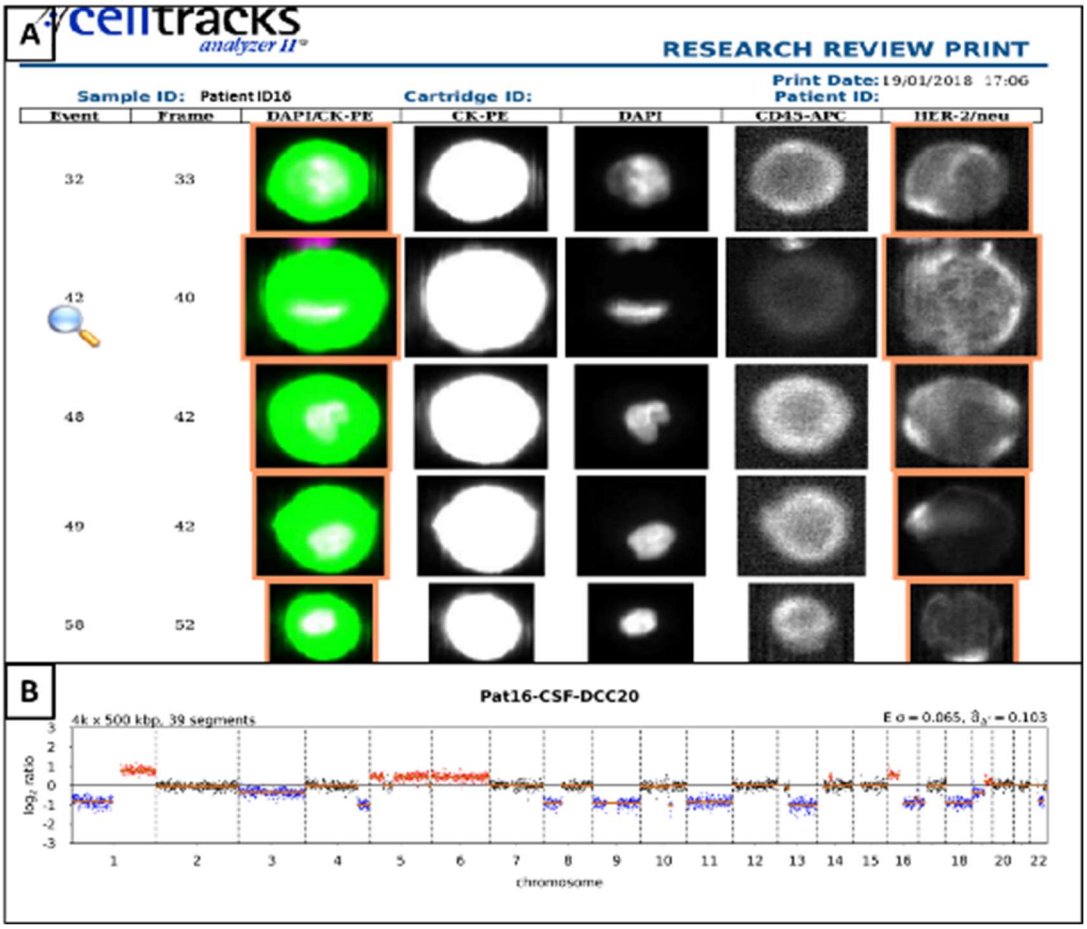

Figure 28 Excerpt of a CellSearch® Gallery from cerebrospinal fluid (CSF) analysis.
A: CSF breast cancer sample ID16 enriched by the CellSearch® CTC-Kit, detected and counted by the CellTracks Analyzer II®, where the DAPI, the Cytokeratin but also the ERBB2 (Her2) signal is shown. **B**: Copy number variation (CNV) profile of a disseminated cancer cell (DCC20) isolated from the CSF of breast cancer patient ID16 where no ERBB2 amplification (17q) was detectable by CNV analysis.

The common variations on Chromosomes (Chr) 1q (gain), 16q (loss) and 8p (loss) connected to tumor progression and aggressivity were detected in almost all the breast cancer samples and the lung samples. The CNV profiles of CUP (e.g., Figure 27),

gastric cancer, and melanoma (Figure 29) showed more different CNV patterns concerning those regions.

In the melanoma sample (ID65, Figure 29) a gain of Chr 8q is striking which is obviously connected to a *MYC* gene amplification and could also be confirmed in the statistical gene analysis of the CNV profile (ploidy in coding region of *MYC* gene = 4). The Chr 1q gain and the 16q loss were also visible through all isolated CSF single cells likewise the gain on Chr 20 which is correlated to tumorigenic process in different cancer types amongst others in melanoma. Interestingly, two CUP patients were analyzed within this collective. By comparing the appearing copy number variations no clear tendency concerning the primary tumor is visible. Also, the CNV profile of patient ID10 (Figure 30) does not show a typically cancer type assigned pattern but a gain of Chr 3q has been recognized which can also be found to be connected to other cancer types. For CUP patients, drawing a conclusion to cancer type is not feasible only by CNV profiles. But they could provide in general important molecular information to guide the direction for further molecular analysis.

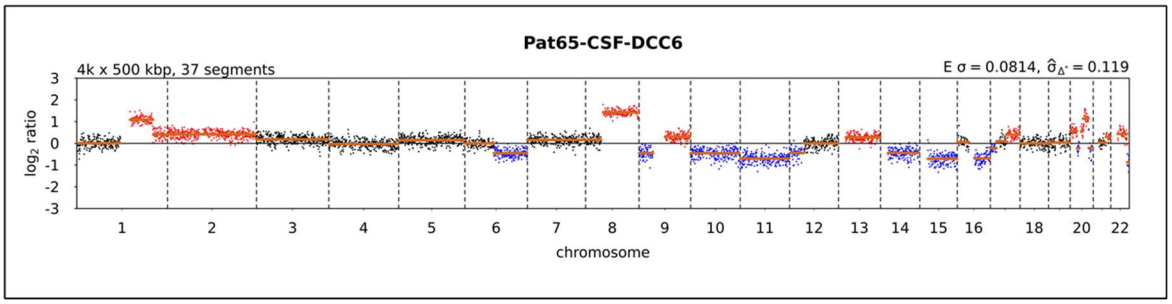

Figure 29 Copy number variation (CNV) profile of a melanoma single cell.
Isolated single disseminated cancer cell (DCC6) from cerebrospinal fluid (CSF) of melanoma patient ID65.

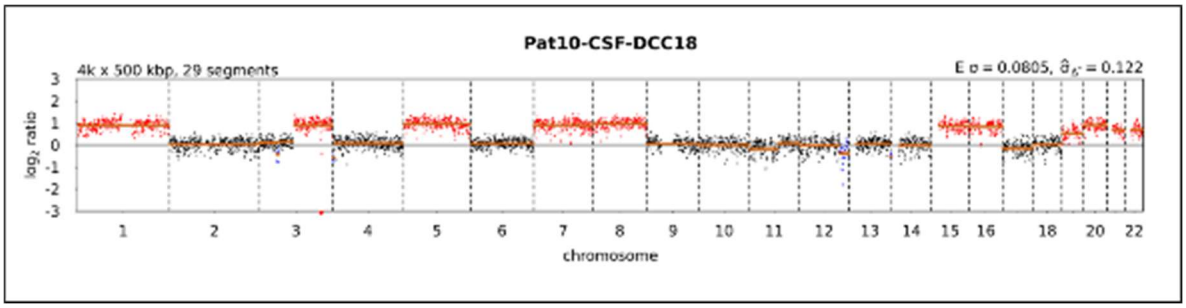

Figure 30 Copy number variation (CNV) profile of a cancer of unknown primary single cell.
Isolated single disseminated cancer cell (DCC18) from cerebrospinal fluid (CSF) of cancer of unknown primary patient ID10.

3.9 Isolation of circulating cell-free DNA from CSF samples

In addition to DCCs, also circulating tumor cell free DNA (cfDNA) can be a liquid biopsy approach containing additional valuable genetic information. It is described as an apparently easily accessible biomarker with fast analysis possibilities. It can´t be found only in blood even if mostly described in blood plasma with an increased concentration in tumor patients. Considering the generally cell rare CSF as source for cfDNA, it can be assumed that its detection amount is even less compared to plasma. However, it may provide more precise information concerning CNS affection. Considering the different tumor entities from various carcinoma types but also melanoma in this collective 30 % LM detection reflects a realistic average. Nevertheless, the clinical suspicion of LM in the residual 70 % of patients persisted and the enhancement of the DCC results by means of additional CSF analysis was aspired. Therefore, the option for using the cell free DNA compartment separated from the CSF samples prior to DCC analysis was obvious. Together with an affiliated medical doctoral thesis the cell free DNA of 29 CSF samples was analyzed within this project. While the sample IDs 14 – 24 (n = 8) were isolated, quantified and sequenced by me the residual samples (IDs 25 – 66, n = 21) were isolated, quantified, and sequenced by Lena Moser and compared to exosomes, which were part of her project. As agreed, the isolation, quantification and sequencing data derived from both of us are allowed to be used for evaluating important points of project specific topics of both theses.

3.9.1 Sample characteristics – Volumes and quantification

Within this collective 29 CSF samples with volumes between 0.65 and 2 ml (median 1,3 ml) were available to be processed for cfDNA isolation. While 19 samples showed a median DNA concentration of 0.304 ng/µl (range 0,13 – 1,83 ng/µl) and for ten samples cfDNA was not even detectable (under the detection limit of 0,05 ng/µl; Table 26). These very low amounts of cfDNA rendered most samples inaccessible for further molecular analysis, because the success of a molecular downstream analysis is also dependent from enough input. We therefore utilized the adapted WGA-based amplification procedure for all cfDNA samples (Chapter 2.16), also the ones with

potentially enough cfDNA, to perform an amplification which was resulting in an up to 80-fold higher cfDNA amount (median 24,6 ng/µl; range: 2,56 – 82,4 ng/µl). Interestingly, it was possible to reach the required DNA amount also for the ten samples with no DNA detected after isolation from CSF. There was no direct correlation between the input amount before amplification and the output after the amplification.

Table 26 Overview of cerebrospinal fluid (CSF) samples
analyzed for cell-free tumor DNA. Sample IDs >25 were processed by Lena Moser.

ID	Tumor Entity	Sex	Age at withdrawal	Analysed volume supernatant [ml]	DNA concentration before amplification [ng/µl]	DNA concentration after amplification [ng/µl]
14	**Breast**	f	71	1,5	< 0,05	39,2
15	**Lung**	m	52	2	< 0,05	35,9
16	**Breast**	f	71	0,8	< 0,05	38,3
17	**Breast**	f	81	1,1	< 0,05	35
18	**Breast**	f	71	1	< 0,05	34,7
21	**Breast**	f	47	1	< 0,05	29,5
22	**CUP**	f	74	1	< 0,05	38,3
24	**Colon**	m	73	1,4	< 0,05	35,5
25	**Melanoma**	f	59	1,2	0,354	7,9
28	**Breast**	f	76	0,9	0,284	14,9
29	**Breast**	f	59	1,8	0,308	13,4
31	**Lung**	f	39	0,8	0,3	20,8
35	**Breast**	f	61	1,6	0,168	49,6
38	**Melanoma**	f	59	1,8	0,258	82,4
39	**CUP**	m	70	1,5	0,352	67,6
45	**Larynx**	f	71	1,1	< 0,05	3,09
46	**Breast**	f	48	1,5	0,384	3,58
47	**Lung**	f	71	1,2	0,818	7,46
48	**Lung**	f	67	1	0,13	24,6
49	**Melanoma**	f	80	1,8	< 0,05	2,56
53	**Melanoma**	m	76	1,2	0,438	9,18
55	**Breast**	f	43	1,5	0,21	9,5
56	**Gastric**	f	62	1,6	1,19	34,4
57	**Lung**	m	56	1,4	0,4	17,5
58	**Melanoma**	f	57	1,8	0,166	33,6
62	**Lung**	m	69	0,65	0,304	39,8
64	**Breast**	f	68	0,85	0,216	13,6
65	**Melanoma**	m	52	1,2	1,83	16,1
66	**Lung**	m	38	1,4	0,22	9,36

This means that samples with a very low input of < 0,05 ng/µl could reach a very high amount (e.g., ID 22) and the other way around (e.g., ID 65) (Figure 31). Both groups were analyzed with the paired, two-tailed t-test (Vassarstats) and the p <0.001 showed that there is a significant difference between the two groups before and after amplification.

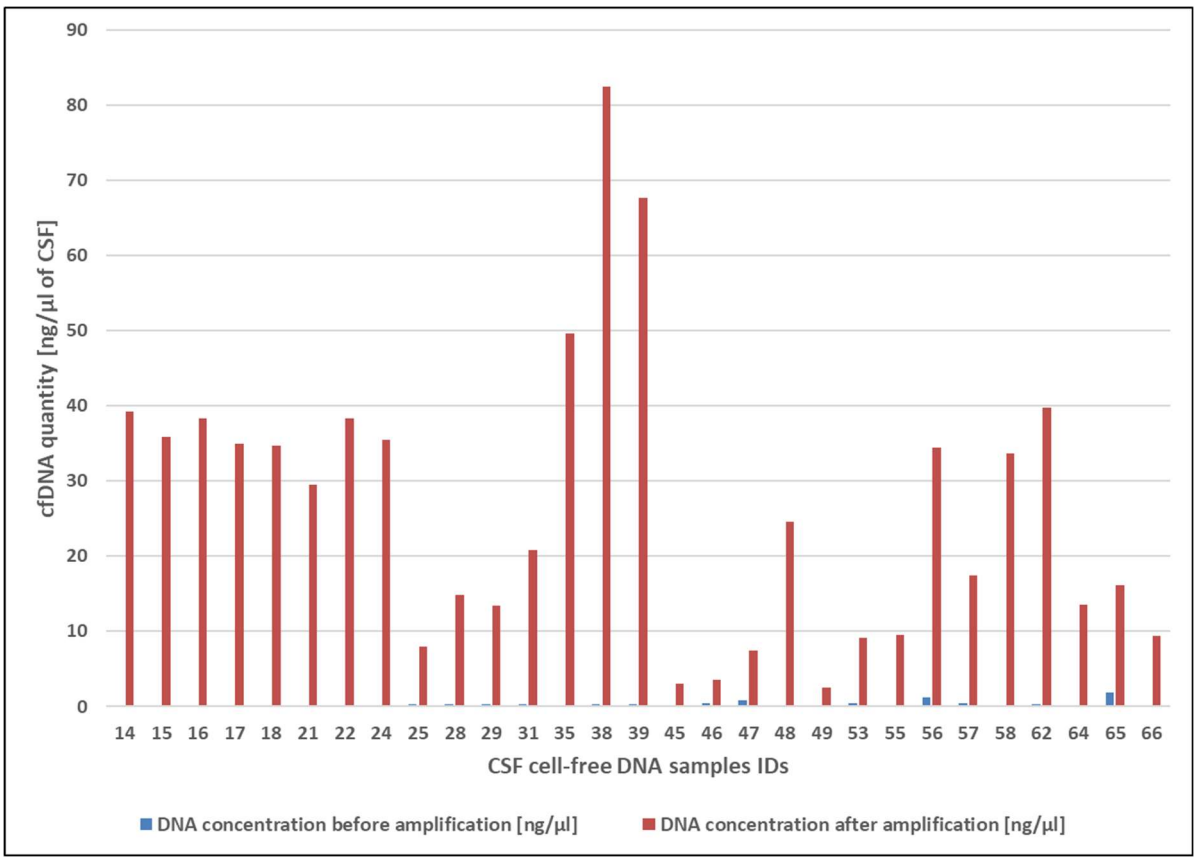

Figure 31 Quantity of cell free DNA (cfDNA) isolated from cerebrospinal fluid (CSF). cfDNA values before amplification directly after isolation (blue) and after amplifcation (red) measured by QuBit high sensitivity assay for patients IDs (14, 15, …66). P < 0.001 (paired t-test, www.vassartats.com)

The tendency that the concentration of cfDNA is dependent on tumor type appeared, and interestingly the amount for melanoma patients was highest with a median of 0,304 ng/µl (range: <0,05 – 1,83 ng/µl) followed by lung cancer (median = 0,3 ng/µl; range: <0,05 – 0,82 ng/µl), cancer of unknown primary (median = 0,2 ng/µl; range: <0,05 – 0,352 ng/µl) and breast cancer (median = 0,17 ng/µl; range: <0,05 – 0,384 ng/µl). Considering the number of samples, a meaningful statement for entities with only one sample (gastric, larynx, colon cancer) cannot be done (Figure 32 A).

The cfDNA concentration was higher in male than female patients and highest in the age group between 51 – 60 (Figure 32 B, C) but no correlation was detected including the analyzed volume (data not shown – evaluated by Lena Moser). Although data does exist in literature with a mean cfDNA amount of CSF in tumor patients, it is very challenging to define the cfDNA amount in CSF in healthy donors because only a secured suspicion of a disease of the central nervous system (CNS) justifies a CSF withdrawal. Trying to find a mean reference CSF cfDNA concentration the collective was divided in patients positive for LM (n = 13) spread by one of the Gold Standard methods, either MRI or CSF cytology and negative (n = 10) for these methods, knowing well, that all patients were diagnosed positive for any kind of primary tumor and/or extra CNS metastases.

With a median of 0,21 ng/µl for LM negative and a median of 0,23 ng/µl for LM positive patients no significant difference could be confirmed (Figure 32 D).

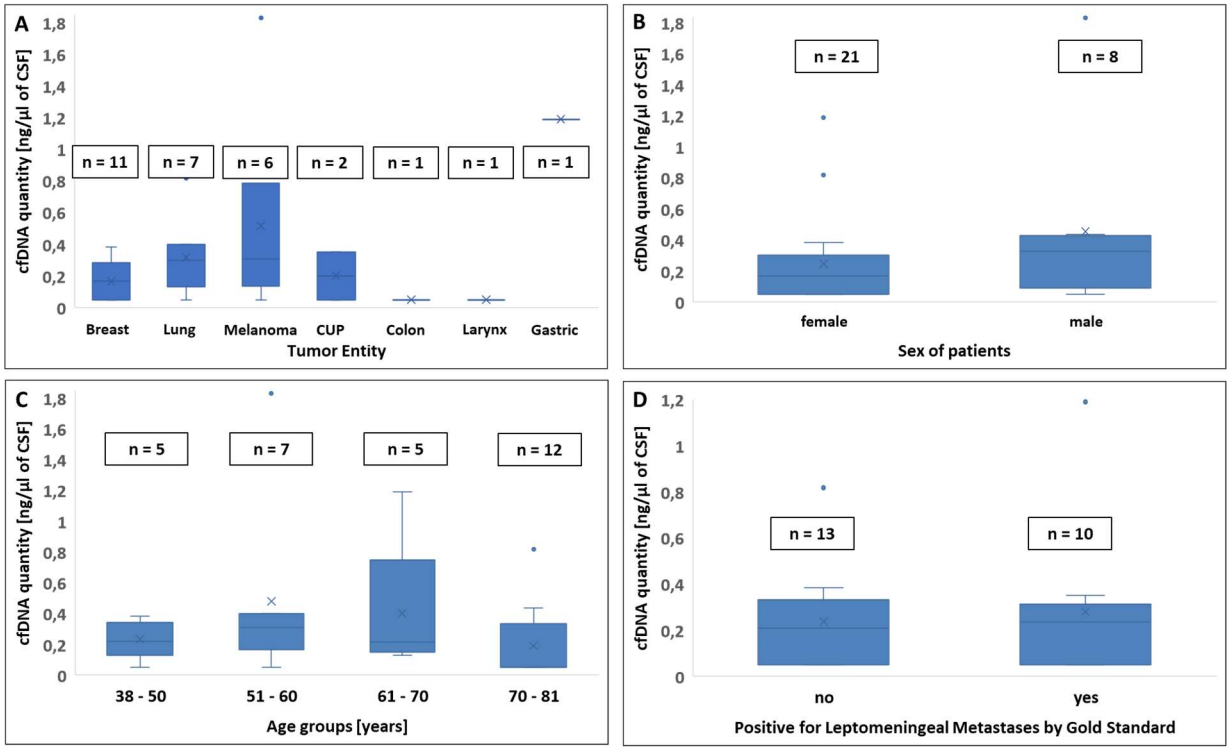

Figure 32 ctDNA concentration of cerebrospinal fluid (CSF) samples.
Correlations from circulating tumor DNA (ctDNA) concentration of patients with suspected leptomeningeal metastases and different primary tumors. A: Correlation of cfDNA quantity and tumor entity (n = 29). B: Correlation of cfDNA quantity and sex of patients (n = 29). C: Correlation of cfDNA quantity and age of patients (n = 29). D: Correlation of confirmed leptomeningeal metastases spread by at least one of the two gold standard methods (either CSF cytology or magnetic resonance imaging (MRI)).

3.9.2 Fragmentation of CSF cfDNA

The fragmentation of all CSF cfDNA samples was performed with the Bioanalyzer High sensitivity assay (Agilent, 2.19). These are the eight samples (ID 14 – 24, Figure 33) that I processed independently for further analysis, chosen as representative for the size distribution. On closer inspection, all eight samples showed a peak at 200 – 400 bp, which represents a fraction of smaller fragments, but also samples with additional higher peaks (> 500 bp; ID17, 21), exist. The two samples with higher fragments (ID17, 21) showed indeed a balanced CNV profile whereas the samples with clearly defined shorter fragments (ID14, 18, 22, 24) were aberrant. It must, however, be mentioned that also ID 18 shows fragments higher than 500 bp. But due to the low concentration and the sharply defined peaks at 200 and 400 bp, the circulating tumor DNA was high enough to create a meaningful aberrant profile. Unfortunately, two samples (ID15 = 0 DCCs, ID16 = 114 DCCs) could not be evaluated for cfDNA due to a widespread or low amount of data points in the CNV analysis. The assumption that this might be correlated to the more “one single peak” shape could not be confirmed considering the

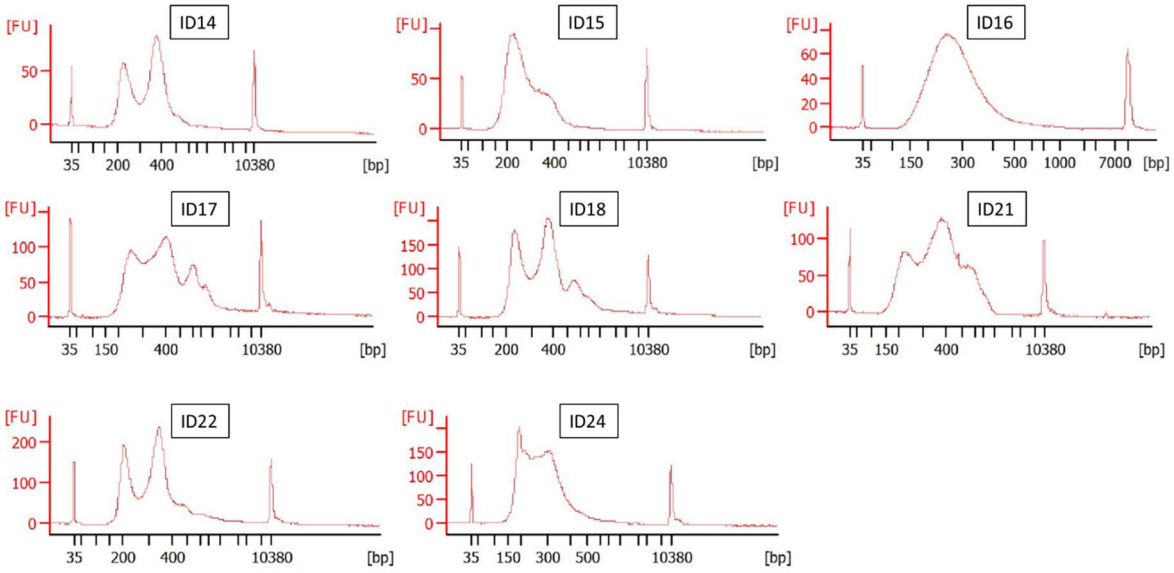

Figure 33 Fragmentation profiles of cerebrospinal fluid (CSF) derived cell free DNA.
Eight representative samples from patient ID14 – 24 analyzed with the Bioanalyzer high sensitivity kit (Agilent). All fragmentation profiles show the low marker (35 base pairs (bp) – X-Axis), the high marker (10380 bp – X-Axis) and a typically fragment distribution of cfDNA with two peaks at 200 and 400 bp with a concentration around 150 fluorescent units (FU, Y-Axis). Some samples show additional peaks (ID17, ID21) or only one peak (ID16) which can be caused by the release mechanism of circulating DNA.

additional cfDNA samples (n = 21, sample ID 25 – 66, doctoral thesis Lena Moser) of this collective.

3.9.3 CNV analysis of amplified cfDNA

The CNV calling was performed for all cfDNA samples (n = 29). Twenty-one % showed an aberrant, 52 % a balanced and 27 % of the samples a not evaluable profile (e.g., CNV profiles of breast cancer patients in Figure 34). Returning to the latter, no correlation concerning cfDNA concentration (median before amplification: 0,29 ng/µl) and CNV success rate could be detected because even samples with the lowest (< 0,05 ng/µl, e.g., ID15, 16) but also the highest (1,83 ng/µl, ID65) isolated DNA amount showed not evaluable CNV profiles. This accounted also for the comparison after the amplification step (range 9,36 – 38,8 ng/µl) and vice versa for the evaluable profiles (median before amplification: 0,3 ng/µl).

For all 29 cfDNA samples, the cell fraction of the CSF sample was enriched for detecting DCCs, while eight samples were confirmed DCC positive and 21 negative.

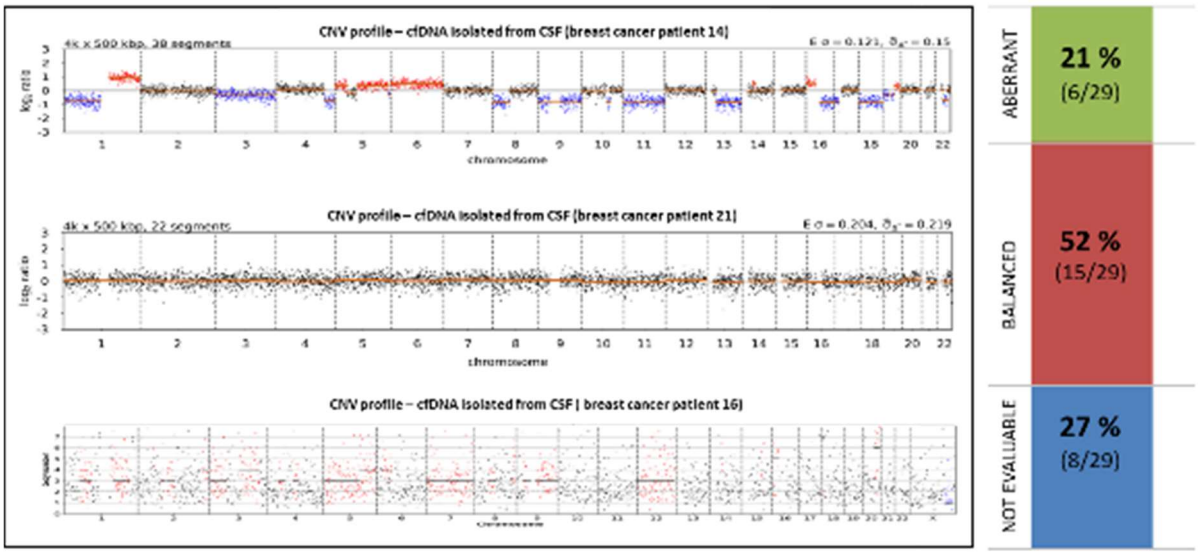

Figure 34 Copy Number Variation profiles of ctDNA isolated from CSF.
Representative for 21 % of aberrant profiles the upper profile of cell free tumor DNA (ctDNA) isolated from cerebrospinal fluid (CSF) of breast cancer patient 14, for 52 % of balanced profiles the middle profile of breast cancer patient 21 and for 27 % of not evaluable profiles the lower profile of breast cancer patient 16. The lowest profile was analyzed with a preliminary version of the bioinformatician pipeline for copy number variation (CNV) analysis that's why the picture is different two the upper ones. Analyzed with the new software version those profiles would bring the message "not evaluable" an no CNV profile would be analyzed.

Including all samples, a direct comparison between DCCs and cfDNA results mirrored a concordance of 59 % (17/29) regardless of whether the samples were concordant aberrant or balanced. Unfortunately, only 27,5 % (8/29) of analyzed samples were not evaluable for cfDNA, either because of widespread or a low number of reads in sequencing, which revealed a high dropout rate of quarter of samples for the cfDNA approach. If only the evaluable cfDNA profiles are highlighted (n = 21) a concordance of 81 % (17/21) between the CNV evaluation of cfDNA (balanced or aberrant) and the DCC availability was detected (see Figure 35), when DCC negativity equates to a balanced cfDNA profile and DCC positivity to an aberrant cfDNA profile. This reveals that both, either DCC or cfDNA enrichment technologies, provide valuable and comparable molecular information about tumor DNA.

For the sake of completeness, it must be augmented that by reducing the sample number from 29 to 21 concerning the evaluability of CNV cfDNA profiles, four DCC positive (and 4 DCC negative) samples were excluded. This makes the data (Figure 35) seem to support the sensitivity of the cfDNA approach while in total (n = 29) twelve

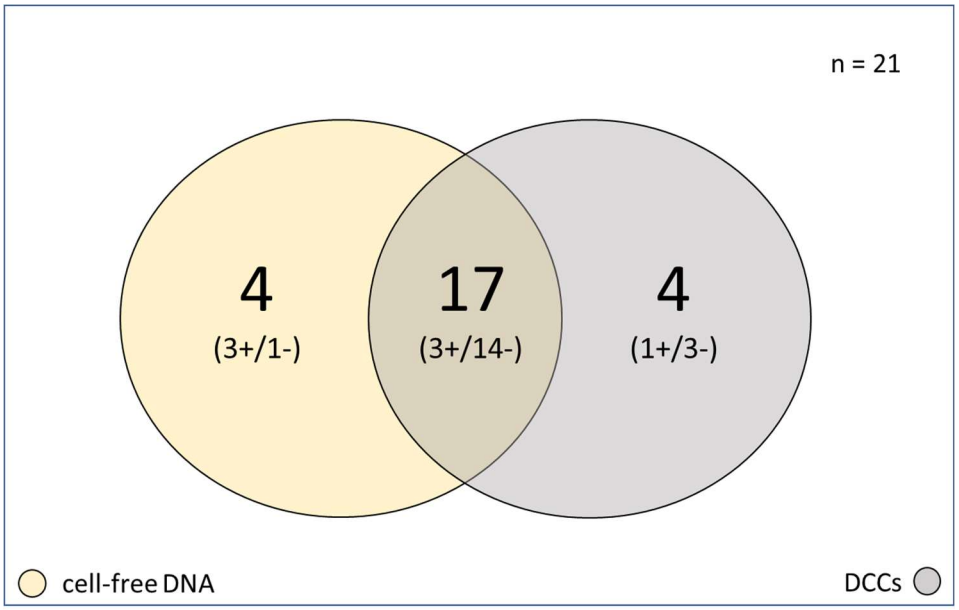

Figure 35 Concordance of copy number variation analysis of ctDNA and DCC detection. Circulating tumor DNA (ctDNA) and disseminated cancer cells (DCCs) from corresponding cerebrospinal fluid (CSF) samples. cfDNA balanced CNV profiles and DCC negative counts just as well as vice versa cfDNA aberrant CNV profiles and DCC positive counts. Not pictured are the n = 8 samples which were not evaluable for cfDNA analysis but DCC positive (n=4) and DCC negative (n=4).

samples were confirmed DCC positive and six samples only could be confirmed tumor derived via an aberrant CSF cfDNA profile.

3.9.4 ctDNA and DCCs of related CSF samples show similar CNV profiles

For one breast cancer patient, molecular information from DCC and circulating tumor DNA (ctDNA) exists. For this patient, a serial CSF withdrawal was performed at three different timepoints, sample ID14 (27.10.2017), ID16 (19.02.1018) and ID18

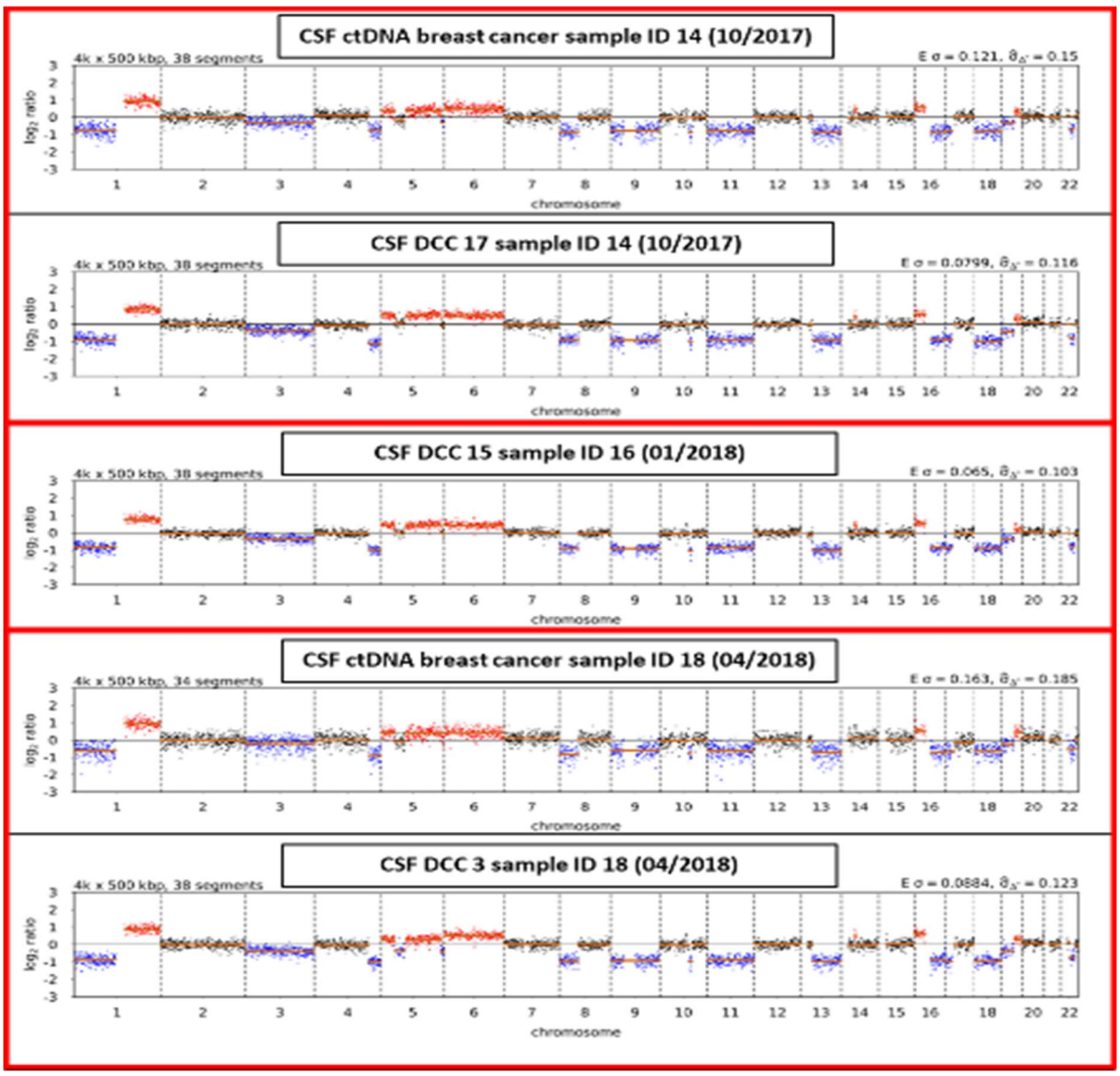

Figure 36 CNV profiles from serial CSF assessment of DCCs and ctDNA.
Copy number variation (CNV) profiles of isolated cerebrospinal fluid (CSF) single disseminated cancer cell (DCC) and cell free tumor DNA (ctDNA) from one breast cancer patient with serial CSF assessment (ID14 – 10/2017, ID16 – 01/2018, ID18 – 04/2018).

(13.04.2028). While for ID14 and 16 both data sets exist, the cfDNA analysis of ID16 was not evaluable. It can be seen (Figure 36) that both the DCCs of the three different time points and the correlating circulating tumor DNA derive from the same subclone of the tumor because they share gains and losses identically.

These results were not surprising because the withdrawal intervals of three months were very short. It was still possible to follow this patient during seven months of therapy by CSF analysis. On the long run, this might be an option to monitor the progress of the disease very continuously and detect changes under therapy conditions timely.

3.10 CNS specific subclones confirmed by FFPE derived tumor cell pools

In these, collective patients with different non central nervous system (CNS) primary tumors, as carcinoma and melanoma, are included. They were additionally diagnosed for leptomeningeal spread, mostly after years of primary detection and molecular data were generated from different sources of biomarkers, blood, or CSF at this later timepoints. Going back to the molecular analysis of primary tissue or different metastases, even from CNS, the question, if tumor cell clones passing the blood-brain-barrier to form CNS metastases differ from other subclones found in tissue material, should be answered.

3.10.1 Sample characteristics – Availability and isolated populations

In total, 22 tissue samples were available from twelve patients (nine female, three male) with suspected leptomeningeal metastases included in this cohort (additional sample information see Table 1A, Appendix). Due to the critical nature, surgery close to CNS, must be weighed up keenly and it is always an individual decision if material different metastatic tissue material, CNS and non-CNS derived, of included patients (Figure 37) for generating valuable data.

Since most patients in the collective are breast, melanoma, and lung cancer patients (3.2) it is not surprising that the majority of the available tissue samples derived from those entities. Seven breast, two lung, one gastric cancer, and two melanoma patients

are represented in the FFPE collective while also up to three different FFPE samples from one single patient were available.

According to tissue size and residual material left on the FFPE block, slices between 40 µm (2 x 20 µm; all brain metastases), 50 µm and 100 µm (2 x 50 µm) were dissociated. They resulted in cell suspensions (tumor plus stromal cells) with a median cell number of 792750 (range 6000 – 4023000 cells) whereas no correlation between the thickness and the cell number was detected (Hoechst 33342, Countess - LifeTechnologies, ImageJ, see 2.10). Samples with the lowest cell numbers were derived from pleural effusion (6000 cells), lymph node (58.500 cells) and bone (median 141900 cells, n = 2) material. This might in case of the pleural effusion and the lymph node sample be connected to the enrichment procedure before embedding but could also be a matter of digestion time. Normally the digestion procedure from connected cells to single cells can take up to 45 minutes and is surveyed every ten minutes. With this an over digestion of the sample resulting in released DNA but not in a cell suspension with intact cells should be avoided. It was not surprising that the digestion time for the pleural effusion sample was very short with 10 minutes because the embedding input is already a single cell suspension re-clustered by centrifugation prior to storage in paraffin. It seemed that for samples of this texture ten minutes incubation led already to an over digestion resulting in low cell numbers considering that only one pleural effusion sample was analyzed but with a significant low cell number.

Concerning the low cell number from cell suspensions of bone material it must be admitted that the dissociation procedure with the FFPE sample Prep Kit (MSB) was not especially developed for strong bone material. Even after a 45-minute digestion the bone material was still visible.

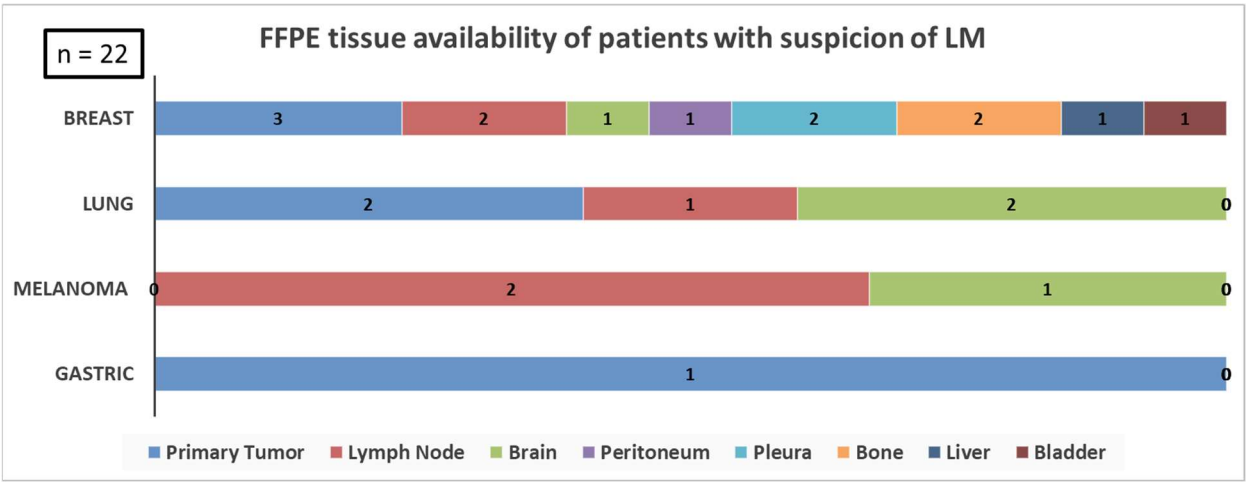

Figure 37 Sample availability of FFPE tissue material.
Analyzed formalin fixed paraffin embedded (FFPE) tissue of included patients with different primary tumors but suspicion of leptomeningeal metastases (LM). In total 22 samples from twelve patients were available among them primary tumor (n = 6) and different metastases as lymph node (n = 5), brain (n = 4), peritoneum (n = 1), pleural effusion (n = 2), bone (n = 2), liver (n = 1) and bladder (n = 1).

3.10.2 Isolation of tumor cell populations with the DEPArray™ technology

By processing the samples with the DEPArray™ sample prep Kit stromal cell populations are defined by the Vimentin antibody, tumor cell populations by Cytokeratin in connection to a DAPI nuclear staining. Up to 500.000 cells (Countess, LifeTechnologies) were stained from each cell suspension. One stromal cell population (n = 22) and up to three different tumor cell populations (n = 29) were isolated in total (n = 51). The cell selection and assignment to the appropriate populations is performed automatically with the system integrated CellBrowser software. The fact that more than one tumor cell population can be available per sample is connected to the automatically calculated “DNA Index”. Therefore, the mean DAPI signal of all diploid cells (equivalent to DNA content of Vimentin positive cells) is determined and set as a benchmark per definition 1. Correlating this to the DAPI signal of the Cytokeratin positive detected cells, the DNAIndex is calculated and cells with similar results are grouped. A DNAIndex close to one mirror a pseudo-diploid tumor fraction, whereas cells with a DNAIndex < 1 might be more the fragmented, necrotic, and apoptotic cells. The hyper-diploid tumor cell fraction is represented by a DNAIndex > 1 whereas it is essential that the more far the DNAIndex from 1 the higher the DNA content and thereby the more

probable pure tumor cells are included. For two samples (lymph node metastases ID53, 66) the DNAIndex could not be calculated due to technical issues. Those cell populations were selected one by one on basis of the fluorescent images presented from the system. It might be that the low tumor cell number of these samples was influencing the DNAIndex determination.

From the FFPE samples tumor cell populations with a median DNAIndex of 1,195 (range 0,77 – 2,57) were isolated. The population size varied between 2 and 468 and was dependent on the availability of cells. On trend a lower cell number was detected for the stromal cell populations (median 122, range 2 – 352) which is explainable that during the surgery the tumor tissue shall be removed completely but preferably without too much surrounding healthy tissue. The cell number of the tumor cell populations (median 136, range 18 – 468) can be dependent from different factors among others the content of tissue (e.g., sample with lowest (A) and highest (B) cell number, Figure 38), the tumor size, the thickness of slices and the cell amount involved, and the quality state, important for successful isolation of the cells, are most influencing.

After isolation the populations were amplified following the protocol for the whole genome amplification (2.12) but quality was not assessed by the connected QC assay because the used primer pairs were not giving meaningful results for higher fragmented FFPE material.

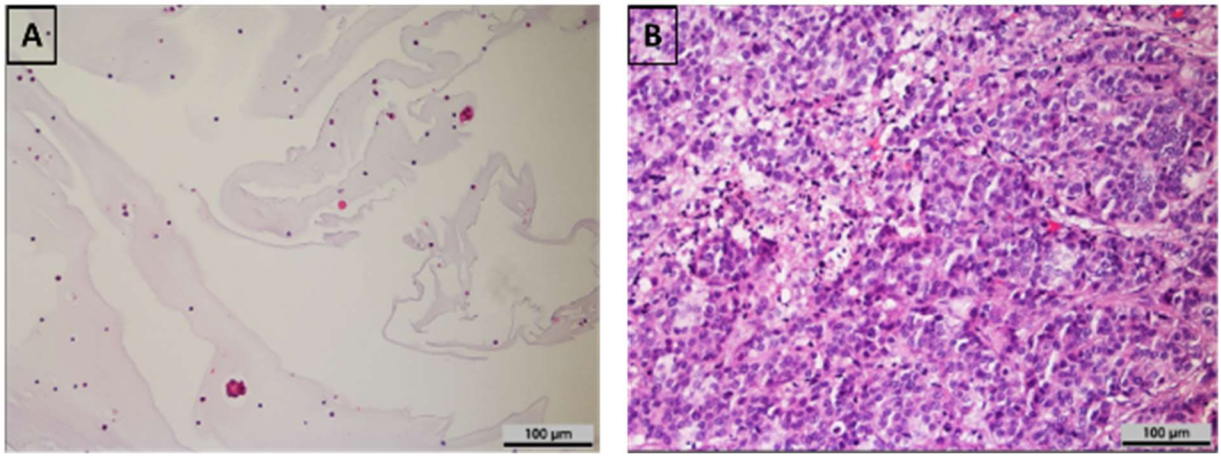

Figure 38 Hematoxylin-Eosin (HE) staining of FFPE slices.
Stained tumor tissue from patients with breast cancer and suspicion of leptomeningeal metastases (LM). A: HE stained formalin fixed paraffin embedded (FFPE) material of a pleural effusion patient ID21 (20 µm). B: HE stained FFPE material of a lymph node patient ID29 (20 µm). Violet dots are representing tumor cells while sample A (left) represent a sample with a low tumor content and sample B (right) a sample with a high tumor content.

3.10.3 DNA quality of FFPE derived cell populations

Prior to CNV analysis, the fragmentation and DNA amount was determined using the Bioanalyzer system (2.19). In general, one broad peak was detected at 200 – 700 bp (peak ~ 380 bp, **Figure 39** B) which represented the high fragmentation expected in DNA passed through the FFPE workflow independent of cell type (stromal, tumor). This was also confirmed by comparing the fragment size of DCCs isolated of CSF with main peaks around 700 bp. The isolated cell number is significantly correlated with the DNA concentration specified by the fluorescent units (FU) in the fragmentation profiles (**Figure 39**). Four samples (three stromal cell and one tumor cell population) could not be further processed because the DNA amount input would have been too low. It is not wondering that those samples are also the ones with the lowest cell numbers.

The storage period, the storage conditions and the embedding process of tissue can have an impact on the quality of DNA and the success of further downstream analysis. But since the analyzed tissues derived from different clinics no conclusion concerning storage conditions and embedding process could be performed. It can only be mentioned that the storage period of the samples cannot be correlated with the quality of DNA measured by fragmentation.

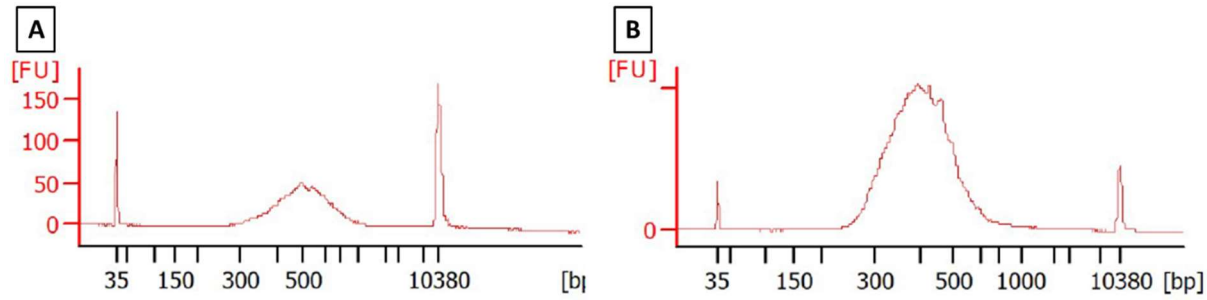

Figure 39 Fragmentation profiles of amplified cell populations from FFPE tissue.
Formalin fixed paraffin embedded (FFPE) tissue isolated from single cell suspension with the DEPArray™ technology and analyzed with the Bioanalyzer high sensitivity kit (Agilent). A: Isolated stromal cell population (size n = 2 cells) of FFPE pleural effusion tissue of breast cancer patient ID21 after whole genome amplification (WGA). B: Isolated tumor cell population (size n = 468 cells) of FFPE lymph node tissue of breast cancer patient ID29 after whole genome amplification (WGA).

3.10.4 CNV analysis of FFPE isolated cell populations

The CNV analysis was successful in 82 % (42/51) of processed samples. Nine samples (6 stromal, 3 tumor) could not provide evaluable data which was connected to the insufficient DNA amount necessary for sequencing (n = 4) or no sequencing output (n

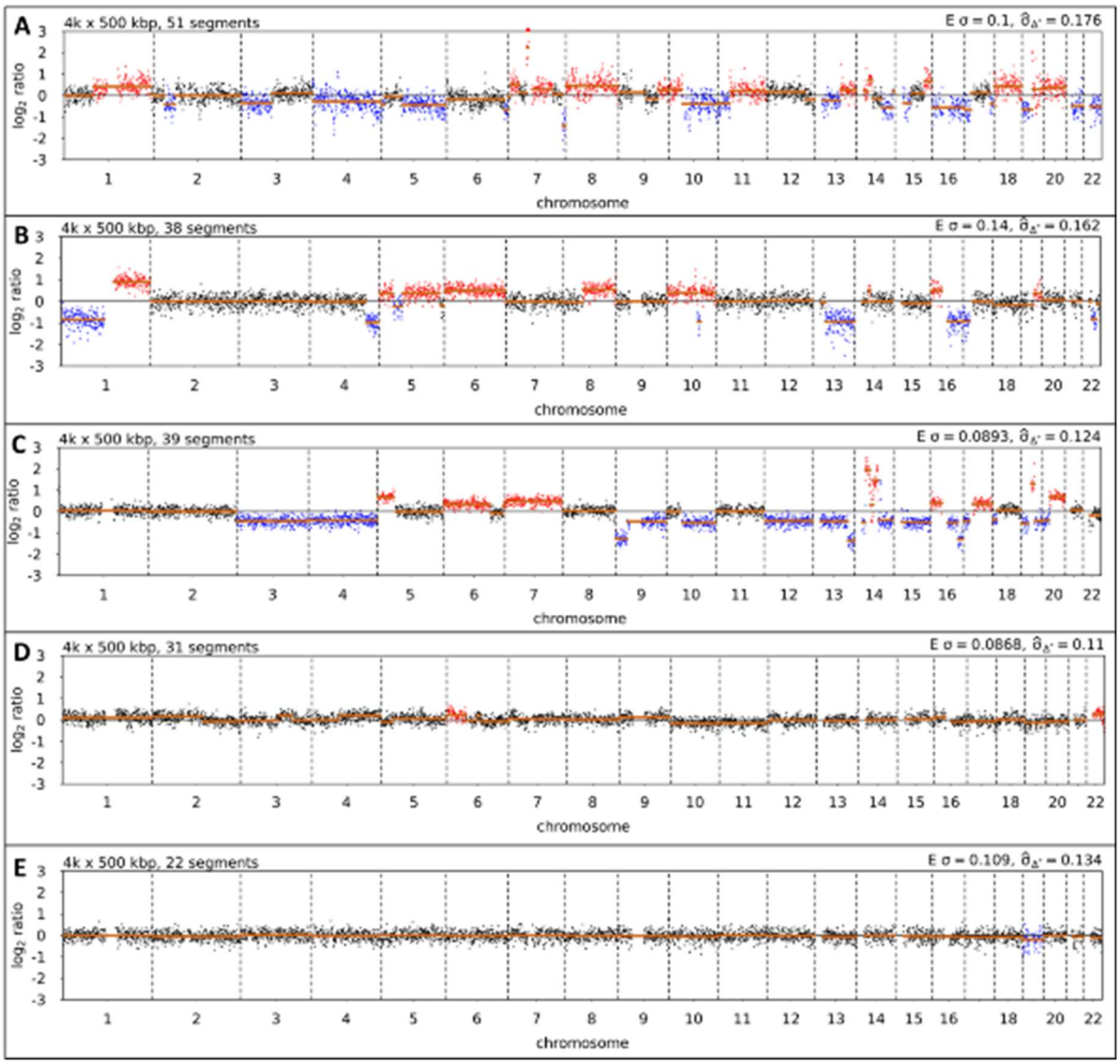

Figure 40 Copy Number Variation (CNV) profiles of FFPE isolated tumor cell populations. Formalin fixed paraffin embedded (FFPE) tissue derived tumor cell populations isolated with the DEPArray™ technology from three different patients with suspicion of leptomeningeal metastases. **A**: Aberrant CNV profile derived from primary tumor of gastric cancer patient ID56. **B**: Aberrant CNV profile derived from peritoneal metastasis of breast cancer patient ID14. **C**: Aberrant CNV profile derived from brain metastasis of lung cancer patient ID66. **D**: Slightly aberrant CNV profile derived from lymph node metastasis of melanoma patient ID38. **E**: Balanced CNV profile derived from peritoneal metastasis of breast cancer patient ID14. Evaluation of profiles see 2.22.

= 5). Going back to raw data those were also the samples with either a DNAIndex close to 1 or a low population number. So, the number of evaluable CNV profiles was reduced to 16 stromal cell populations and 26 tumor cell populations.

The isolated tumor cell populations were in 81 % (21/26) of the cases confirmed by aberrant CNV profiles as tumor DNA (e.g., Figure 40, A-C). Only two of them showed a slightly aberrant profile (e.g., Figure 40, D) with low copy number variations but also here DNAIndex (average 0,874) and the ratio between pseudo-diploid and hyper-diploid cells within the isolated population may assume a role. The latter is known to be important for the correct data interpretation because the higher the tumor cell content in the isolated cell population the more precise can aberrancies be detected (75). Five of 26 (9 %) isolated putative tumor cell populations showed a balanced CNV profile while three of them were derived from primary tumor. Interestingly further isolated tumor cell populations from additional metastases of those patients showed also balanced CNV profiles so that an individual sample related reason cannot be excluded.

The isolated and evaluable stromal cell populations (n = 16) were confirmed in 88 % (14/16) by a balanced CNV profile. The loss effect seen on Chromosome 19 (e.g., Figure 40, E) occurred in almost all balanced profiles and after consulting the bioinformatician experts this might be a technical effect only seen in FFPE derived samples.

3.10.5 Evaluation of patient specific data from different Biomarkers

The possibility to compare primary tumor tissue material and DCCs, both resected resp. withdrawn at the same timepoint, was given in gastric patient sample ID56 (Figure 41). On Chr 7p a gain is detected in both sample types, which is correlated to the EGFR gene (also confirmed by CNV statistic. Multiple variations in Chr 10q, 11p and 13 of the CSF isolated DCCs could argue that those aberrations facilitate cells to reach the CNS because they are missed in the primary tumor. In general, a lot of genetic similarities can be found in both sample types which confirms on the one hand

the tumor affiliation of the DCCs but shows on the other hand also their ability to develop individual CNS seeking potential.

As described above from some tissue the isolation of more than one tumor cell population was performed which represent tumor cells varying in ploidy measured by the DAPI signal intensity ratio (DNAIndex). In one breast cancer patient (sample ID64) the primary tumor was detected in 2015 but could unfortunately not be processed for research purposes. The tissue material from a lymph node metastasis removed in 2019 delivered two different tumor cell populations (DNAIndex 1,64 and 1,03). Interestingly, the three isolated CSF-DCCs from 2021 could be assigned to the two different tumor cell groups (Figure 42). While DCC4 shows the same variation pattern than the tumor cell population with DNAIndex 1,64 the DCC1 might be more related to the tumor cell population with the DNAIndex 1,03. Considering the number of DNA

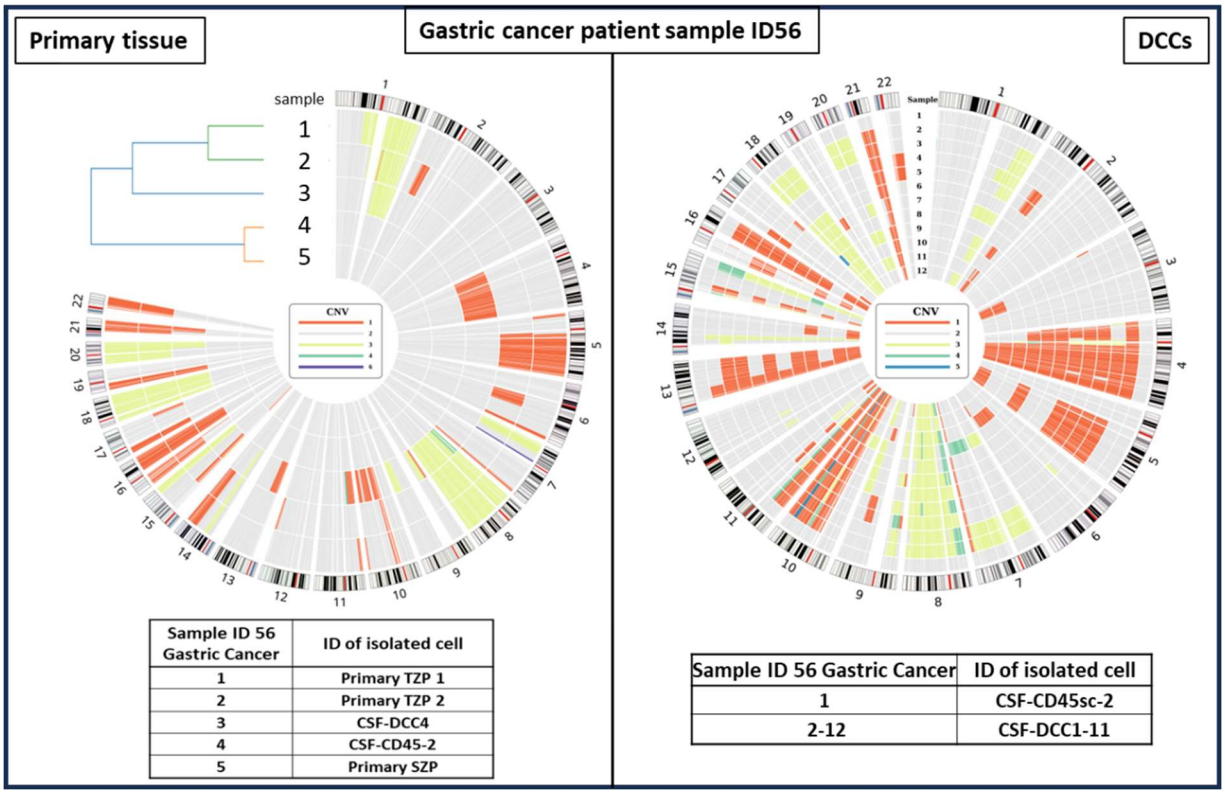

Sample ID 56 Gastric Cancer	ID of isolated cell
1	Primary TZP 1
2	Primary TZP 2
3	CSF-DCC4
4	CSF-CD45-2
5	Primary SZP

Sample ID 56 Gastric Cancer	ID of isolated cell
1	CSF-CD45sc-2
2-12	CSF-DCC1-11

Figure 41 Circosplot of CNV analysis from gastric cancer patient sample ID56.
Left: Copy number variation (CNV) profiles derived from primary tumor cell populations (TZP, sample 1, 2) and stromal cell population (SZP, sample 5) of formalin fixed paraffin embedded (FFPE) tissue compared to one single DCC (sample 3) and one single CD45 positive cell (sample 4) both cerebrospinal fluid (CSF) derived. **Right**: CD45 positive (sample 1) and disseminated cancer cells (DCCs, sample 2-12) isolated from the same CSF sample. Colors in the middle of the plot represent the ploidy of colored regions in the profiles.

variations in the tumor cell populations, it could be confirmed that the higher the DNAIndex resp. the higher DAPI signal intensity, the more alterations can be detected in the isolated DNA. This makes the DNAIndex a trustable variable for selecting cells predestinated for generating valuable molecular information.

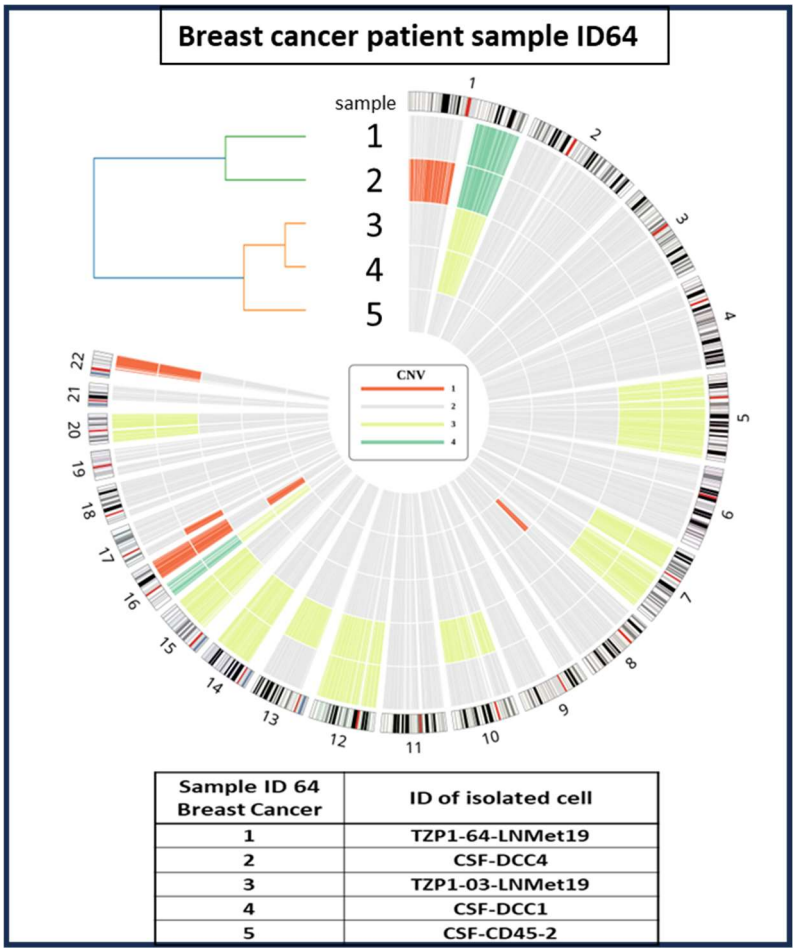

Sample ID 64 Breast Cancer	ID of isolated cell
1	TZP1-64-LNMet19
2	CSF-DCC4
3	TZP1-03-LNMet19
4	CSF-DCC1
5	CSF-CD45-2

Figure 42 Circosplot of copy number variation (CNV) profiles patient ID64.
Formalin fixed paraffin embedded (FFPE) lymph node tissue from breast cancer patient ID64. Isolated tumor cell populations (TZP, sample 1, 3) compared to single DCCs (sample 2,4) and a single CD45 positive cell (sample 5) all cerebrospinal fluid (CSF) derived from the same patient. Colors in the middle of the plot represent the ploidy of colored regions in the profiles.

Another patient with molecular information from two different sources is a melanoma patient (sample ID38). A lymph node metastasis detected in 2018 was analyzed by CNV analysis and compared to CSF derived DCCs from 2020. Unfortunately, the DNAIndex of the isolated tumor cell population was 0,779 why the aberration pattern seems to be doubtful because most of the profile is balanced. Even though both gains

on Chr 6q and 22 (Figure 43 A) were retrieved also in the molecular analysis of the years later isolated CSF-DCCs (Figure 43 B), a comparison of both biomarker is not senseful and less valuable. Nevertheless, a comparison of molecular information from different sources can be a useful option not only to determine clinically relevant information but also to monitor the disease in a chronological sequence to quickly intervene if changes are detected.

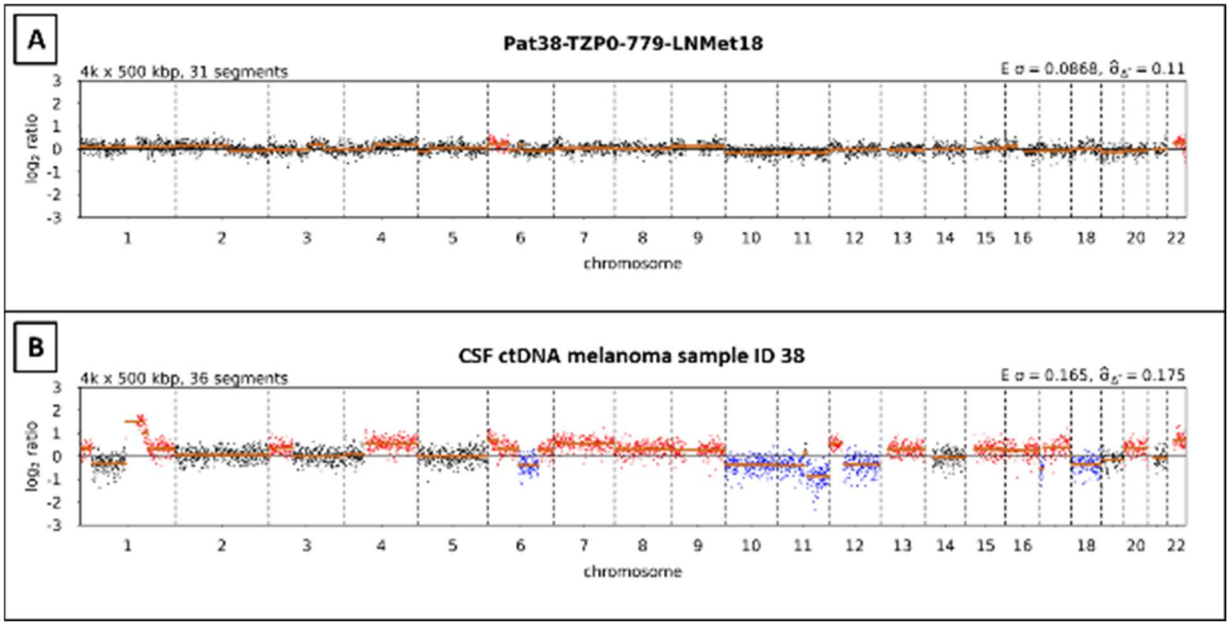

Figure 43 CNV profiles from melanoma patient sample ID38.
Copy number variation (CNV) profiles from **A**: 2018 isolated tumor cell population (TZP, DNAIndex 0,779) from a formalin fixed paraffin embedded (FFPE) lymph node metastasis. **B**: CNV profile of circulating tumor DNA (ctDNA) isolated from cerebrospinal fluid (CSF)from the same patient.

3.10.6 Serial CSF sampling of a breast cancer patient

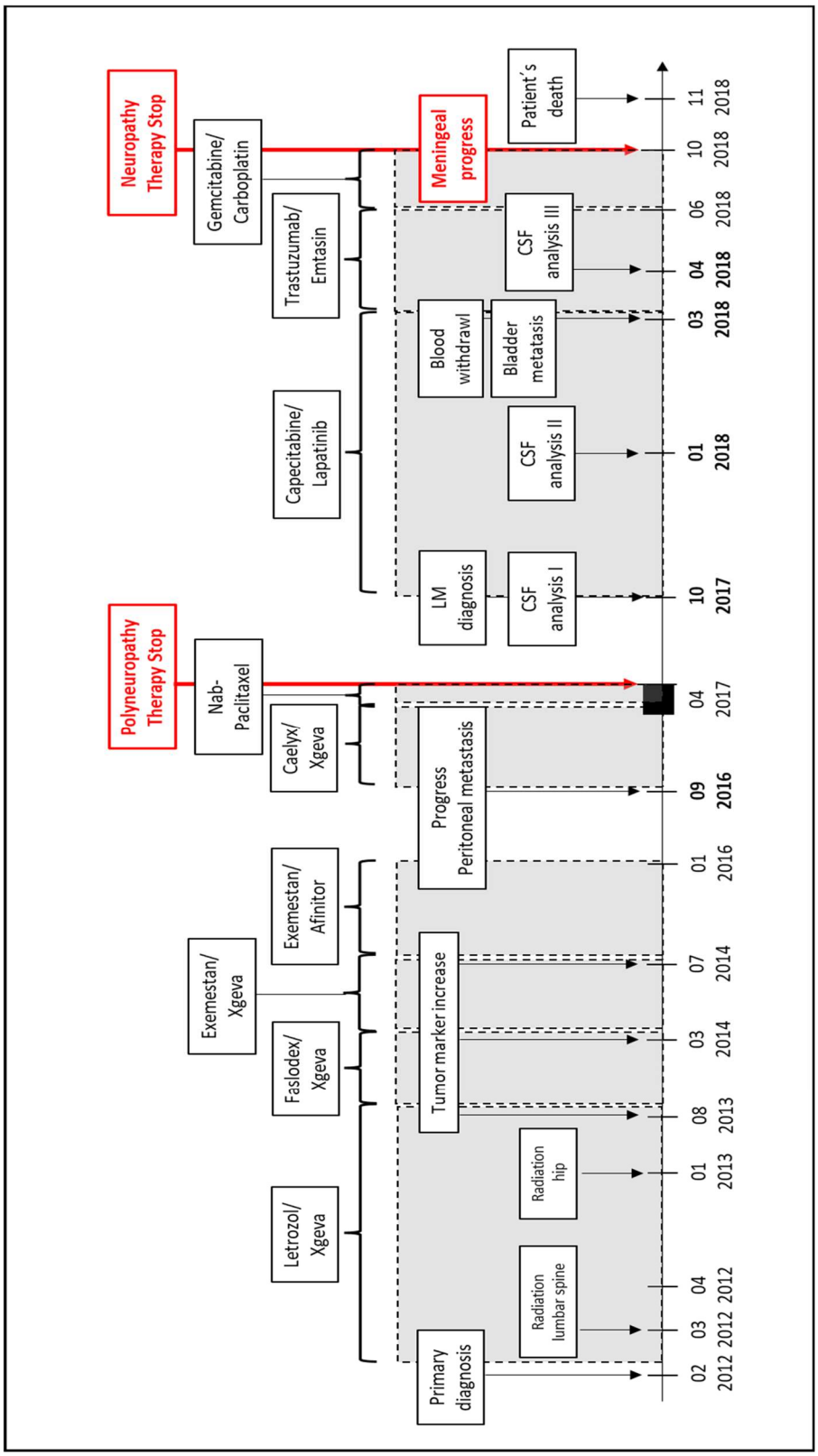

Figure 44 Course of disease of breast cancer patient ID14.
Therapy timepoints, sample withdrawal and progress of breast cancer ID14 with the analysis of serial CSF sampling.

In an individual index patient with breast cancer, we were able to collect three CSF samples at three different timepoints (Figure 44). For a more comprehensive analysis of this index patient, we additionally collected FFPE tissue from a peritoneal metastasis (2016) and bladder metastases (2018). In both FFPE specimen, we confirmed high tumor content by HE staining (Figure 45) and subsequently isolated pure tumor cell and stromal cell populations (average cell number for all isolated cell populations 150) using the DEPArray™ FFPE sample prep workflow and isolation protocol.

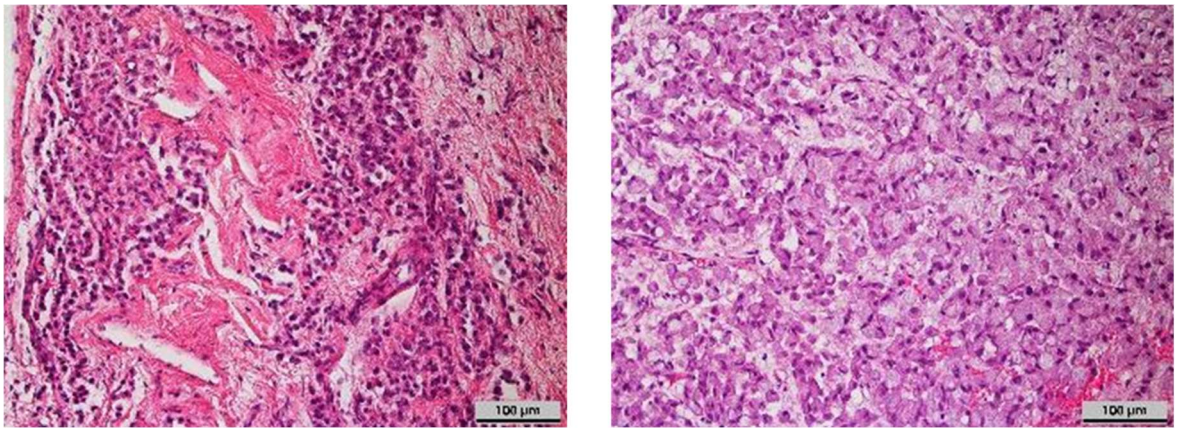

Figure 45 Hematoxylin/Eosin staining of FFPE tissue.
Formalin fixed paraffin embedded (FFPE) tissue derived from breast cancer ID14. Left: Peritoneal metastases 2016; Right: Bladder metastases 2018.

Interestingly, we were able to define two distinct tumor cell subpopulations in the peritoneal metastasis based on the DNA Index, a surrogate for aneuploidy of isolated cells. The isolated cell populations were subjected to WGA following CNV analysis. Comparing the CNV profiles of the isolated tumor cell populations of the peritoneal and the bladder metastases, we observed that they derive most likely from the same subclone (Figure 46).

Moreover, those cells from tissue of visceral metastasis were highly like CNV profiles obtained from CTCs from blood. Interestingly, the DCCs from CSF harbored distinct CNVs (i.e., on chromosomes 8, 9, 11, and 18) indicating that these cells originate from a distinct subclone specific for the CNS (Figure 47, Figure 48).

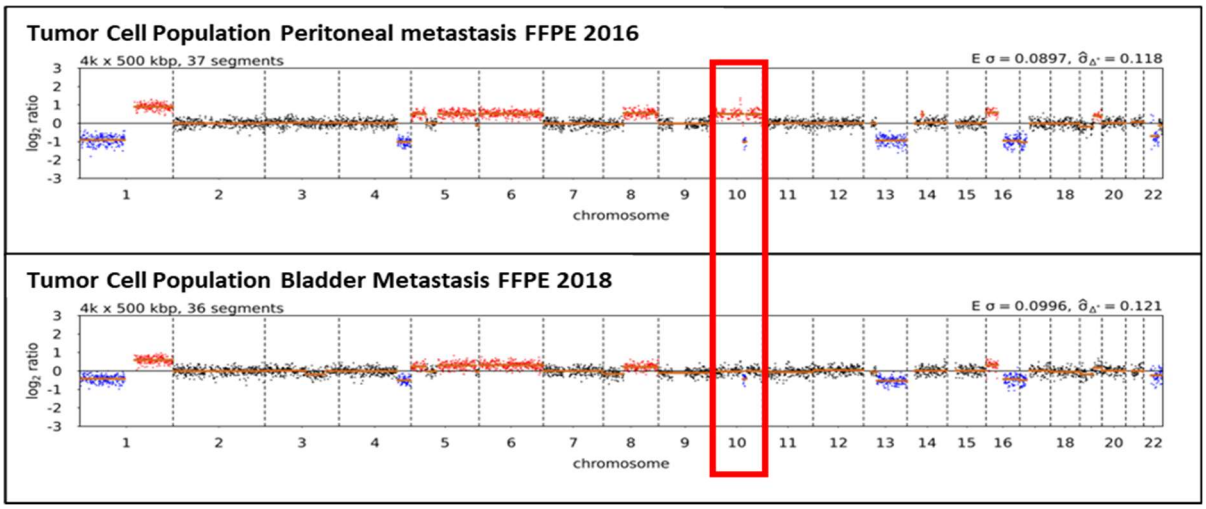

Figure 46 Copy number variation analysis of FFPE tissue from patient ID14.
CNV profiles of formalin fixed paraffin embedded (FFPE) tissue slices of breast cancer ID14. Up: Tumor cell population isolated with the DEPArrayTM system from the peritoneal metastasis in 2016. Below: Tumor cell population isolated with the DEPArray TM system from the bladder metastases in 2018.

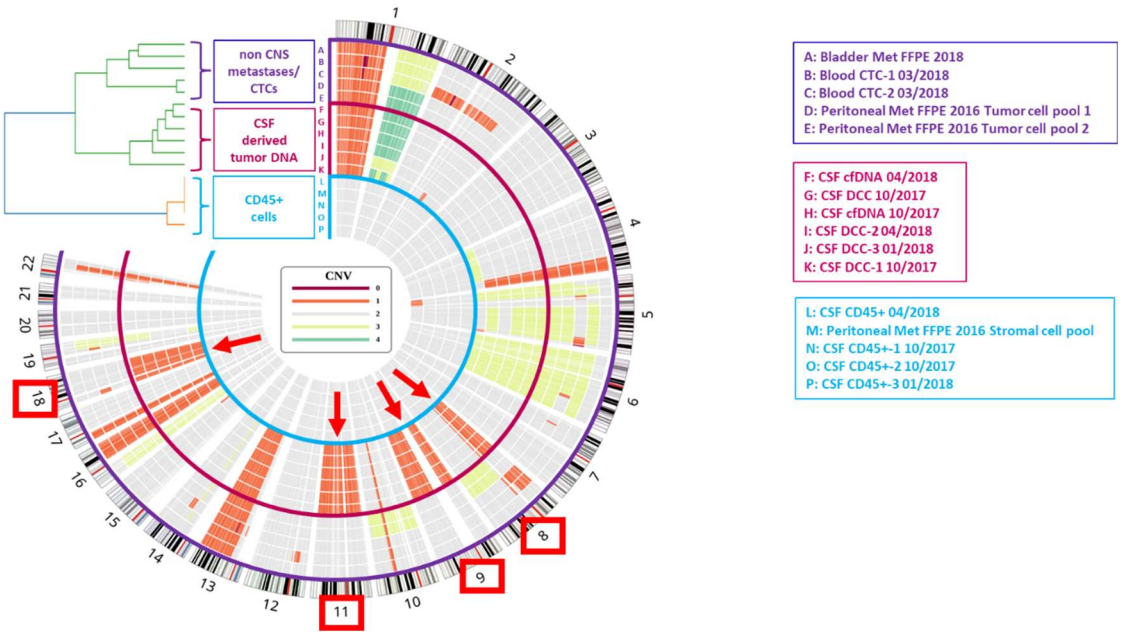

Figure 47 Circosplot of CNV profiles from breast cancer patient ID14.
Samples are derived from formalin fixed paraffin embedded (FFPE) bladder and peritoneal metastases tissue, compared to single DCCs and single CD45 positive cells from cerebrospinal fluid (CSF) and stromal cell populations as well as from circulating tumor cells (CTCs) from blood derived from the same patient. Colors in the middle of the plot represent the ploidy of colored regions in the profiles, input of the figure are the copy number variation (CNV) profiles of the samples.

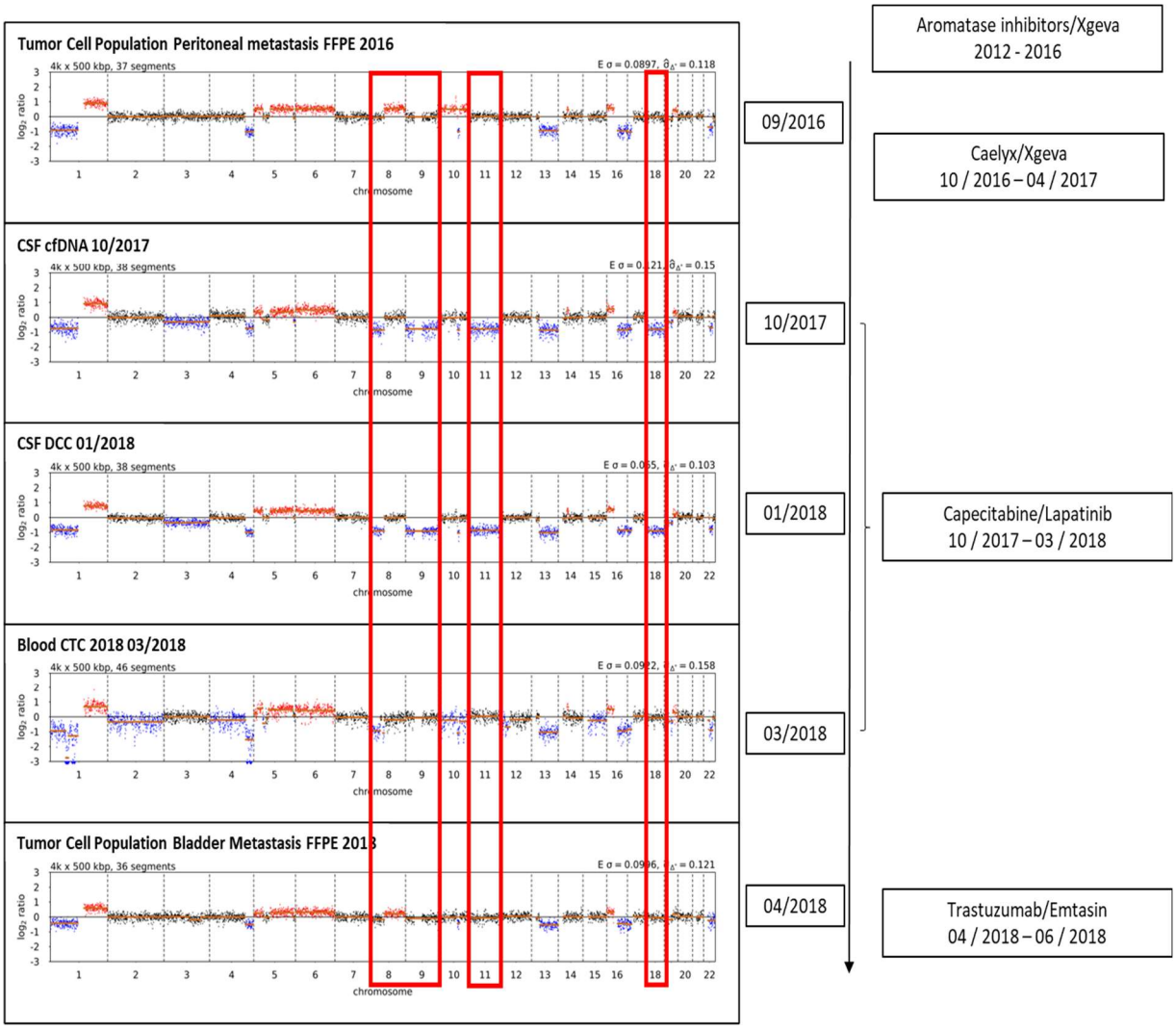

Figure 48 Copy number variation (CNV) profiles.
Aberrant CNV profiles of different biomarkers derived from breast cancer patient ID14 under therapy.

3.11 MRI and Cytology – the gold standard for examination of LM

Following the guidelines of the European Association of Neuro-Oncology (EANO) and European Society for Medical Oncology (ESMO), the gold standard examination for patients with solid cancer and leptomeningeal spread is neuroimaging, CSF cytology and leptomeningeal biopsy, if possible. The purpose of this thesis was not only to highlight the molecular aspect of the liquid biopsy CSF analysis of DCCs and cfDNA but also to verify the sensitivity of the molecular liquid biopsy assay by results of parallel performed cytological CSF analysis.

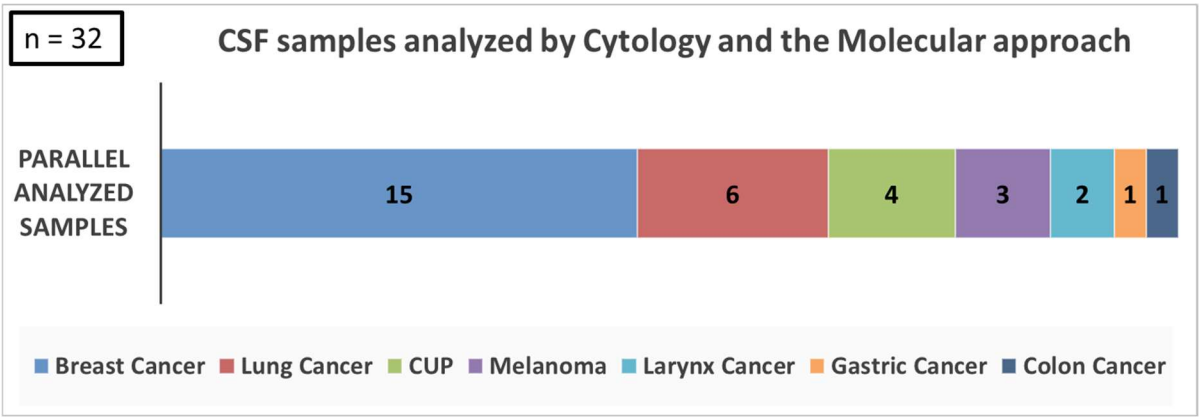

Figure 49 Cerebrospinal fluid (CSF) sample availability for parallel analysis.
Samples compared with the two technologies CellSearch™ Liquid Biopsy and Cytological analysis. In total 32 samples from 29 patients were available among them breast cancer (n = 15), lung cancer (n = 6), cancer of unknown primary (CUP) (n = 4), melanoma (n = 3), larynx (n = 2), gastric (n = 1) and colon cancer (n = 1).

3.11.1 Cytology results

Therefore, 32 CSF samples were analyzed in parallel (Figure 49) by cytology and the molecular CSF approach (CellSearch® enrichment and ctDNA analysis) to verify the reliability of the latter. 32 % (10/32) of samples were positive by cytology, while the detection rate for LM of the molecular approach was slightly higher with 38 %. This means that the molecular approach seems to be at least as reliable than the CSF cytology elsewise more. But going more in detail, 82 % (26/32) of samples showed concordant results. While eight were positive and 18 negative for cancer cell detection six samples remained different, three CUP, two breast and one colon carcinoma. Two

were detected only by the cytological (ID27, ID21) and four by the molecular CSF approach (ID4, 10, 22, 24, Figure 50). It must be admitted that two of the negative samples in cytology were positive counted via ctDNA in the molecular approach and no cells were detected only by the CellSearch® workflow. But the combination of both approaches in the molecular liquid biopsy analysis resulted in four more positive detections of LM than in the cytological approach.

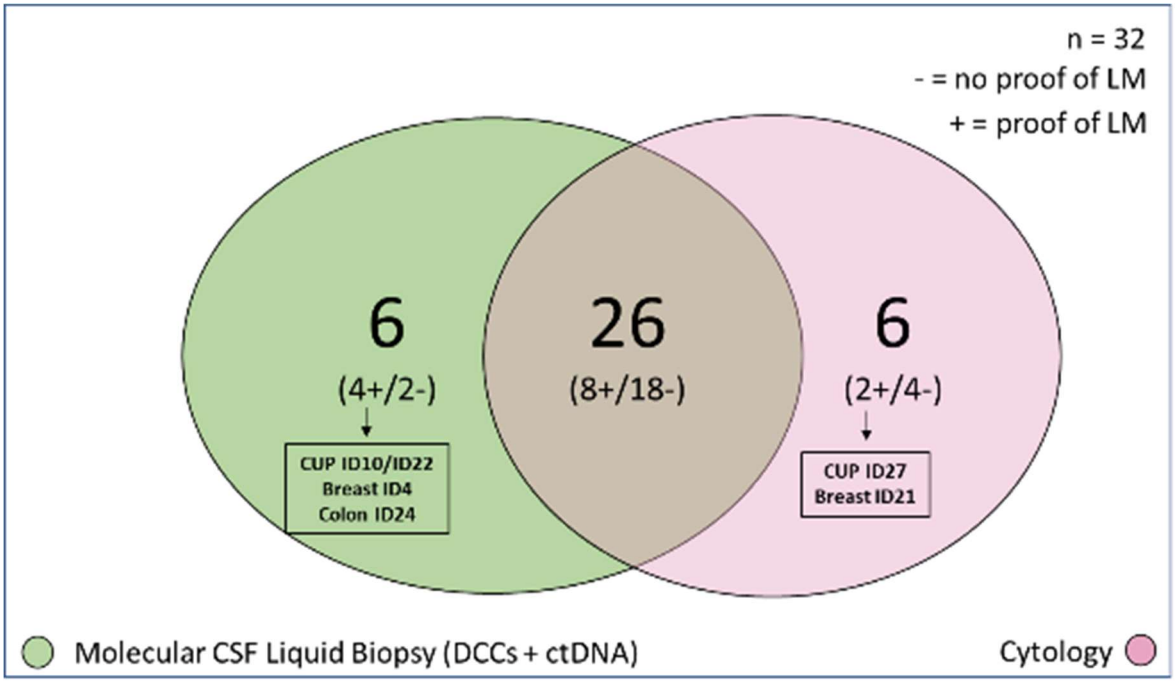

Figure 50 Results of parallel analyzed cerebrospinal fluid (CSF) samples.
Thirtytwo samples were analyzed with the molecular CSF Liquid biopsy approach, combining disseminated cancer cell (DCCs) and circulating tumor DNA (ctDNA) enrichment and the Cytological approach. Results are illustrated in a Venn diagram. 26 samples show concordant results, while 8 were positive ("+") for leptomeningeal metastases (LM) and in 18 samples no cells were detected ("-"). Six sampes in total showed different results while two were only positive for Cytology (rosa, CUP ID27, Breast ID21) and two were positive only for the CellSearch™ approach (green, CUP ID27, Breast ID21). P = 0,0003, Cramers V Test = 0,71

3.11.2 MRI results

To have a reference for both CSF analysis methods the imaging data of patients derived from the timepoint of CSF withdrawal were considered (n = 30; Figure 51). 13 (43 %) of those were confirmed for leptomeningeal spread while 17 (57 %) were negative in the MRI.

Compared to the molecular CSF analysis the MRI data were concordant in only 50 % of samples (15/30) while the sensitivity for both methods was similar with 40 % (molecular CSF, 12 positive) and 43 % (imaging, 13 positive, Figure 52).

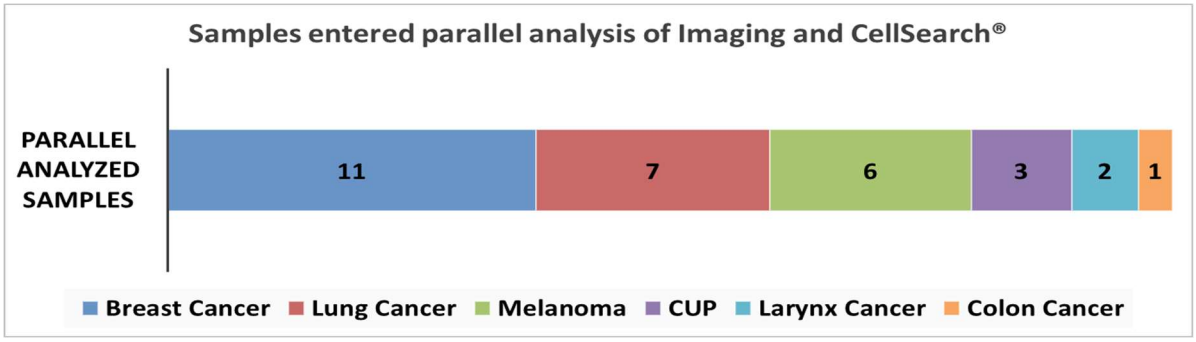

Figure 51 Cerebrospinal fluid (CSF) sample availability for parallel analysis.
In total 29 samples of 27 patients were analyzed with the two technologies CellSearch® Liquid Biopsy and imaging. Among them breast cancer (n = 11), lung cancer (n = 7), melanoma (n = 6), cancer of unknown primary (CUP) (n = 3), larynx (n = 2) and colon cancer (n = 1).

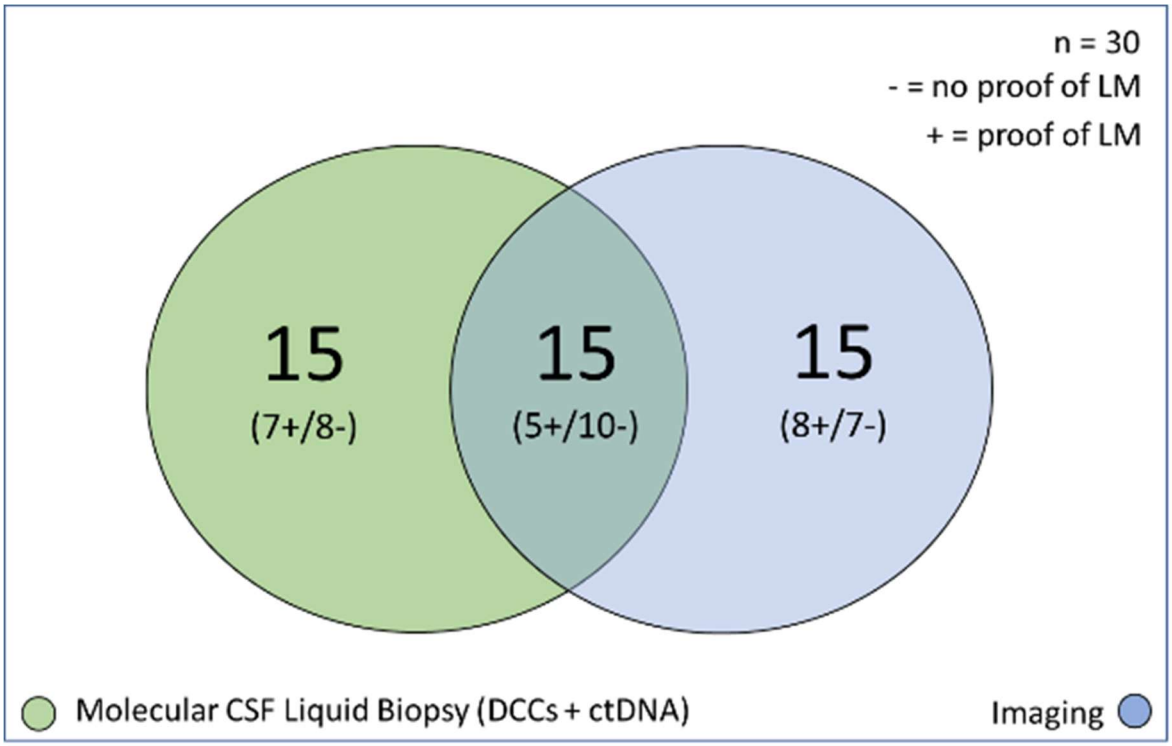

Figure 52 Results of parallel analyzed cerebrospinal fluid (CSF) samples.
In total thirty samples were analyzed with the CSF liquid biopsy approach combining disseminated cancer cell (DCC) and circulating tumore cell (ctDNA) enrichment. Results are illustrated in a Venn diagram. 15 samples showed concordant results, while 5 were positive ("+") for leptomeningeal metastases (LM) and in 10 samples no cells were detected ("-"). 15 samples in total showed different results while eight were positive only for imaging (blue) and seven were positive only for the CellSearch® approach (green).

3.11.3 Gold standard versus molecular CSF liquid biopsy analysis

LM are classified as confirmed if the cytology and/or the imaging data show a positive result. The relative detection rate for LM was higher by imaging (43 %, 13/30) than cytology (32 %, 10/32) which pointed already out that a difference in the detection reliability exists (Figure 53). 24 samples could be compared directly in parallel for both standard methods, and data confirmed that the imaging performed better with 38 % (9/24) positive samples than the cytology with 29 % (7/24) LM detection. Five positive samples could only be detected by imaging and three only by cytology, which resulted

in a final concordance in 67 % of samples (4 positive, 12 negative) and means that the result for every third sample is different (Figure 53, “Comparison”).

The question, if the molecular CSF liquid biopsy approach, including enrichment of DCCs and cfDNA, is an alternative for a reliable statement about leptomeningeal affection or not could be solved with Figure 54. Opposing the molecular CSF liquid biopsy results to those methods most of the LM positive samples could be detected by our approach (n = 10), followed by MRI (n = 9) and cytology (n = 7). This showed that all positive sample could be covered by imaging and the molecular CSF liquid biopsy analysis.

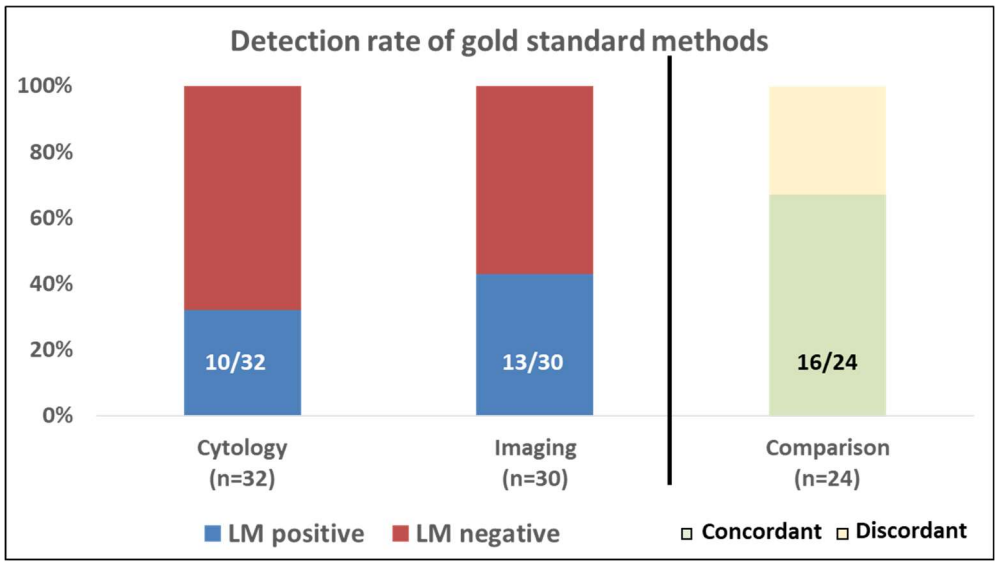

Figure 53 Detection rate of LM by the gold standard methods.
Cytology and imaging are the gold standard for leptomeningeal metastases (LM) diagnosis, while 32 % of sample were detected LM positive with the cytological approach and 43 % samples were positive by imaging. 24 samples could be compared in parallel and 67 % of them showed concordant results, meaning that ever third result is different.

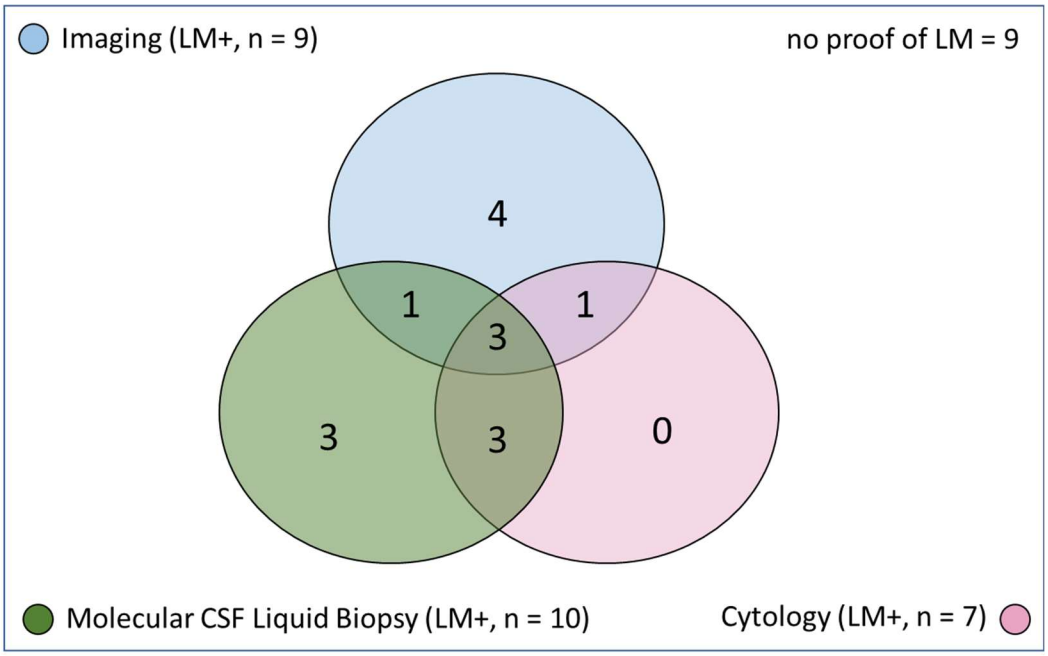

Figure 54 Results of parallel analyzed cerebrospinal fluid (CSF) samples.
In total twenty-four samples were analyzed with the CellSearch® CSF Liquid biopsy (DCCs and ctDNA), the cytology approach, and the imaging. Nine of 24 samples were negative for leptomeningeal spread in all three methods. and the Cytological approach illustrated in a Venn diagram. 28 samples show concordant results, while 8 were positive ("+") for leptomeningeal metastases.

4. Discussion

As leptomeningeal metastases (LM) are associated with a poor prognosis, the clinical objective is to support patients by managing symptoms, controlling disease progression, and thus improving quality of life (76). Although cerebrospinal fluid (CSF) cytology and imaging can detect tumor involvement of the central nervous system (CNS), both methods are known to have low sensitivity and limitations (8). These become evident in the field of molecular characterization for assessing predictive tumor biomarkers, which is one of the mainstays for personalized treatment decisions. Here, liquid biopsy analysis of CSF can be a valuable resource for clinical decision-making. Therefore, the aim of the study was to investigate the potential of a workflow enabling the detection and analysis of tumor DNA, including single tumor cells and ctDNA, from CSF to increase the likelihood of confirming leptomeningeal spread and to enable therapy prediction through genetic analysis in the future. By incorporating the analysis of extra-CNS tumor tissue (primary tumor or visceral metastases), this workflow also represents a novel tool for investigating cellular heterogeneity of systemic cancer and defining the genetic landscape of CNS-seeking subclones.

4.1 The additional value of the molecular CSF liquid biopsy

The enrichment of EpCAM/CK positive cells with the CellSearch® workflow is a trustable and competitive alternative to the cytological gold standard for CSF analysis. Considering the number of cases and the different entities in this thesis it seems that the ferrofluidic capturing is more sensitive than cytology for detecting both high and low cell numbers, regardless of the primary tumor type. Twelve of thirteen (92 %) positive CellSearch enriched DCC samples could be confirmed as tumor derived. Although if the CellSearch® system was initially developed for detecting circulating tumor cells (CTCs) in blood (31) it has shown increasing success in analyzing other liquid biopsy sources (8,10,33,47,48) in recent years, as supported by our data.

Furthermore, our method offers an additional benefit compared to conventional cytology: the ability to perform molecular downstream analysis on disseminated cancer

cells isolated from CSF. We confirmed the tumor origin in 98 % of the EpCAM/CK-positive cells enriched with the CellSearch® workflow by identifying aberrant copy number variation (CNV) profiles, thus validated the method through molecular analysis. This enrichment method demonstrates a very high specificity of 92 % (12/13) for DCC positive samples (determined by fluorescent signal after the magnetic bead enrichment) compared to sensitivity of MRI and CSF cytology (77–79). These findings were further supported by the balanced profiles of CD45-positive cells derived in 11 out of 13 cases, indicating that the CellSearch® workflow is a reliable approach for detecting and selecting real tumor cells.

The molecular data offered a valuable source for gaining important insights into the genetic landscape of cancer. Analysis revealed known cancer-related mutations not only in DCCs but also in circulating tumor DNA (ctDNA). For many cancer types, gene variations are well studied and often associated with therapy response (80–87). For instance, in breast cancer, amplifications are primarily focused on *ERBB2*, *CCND1*, *PIK3A*, and *EGFR*, while deletions accumulate in *PTEN, CDKN2A, KMT2C (MLL3)*, and *MAP2K* (88–90). By analyzing single cells isolated from CSF, we were able to confirm cancer related changes by copy number variation for the patients within this collective. This included cancer of unknown primary (CUP) patient samples, in which gains described in various cancer types could be detected, e.g. cervical cancer (91), non-small cell lung cancer (92) but also various types of leukemia, in particular acute myeloid leukemia (93,94). Even if this was not analyzed in a systematic way in this thesis this possibility underscores the potential of DNA isolation from CSF for further molecular examinations, both to characterize tumor type or landscape for patients not yet diagnosed but evidently affected by cancer, and to facilitate more targeted analysis for rapid clinical decision-making.

4.2 Further validation needed for CSF DCC detection in lung cancer patients

For lung cancer, only one of eight CSF samples was positive with the molecular liquid biopsy workflow. None of these eight samples were confirmed to have leptomeningeal metastases (LM) by imaging or cytological analysis. It appears that the various types of lung cancer included, such as small cell lung cancer, non-small cell lung cancer, and bronchial carcinoma, collectively represent true negative samples. Despite the fact that lung cancer is associated with a high percentage of circulating tumor cells, at least in blood (46,95), and is one of the three common causes of LM (5) this could not be confirmed for CSF samples from lung cancer patients analyzed in our study. Data from other studies in our laboratory also indicated difficulties in the enrichment of lung cancer circulating tumor cells with the CellSearch® system, at least in blood. This may be due to a highly variable cytokeratin expression pattern among different lung cancer subtypes and their individual likelihood for LM development (5,96,97). In a separate study focusing specifically on the subtype of lung cancer patients, this effect could be further investigated in detail by including different marker, technologies but also by comparing the value of different biomarker.

4.3 Multiple markers could raise DCC detection in melanoma patients

LM spread is described in 5 up to 25 % of melanoma patients (2,15) which aligns with the positivity rate of our CSF liquid biopsy approach (2 out of 8 positive samples). Similarly, only one case was detected by conventional CSF cytology, while imaging of those eight patients resulted in a detection rate for LM of 63 % (5 out of 8). This raises questions about these discrepancies and the utility of molecular analysis of CSF in melanoma patients.

Intratumor heterogeneity is well-documented in various solid cancer types (98) and metastatic melanoma is known to be a highly heterogeneous tumor (99). Therefore, the methods to analyze circulating tumor derived cells should address this diversity. The most common marker used for CTC enrichment in melanoma patients is the

surface melanoma-associated chondroitin sulphate proteoglycan (MCSP), also known as CSPG4, HMW-MAA and MSK16, which plays a role in cell adhesion, migration, and invasion. Its expression in CTCs, correlated with the clinical stage of the patient (100), confirms its reliability. Additionally, the melanoma cell adhesion molecule (MCAM, CD146) is often used as a detection marker for circulating tumor cell, playing a pivotal role in the progression of this malignant disease (101,102).

In our approach the HMB45 antibody was used as a diagnostic marker targeting the gp100 (Pmel17) protein, a melanocyte differentiation antigen, to identify melanocytic lesions. This biomarker has been widely shown to identify melanocytic lesions, including melanoma, and can aid in distinguishing them from other types of tumors and lesions (103–105). Although it is possible to detect and isolate melanoma CTCs using this biomarker in a single staining approach, the additional value of using a combination of markers could be substantial (106,107).

To enhance the yield of disseminated cancer cells in CSF from melanoma patients, a combination of the most promising marker could be an option. Several enrichment methods would be possible, but an automated option for reproducible results, such as the CellSearch® system with the Circulating Melanoma Cell (CMC) assay, which already includes a combination of MCAM and MCSP as enrichment and detection marker with further possibilities for a third specific marker, could be considered. Although limited data are available, the CellSearch® assay for melanoma is described as a successful analysis methods for CTCs in melanoma patients with advanced disease stages (108–110). Nevertheless, we believe that a combination of melanoma markers for detecting DCCs in CSF, regardless of the underlying technology, could be beneficial for generating individual molecular profiles valuable for therapeutic decision-making.

4.4 Standardized quantification of DCCs from CSF necessary

Typically, subsequent cell detection after CellSearch® enrichment is conducted using the automated CellTracks AnalyzerII® device, relying on the fluorescent signal of the cells. However, our data revealed that the system encountered issues in approximately

two-thirds of the samples (20 out of 31), struggling to find the focus for automated cell detection. This observation aligns with findings from studies utilizing the CellSearch® system to detect DCCs in CSF (33). The cause for those difficulties might be the fact, that CSF is a very cell rare fluid (111) even though higher cell numbers are anticipated in diseased individuals.

The CellTracks Analyzer II® relies on detecting a signal, usually the DAPI signal of CD45-positive blood cells, to ensure the identification of putative tumor cells in the correct focus. However, if the analyzed solution lacks these cells, as in CSF, the system fails to locate the correct focus and cannot scan the cartridge. This could be an explanation for samples with no DCCs detected or a very low cell number (<70 cells), but we observed this effect even in samples with very high cell numbers (>20.000 cells). A reliable automated count for CSF samples was only achievable for a medium cell number range (70 – 20.000 cells). For very low or very high cell numbers, manual counting under the fluorescence microscope was necessary.

To overcome these difficulties and to achieve continuous, standardized screening conditions, DAPI fluorescent magnetic beads, such as Dynabeads (ThermoFisher), could be a solution. By adding a defined number of these beads to the sample, the system would be able to find the focus necessary for counting real cells. Since the CellSearch® workflow itself includes a cell specific marker, cells and beads should be distinguishable by the automated CellTracks AnalyzerII® and yield reliable results regardless of the tumor cell number in the sample.

This step in our single-cell enrichment workflow holds significant importance in various aspects. Firstly, circulating tumor cells, particularly in blood, and their quantity, are recognized as predictors of disease progression, overall survival, treatment response, and prognosis in various cancer types (10,34,100,112–115). It has recently been confirmed for circulating cells detected in CSF as well (47). With reliable, standardized counts, monitoring patients under therapy through serial CSF analysis could provide valuable insights.

Furthermore, quantification enables the selection of samples with a promising DCC yield for isolation. This is crucial for determining the appropriate isolation method, whether manual for very low numbers or automated for higher cell counts. Additionally, the sample screening and counting step under the microscope offer insights into the sample quality through morphological examination. DCC morphology can vary widely depending on factors such as origin, differentiation stage, and enrichment method (116,117). We confirmed that cells with intact nuclei and clear cytoplasm have a better preserved DNA and are more suitable for molecular downstream analysis (61). In daily laboratory practice, attention to sample viability and morphology during the initial screening step is valuable for pre-assessing samples for successful downstream molecular analysis and for optimizing time and resources.

4.5 High quality CSF single cells for molecular downstream analysis

The isolation of DCCs from CSF yielded single cells with significantly higher quality (76%) compared to circulating tumor cells (CTCs) isolated from blood (36%). Since the quality of cells is known to be correlated with successful downstream analysis (61), CSF emerges as a valuable source for generating reliable molecular data from DCCs (26). Interestingly, the data suggested that cell quality might be linked to tumor type, as indicated by the lower genomic integrity index (GII) observed in melanoma samples compared to carcinoma.

While such a correlation has not been described in the literature, it is more likely attributed to technical factors. For melanoma cells, the isolation process was conducted from glass adhesion slides, where cell detachment is achieved by scratching. This procedure, less gentle than isolating cells from solution as performed for carcinoma samples, may impact cell quality.

Furthermore, this assumption is supported by quality differences observed in cells isolated manually from suspension versus those isolated automatically with the DEPArray^{TM} system. Less than half (46 %) of cells isolated with the automatic system reached a quality suitable for molecular analysis (61). Considering the sample number

evaluable for this direct comparison (n = 2), it may represent an isolated issue requiring further investigation on a larger scale. Nonetheless, these findings suggest that the isolation method influences cell quality, with micromanipulation-based isolation from suspension being gentler on cells, albeit more time-consuming for the user.

4.6 CSF – a possible source for functional analysis

In general, DNA analysis of circulating tumor cells, holds the potential to provide crucial insights into the genetic landscape of cancer, thereby improving diagnosis, therapy development, and treatment outcomes for patients. By examining genetic heterogeneity (118–122) and mutations it becomes possible to identify genetic alterations driving cancer progression, thus pinpointing potential therapeutic targets (37,123–125). Moreover, RNA analysis of CTCs offers additional advantages in dynamic gene expression patterns. The high-quality DCCs isolated from CSF present an opportunity to identify RNA-specific molecules as predictive or prognostic biomarkers (126,127) for diagnosis, prognosis or therapy monitoring.

In addition to molecular analysis of high-quality good DNA from DCCs, CSF can also serve as an option for functional analysis to gain future insights into various cancer types. In 2013 Zhang et al. (128) established the first primary cultures from CTCs obtained from patients with advanced-stage breast cancer, enabling the isolation of long-term cultures of human breast cancer CTCs and identification of markers for brain metastasis signature. In recent years, several groups have demonstrated the feasibility of establishing different models, including in-vitro cell cultures, in-vivo animal models, as well as tissue and organoid models (129). These models can be utilized for analyzing tumor biology and metastasis, identifying new therapeutic targets, and predicting therapy resistance and drug response (130–132).

To generate these models, it is necessary to enrich viable cells with the potential to expand. The high DNA quality and the intact morphology of DCCs isolated from CSF present a promising option for generating these cell cultures. In our cohort we tried to

cultivate cells from CSF of eight samples under organoid conditions. In one case, six small organoids were successfully isolated and confirmed as tumor material through downstream molecular analysis, although LM positivity could not be detected by the CellSearch® enrichment. Nevertheless, even if the cultivation conditions must be optimized, the potential for CSF-DCCs as for establishing a cell model for functional analysis remains.

4.7 CSF circulating tumor DNA - an important supplemental biomarker

In addition to DCCs, also circulating tumor cell free DNA (cfDNA) represents another liquid biopsy approach containing valuable genetic information (133). It is described as an easy accessible biomarker with rapid analysis capabilities, not limited to blood (134,135). Previous studies predominantly focus on blood plasma, confirming that ctDNA concentration is clearly increased in tumor patients (16,17,134) and correlates with tumor stage, metastatic disease, and tumor burden (136,137). While cfDNA sourced from cerebrospinal fluid (CSF), typically depleted of cells, may exhibit lower detection rates compared to plasma, it offers more precise insights into CNS involvement, particularly for primary CNS tumors (133,138) and non-CNS primary tumors (139).

Our observations indicate that DCC enrichment confirms the presence of LM in 37 % patients (15 out of 41). As ctDNA can be detected in approximately 75 % of metastasized patients this biomarker increasingly complements or even supplants circulating tumor cell analysis in clinical diagnostics (140,141). Although high ctDNA concentrations correlate with tumor burden and metastatic disease (142,143) and circulating tumor cells serve as an independent prognostic factor (123,144) we did not find evidence linking high DCC numbers to increased ctDNA concentration. The cfDNA amount appears more closely related to its release mechanism, reflected in the size of the circulating tumor DNA fragments.

Analyzing the fragmentation profile gives the possibility to distinguish between DNA derived from apoptosis (comprising smaller fragments) (145,146) and necrosis (comprising larger fragments > 500 bp) (86). Circulating tumor DNA tends to be shorter

than non-tumoral cell-free DNA (147), particularly in blood. Because in our collective around 50 % of samples were balanced and only 21 % of samples could be confirmed tumor derived the fragmentation size may serve as a useful preselecting criterion before proceeding with molecular ctDNA analysis.

Obtaining a sufficient amount of cfDNA for downstream analysis can be challenging (18,19) and in many of our samples we could not even detect a DNA amount after isolation from CSF. To address this, we introduced a new amplification step in our established ctDNA protocol (dveloped by G. Feliciello) overcoming the issue of sample loss for molecular analysis. With this enhancement, we successfully detected circulating cell-free tumor DNA in two CSF samples undetected by other methods used in this approach, including MRI, cytology, and CellSearch®.

Even if the reliability and expressiveness of ctDNA in our cohort was significantly lower compared to DCCs, ctDNA offers a rapid and cost-effective method for CSF analysis. Combining both biomarkers in a comprehensive analysis workflow could maximize benefits. Initial ctDNA analysis could provide quick insights into the sample, guiding subsequent in-depth molecular analysis of individual cells. This hybrid approach capitalizes on the advantages of rapid analysis while ensuring the generation of meaningful results, ultimately enhancing clinical decision-making for patients with suspected LM.

4.8 Central nervous system specific subclones

It has long been recognized that intratumorally landscape exhibits heterogeneity (148) a factor crucial in various aspects of tumor disease such as development, progression, therapy resistance and treatment outcomes (149,150). Therefore, the analysis of primary tumor tissue remains the first decision-making for determining diagnosis, staging, and treatment strategies. However, by expanding the analysis to include liquid biopsy of circulating tumor DNA from blood, the picture of tumor involvement in metastatic patients can become clearer. It offers significant advantage for therapy decision, as demonstrated in numerous studies (151–156), including the DETECT breast cancer study (157). In our research, we observed differences in the copy

number of DNA isolated from different compartments, corroborating findings in the literature (158,159). This suggests that cells dissociated from the primary tumor undergo specific alterations to enable their migration to the CNS. Molecular analysis of these CNS-seeking subclones may reveal alterations and potentially new therapeutic targets, offering a more precise and personalized approach to therapy that may otherwise be overlooked by analyzing only samples derived from visceral tissues.

4.9 Conclusion

This study demonstrates that the CellSearch® enrichment workflow for circulating tumor cells could be adapted from blood to cerebrospinal fluid (CSF) on patients with suspected leptomeningeal metastases (LM). If offers a sensitive and reliable alternative to the conventional cytology approach with the additional benefit of molecular downstream analysis. Nevertheless, the efficient detection and enrichment of disseminated cancer cells (DCCs) from lung cancer samples remains to be improved. To stabilize the automated counting step with the CellTrack® analyzer II after the enrichment a workflow for DAPI stained beads must be established. Once the final proof has been provided it could be applied to patient samples, having the opportunity to define patient samples optimal for successful downstream analysis but also serial tracking of patients under therapy conditions would be possible. Furthermore, besides the high quality of DCCs from CSF for a DNA downstream analysis our approach offers the possibility to cultivate viable cells under organoid conditions. After defining the best cultivation options the analysis of new biomarker and functional tests could deliver further options on molecular or drug testing, also for patients diagnosed with cancer of unknown primary. Including tissue analysis derived not from the central nervous system (CNS) confirmed that molecular data derived from CSF tumor DNA, DCCs but also circulating cell free tumor DNA (ctDNA), show the evident for heterogeneous subclones delivering the options for detecting new drug targets. Our molecular liquid biopsy approach is a practical workflow possible to be implemented in the daily clinical routine for the analysis of CSF instead of conventional cytology. It enables a multifaceted, unprecedented option for the molecular analysis of DCCs and ctDNA from CSF with the possibility to study new CNS individual biomarker for clinical decision-making.

5. Appendix

Table of figures II - Appendix

Table of tables II - Appendix

TableA 1 Sample list – Overview about samples, analysis methods and results

ID	Research Number	Sex	Age at withdrawal	Indication Cytology	Indication MRI	Indication molecular liquid biopsy	# Cells detected	Nr of tumor cells isolated	# high quality tumor cells	LowPass evaluation tumor cells	# of CD45+ cells isolated	# high quality CD45+ cells	LowPass evaluation CD45+ cells	cfDNA isolated	LowPass evaluation cfDNA
3	NSCLC15-0214 Liq	w	65	n.a.	n.a.	positiv	10	10	9	aberrant	2	2	balanced	n.a.	n.a.
4	MC15-0253 Liq	w	56	negativ	nein	positiv	9	9	8	aberrant	2 + Pool	2	balanced	n.a.	n.a.
5	MC15-0270 Liq	w	65	positiv	nein	positiv	334	15	14	aberrant	2 Pools	2	aberrant! Contaminated with TZ	n.a.	n.a.
6	MC16-0403 Liq	w	70	negativ	nein	negativ	0	0	0	n.a.	n.a.	n.a.	n.a.	n.a.	n.a.
7	MC16-0409 Liq	w	70	n.a.	n.a.	negativ	0	0	0	n.a.	n.a.	n.a.	n.a.	n.a.	n.a.
10	CUP16-0523 Liq	w	44	negativ	ja	positiv	363	20	20	aberrant	2 + Pool	2	balanced	n.a.	n.a.
12	MM16-0575 Liq	w	54	negativ	nein	negativ	0	0	0	n.a.	n.a.	n.a.	n.a.	n.a.	n.a.
14	MC17-256 Liq	w	71	positiv	ja	positiv	20000	93	69	aberrant	6 + 3 Pools	6	balanced	yes	aberrant
15	SCLC18-0013 Liq	m	52	negativ	nein	negativ	0	0	0	n.a.	0	0	n.a.	yes	not eval.
16	MC18-0019 Liq	w	71	positiv	n.a.	positiv	114	20	19	aberrant	2 + Pool	3	balanced	yes	not eval.
17	MC18-0087 Liq	w	81	n.a.	nein	positiv	190	20	20	aberrant	2 + Pool	3	balanced	yes	balanced
18	MC18-0123 Liq	w	71	positiv	nein	positiv	145	20	20	aberrant	2 + Pool	3	balanced	yes	aberrant
21	MC18-201 Liq	w	47	positiv	ja	negativ	5	5	5	4 balanced/ 1 aberrant	2 + Pool	3	balanced	yes	balanced
22	CUP18-210 Liq	w	74	negativ	nein	negativ	0	0	0	n.a.	0	0	n.a.	yes	aberrant
24	CC19-027 Liq	m	73	negativ	nein	negativ	0	0	0	n.a.	0	0	n.a.	yes	aberrant/Sex?
25	MM19-285-Liq	w	59	negativ	n.a.	negativ	0	0	0	n.a.	0		n.a.	yes	balanced
27	CUP19-322-Liq	m	21	positiv	n.a.	negativ	0	0	0	n.a.	0	0	n.a.	n.a.	n.a.
28	MC19-339-Liq	w	76	negativ	ja	negativ	0	0	0	n.a.	0	0	n.a.	yes	balanced
29	MC19-355-Liq	w	59	negativ	n.a.	negativ	0	0	0	n.a.	0	0	n.a.	yes	balanced
31	SCLC19-370 Liq	w	39	negativ	ja	negativ	0	0	0	n.a.	0	0	n.a.	yes	not eval.

ID	Research Number	Sex	Age at withdrawal	Indication Cytology	Indication MRI	Indication molecular liquid biopsy	# Cells detected	Nr of tumor cells isolated	# high quality tumor cells	LowPass evaluation tumor cells	# of CD45+ cells isolated	# high quality CD45+ cells	LowPass evaluation CD45+ cells	cfDNA isolated	LowPass evaluation cfDNA
32	MC20-003 Liq	w	61	negativ	n.a.	negativ	0	0	0	n.a.	0	0	n.a.	n.a.	n.a.
35	MC20-056 Liq	w	61	negativ	nein	negativ	0	0	0	n.a.	0	0	n.a.	yes	balanced
38	MM20-076 Liq	w	59	positiv	ja	negativ (GII<1)	10	10	0	n.a.	2+Pools	1	n.a.	yes	aberrant
39	CUP20-080 Liq	m	70	positiv	nein	positiv	70	19	13	aberrant	5 + 2 Pools	5	balanced	yes	aberrant
44	D-HN20-223-Liq	w	71	negativ	nein	negativ	0	0	0	n.a.	0	0	n.a.	no	balanced
45	D-HN20-228-Liq	w	71	negativ	nein	negativ	0	0	0	n.a.	0	0	n.a.	no	balanced
46	MC20-250-Liq	w	48	negativ	n.a.	negativ	0	0	0	n.a.	0	0	n.a.	yes	balanced
47	BC20-273-Liq	w	71	negativ	nein	negativ	0	0	0	n.a.	0	0	n.a.	yes	balanced
48	BC20-279-Liq	w	67	negativ	nein	negativ	1	0	0	n.a.	0	0	n.a.	yes	balanced
49	MM20-301_Liq	w	80	n.a.	n.a.	negativ	0	0	0	n.a.	0	0	n.a.	yes	balanced
53	MM20-327-Liq	m	67	n.a.	ja	negativ	0	0	0	n.a.	0	0	n.a.	yes	balanced
55	MC20-028-Liq	w	43	negativ	n.a.	negativ	0	0	0	n.a.	0	0	n.a.	yes	balanced
56	MA20-334-Liq	w	62	positiv	n.a.	positiv	100000	12	12	aberrant	2 + 1 Pool	3	balanced	yes	not eval.
57	BC20-335-Liq	m	56	negativ	nein	negativ	0	0	0	n.a.	0	0	n.a.	yes	balanced
58	MM20-337-Liq	w	57	n.a.	ja	negativ	0	0	0	n.a.	0	0	n.a.	yes	not evaluable
62	BC21-352-Liq	m	69	negativ	nein	negativ	0	0	0	n.a.	0	0	n.a.	yes	balanced
64	MC21-362-Liq	w	68	positiv	ja	positiv	5	4	3	aberrant	2 + 1 Pool	3	balanced	yes	not eval.
65	MM21-367-Liq	m	52	n.a.	ja	positiv	20	16	16	aberrant	2 + 1 Pool	3	aberrant! Contaminated with TZ	yes	not eval.
66	BC21-395 Liq	m	38	negativ	nein	negativ	0	0	0	n.a.	0	0	n.a.	yes	not evaluable
67	MC21-414-Liq	w	70	negativ	ja	negativ	0	0	0	n.a.	0	0	n.a.	n.a.	n.a.
69	MM21-423-Liq	m	71	n.a.	ja	negativ	0	0	0	n.a.	0	0	n.a.	n.a.	n.a.

ID	Research Number	FFPE Brain Metastases	FFPE Brain Mets LowPass	FFPE Primary Tumor	FFPE Primary Tumor LowPass	FFPE Metastases	FFPE Metastases LowPass	Organoids available	Organoids LowPass
3	NSCLC15-0214 Liq	n.a.	n.a.	n.a.	n.a.	n.a.	n.a.	n.a.	n.a.
4	MC15-0253 Liq	4_NP_MC15-0253 _Liq_GehirnMet	n.a.	n.a.	n.a.	n.a.	n.a.	n.a.	n.a.
5	MC15-0270 Liq	no	no	n.a.	n.a.	n.a.	n.a.	n.a.	n.a.
6	MC16-0403 Liq	no	no	yes	tumor - abberrant/ stromal - balanced	6_2_MC16-0403 _FFPE_LK16_1A	n.a.	0,5 ml cultivated - n.a.	n.a.
7	MC16-0409 Liq	n.a.	n.a.	n.a.	n.a.	n.a.	n.a.	0,5 ml cultivated - n.a.	n.a.
10	CUP16-0523 Liq	10_NP_CUP16-0523 _Liq_GehirnMet	n.a.	n.a.	n.a.	n.a.	n.a.	? ml cultivated - n.a.	n.a.
12	MM16-0575 Liq	12_NP_MM16-0575 _Liq_GehirnMet	n.a.	n.a.	n.a.	n.a.	n.a.	n.a.	n.a.
14	MC17-256 Liq	n.a.	n.a.	n.a.	n.a.	yes 14_1_3:MC17-256 _FFPE_Perit16_1& MC17-256_FFPE_ZP 14_2_MC17-256 _FFPE_Blase18	14_1/3 TZP aberrant/SZP balanced 14_2: TZP aberrant SZP n.eval.	n.a.	n.a.
15	SCLC18-0013 Liq	n.a.	n.a.	n.a.	n.a.	15_1_SCLC18-0013 _FFPE_LKMet17_ZP 15_2_SCLC18-0013 _FFPE_LKMet17_FL	n.a.	0,1 ml cultivated - n.a.	n.a.
16	MC18-0019 Liq	n.a.	n.a.	s. 14/18	s. 14/18	s. 14/16	s. 14/18	0,05 ml 3D/mouse - no tumor	n.a.
17	MC18-0087 Liq	n.a.	n.a.	yes	tumor - balanced stromal - n.a.	LK17: 17 3A	tumor - balanced stromal - balanced	0,05 ml 3D/mouse - no tumor	n.a.
18	MC18-0123 Liq	n.a.	n.a.	s. 14/16	s. 14/16	s. 14/16	s. 14/16	? ml cultivated - n.a.	n.a.
21	MC18-201 Liq	n.a.	n.a.	n.a.	n.a.	21_1_MC18-201_FFPE_KM17 21_2_MC18-201 _FFPE_Pleura16ZP 21_3_MC18-201 _FFPE_Pleura17ZP	KM17: TZP aberrant/SZP balanced PI16: TZPaberrant/SZP n.evaluable PI17: TZP aberrant/SZP n.eval.	0,05 ml 3D/mouse - no tumor	n.a.
22	CUP18-210 Liq	n.a.	n.a.	n.a.	n.a.	n.a.	n.a.	? ml cultivated - n.a.	n.a.
24	CC19-027 Liq	n.a.	n.a.	n.a.	n.a.	n.a.	n.a.	n.a.	n.a.
25	MM19-285-Liq	n.a.	n.a.	n.a.	n.a.	no	n.a.	? ml cultivated - n.a.	n.a.
27	CUP19-322-Liq	n.a.	n.a.	n.a.	n.a.	n.a.	n.a.	3 ml cultivated - grown/picked	aberrant & balanced
28	MC19-339-Liq	28_NP_MC19-339 _Liq_Gehirnmet	TZP:aberrant SZP: balanced	n.a.	n.a.	28_1_MC19-339 _FFPE_LebMet20	TZP:aberrant SZP: balanced	6 ml cultivated - n.a.	n.a.
29	MC19-355-Liq	n.a.	n.a.	29_1_MC19-355 _FFPE_PT15_1C	TZP:aberrant SZP: balanced	29_2_MC19-355 _FFPE_LKMet_3A	TZP:aberrant SZP: balanced	6 ml cultivated - n.a.	n.a.
31	SCLC19-370 Liq	n.a.	n.a.	n.a.	n.a.	n.a.	n.a.	n.a.	n.a.

ID	Research Number	FFPE Brain Metastases	FFPE Brain Mets LowPass	FFPE Primary Tumor	FFPE Primary Tumor LowPass	FFPE Metastases	FFPE Metastases LowPass	Organoids available	Organoids LowPass
32	MC20-003 Liq	n.a.	n.a.	32_1_MC20-003 _FFPE_PT19_E	n.a.	n.a.	n.a.	6 ml cultivated - n.a.	n.a.
35	MC20-056 Liq	n.a.	n.a.	n.a.	n.a.	n.a.	n.a.	n.a.	n.a.
38	MM20-076 Liq	n.a.	n.a.	n.a.	n.a.	LKMet:18 2C	TZP: slightly aberrant - gain 6p SZP: balanced but loss 19	6 ml cultivated - n.a.	n.a.
39	CUP20-080 Liq	n.a.	n.a.	n.a.	n.a.	n.a.	n.a.	n.a.	n.a.
44	D-HN20-223-Liq	n.a.	n.a.	44_1_D-HN20-223 _FFPE_PT20_J	n.a.	n.a.	n.a.	n.a.	n.a.
45	D-HN20-228-Liq	n.a.	n.a.	44_1_D-HN20-223 _FFPE_PT20_J	n.a.	n.a.	n.a.	n.a.	n.a.
46	MC20-250-Liq	n.a.	n.a.	n.a.	n.a.	n.a.	n.a.	n.a.	n.a.
47	BC20-273-Liq	n.a.	n.a.	n.a.	n.a.	n.a.	n.a.	n.a.	n.a.
48	BC20-279-Liq	n.a.	n.a.	n.a.	n.a.	48_1_BC20-279 _FFPE_LK20_1 48_2_BC20-279 _FFPE_LK20_2	n.a.	n.a.	n.a.
49	MM20-301_Liq	n.a.	n.a.	n.a.	n.a.	n.a.	n.a.	n.a.	n.a.
53	MM20-327-Liq	53_NP_MM20-382 _Gehirnmet_1	TZP: aberrant SZP: aberrant	n.a.	n.a.	53_1_MM20-382 _FFPELKMet21_1	TZP:aberrant SZP:aberrant	n.a.	n.a.
55	MC20-028-Liq	n.a.	n.a.	n.a.	n.a.	n.a.	n.a.	n.a.	n.a.
56	MA20-334-Liq	n.a.	n.a.	56_1_MA20-334 _FFPE_PT20	TZP:aberrant SZP: balanced	n.a.	n.a.	n.a.	n.a.
57	BC20-335-Liq	n.a.	n.a.	n.a.	n.a.	n.a.	n.a.	n.a.	n.a.
58	MM20-337-Liq	n.a.	n.a.	n.a.	n.a.	n.a.	n.a.	n.a.	n.a.
62	BC21-352-Liq	62_NP_BC21-352 _Liq_Gehirnmet	TZP&SZP: balanced	62_1_BC21_352 _FFPE_PT2_B	TZP&SZP: balanced	n.a.	n.a.	n.a.	n.a.
64	MC21-362-Liq	n.a.	n.a.	64_1_MC21-362 _FFPE_PT15	n.a. for research	64_2_MC21-362 _FFPE_KnochMet19	TZP:aberrant SZP: n. evaluable	n.a.	n.a.
65	MM21-367-Liq	n.a.	n.a.	n.a.	n.a.	n.a.	n.a.	n.a.	n.a.
66	BC21-395 Liq	66_NP_BC21-395 _Liq_Gehirnmet	TZP:aberrant SZP: balanced	66_1_BC21-395 _FFPE_PT20_B	TZP: balanced SZP: balanced	66_2_BC21_395 _FFPE_LKMet20_3	TZP: aberrant SZP: n.evaluable	n.a.	n.a.
67	MC21-414-Liq	n.a.	n.a.	n.a.	n.a.	different metastases available	to be performed	n.a.	n.a.
69	MM21-423-Liq	n.a.	n.a.	n.a.	n.a.	n.a.	n.a.	n.a.	n.a.

Available information from lung cancer patient ID3 – SCLC15-214:

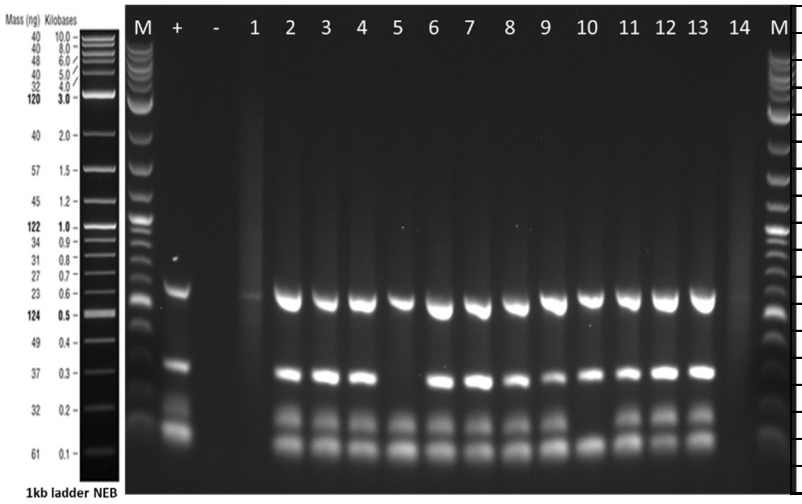

M	1 kb ladder NEB	GII
+	Positive control	4
-	Negative control	0
1	SCLC15-214 Liq_PK	0
2	SCLC15-214 Liq_Pool	4
3	SCLC15-214 Liq_NZ1	4
4	SCLC15-214 Liq_NZ2	4
5	SCLC15-214 TZ1	3
6	SCLC15-214 TZ2	4
7	SCLC15-214 TZ3	4
8	SCLC15-214 TZ4	4
9	SCLC15-214 TZ5	4
10	SCLC15-214 TZ6	3
11	SCLC15-214 TZ7	4
12	SCLC15-214 TZ8	4
13	SCLC15-214 TZ9	4
14	SCLC15-214 TZ10	0
M	1 kb ladder NEB	-

FigureA 1 Agarosegel picture of quality control PCR patient ID3
Mulitplex (4x) of single disseminated cancer cells isolated from CSF of lung cancer patient ID3 – SCLC15-214, including a size marker, a positive and a negative control and a sample list on the right. The genomic integrity index (GII) defines high quality cells (GII 2-4) or low quality cells (GII 0-1). Cells were enriched by the CellSearch system and isolated manually by micromanipulation.

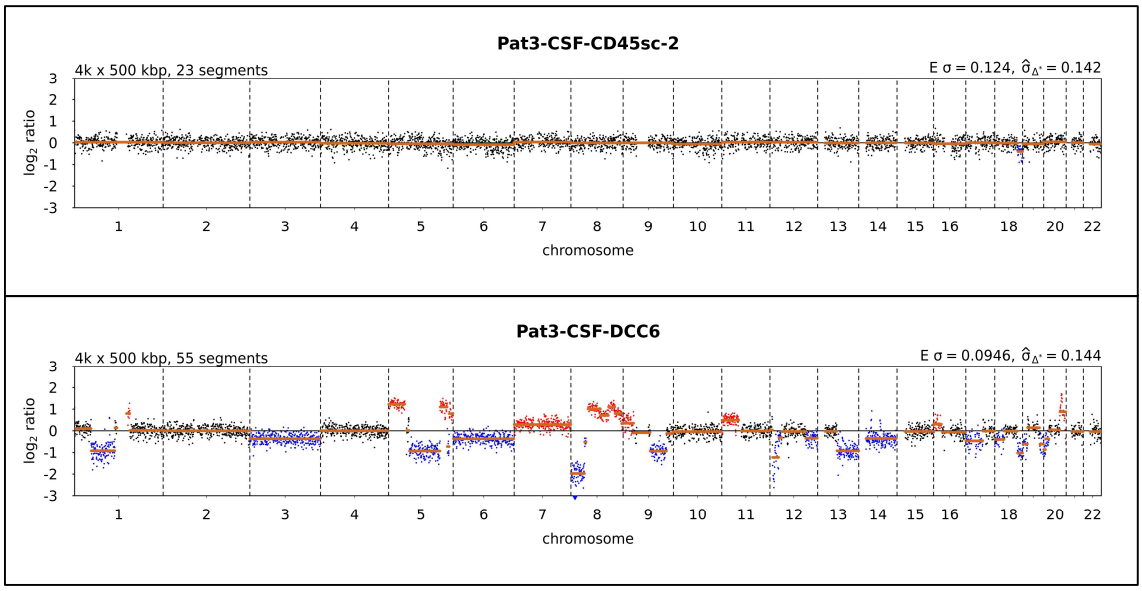

FigureA 2 Copy number variation profiles of single cells patient ID3
Above: Balanced copy number variation profile of CD45 positive cell 2.
Below: Aberrant copy number variation profile of disseminated cancer cell (DCC) 6. Cells were enriched with the CellSearch system and isolated from lung cancer patient ID3 – SCLC15-214 by micromanipulation. Interpretation of profiles in 2.22.

Available information from breast cancer patient ID4 – MC15-253:

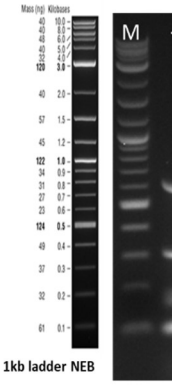

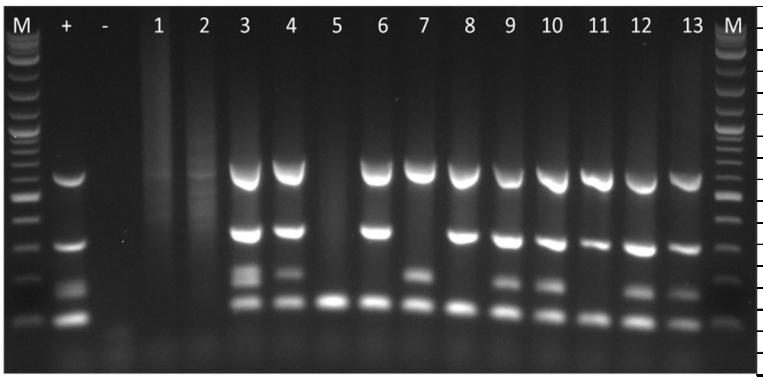

M	1 kb ladder NEB	GII
+	Positive control	4
-	Negative control	0
1	MC15-0253_PK	0
2	MC15-0253_Pool	0
3	MC15-0253_NZ 1	4
4	MC15-0253_NZ 2	4
5	MC15-0253_TZ 1	1
6	MC15-0253_TZ 2	3
7	MC15-0253_TZ 3	3
8	MC15-0253_TZ 4	3
9	MC15-0253_TZ 5	4
10	MC15-0253_TZ 6	4
11	MC15-0253_TZ 7	3
12	MC15-0253_TZ 8	4
13	MC15-0253_TZ 9	4
M	1 kb ladder NEB	-

FigureA 3 Agarosegel picture of quality control PCR patient ID4
Mulitplex (4x) of single disseminated cancer cells isolated from CSF of breast cancer patient ID4 – MC15-253, including a size marker, a positive and a negative control and a sample list on the right. The genomic integrity index (GII) defines high quality cells (GII 2-4) or low quality cells (GII 0-1). Cells were enriched by the CellSearch system and isolated manually by micromanipulation.

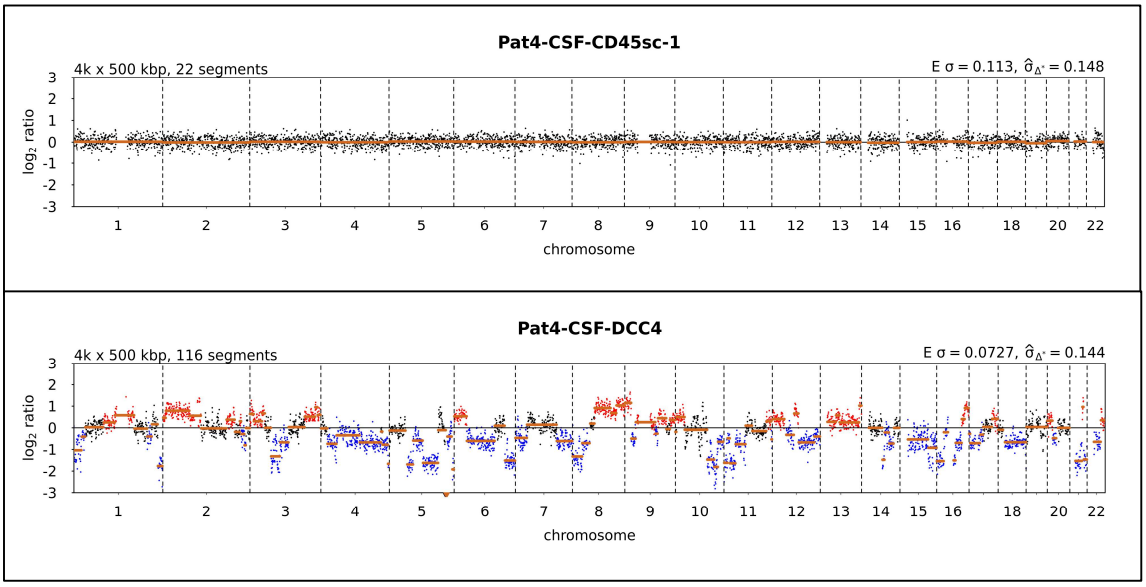

FigureA 4 Copy number variation profiles of single cells patient ID4
Above: Balanced copy number variation profile of CD45 positive cell 1.
Below: Aberrant copy number variation profile of disseminated cancer cell (DCC) 4.
Cells enriched with the CellSearch system and isolated from lung cancer patient ID4 – MC15-253 by micromanipulation. Interpretation of profiles in 2.22.

Available information from breast cancer patient ID5 – MC15-270:

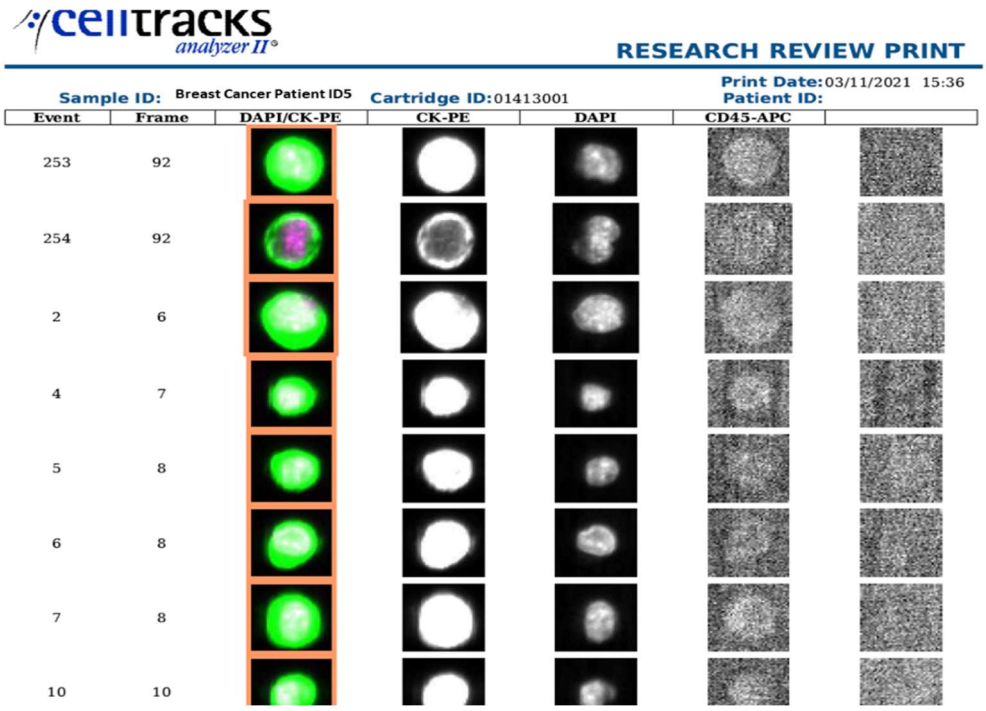

FigureA 5 Excerpt of the CellSearch Gallery patient ID5
Representative for the 334 disseminated cancer cells found in the cerebrospinal fluid (CSF) enrichment of breast cancer ID5 – MC15-270 the first eight cells from the CellSearch Gallery. First the event number, the frame in which the cells can be found, a DAPI/CK overlay channel, the CK-PE channel, the DAPI and the CD45-APC channel.

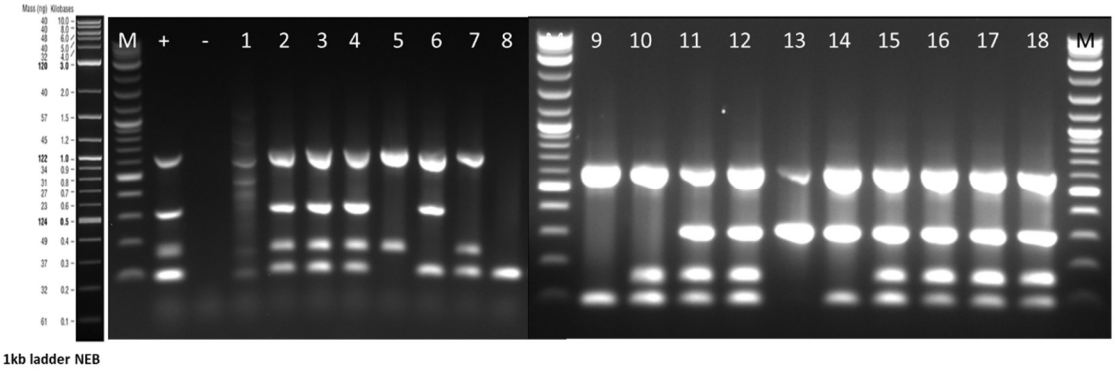

FigureA 6 Agarosegel picture of quality control PCR patient ID5
Mulitplex (4x) of single disseminated cancer cells isolated from CSF of breast cancer patient ID5 – MC15-270, including a size marker, a positive and a negative control and a sample list below. The genomic integrity index (GII) defines high quality cells (GII 2-4) or low quality cells (GII 0-1). Cells were enriched by the CellSearch system and isolated manually by micromanipulation.

TableA 2 Sample list of Agarosegel picture of quality contol PCR patient ID5 above

M	1 kb ladder NEB	GII
+	Positive control	4
-	Negative control	0
1	MC15-0270 PK	0
2	MC15-0270 Zellpool 1	4
3	MC15-0270 Zellpool 2	4
5	MC15-0270 TZ1	3
6	MC15-0270 TZ2	3
7	MC15-0270 TZ3	3
8	MC15-0270 TZ4	1
9	MC15-0270 TZ5	2
4	MC15-0270 TZ6	4
10	MC15-0270 TZ7	3
11	MC15-0270 TZ8	4
12	MC15-0270 TZ9	4
13	MC15-0270 TZ10	3
14	MC15-0270 TZ11	3
15	MC15-0270 TZ12	4
16	MC15-0270 TZ13	4
17	MC15-0270 TZ14	4
18	MC15-0270 TZ15	4
M	1 kb ladder NEB	GII

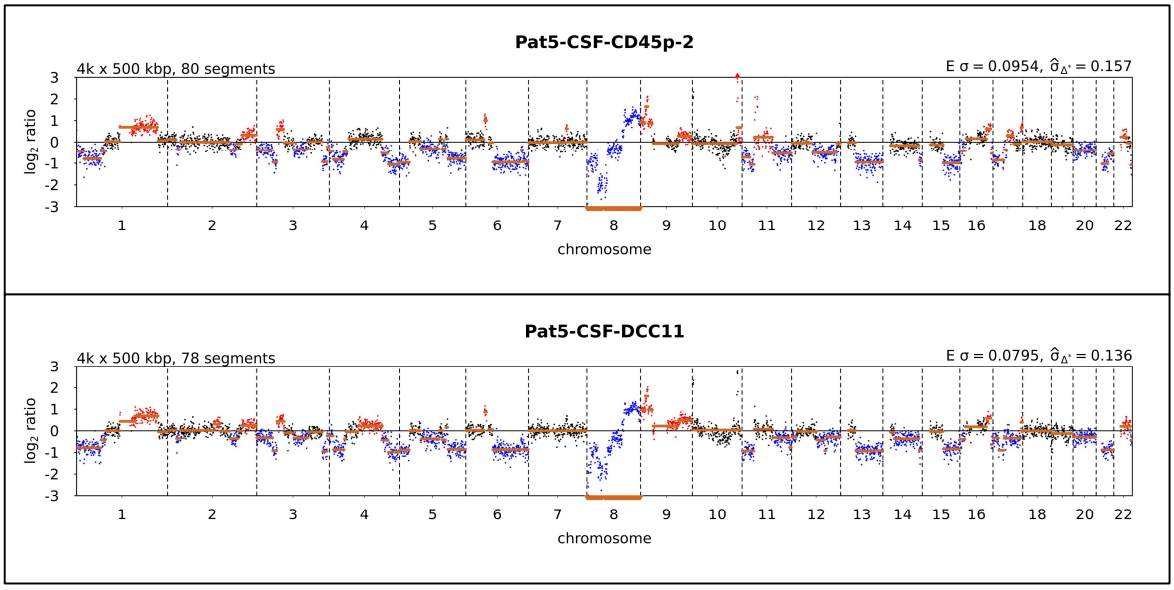

FigureA 7 Copy number variation profiles of single cells patient ID5
Above: Balanced copy number variation profile of a CD45 positive cellpool 2.
Below: Aberrant copy number variation profile of disseminated cancer cell (DCC) 11. Cells enriched with the CellSearch system and isolated from breast cancer patient ID5 – MC15-270 by micromanipulation. Interpretation of profiles in 2.22.

Available information from breast cancer patient ID6 – MC16-0403:

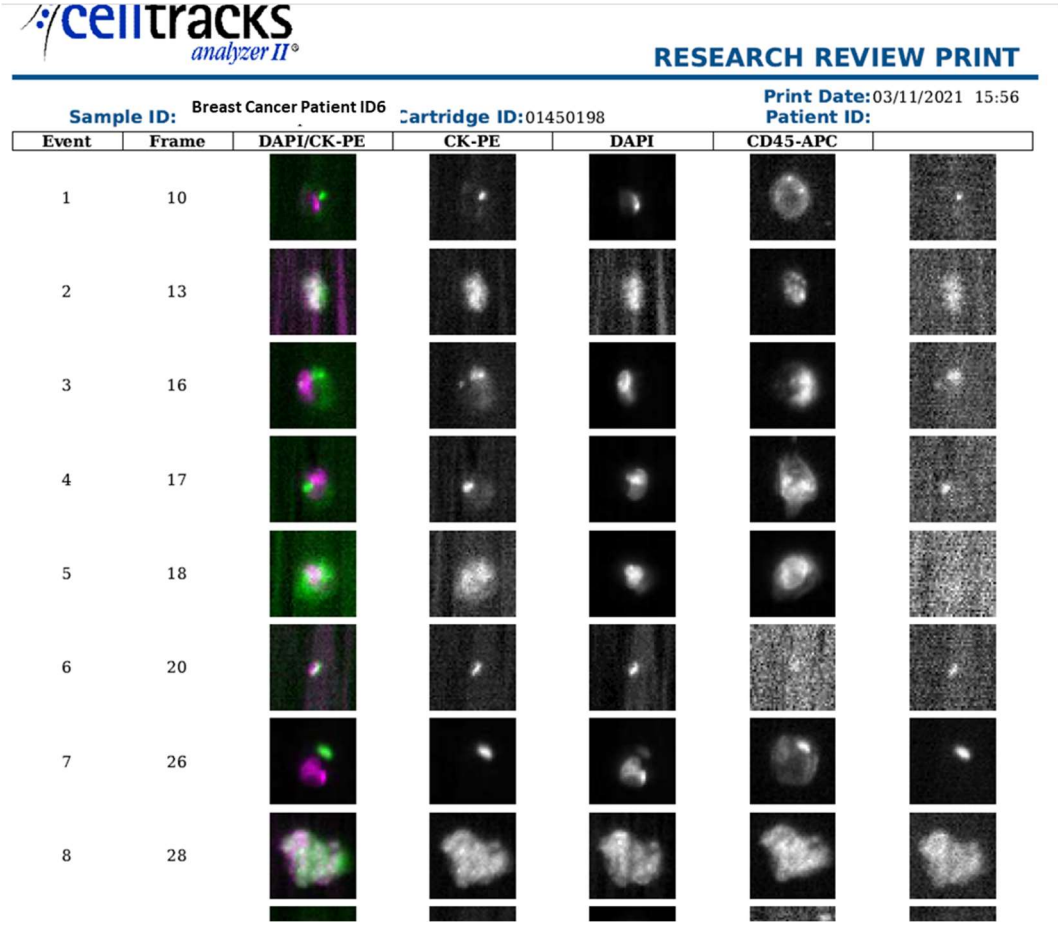

FigureA 9 Excerpt of the CellSearch Gallery patient ID6
No cancer cells were found in the cerebrospinal fluid (CSF) enrichment of breast cancer ID6 – MC16-0403, representative the first eight cells from the CellSearch Gallery with no clear cancer cell staining in the individual channels. First the event number, the frame in which the cells can be found, a DAPI/CK overlay channel, the CK-PE channel, the DAPI and the CD45-APC channel.

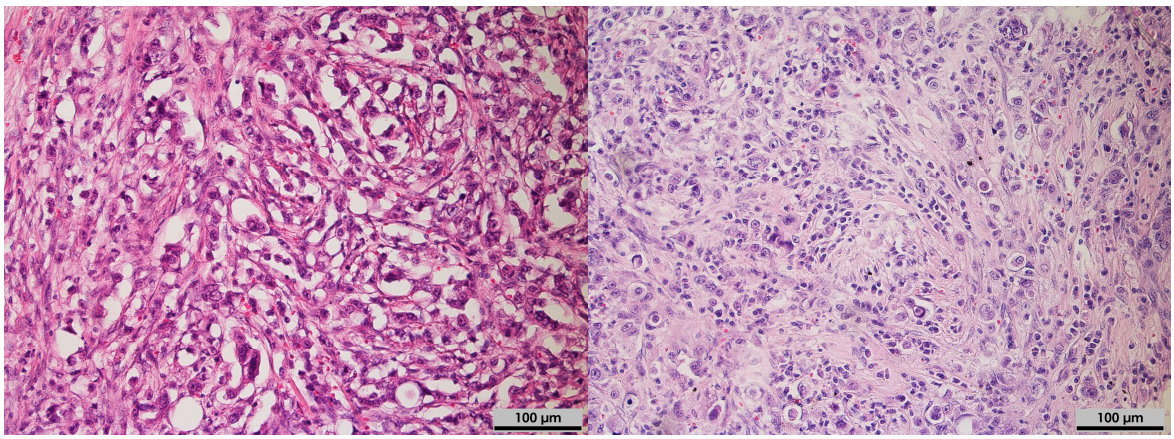

FigureA 8 Hematoxylin-Eosin staining of FFPE slices from patient ID6
Stained tumor tissue from breast cancer ID6 – MC16-0403, left: primary tumor. right: lymph node Violet dots are representing tumor cells, scale 100 µm.

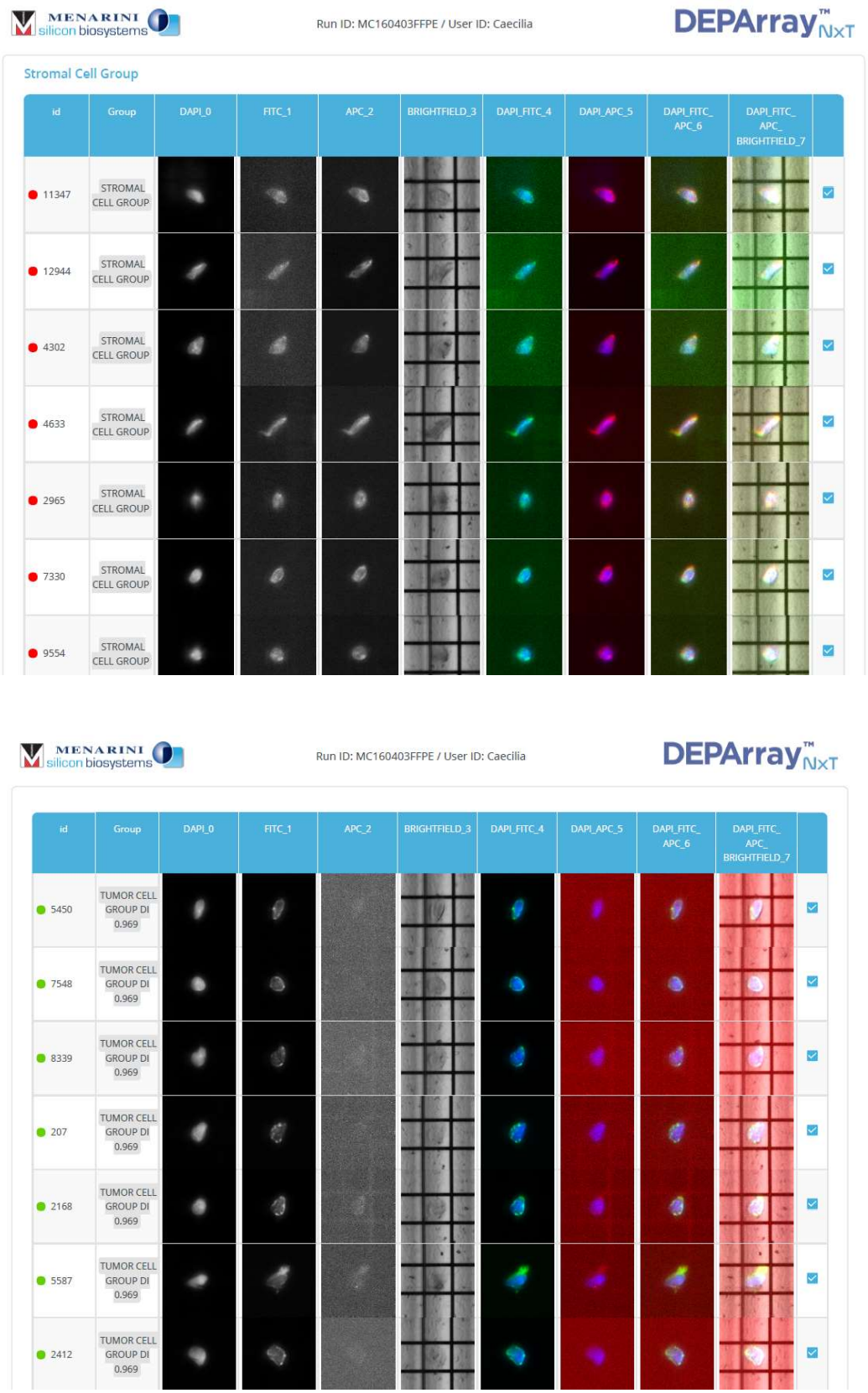

FigureA 10 Excerpt of the DEPArray Gallery patient ID6
Above: Representative the firt single CD45 positive cells. **Below:** Representative the first single disseminated cancer cells. Both cell populations isolated from CSF of breast cancer patient ID6 – MC16-04043 with the automated DEPArray system.

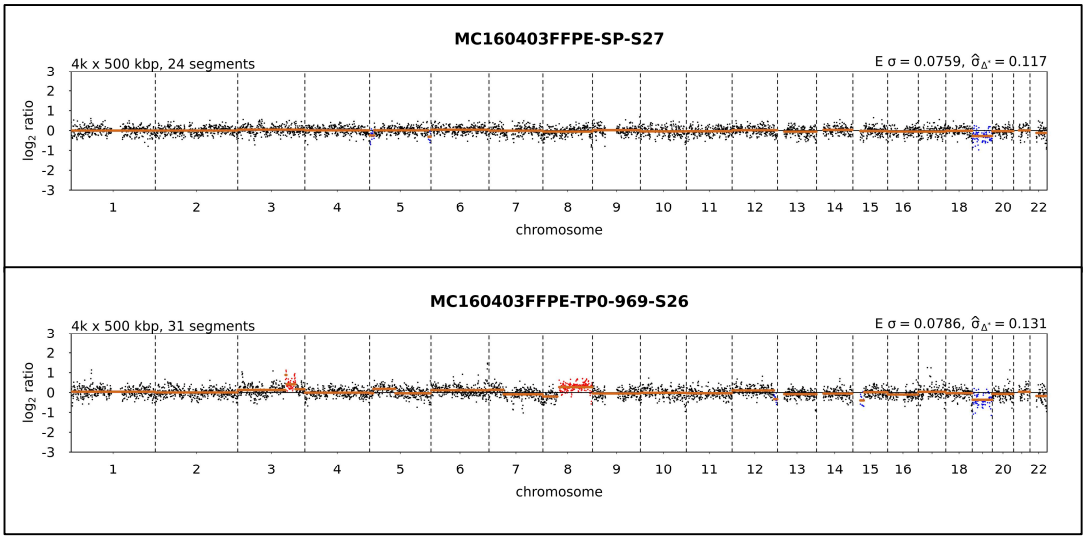

FigureA 11 Copy number variation profiles of single cells patient ID6
Above: Balanced copy number variation profile of a CD45 positive stromal cellpool.
Below: Copy number variation profile of tumor cell population. Cells enriched with the CellSearch system and isolated from the primary tumor tissue of breast cancer patient ID6 – MC16-0403 automatically with the DEPArray system. Interpretation of profiles in 2.22.

Available information from cancer of unknown primary ID10 – CUP16-0523:

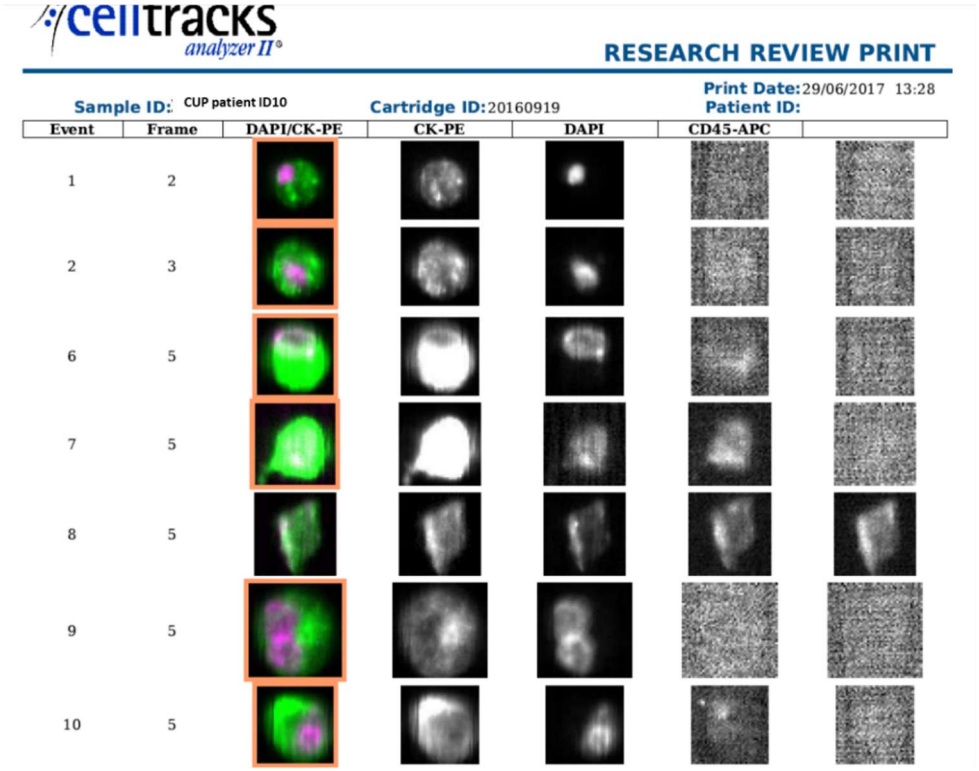

FigureA 12 Excerpt of the CellSearch Gallery patient ID10
Representative for the 363 disseminated cancer cells found in the cerebrospinal fluid (CSF) enrichment of breast cancer ID10 – CUP16-0523 the first seven cells from the CellSearch Gallery. First the event number, the frame in which the cells can be found, a DAPI/CK overlay channel, the CK-PE channel, the DAPI and the CD45-APC channel.

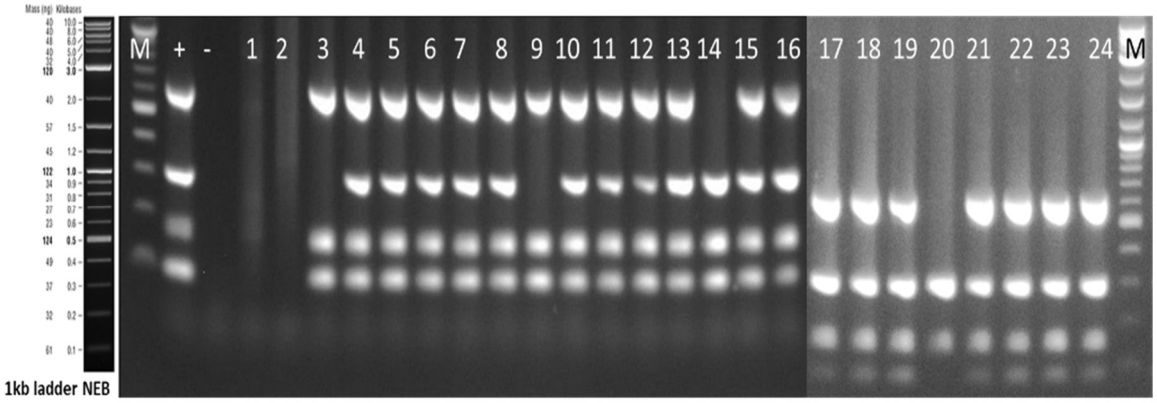

FigureA 13 Agarosegel picture of quality control PCR patient ID10
Mulitplex (4x) of single disseminated cancer cells isolated from CSF of cancer of unknown primary patient ID10 – CUP16-523, including a size marker, a positive and a negative control and a sample list below. The genomic integrity index (GII) defines high quality cells (GII 2-4) or low quality cells (GII 0-1). Cells were enriched by the CellSearch system and isolated manually by micromanipulation.

TableA 3 Sample list of Agarosegel picture of quality contol PCR patient ID5 above

M	1 kb ladder NEB	GII
+	Positive control	4
-	Negative control	0
1	CUP16-523 Liq_PK	0
2	CUP16-523 Liq_Pool	0
3	CUP16-523 Liq_NZ1	3
4	CUP16-523 Liq_NZ2	4
5	CUP16-523 Liq_TZ 01	4
6	CUP16-523 Liq_TZ 02	4
7	CUP16-523 Liq_TZ 03	4
8	CUP16-523 Liq_TZ 04	4
9	CUP16-523 Liq_TZ 05	3
10	CUP16-523 Liq_TZ 06	4
11	CUP16-523 Liq_TZ 07	4
12	CUP16-523 Liq_TZ 08	4
13	CUP16-523 Liq_TZ 09	4
14	CUP16-523 Liq_TZ 10	3
15	CUP16-523 Liq_TZ 11	4
16	CUP16-523 Liq_TZ 12	4
17	CUP16-523 Liq_TZ 13	4
18	CUP16-523 Liq_TZ 14	4
19	CUP16-523 Liq_TZ 15	4
20	CUP16-523 Liq_TZ 16	3
21	CUP16-523 Liq_TZ 17	4
22	CUP16-523 Liq_TZ 18	4
23	CUP16-523 Liq_TZ 19	4
24	CUP16-523 Liq_TZ 20	4
M	1 kb ladder NEB	-

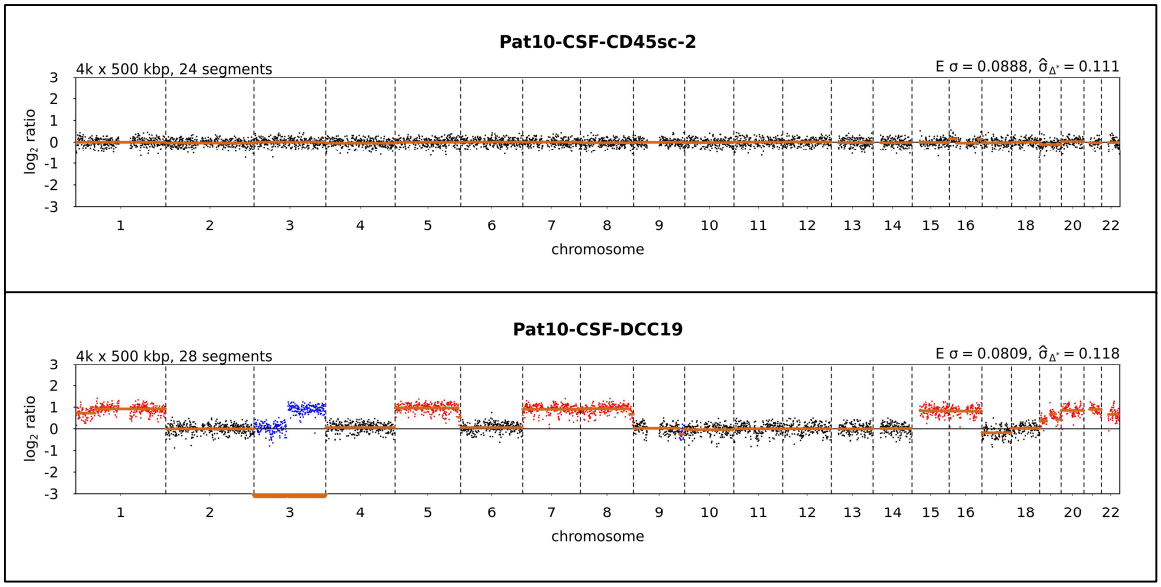

Figure 14 Copy number variation profiles of single cells patient ID10
Above: Balanced copy number variation profile of a CD45 positive single cell 2. **Below:** Copy number variation profile of disseminated cancer cell 19. Cells enriched with the CellSearch system and isolated from CSF of breast cancer patient ID10 – CUP16-0523 by micromanipulation. Interpretation of profiles in 2.22.

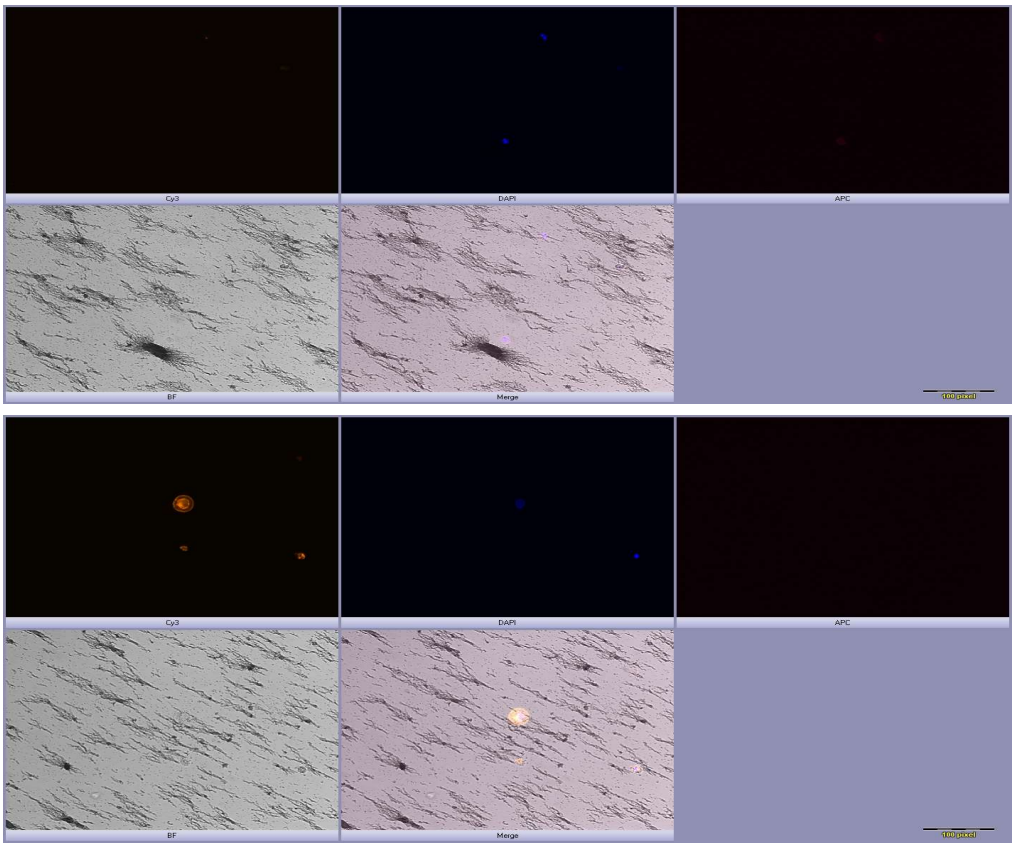

Figure 15 Microscope picture of single cells patient ID10
Above: CD45 positive single cell 2. **Below:** Disseminated cancer cell 19. Both isolated from CSF of patient ID10 – CUP16-523. The different channels are: Cy3 (left up), DAPI (middle up), APC (right up), brightfield (left down), merge (middle down), scale bar 100 pixel.

Available information from breast cancer patient **ID14 – MC17-256 (timepoint 1)**,

ID16 – MC18-019 (timepoint 2), ID18 – MC 18-123 (timepoint 3) – represent one patient

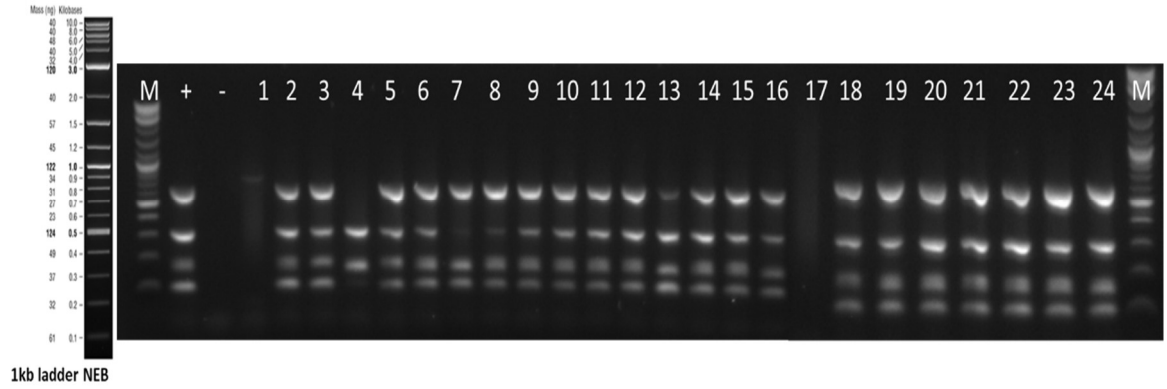

FigureA 16 Agarosegel picture of quality control PCR patient ID14
Mulitplex (4x) of single disseminated cancer cells isolated from CSF of breast cancer patient ID14 MC17-256, including a size marker, a positive and a negative control and a sample list below. The genomic integrity index (GII) defines high quality cells (GII 2-4) or low quality cells (GII 0-1). Cells were enriched by the CellSearch system and isolated manually by micromanipulation.

TableA 4 Sample list of Agarosegel picture of quality contol PCR patient ID14 above

M	1 kb ladder NEB	GII
+	Positive control	4
-	Negative control	0
1	MC17-256 Liq_PK	0
2	MC17-256 Liq_Pool	4
3	MC17-256 Liq_N1	4
4	MC17-256 Liq_N2	3
5	MC17-256 Liq_TZ 01 M	4
6	MC17-256 Liq_TZ 02 M	4
7	MC17-256 Liq_TZ 03 M	4
8	MC17-256 Liq_TZ 04 M	4
9	MC17-256 Liq_TZ 05 M	4
10	MC17-256 Liq_TZ 06 M	4
11	MC17-256 Liq_TZ 07 M	4
12	MC17-256 Liq_TZ 08 M	4
13	MC17-256 Liq_TZ 09 M	4
14	MC17-256 Liq_TZ 10 M	4
15	MC17-256 Liq_TZ 11 M	4
16	MC17-256 Liq_TZ 12 M	4
17	MC17-256 Liq_TZ 13 M	4
18	MC17-256 Liq_TZ 14 M	4
19	MC17-256 Liq_TZ 15 M	4
20	MC17-256 Liq_TZ 16 M	4
21	MC17-256 Liq_TZ 17 M	4
22	MC17-256 Liq_TZ 18 M	4
23	MC17-256 Liq_TZ 19 M	4
24	MC17-256 Liq_TZ 20 M	4
M	1 kb ladder NEB	GII

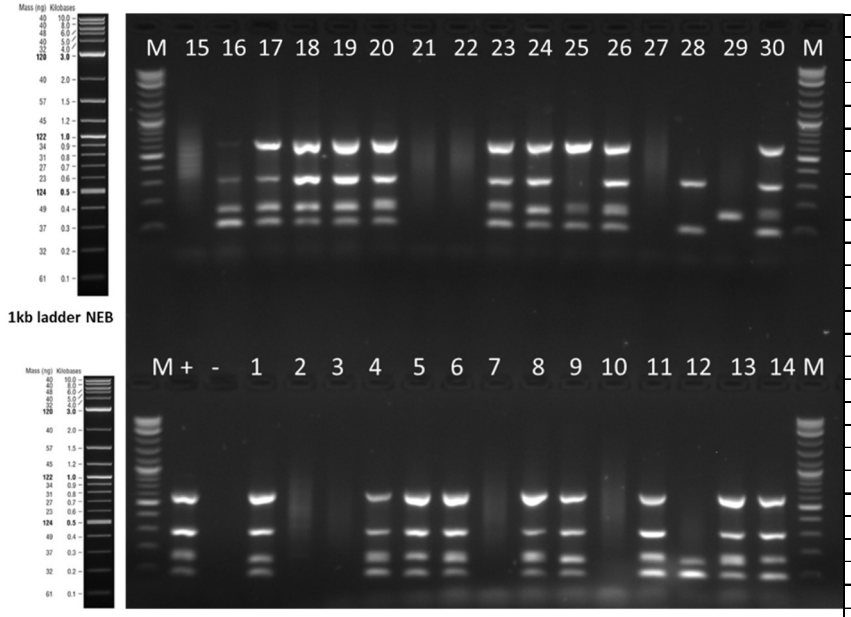

M	1 kb ladder NEB	GII
+	Positive control	4
-	Negative control	0
1	MC17-256 Liq_TZ 01 D1	4
2	MC17-256 Liq_TZ 02 D1	0
3	MC17-256 Liq_TZ 03 D1	0
4	MC17-256 Liq_TZ 04 D1	4
5	MC17-256 Liq_TZ 05 D1	4
6	MC17-256 Liq_TZ 06 D1	4
7	MC17-256 Liq_TZ 07 D1	0
8	MC17-256 Liq_TZ 08 D1	4
9	MC17-256 Liq_TZ 09 D1	4
10	MC17-256 Liq_TZ 10 D1	0
11	MC17-256 Liq_TZ 11 D1	4
12	MC17-256 Liq_TZ 12 D1	2
13	MC17-256 Liq_TZ 13 D1	4
14	MC17-256 Liq_TZ 14 D1	4
M	1 kb ladder NEB	-
15	MC17-256 Liq_TZ 15 D1	0
16	MC17-256 Liq_TZ 16 D1	4
17	MC17-256 Liq_TZ 17 D1	4
18	MC17-256 Liq_TZ 18 D1	4
19	MC17-256 Liq_TZ 19 D1	4
20	MC17-256 Liq_TZ 20 D1	4
21	MC17-256 Liq_TZ 21 D1	0
22	MC17-256 Liq_TZ 22 D1	0
23	MC17-256 Liq_TZ 23 D1	4
24	MC17-256 Liq_TZ 24 D1	4
25	MC17-256 Liq_TZ 25 D1	3
26	MC17-256 Liq_TZ 26 D1	4
27	MC17-256 Liq_PK D1	0
28	MC17-256 Liq_NZ1 D1	2
29	MC17-256 Liq_NZ2 D1	2
30	MC17-256 Liq_Pool D1	4
M	1 kb ladder NEB	-

FigureA 18 Agarosegel picture of quality control PCR patient ID14
Mulitplex (4x) of single disseminated cancer cells isolated from CSF of breast cancer patient ID14 – MC17-256, including a size marker, a positive and a negative control and a sample list on the right side. The genomic integrity index (GII) defines high quality cells (GII 2-4) or low quality cells (GII 0-1). Cells were enriched by the CellSearch system and isolated manually by micromanipulation.

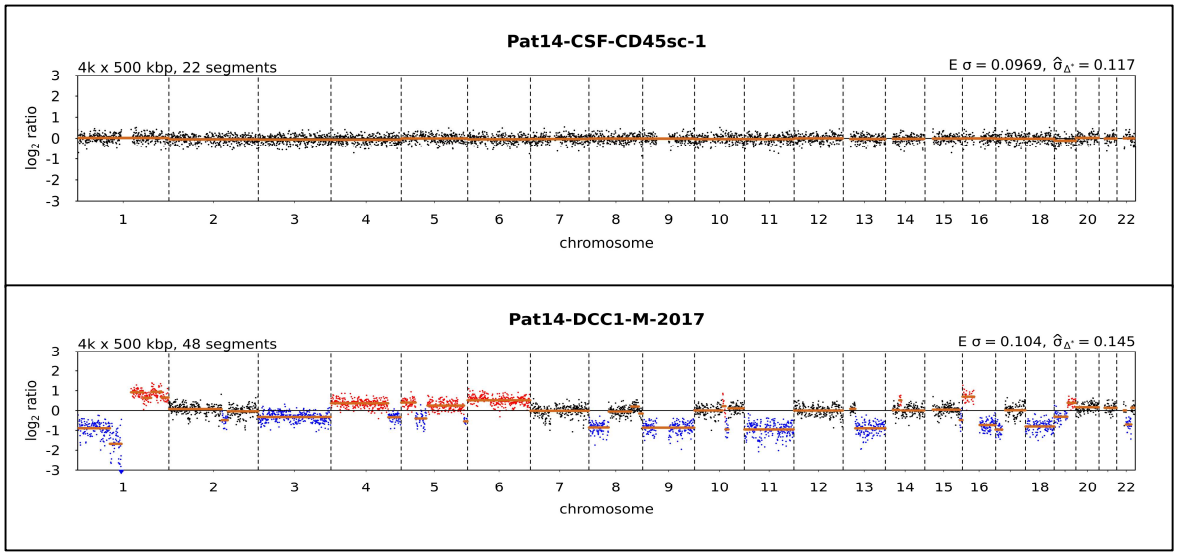

FigureA 17 Copy number variation profiles of single cells patient ID14
Above: Balanced copy number variation profile of a CD45 positive single cell 1.
Below: Copy number variation profile of disseminated cancer cell 1. Cells enriched with the CellSearch system and isolated manually by micromanipulation from CSF of breast cancer patient ID14 – MC17-256 (timepoint 1). Interpretation of profiles in 2.22

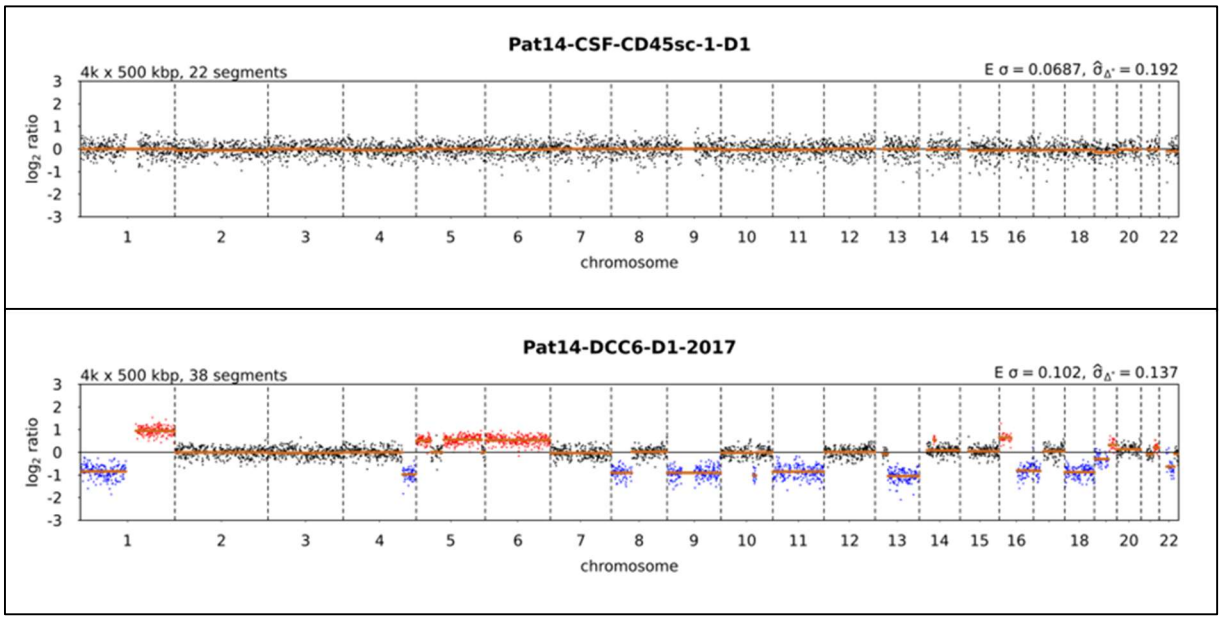

FigureA 19 Copy number variation profiles of single cells patient ID14
Above: Balanced copy number variation profile of a CD45 positive single cell 1.
Below: Copy number variation profile of disseminated cancer cell 1. Cells enriched with the CellSearch system and isolated automatically with the DEPArray system from CSF of breast cancer patient ID14 – MC17-256 (timepoint 1). Interpretation of profiles in 2.22.

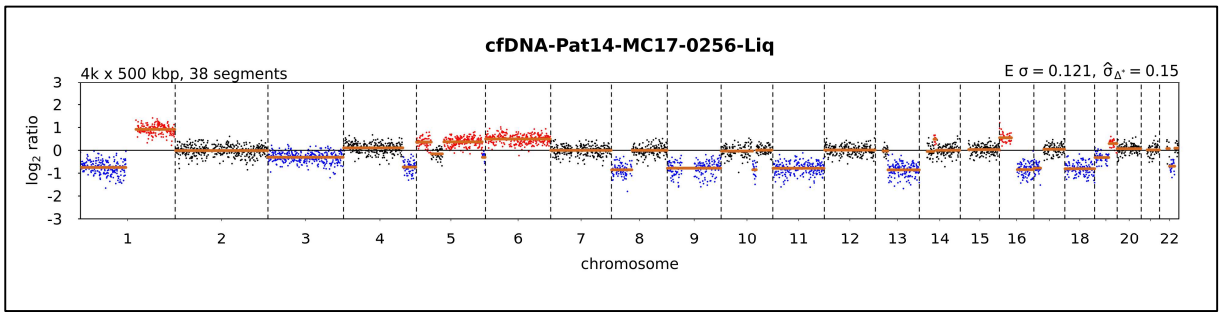

FigureA 20 Copy number variation profile of ctDNA of patient ID14
Aberrant copy number variation profile of circulating cell free tumor DNA (ctDNA) isolated from CSF of breast cancer patient ID14 – MC17-256 (timepoint 1). Interpretation of profiles in 2.22.

Available information from breast cancer patient **ID16 – MC18-019 (timepoint 2),** ID14 – MC17-256 (timepoint 1), ID18 – MC 18-123 (timepoint 3) – represent one patient

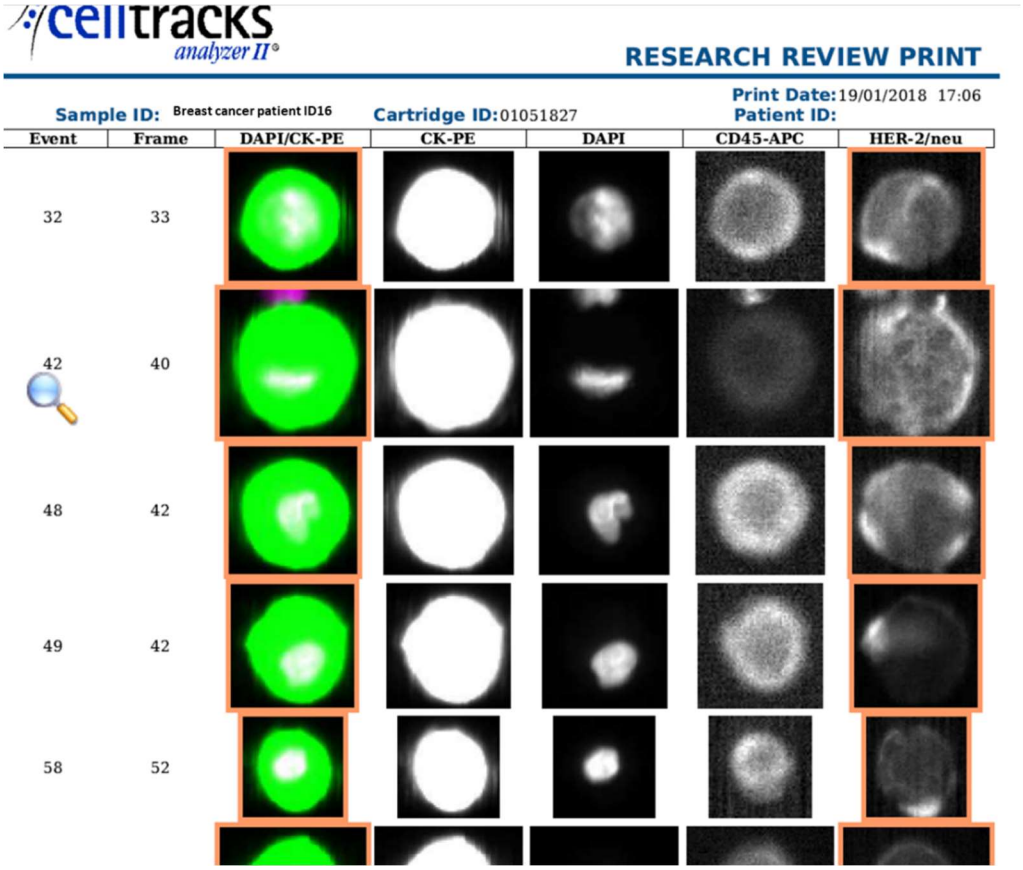

FigureA 21 Excerpt of the CellSearch Gallery patient ID16
Representative for the 114 disseminated cancer cells found in the cerebrospinal fluid (CSF) enrichment of breast cancer ID16 – MC18-019 the first five cells from the CellSearch Gallery. First the event number, the frame in which the cells can be found, a DAPI/CK overlay channel, the CK-PE channel, the DAPI and the CD45-APC channel.

TableA 5 Sample list of Agarosegel picture of quality contol PCR patient ID16 above

M	1 kb ladder NEB	GII
+	Positive control	4
-	Negative control	0
1	MC18-019 Liq_PK	0
2	MC18-019 Liq_Pool	4
3	MC18-019 Liq_NZ1	3
4	MC18-019 Liq_NZ2	4
5	MC18-019 Liq_TZ 01	2
6	MC18-019 Liq_TZ 02	4
7	MC18-019 Liq_TZ 03	4
8	MC18-019 Liq_TZ 04	4
9	MC18-019 Liq_TZ 05	4
10	MC18-019 Liq_TZ 06	4
11	MC18-019 Liq_TZ 07	4
12	MC18-019 Liq_TZ 08	0
13	MC18-019 Liq_TZ 09	4
14	MC18-019 Liq_TZ 10	4
15	MC18-019 Liq_TZ 11	4
16	MC18-019 Liq_TZ 12	4
17	MC18-019 Liq_TZ 13	4
18	MC18-019 Liq_TZ 14	4
19	MC18-019 Liq_TZ 15	4
20	MC18-019 Liq_TZ 16	4
21	MC18-019 Liq_TZ 17	4
22	MC18-019 Liq_TZ 18	4
23	MC18-019 Liq_TZ 19	4
24	MC18-019 Liq_TZ 20	4
M	1 kb ladder NEB	-

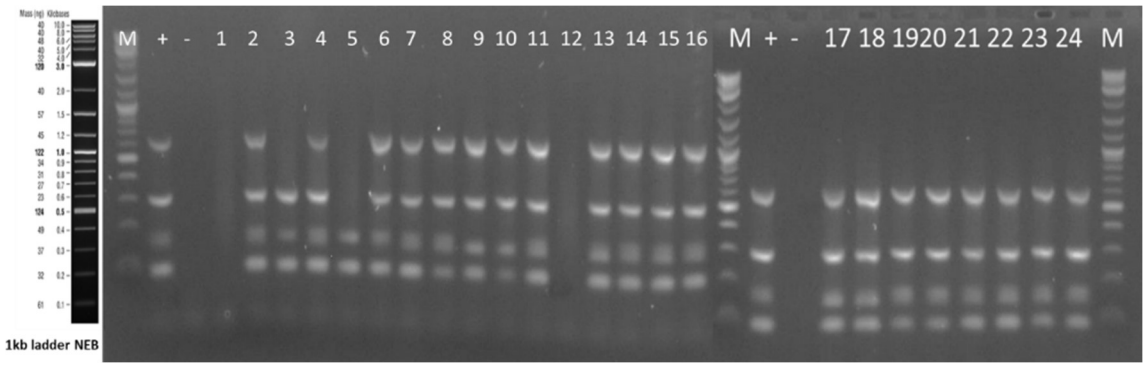

FigureA 22 Agarosegel picture of quality control PCR patient ID16
Mulitplex (4x) of single disseminated cancer cells isolated from CSF of breast cancer patient ID16-MC18-019, including a size marker, a positive and a negative control and a sample list below. The genomic integrity index (GII) defines high quality cells (GII 2-4) or low quality cells (GII 0-1). Cells were enriched by the CellSearch system and isolated manually by micromanipulation.

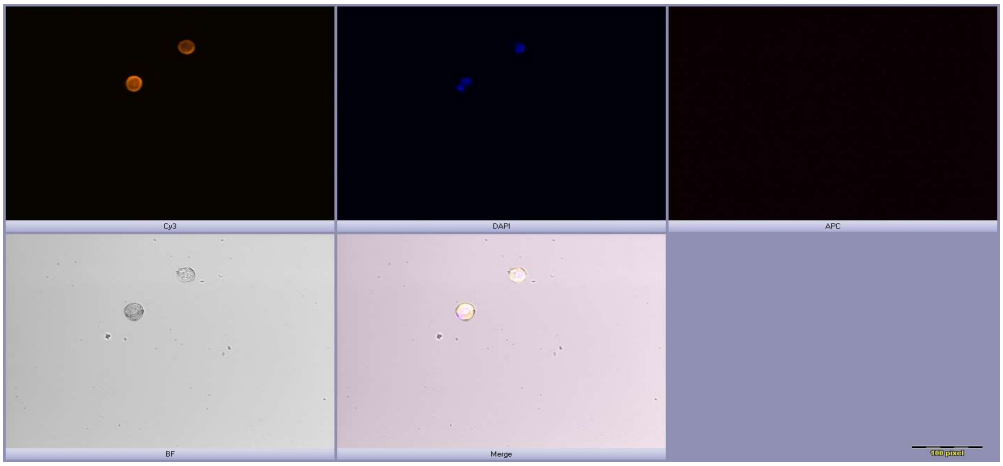

FigureA 23 Microscopy picture of single cells patient ID16
Disseminated cancer cell 13 (left below) and 14 (right up). Both isolated from CSF of patient ID16 – MC18-019 (timepoint 2). The different channels are: Cy3 (left up), DAPI (middle up), APC (right up), brightfield (left down), merge (middle down), scale bar 100 pixel.

Available information from breast cancer patient **ID18 – MC 18-123 (timepoint 3),** ID14 – MC17-256 (timepoint 1), ID16 – MC18-019 (timepoint 2) – represent one patient

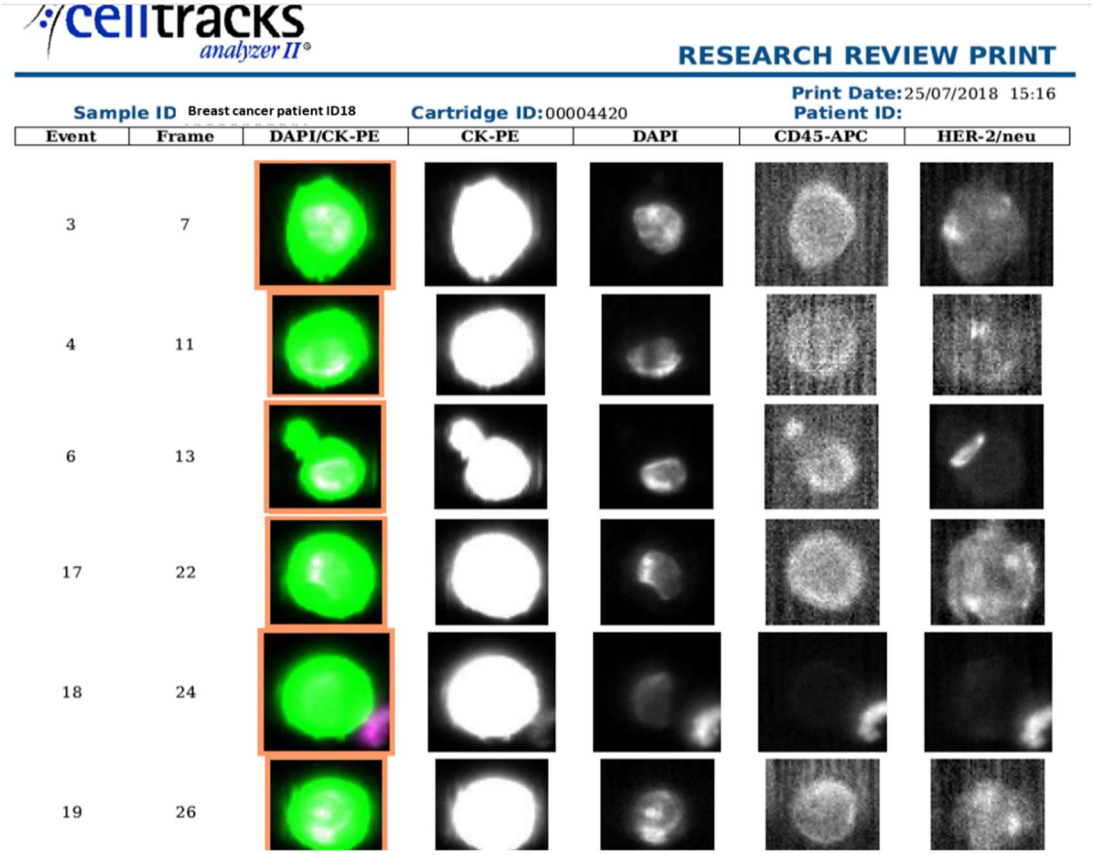

FigureA 24 Excerpt of the CellSearch Gallery patient ID18
Representative for the 145 disseminated cancer cells found in the cerebrospinal fluid (CSF) enrichment of breast cancer ID18 – MC18-123 the first six cells from the CellSearch Gallery. First the event number, the frame in which the cells can be found, a DAPI/CK overlay channel, the CK-PE channel, the DAPI and the CD45-APC channel.

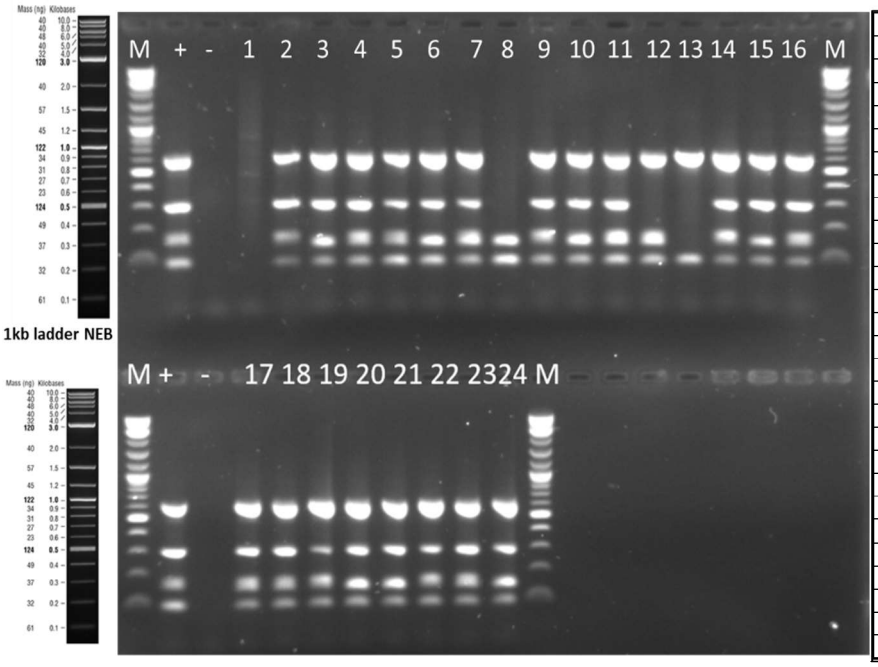

M	1 kb ladder NEB	GII
+	Positive control	4
-	Negative control	0
1	MC18-123 Liq_PK	0
2	MC18-123 Liq_Pool	4
3	MC18-123 Liq_NZ1	4
4	MC18-123 Liq_NZ2	4
5	MC18-123 Liq_TZ 01	4
6	MC18-123 Liq_TZ 02	4
7	MC18-123 Liq_TZ 03	4
8	MC18-123 Liq_TZ 04	2
9	MC18-123 Liq_TZ 05	4
10	MC18-123 Liq_TZ 06	4
11	MC18-123 Liq_TZ 07	4
12	MC18-123 Liq_TZ 08	3
13	MC18-123 Liq_TZ 09	2
14	MC18-123 Liq_TZ 10	4
15	MC18-123 Liq_TZ 11	4
16	MC18-123 Liq_TZ 12	4
17	MC18-123 Liq_TZ 13	4
18	MC18-123 Liq_TZ 14	4
19	MC18-123 Liq_TZ 15	4
20	MC18-123 Liq_TZ 16	4
21	MC18-123 Liq_TZ 17	4
22	MC18-123 Liq_TZ 18	4
23	MC18-123 Liq_TZ 19	4
24	MC18-123 Liq_TZ 20	4
M	1 kb ladder NEB	-

FigureA 25 Agarosegel picture of quality control PCR patient ID18
Mulitplex (4x) of single disseminated cancer cells isolated from CSF of breast cancer patient ID18 – MC18-123, including a size marker, a positive and a negative control and a sample list on the right side. The genomic integrity index (GII) defines high quality cells (GII 2-4) or low quality cells (GII 0-1). Cells were enriched by the CellSearch system and isolated manually by micromanipulation.

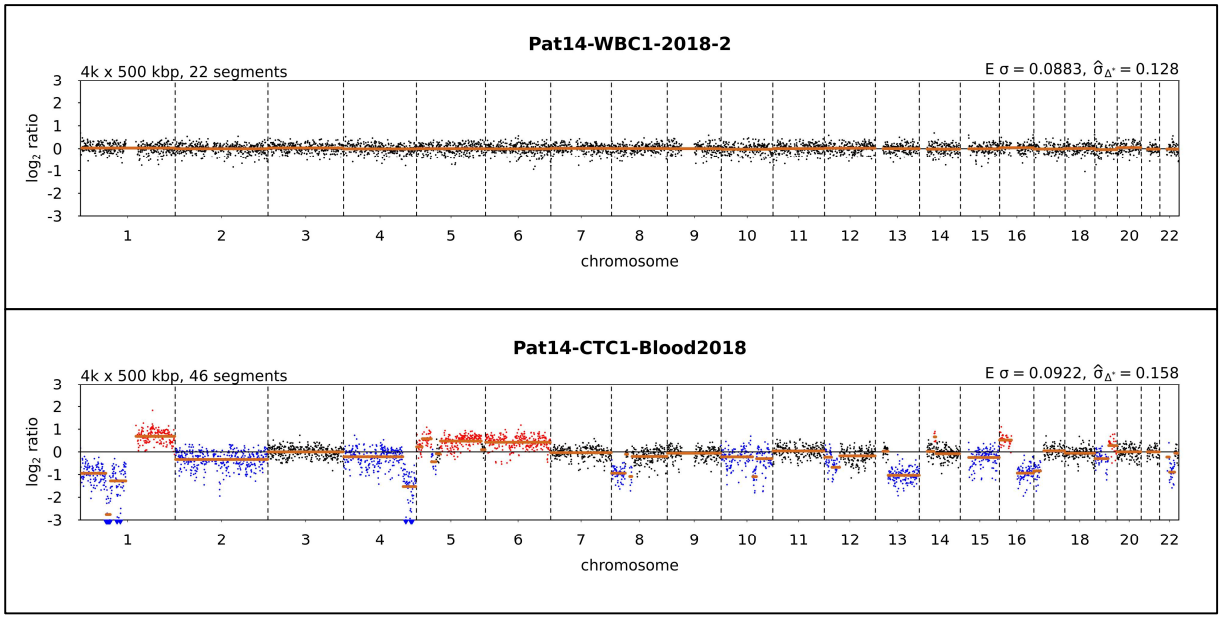

FigureA 26 CNV profiles of single cells from blood patient ID18 – timepoint 3
Above: Balanced copy number variation (CNV) profile of a CD45 positive single cell 2.
Below: CNV profile of a circulating tumor cell 1. Cells enriched with the CellSearch system and isolated manually by micromanipulation of breast cancer patient ID18 – MC18-123 (timepoint 3). Interpretation of profiles in 2.22.

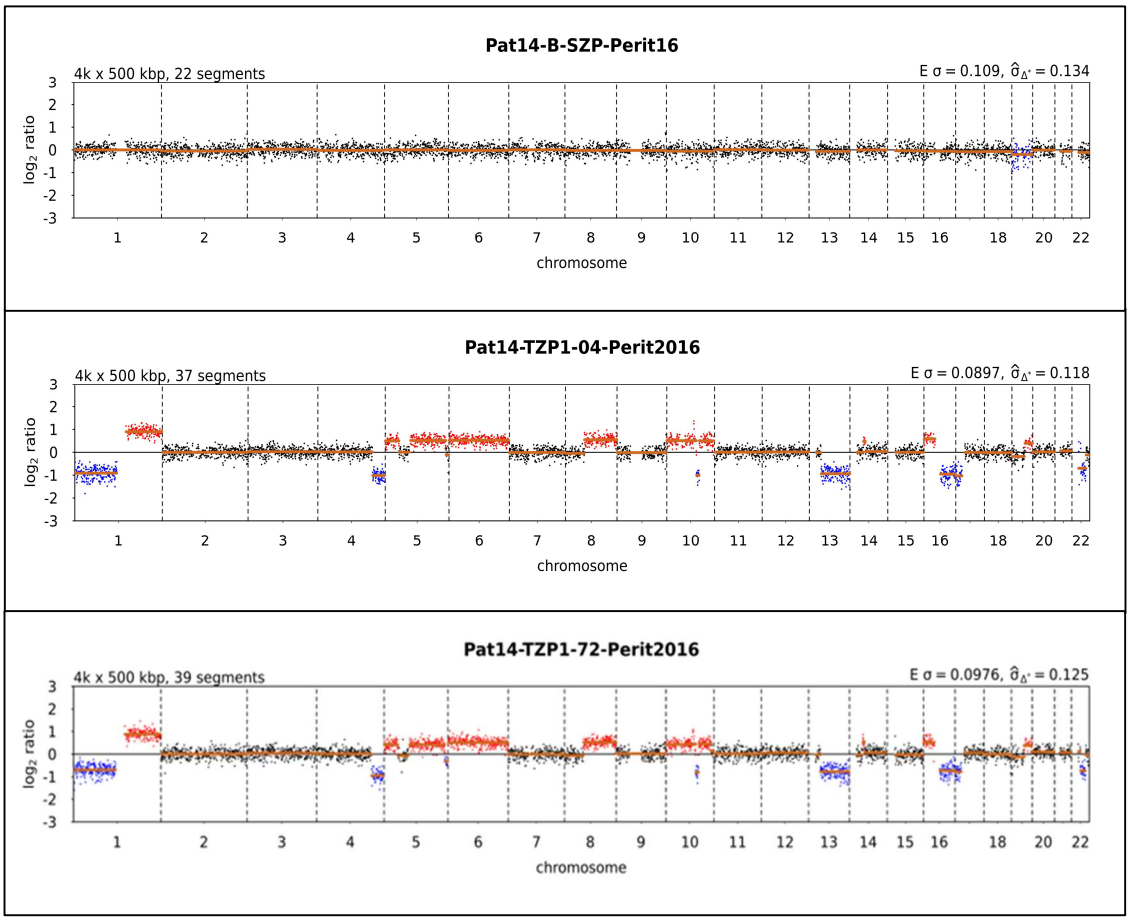

FigureA 27 Copy number variation profiles of tissue from patient ID14/16/18
Above: CNV profile of the isolated stromal cell pool (SZP) from the peritoneal metastases in 2016, **Middle:** CNV profile of an isolated tumor cell pool (TZP) from the peritoneal metastases in 2016 (DNAIndex 1,04), **Below:** CNV profile of an isolated TZP from the peritoneal metastases in 2016 (DNAIndex 1,72). Populations were isolated with the DEPArray. Interpretation of profiles in 2.22.

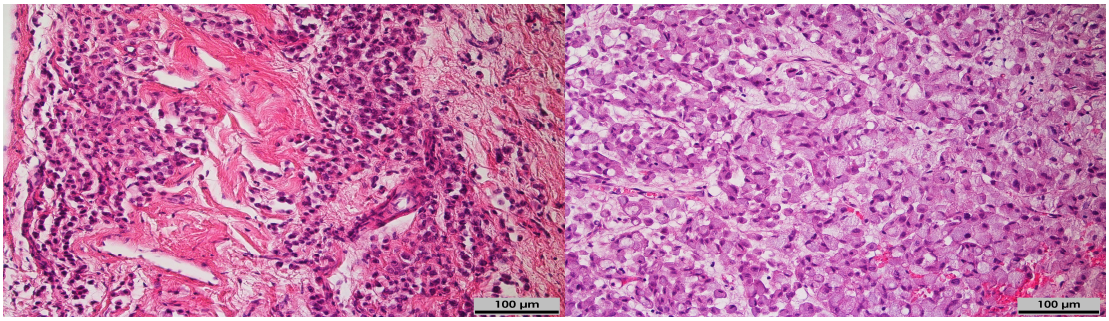

FigureA 28 Hematoxylin-Eosin staining of FFPE slices from patient ID14
Stained tumor tissue from breast cancer ID14 – MC17-256, left: pleura pool (timepoint 1). right: bladder (timepoint 3) metastases. Violet dots are representing tumor cells, scale 100 µm.

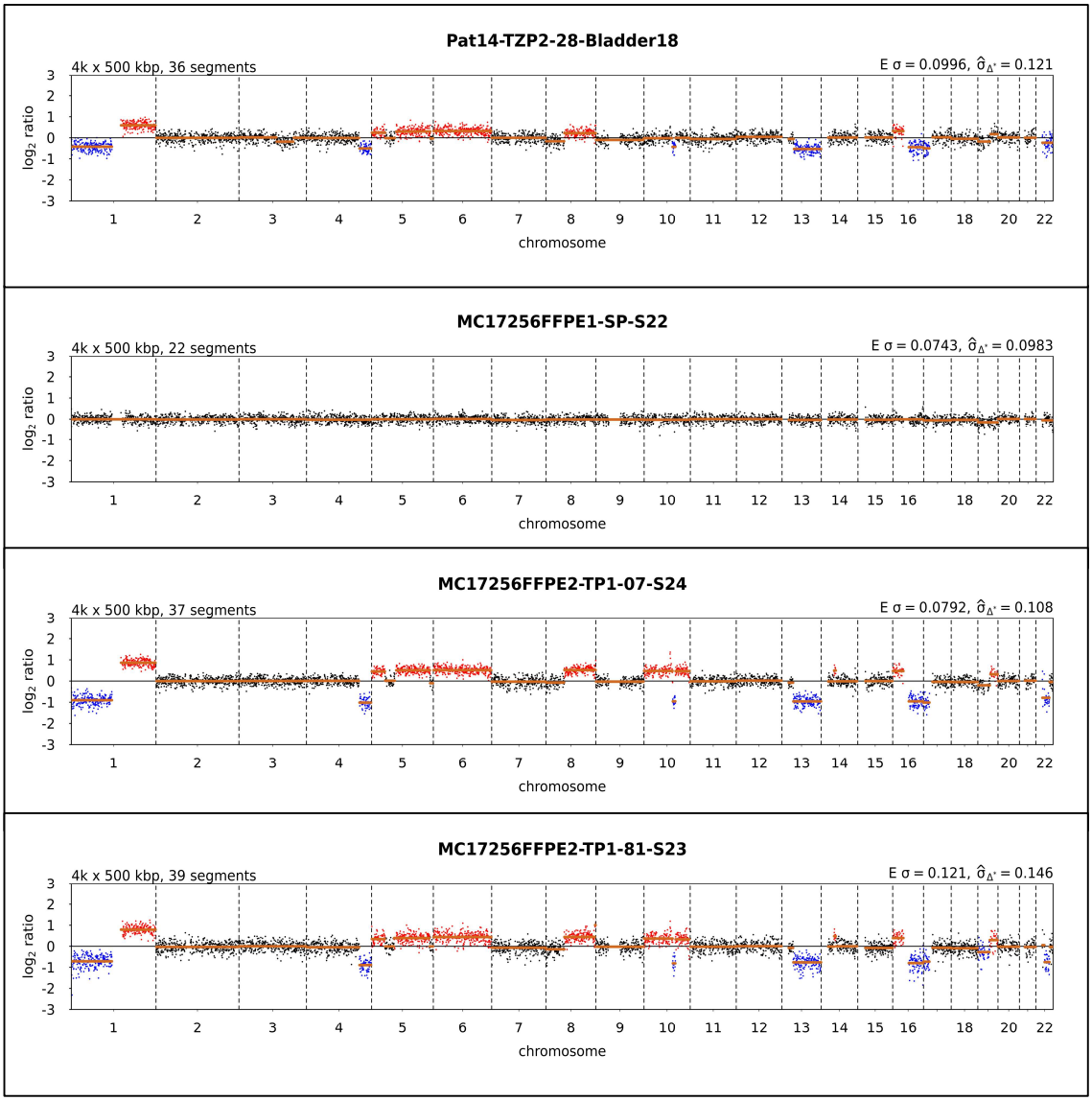

FigureA 29 Copy number variation profiles of tissue from patient ID14/16/18
Above: Aberrant copy number variation (CNV) profile of the isolated tumor cell pool (TZP) from the bladder metastases (ID18 - timepoint 3), **Below:** S22: CNV profile of the isolated stromal cell pool (SZP) from the pleura pool, S24: CNV profile of an isolated TZP from the pleura pool (DNAIndex 1,07), S23: CNV profile of an isolated TZP from the pleura pool (DNAIndex 1,81) all from patient ID14 – timepoint 1.Isolated with the DEPArray. Interpretation of profiles in 2.22.

Available information from lung cancer patient ID 15 – SCLC18-013:

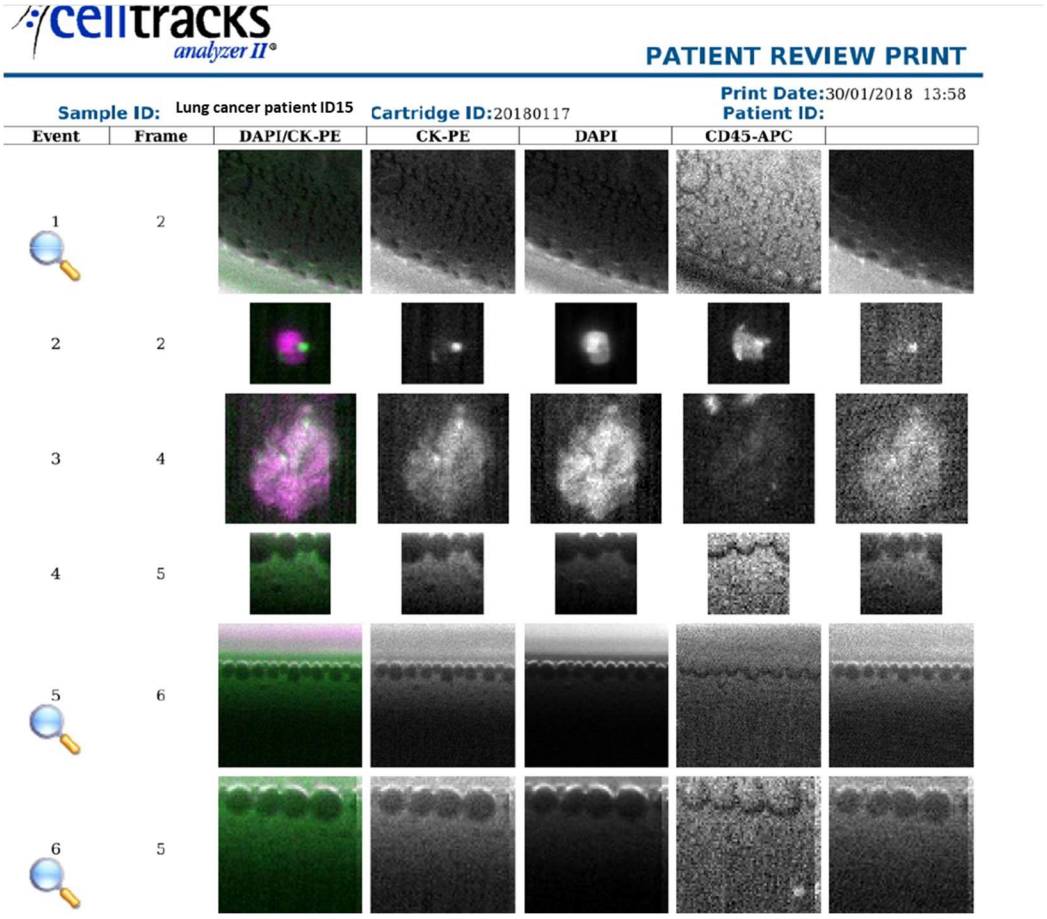

FigureA 30 Excerpt of the CellSearch Gallery patient ID15
No disseminated cancer cells found in the cerebrospinal fluid (CSF) enrichment of lung cancer ID15 – SCLC18-013 First the event number, the frame in which the cells can be found, a DAPI/CK overlay channel, the CK-PE channel, the DAPI and the CD45-APC channel.

Available information from breast cancer patient ID 17 – MC18-087:

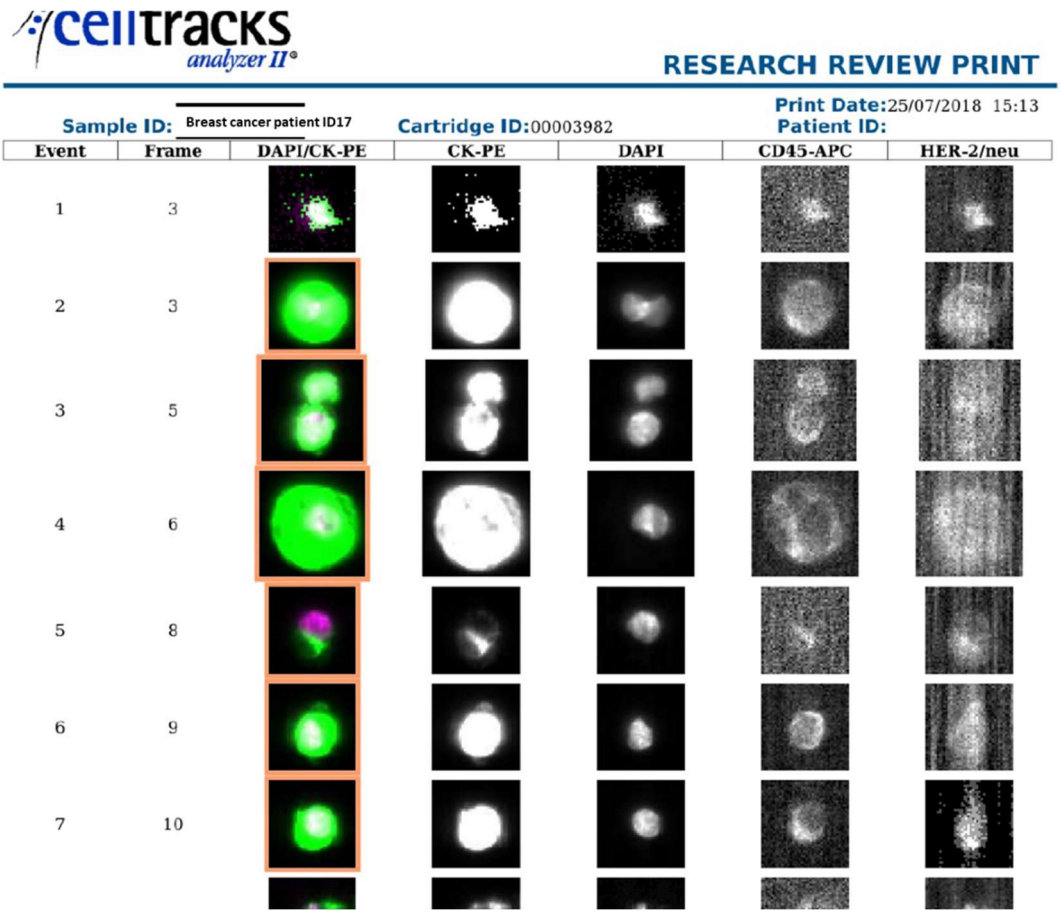

FigureA 31 Excerpt of the CellSearch Gallery patient ID17
Representative for the 190 disseminated cancer cells found in the cerebrospinal fluid (CSF) enrichment of breast cancer ID17 – MC18-187 the first six cells from the CellSearch Gallery. First the event number, the frame in which the cells can be found, a DAPI/CK overlay channel, the CK-PE channel, the DAPI and the CD45-APC channel.

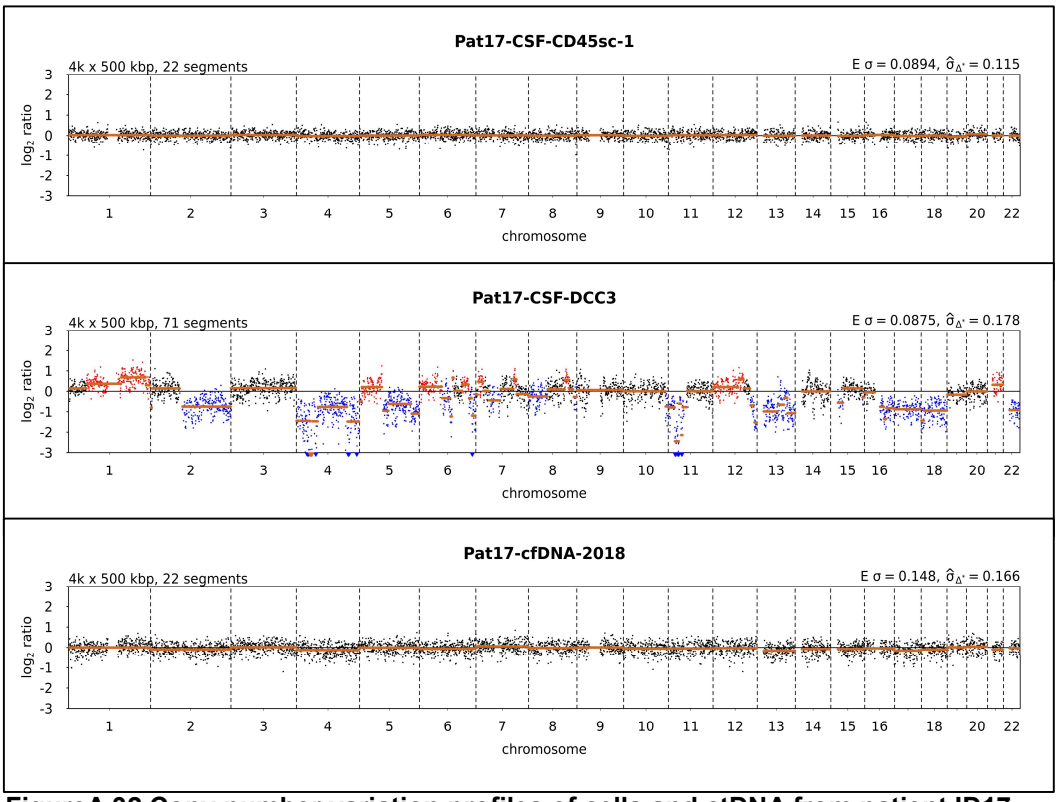

FigureA 32 Copy number variation profiles of cells and ctDNA from patient ID17
Above: Balanced copy number variation (CNV) profile of the isolated CD45 positive single cell1, **Middle:** Aberrant CNV profile of isolated disseminated cancer cell (DCC) 3. Cells are from CSF enriched with the CellSearch system and isolated manually by micromanipulation. **Below:** Balanced CNV profile of circulating cell free tumor DNA (ctDNA) isolated from CSF. Cells and ctDNA are derived from breast cancer patient ID 17 – MC18-087. Interpretation of profiles in 2.22.

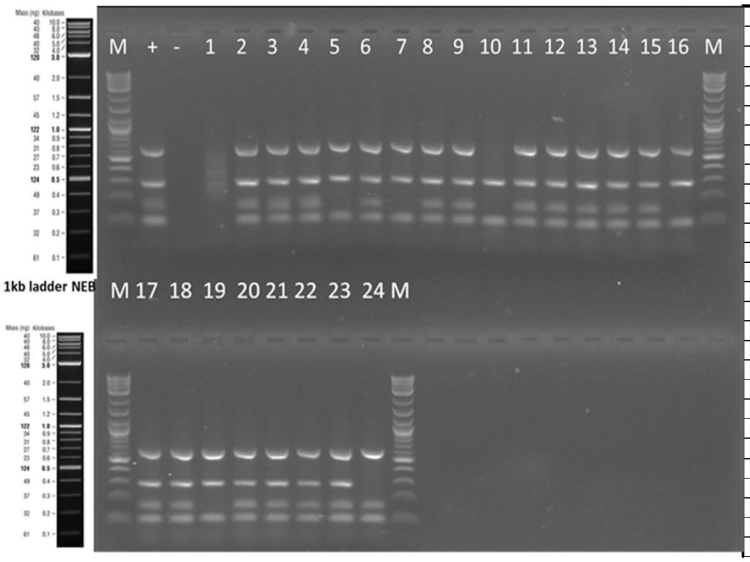

M	1 kb ladder NEB	GII
+	Positive control	4
-	Negative control	0
1	MC18-0087 Liq_PK	0
2	MC18-0087 Liq_Pool	4
3	MC18-0087 Liq_NZ1	4
4	MC18-0087 Liq_NZ2	4
5	MC18-0087 Liq_TZ 01	3
6	MC18-0087 Liq_TZ 02	4
7	MC18-0087 Liq_TZ 03	3
8	MC18-0087 Liq_TZ 04	4
9	MC18-0087 Liq_TZ 05	4
10	MC18-0087 Liq_TZ 06	2
11	MC18-0087 Liq_TZ 07	4
12	MC18-0087 Liq_TZ 08	4
13	MC18-0087 Liq_TZ 09	4
14	MC18-0087 Liq_TZ 10	4
15	MC18-0087 Liq_TZ 11	4
16	MC18-0087 Liq_TZ 12	3
17	MC18-0087 Liq_TZ 13	4
18	MC18-0087 Liq_TZ 14	4
19	MC18-0087 Liq_TZ 15	3
20	MC18-0087 Liq_TZ 16	4
21	MC18-0087 Liq_TZ 17	4
22	MC18-0087 Liq_TZ 18	4
23	MC18-0087 Liq_TZ 19	4
24	MC18-0087 Liq_TZ 20	3
M	1 kb ladder NEB	-

FigureA 33 Agarosegel picture of quality control PCR patient ID17
Mulitplex (4x) of single disseminated cancer cells isolated from CSF of breast cancer patient ID17 – MC18-087, including a size marker, a positive and a negative control and a sample list below. The genomic integrity index (GII) defines high quality cells (GII 2-4) or low quality cells (GII 0-1). Cells were enriched by the CellSearch system and isolated manually by micromanipulation.

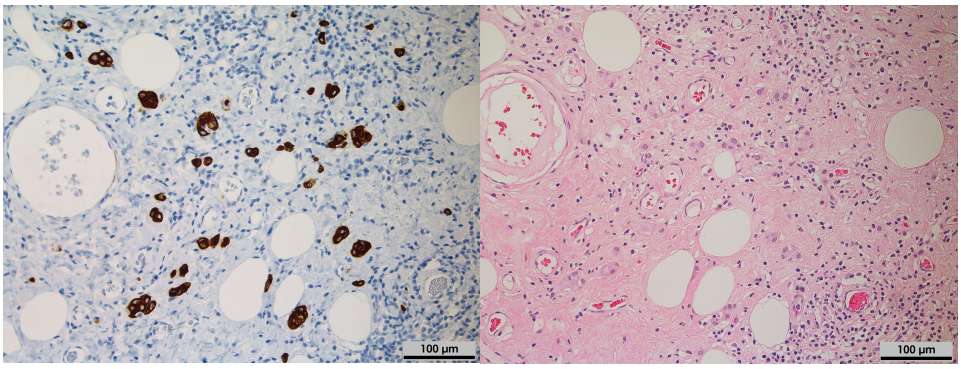

FigureA 34 Cytological staining of FFPE lymphnode slices from patient ID17
Left: Cytokeratin antibody, **Right:** Hematoxylin-Eosin staining.
10 µm tissue slices stained by pathologists of the University of Regensbug from lymph node metastases resected in 2017 of breast cancer ID17 – MC18-087 for defining the tumor content.Violet dots are representing tumor cells, scale bar 100 µm.

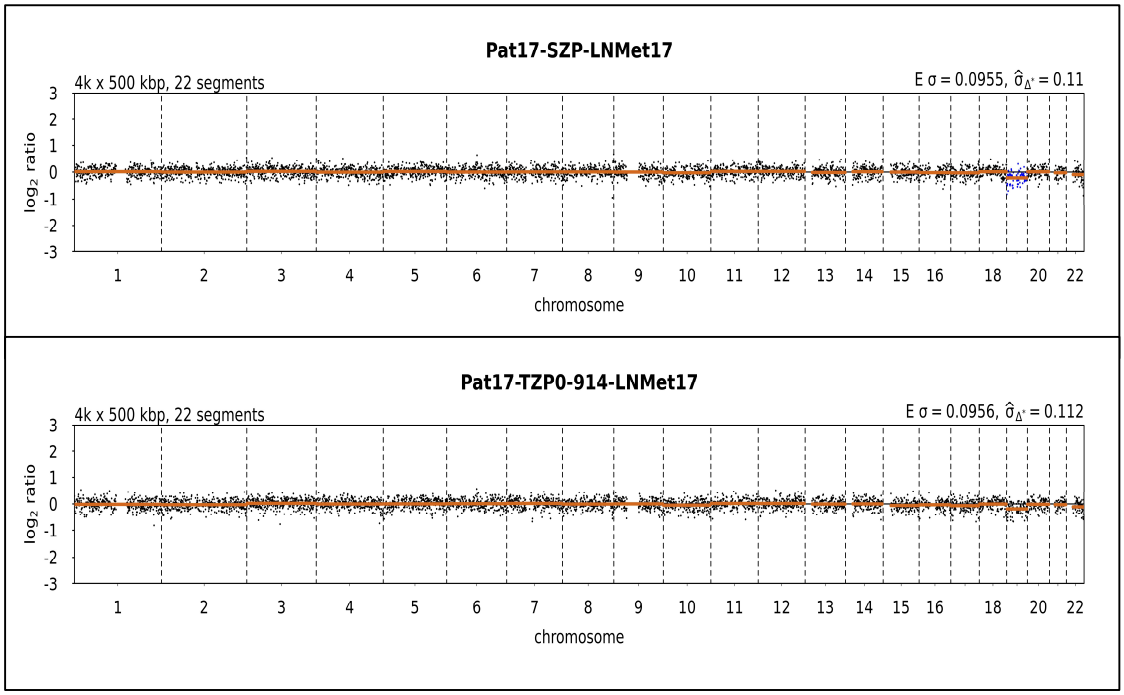

FigureA 35 Copy number variation profiles of lymph node tissue from patient ID17
Above: Balanced copy number variation (CNV) profile of the isolated stromal cell pool.
Below: Aberrant CNV profile of isolated tumor cell pool (DNAIndex 0.914). Cells derived from a lymph node metastases resected in 2017 from breast cancer patient ID17 – MC18-087 isolated automatically with the DEPArray system. Interpretation of profiles in 2.22.

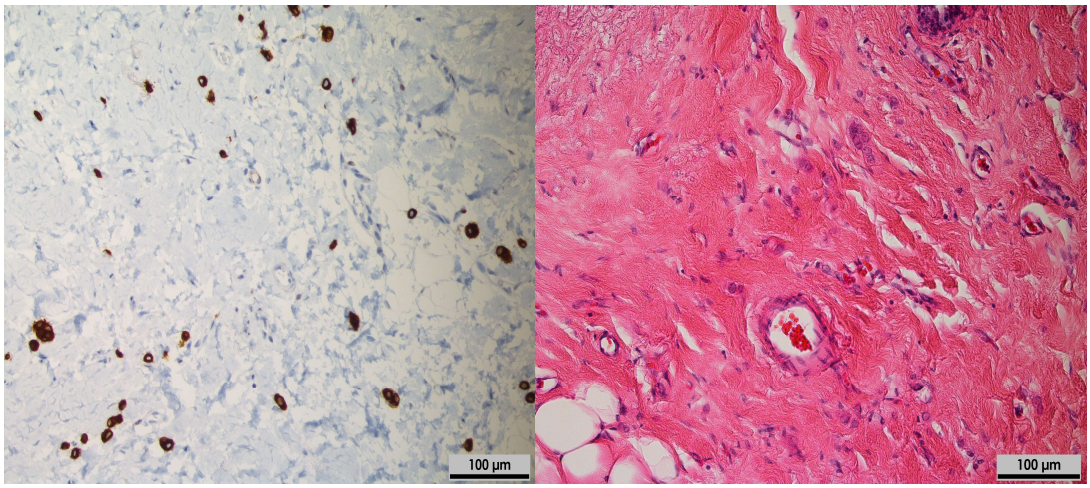

FigureA 36 Cytological staining of FFPE primary tumor from patient ID17
Left: Cytokeratin antibody, **Right:** Hematoxylin-Eosin staining.
10 µm tissue slices stained by pathologists of the University of Regensbug from primary tissue resected in 2017 of breast cancer ID17 – MC18-087 for defining the tumor content.Violet dots are representing tumor cells, scale bar 100 µm.

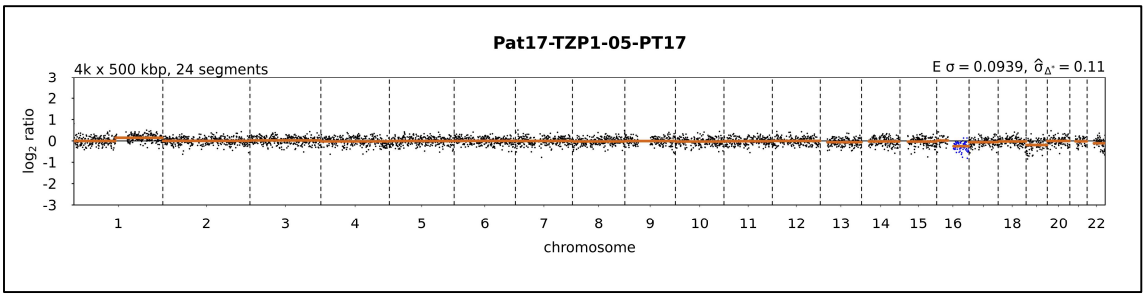

FigureA 37 Copy number variation profiles of tissue from patient ID17
Above: Balanced copy number variation (CNV) profile of the isolated tumor cell pool (DNAInde 1.05). The profile of the stromal cell population did not work in sequencing and cannot be shown here. Cells derived from the primary tumor resected in 2017 from breast cancer patient ID17 – MC18-087 isolated automatically with the DEPArray system. Interpretation of profiles in 2.22.

Available information from breast cancer patient ID 21 – MC18-201:

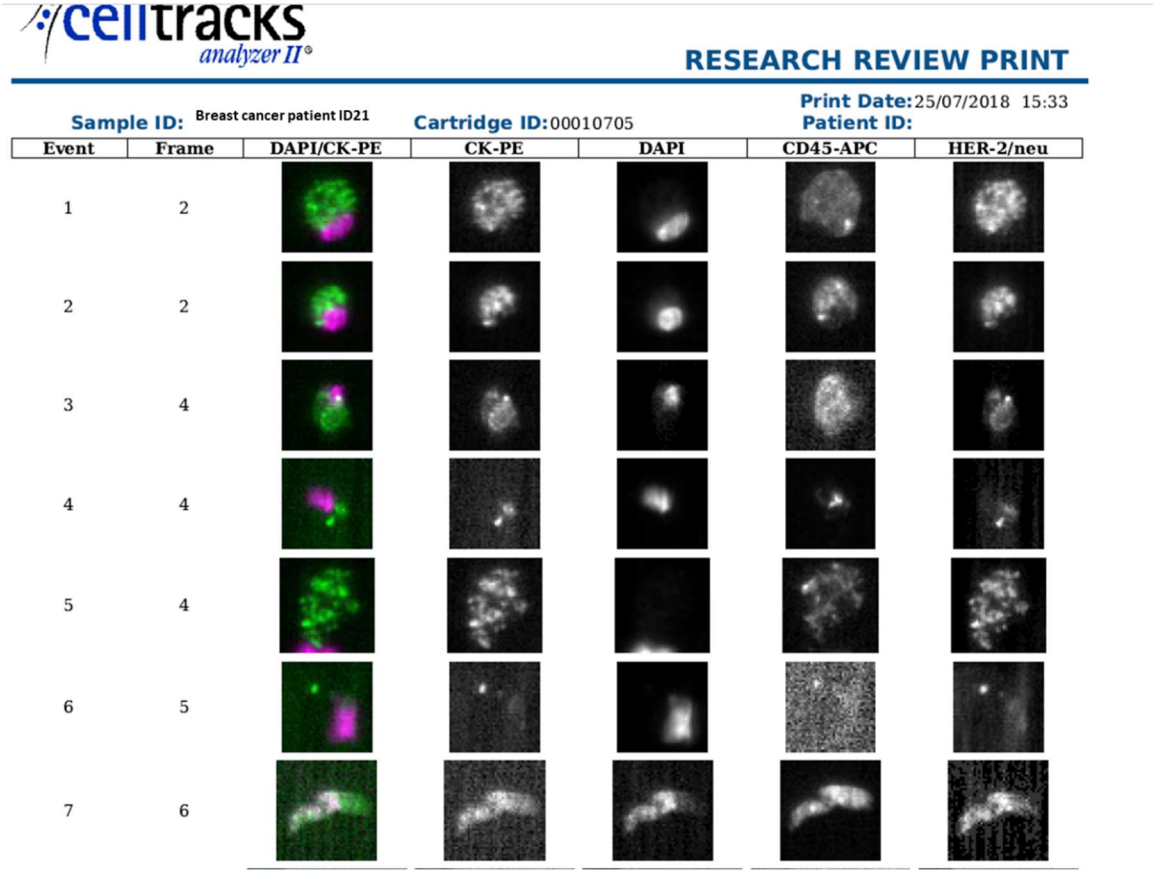

FigureA 38 Excerpt of the CellSearch Gallery patient ID21
Representative for the 5 disseminated cancer cells found in the cerebrospinal fluid (CSF) enrichment of breast cancer ID21 – MC18-201 the first six cells from the CellSearch Gallery. Unfortunately the cells are not marked in this report. First the event number, the frame in which the cells can be found, a DAPI/CK overlay channel, the CK-PE channel, the DAPI and the CD45-APC channel.

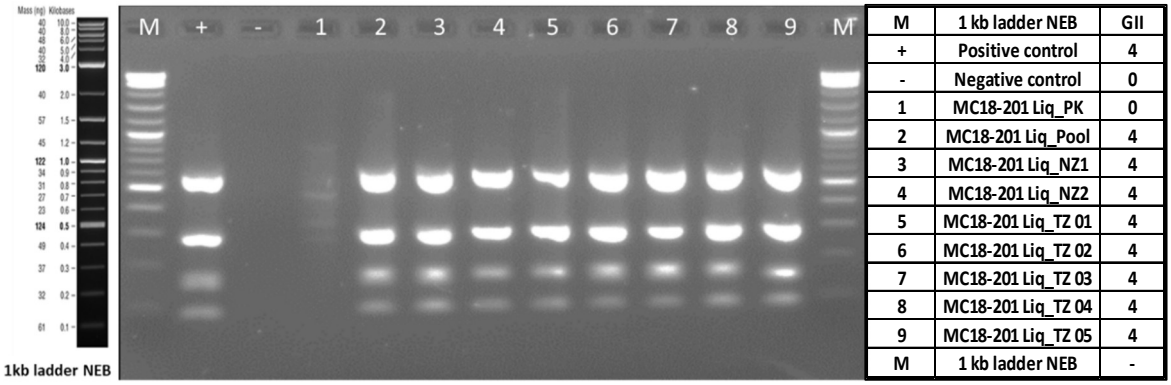

M	1 kb ladder NEB	GII
+	Positive control	4
-	Negative control	0
1	MC18-201 Liq_PK	0
2	MC18-201 Liq_Pool	4
3	MC18-201 Liq_NZ1	4
4	MC18-201 Liq_NZ2	4
5	MC18-201 Liq_TZ 01	4
6	MC18-201 Liq_TZ 02	4
7	MC18-201 Liq_TZ 03	4
8	MC18-201 Liq_TZ 04	4
9	MC18-201 Liq_TZ 05	4
M	1 kb ladder NEB	-

FigureA 39 Agarosegel picture of quality control PCR patient ID21
Mulitplex (4x) of single disseminated cancer cells isolated from CSF of breast cancer patient ID21 MC18-201, including a size marker, a positive and a negative control and a sample list on the right side. The genomic integrity index (GII) defines high quality cells (GII 2-4) or low quality cells (GII 0-1). Cells were enriched by the CellSearch system and isolated manually by micromanipulation.

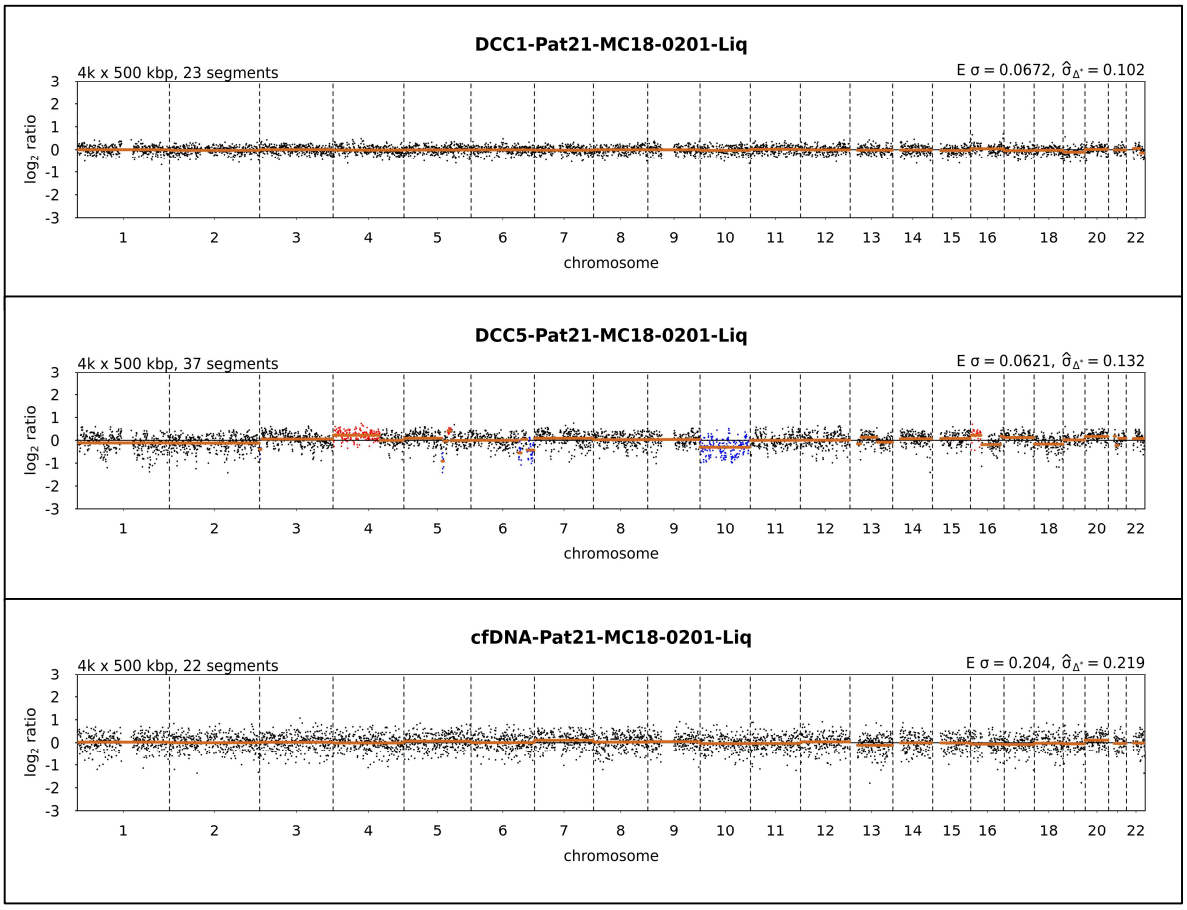

FigureA 41 Copy number variation profiles of cells and ctDNA from patient ID21
Above: Balanced copy number variation (CNV) profile of the isolated disseminated cancer cell (DCC)1**Middle:** Slightly aberrant CNV profile of isolated disseminated cancer cell (DCC)5. Cells are from CSF enriched with the CellSearch system and isolated manually by micromanipulation. **Below:** Balanced CNV profile of circulating cell free tumor DNA (ctDNA) isolated from CSF. Cells and ctDNA are derived from breast cancer patient ID 21 – MC18-201. Interpretation of profiles in 2.22.

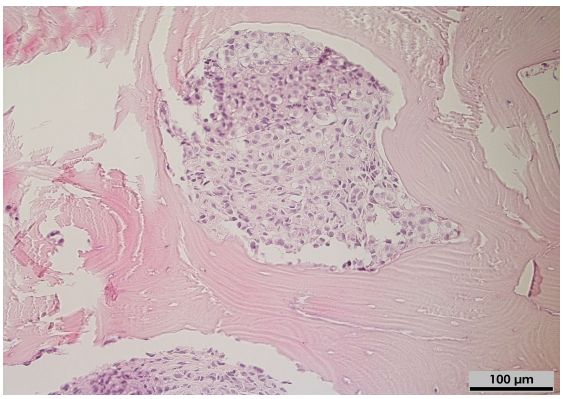

FigureA 40 Cytological staining of FFPE bone metastases from patient ID21
Hematoxylin-Eosin staining of a10 µm tissue slice stained by pathologists of the University of Regensbug from a bone metastases resected in 2017 of breast cancer ID21 – MC18-201 for defining the tumor content.Violet dots are representing tumor cells, scale bar 100 µm.

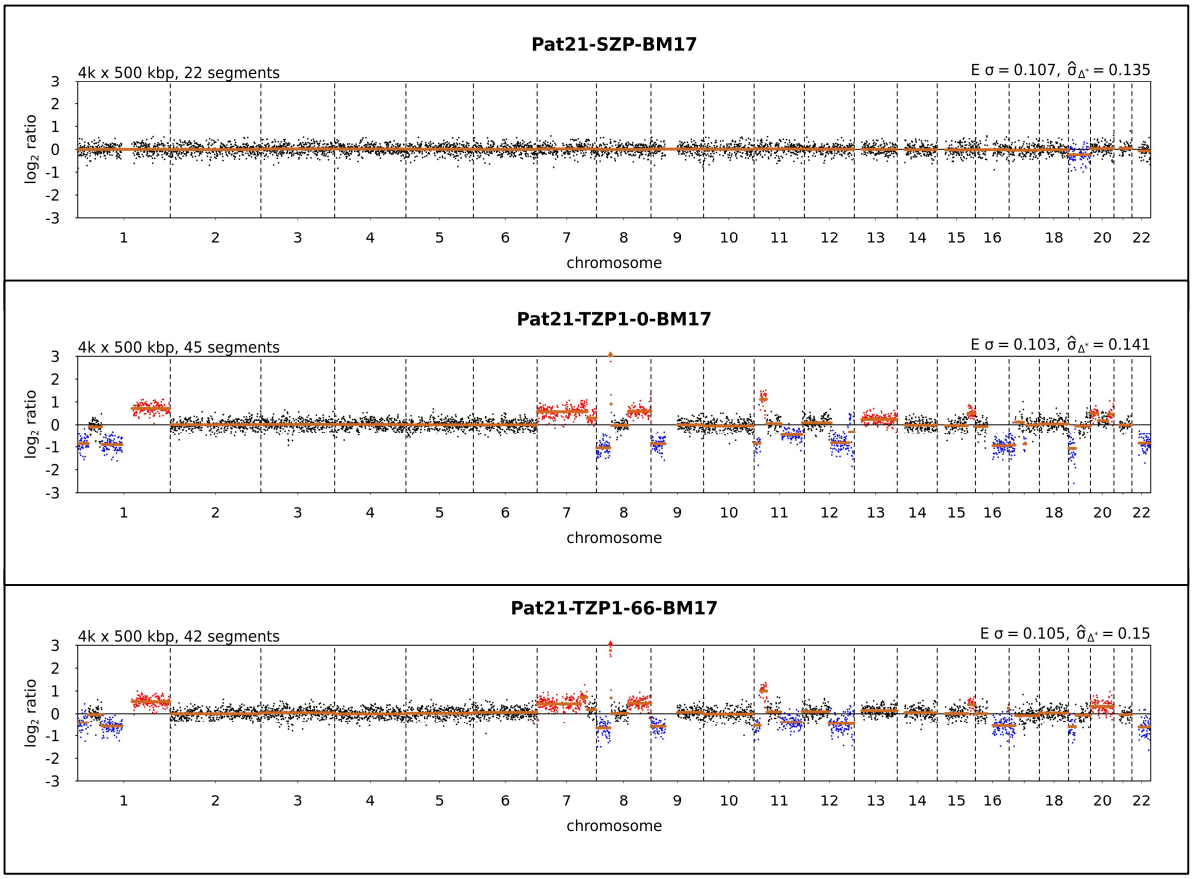

FigureA 42 Copy number variation profiles of tissue from patient ID21
Above: Balanced copy number variation (CNV) profile of the isolated stromal cell pool from the bone metastases.**Middle:** CNV profile of the isolated tumor cell pool (TZP, DNAIndex 1.0) from bone metastases. **Below:** CNV profile of the isolated TZP (DNAIndex 1.66) from bone metastases. Cell were isolated automatically with the DEPArray from a bone metastases detected in 2017 from breast cancer patient ID21 – MC18-201. Interpretation of profiles in 2.22.

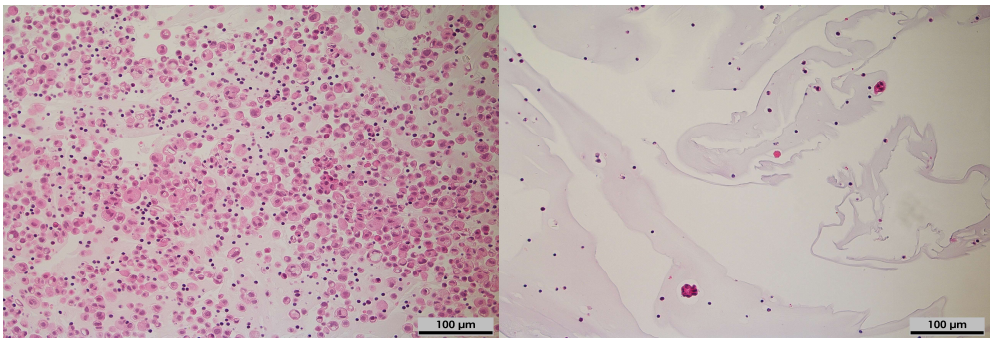

FigureA 43 Cytological staining of FFPE pleura tissue from patient ID21
Left: Hematoxylin-Eosin staining of pleura tissue from 2016, **Right:** Hematoxylin-Eosin staining pleura tissue from 2017.10 µm tissue slices stained by pathologists of the University of Regensbug from pleura tissue resected in 2016/2017 of breast cancer ID21 – MC18-201 for defining the tumor content.Violet dots are representing tumor cells, scale bar 100 µm.

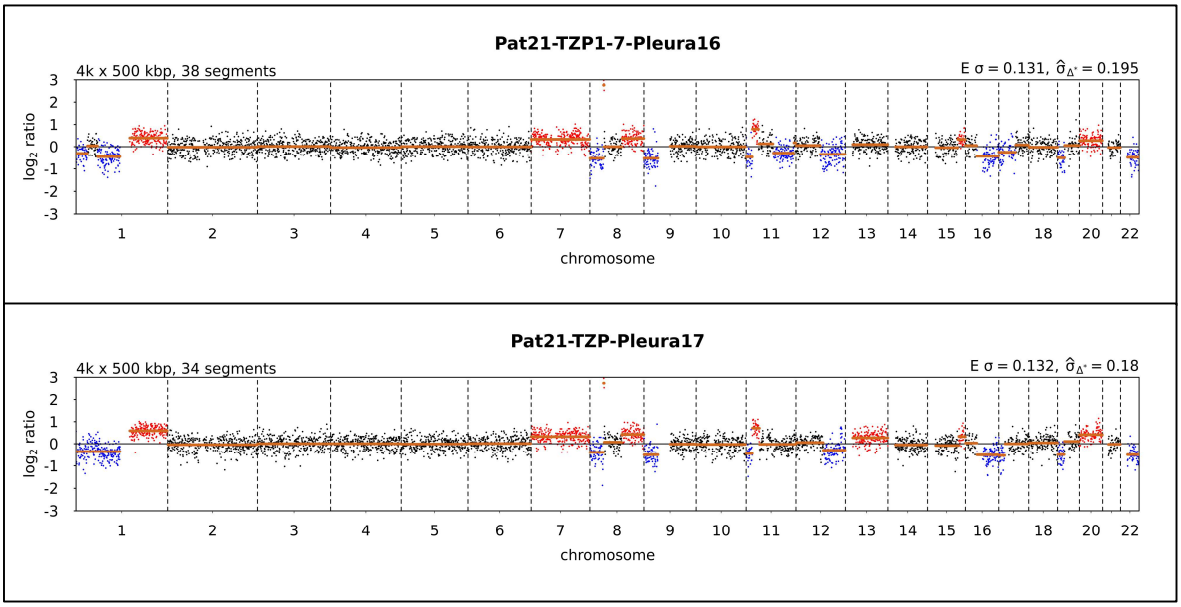

FigureA 44 Copy number variation profiles of tissue from patient ID21
Above: CNV profile of the isolated tumor cell pool (TZP, DNAIndex 1.7) from pleura tissue 2016. **Below:** CNV profile of the isolated TZP (DNAIndex n.a.) from pleura tissue 2017. Cell were isolated automatically with the DEPArray from a pleural effusion embedded in FFPE detected in 2016/2017 from breast cancer patient ID21 – MC18-201. Interpretation of profiles in 2.22.

Available information from cancer of unknown primary patient ID 22 – CUP18-210

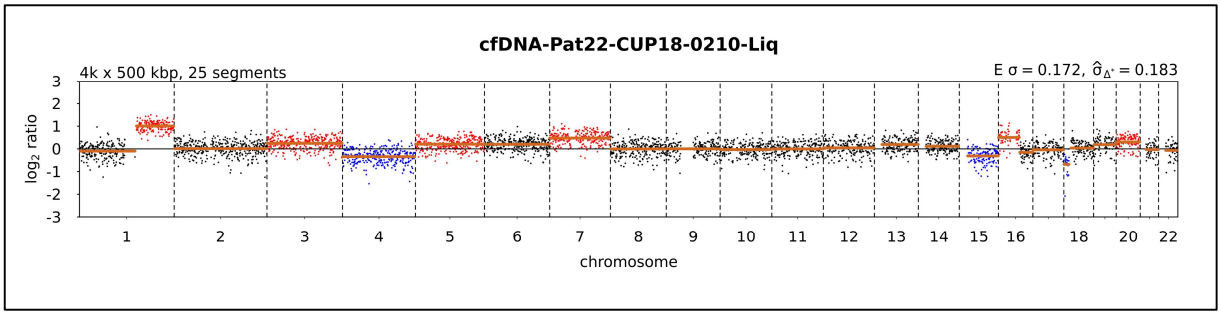

FigureA 45 Copy number variation profiles of cfDNA from patient ID22
Aberrant CNV profile of circulating cell free tumor DNA (ctDNA) isolated from CSF from cancer of unknown primary patient 22 – CUP18-210. Interpretation of profiles in 2.22.

Available information from colon carcinoma patient ID 24 – CC19-027

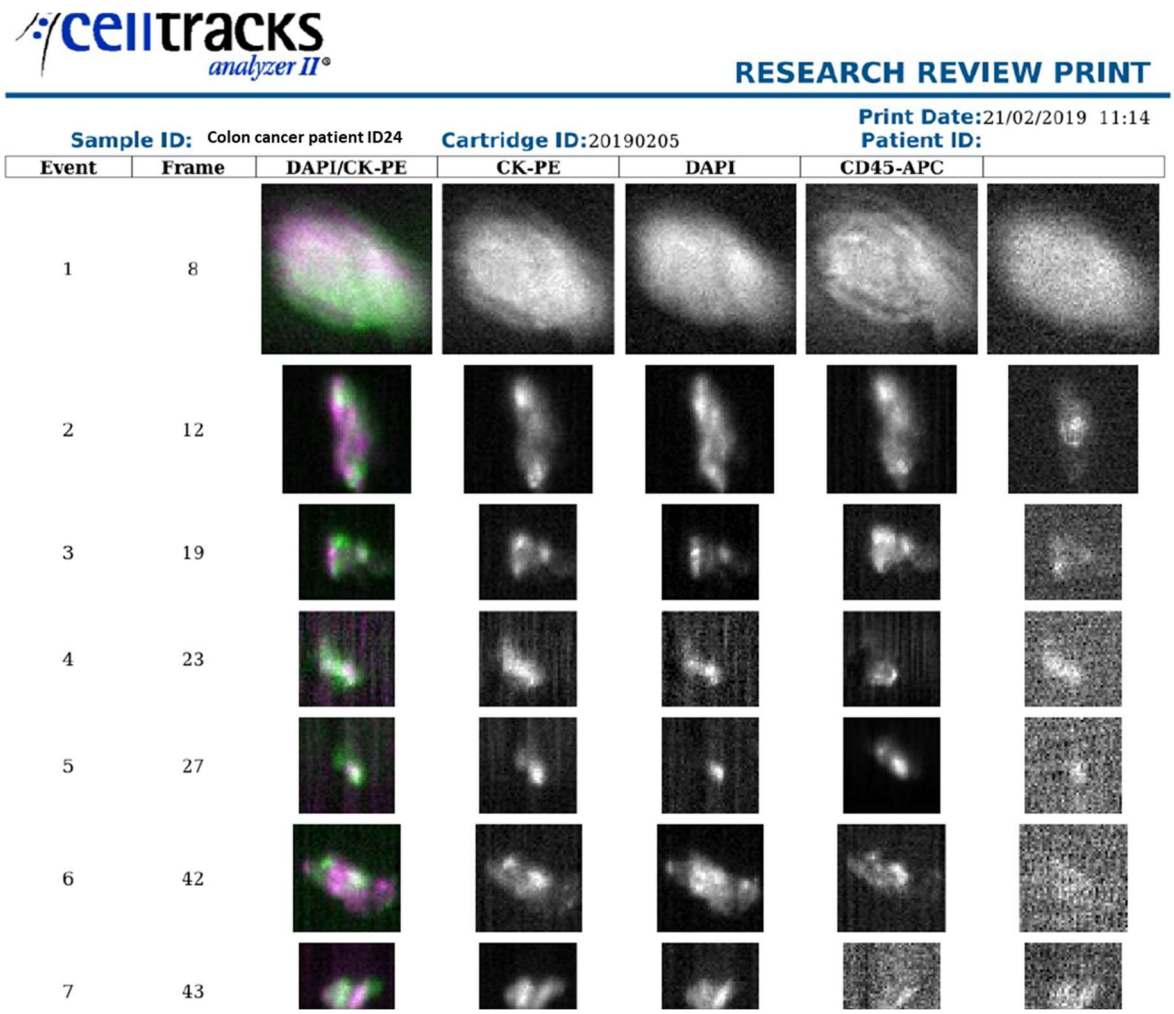

FigureA 46 Excerpt of the CellSearch Gallery patient ID24
No disseminated cancer cells found in the cerebrospinal fluid (CSF) enrichment of colon carcinoma patient ID24 – CC19-027 the first six cells from the CellSearch Gallery. First the event number, the frame in which the cells can be found, a DAPI/CK overlay channel, the CK-PE channel, the DAPI and the CD45-APC channel.

Available information from cancer of unknown primary patient ID 27 – CUP19-322

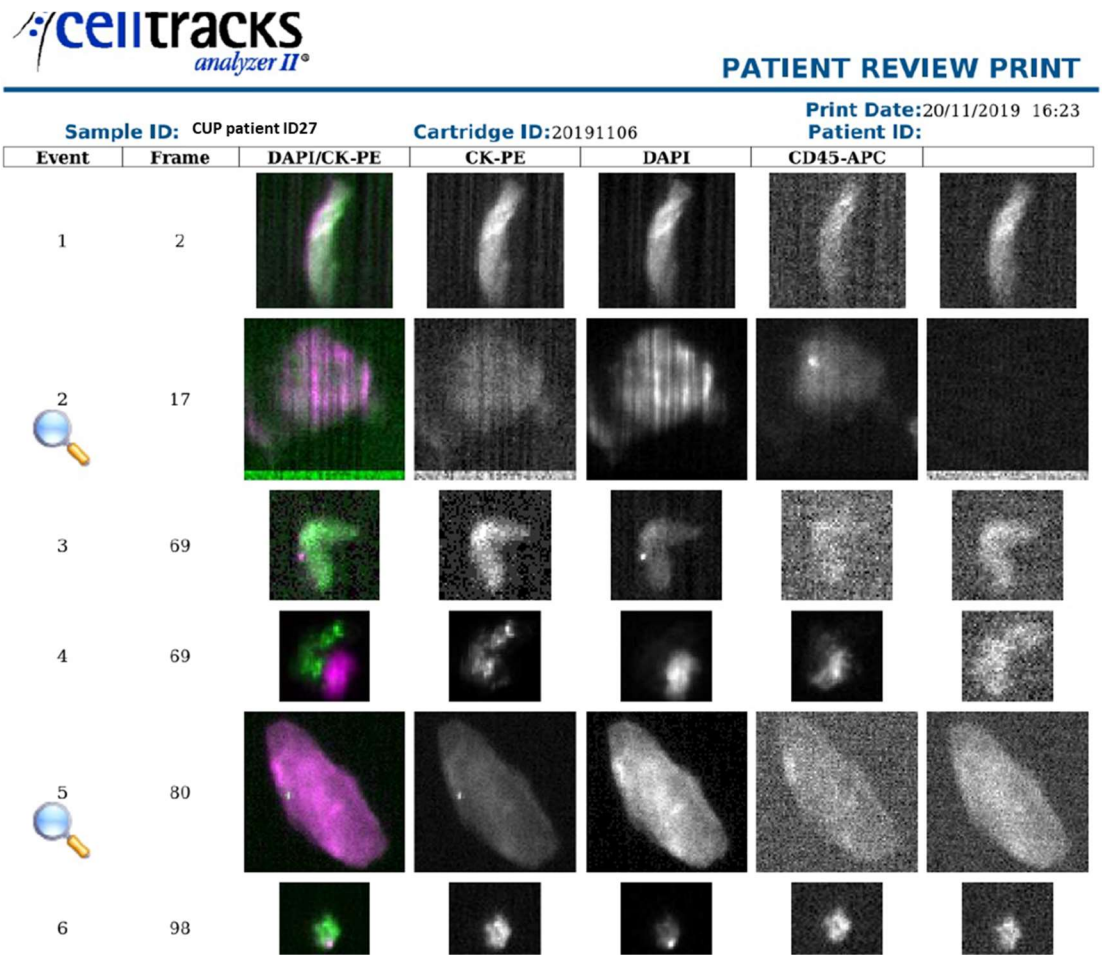

FigureA 47 Excerpt of the CellSearch Gallery patient ID27
No disseminated cancer cells found in the cerebrospinal fluid (CSF) enrichment of cancer of unknown primary patient ID27 – CUP19-322. Representative for the cells the first six cells are shown in this gallery. First the event number, the frame in which the cells can be found, a DAPI/CK overlay channel, the CK-PE channel, the DAPI and the CD45-APC channel.

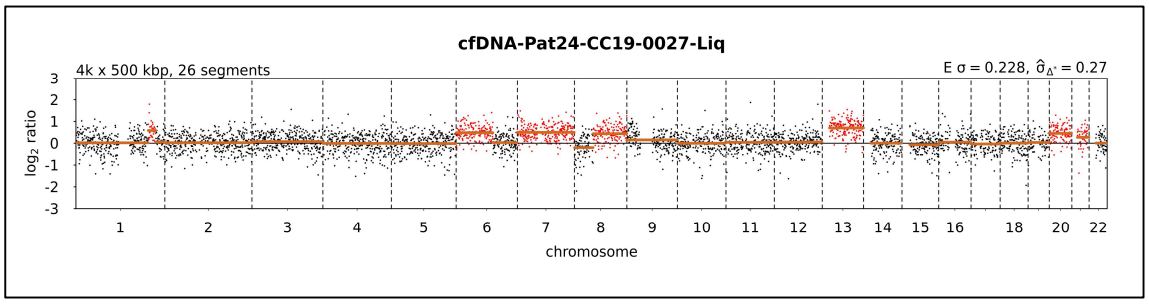

FigureA 48 Copy number variation profiles of cfDNA from patient ID24
Aberrant CNV profile of circulating cell free tumor DNA (ctDNA) isolated from CSF from colon carcinoma patient 24 – CC19-027. Interpretation of profiles in 2.22.

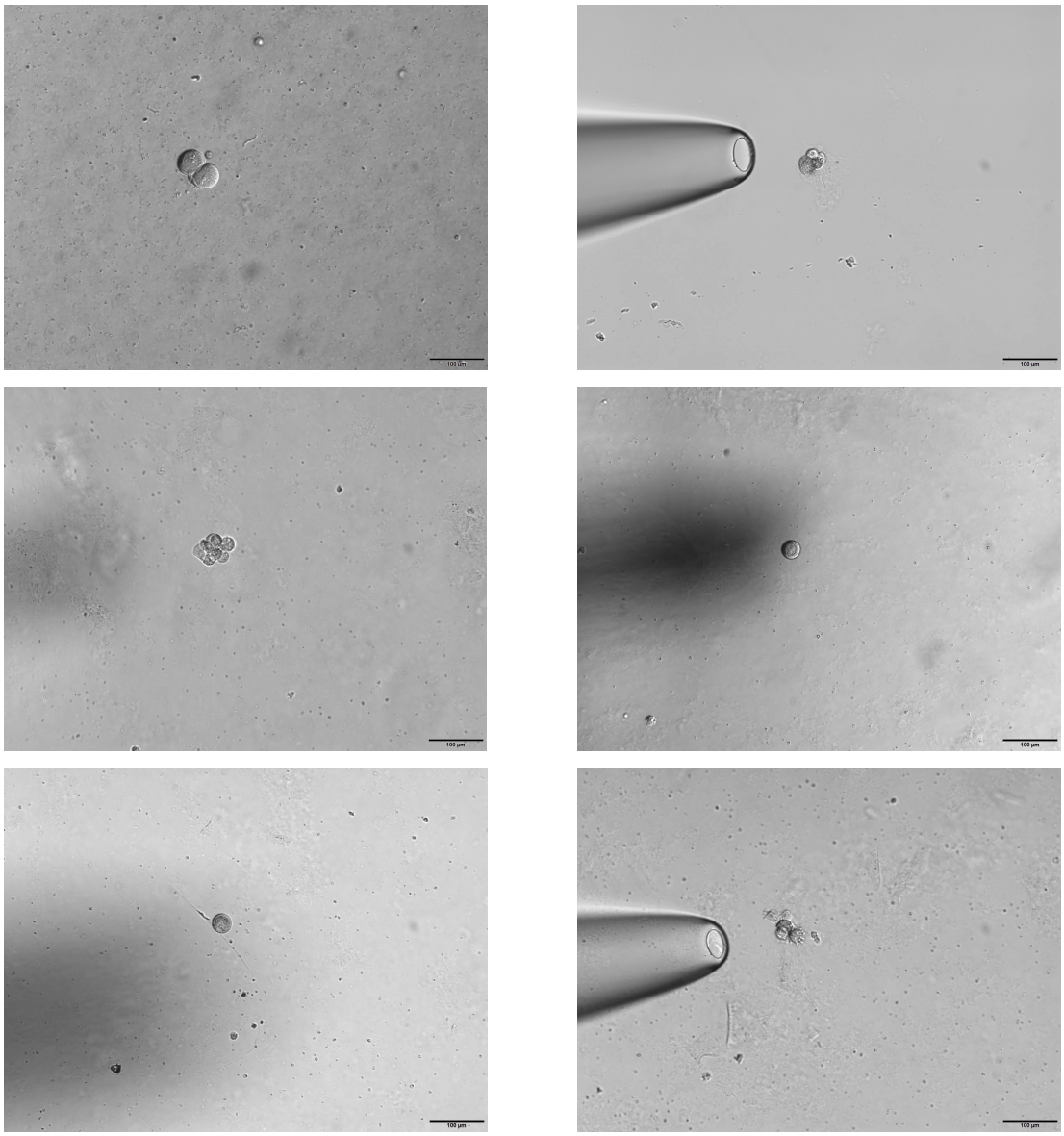

FigureA 49 Brightfield microscopy pictures of organoids patient ID27
Isolation procedure from organoids cultivated from native CSF of cancer of unknown primary patient ID27 – CUP19-322. Left up: Organoid1, Right up: Organoid2, Left middle: Organoid3, Right middle: Organoid4, Left down: Organoid5, Right down: Organoid6. Scale bare 100 µm.

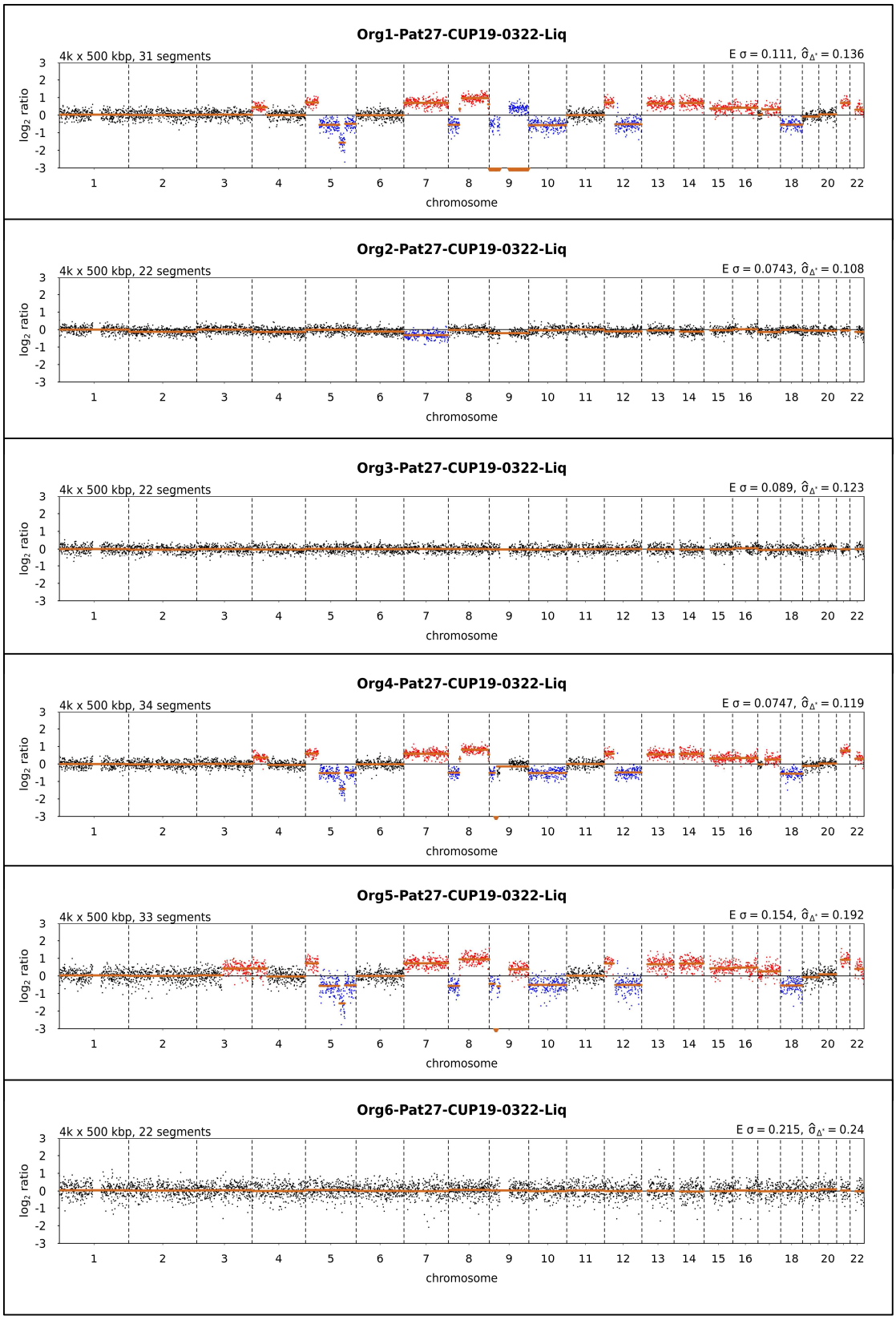

FigureA 50 Copy number variation profiles of organoids from patient ID27
Aberrant/balaned CNV profiles of organoids 1- 6 from native CSF cultivated under 3D conditions and isolated by micromanipluation from cancer of unknown primary patient ID 27 – CUP19-322. Microsope picture in FigureA 49. Interpretation of profiles in 2.22.

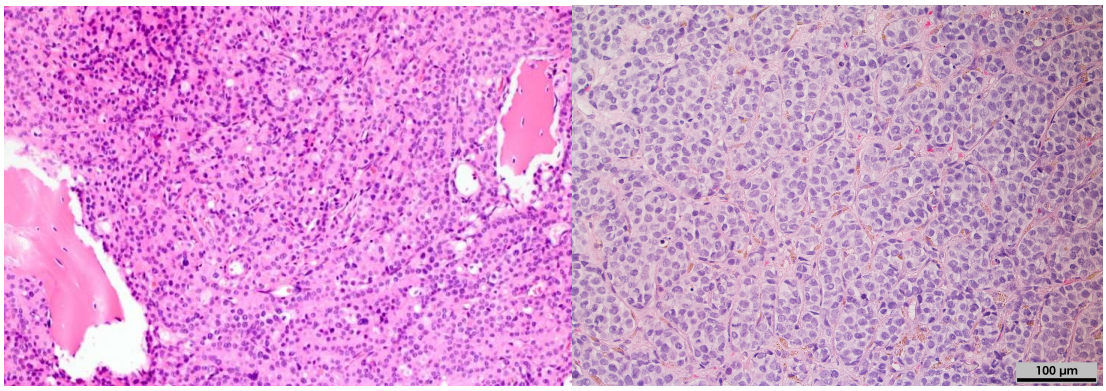

FigureA 51 Cytological staining of FFPE tissue from patient ID28
Left: Hematoxylin-Eosin staining of brain metastases 2016, **Right:** Hematoxylin-Eosin staining of liver metastases.10 µm tissue slices stained by neuropathologists and pathologists of the University of Regensbug from tissue of breast cancer ID28 – MC19-339 for defining the tumor content.Violet dots are representing tumor cells, scale bar 100 µm.

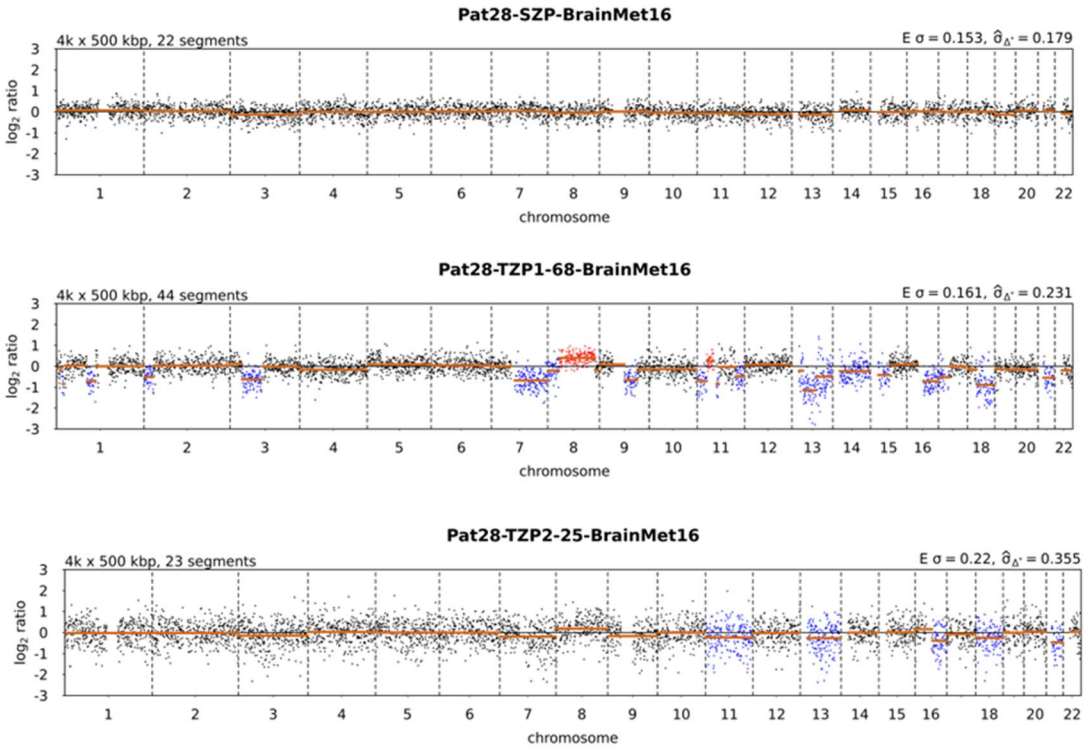

FigureA 52 Copy number variation profiles of tissue from patient ID28
Above: Balanced copy number variation (CNV) profile of the isolated stromal cell pool from the brain metastases.**Middle:** Aberrant CNV profile of the isolated tumor cell pool (TZP, DNAIndex 1.68) from brain metastases. **Below:** Unclear CNV profile of the isolated TZP (DNAIndex 2.25) from brain metastases. Cell were isolated automatically with the DEPArray from a brain metastases detected in 2016 from breast cancer patient ID28 – MC19-339. Interpretation of profiles in 2.22.

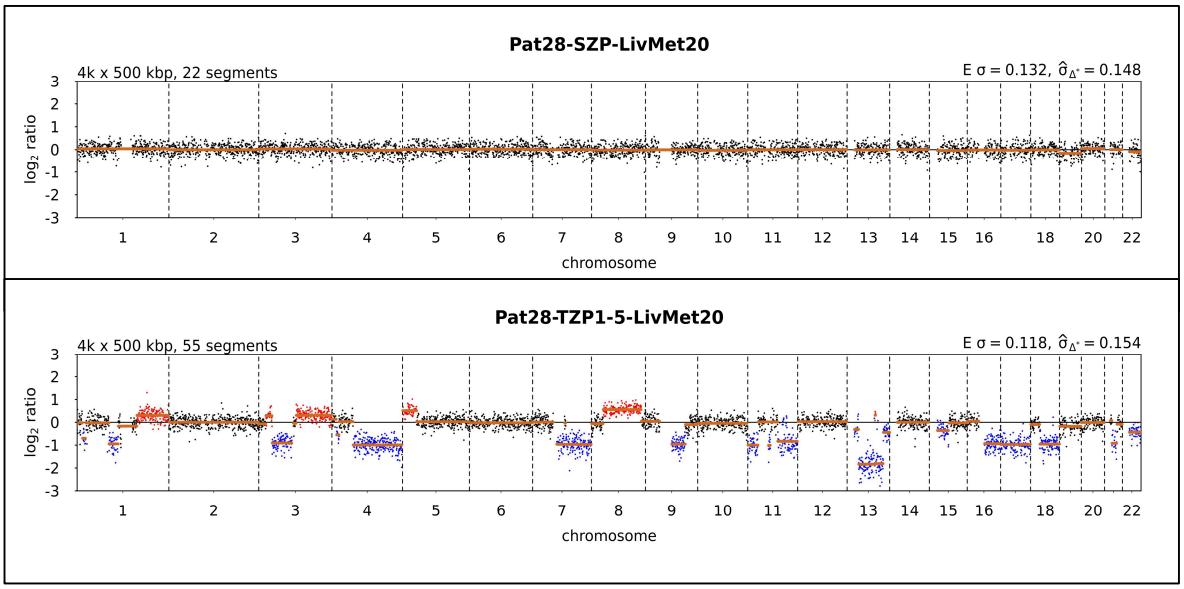

FigureA 53 Copy number variation profiles of tissue from patient ID28
Above: Balanced copy number variation (CNV) profile of the isolated stromal cell pool from the liver metastases.**Below:** Aberrant CNV profile of the isolated tumor cell pool (TZP, DNAIndex 1.5) from liver metastases. Cell were isolated automatically with the DEPArray from a liver metastases detected in 2020 from breast cancer patient ID28 – MC19-339. Interpretation of profiles in 2.22.

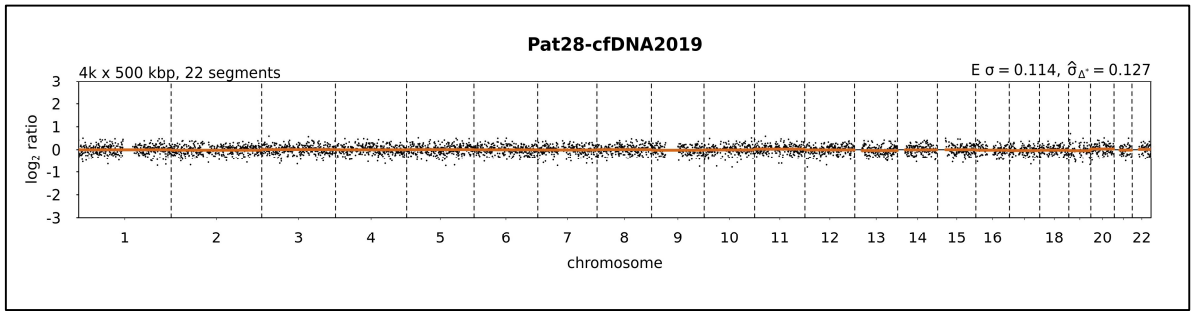

FigureA 54 Copy number variation profiles of cfDNA from patient ID28
Balanced CNV profile of circulating cell free tumor DNA (ctDNA) isolated from CSF from breast cancer patient 28 – MC19-339. Interpretation of profiles in 2.22.

Available information from breast cancer patient ID 29 – MC19-355

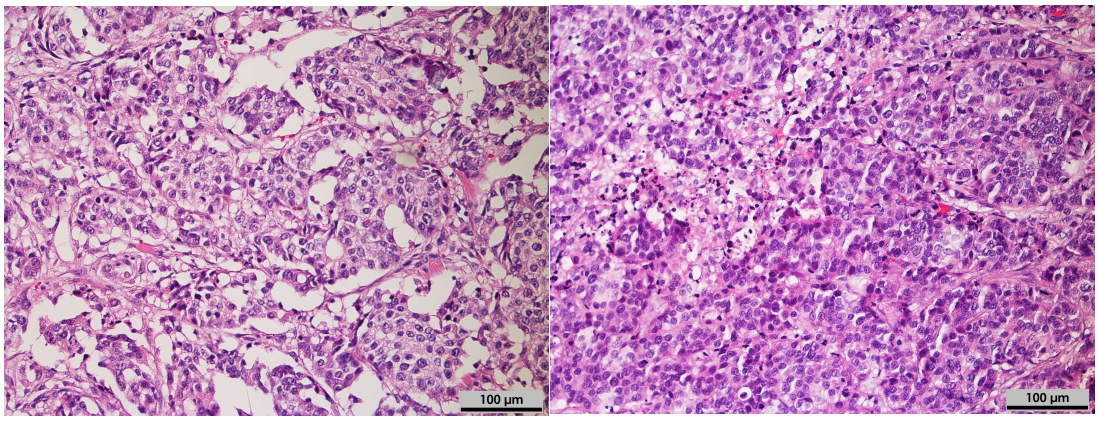

FigureA 55 Cytological staining of FFPE tissue from patient ID29
Left: Hematoxylin-Eosin staining of primary tumor 2015, **Right:** Hematoxylin-Eosin staining of lymph node metastases 2015.10 µm tissue slices stained by pathologists of the University of Regensbug from tissue of breast cancer ID29 – MC19-355 for defining the tumor content.Violet dots are representing tumor cells, scale bar 100 µm.

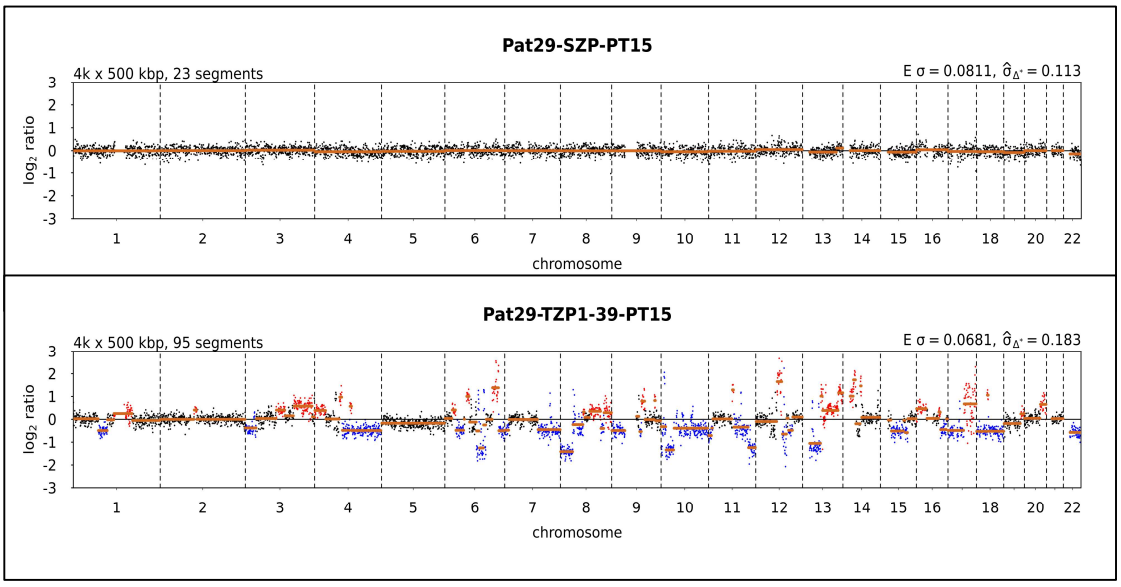

FigureA 56 Copy number variation profiles of tissue from patient ID29
Above: Balanced copy number variation (CNV) profile of the isolated stromal cell pool from the primary tumor.**Below:** Aberrant CNV profile of the isolated tumor cell pool (TZP, DNAIndex 1.39) from the primary tumor. Cell were isolated automatically with the DEPArray from the primary resected in 2015 from breast cancer patient ID29 – MC19-355. Interpretation of profiles in 2.22.

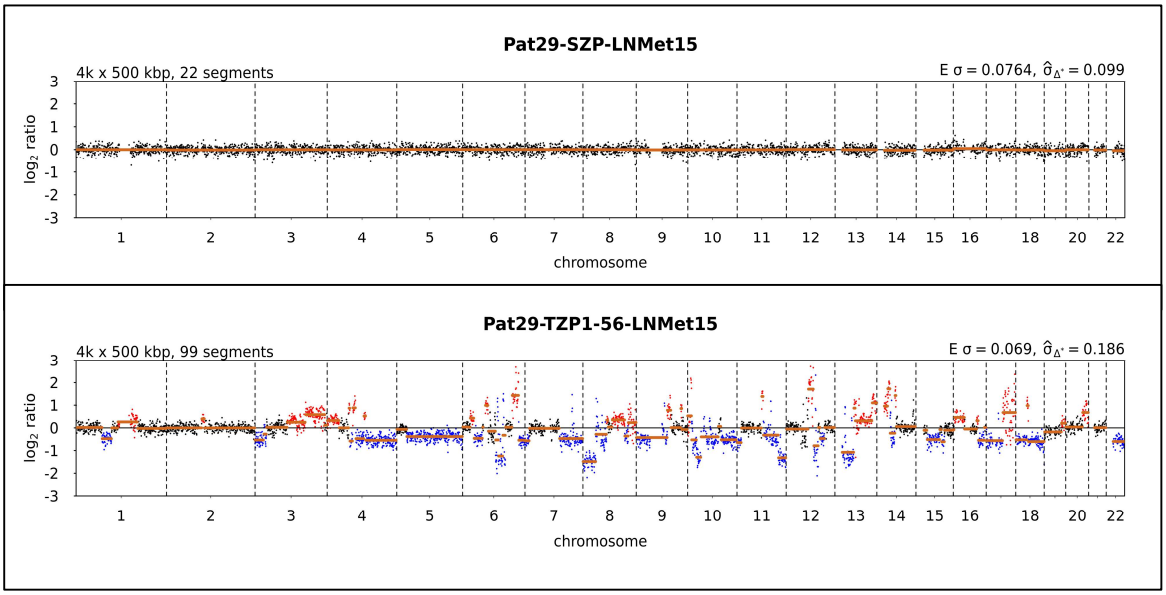

FigureA 57 Copy number variation profiles of tissue from patient ID29
Above: Balanced copy number variation (CNV) profile of the isolated stromal cell pool from the lymph node metastases.**Below:** Aberrant CNV profile of the isolated tumor cell pool (TZP, DNAIndex 1.56) from the lymph node metastases. Cell were isolated automatically with the DEPArray from a lymph node metastases resected in 2015 from breast cancer patient ID29 – MC19-355. Interpretation of profiles in 2.22.

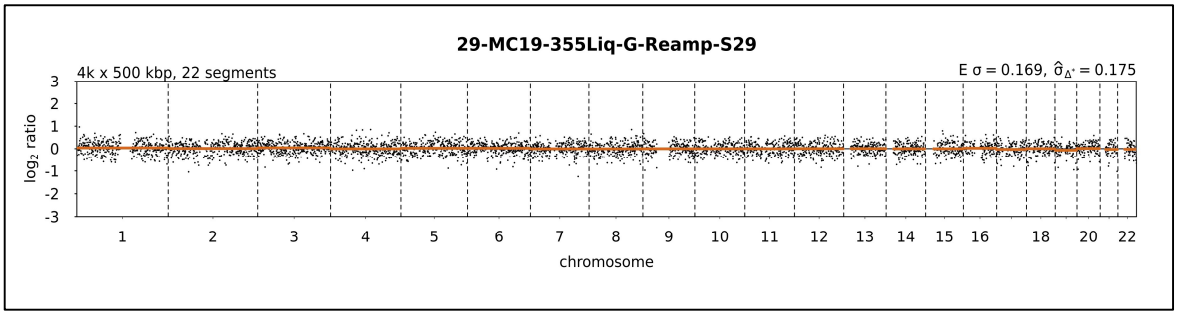

FigureA 58 Copy number variation profiles of cfDNA from patient ID29
Balanced CNV profile of circulating cell free tumor DNA (ctDNA) isolated from CSF from breast cancer patient 29 – MC19-355. Interpretation of profiles in 2.22.

Available information from breast cancer patient ID 35 – MC20-056

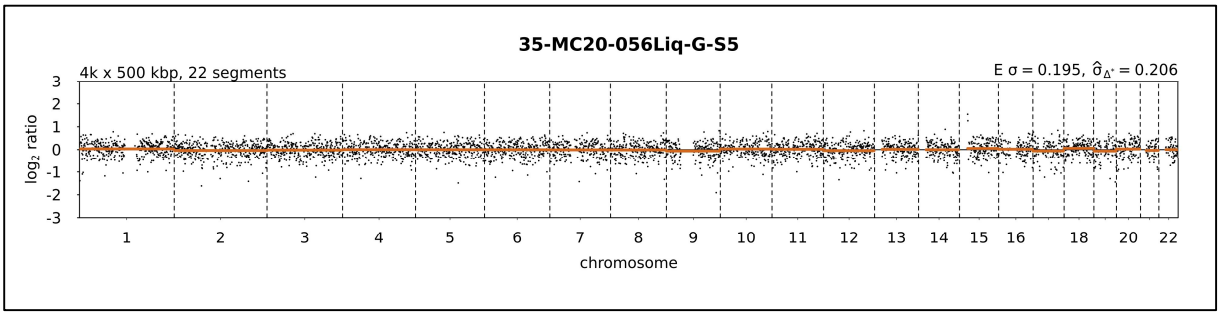

FigureA 59 Copy number variation profiles of cfDNA from patient ID35
Balanced CNV profile of circulating cell free tumor DNA (ctDNA) isolated from CSF from breast cancer patient 29 – MC20-056. Interpretation of profiles in 2.22.

Available information from melanoma cancer patient ID 38 – MM20-076

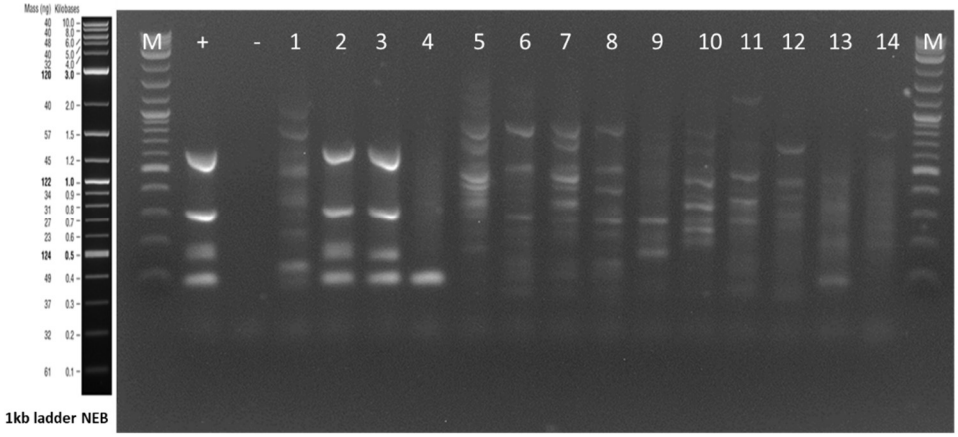

M	1 kb ladder NEB	GII
+	Positive control	4
-	Negative control	0
1	MM20-076 PK	0
2	MM20-076 Pool	4
3	MM20-076 NZ01	4
4	MM20-076 NZ02	1
5	MM20-076 TZ01	0
6	MM20-076 TZ02	0
7	MM20-076 TZ03	0
8	MM20-076 TZ04	0
9	MM20-076 TZ05	0
10	MM20-076 TZ06	0
11	MM20-076 TZ07	0
12	MM20-076 TZ08	0
13	MM20-076 TZ09	0
14	MM20-076 TZ10	0
M	1 kb ladder NEB	-

FigureA 60 Agarosegel picture of quality control PCR patient ID35
Mulitplex (4x) of single disseminated cancer cells isolated from CSF of melanoma patient ID35 MM20-076, including the marker, a positive and a negative control and a sample list on the right. Cells were isolated manually by micromanipulation. Due to the bad genomic integrity index (GII) the cells were not analyzed by copy number variation experiment.

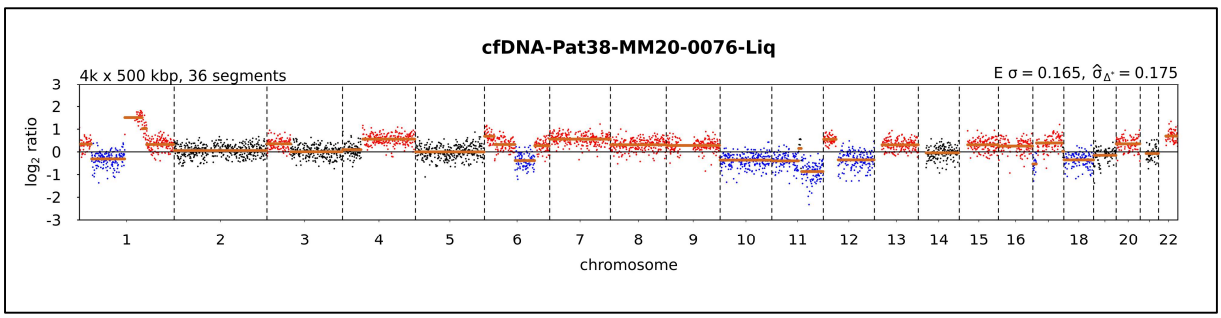

FigureA 61 Copy number variation profiles of cfDNA from patient ID38
Aberrant CNV profile of circulating cell free tumor DNA (ctDNA) isolated from CSF from melanoma patient 35 – MM20-076. Interpretation of profiles in 2.22.

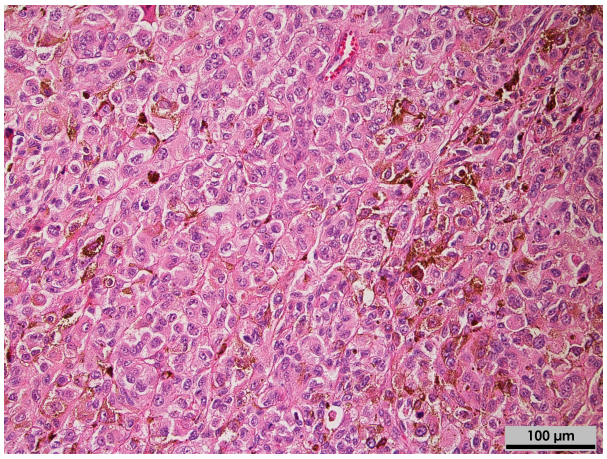

FigureA 62 Cytological staining of FFPE tissue from patient ID35
Hematoxylin-Eosin staining of lymph node metastases, 2018.10 µm tissue slices stained by pathologists of the University of Regensbug from melanoma ID35 – M20-076 for defining the tumor content.Violet dots are representing tumor cells, scale bar 100 µm.

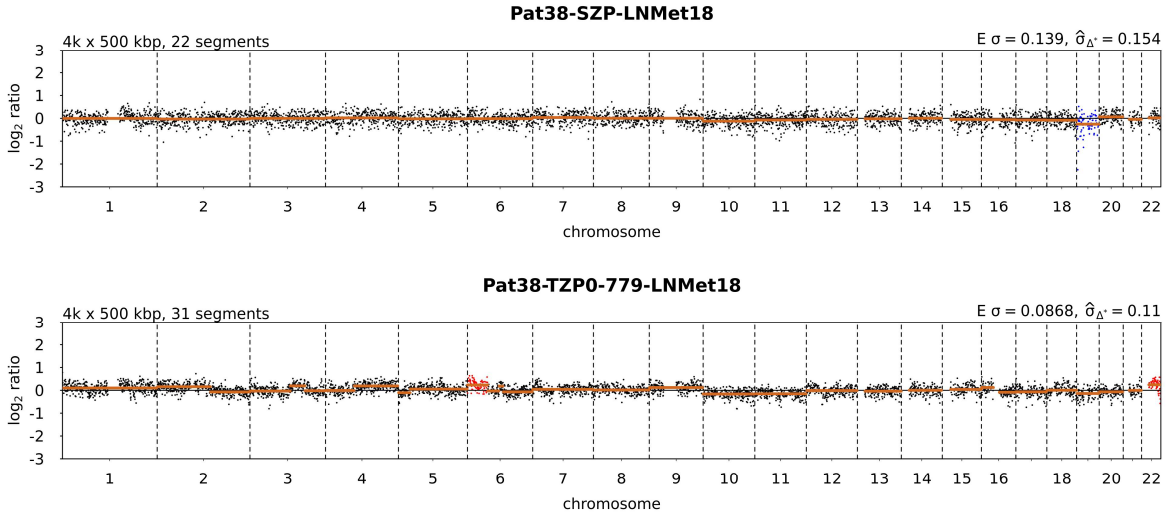

FigureA 63 Copy number variation profiles of tissue from patient ID35
Above: Balanced copy number variation (CNV) profile of the isolated stromal cell pool from the lymph node metastases.**Below:** Slightly aberrant CNV profile of the isolated tumor cell pool (TZP, DNAIndex 0.779) from the lymph node metastases. Cell were isolated automatically with the DEPArray from a lymph node metastases resected in 2018 from melanoma patient ID35 – MM20-076. Interpretation of profiles in 2.22.

Availble information from melanoma cancer patient ID 39 – CUP20-080

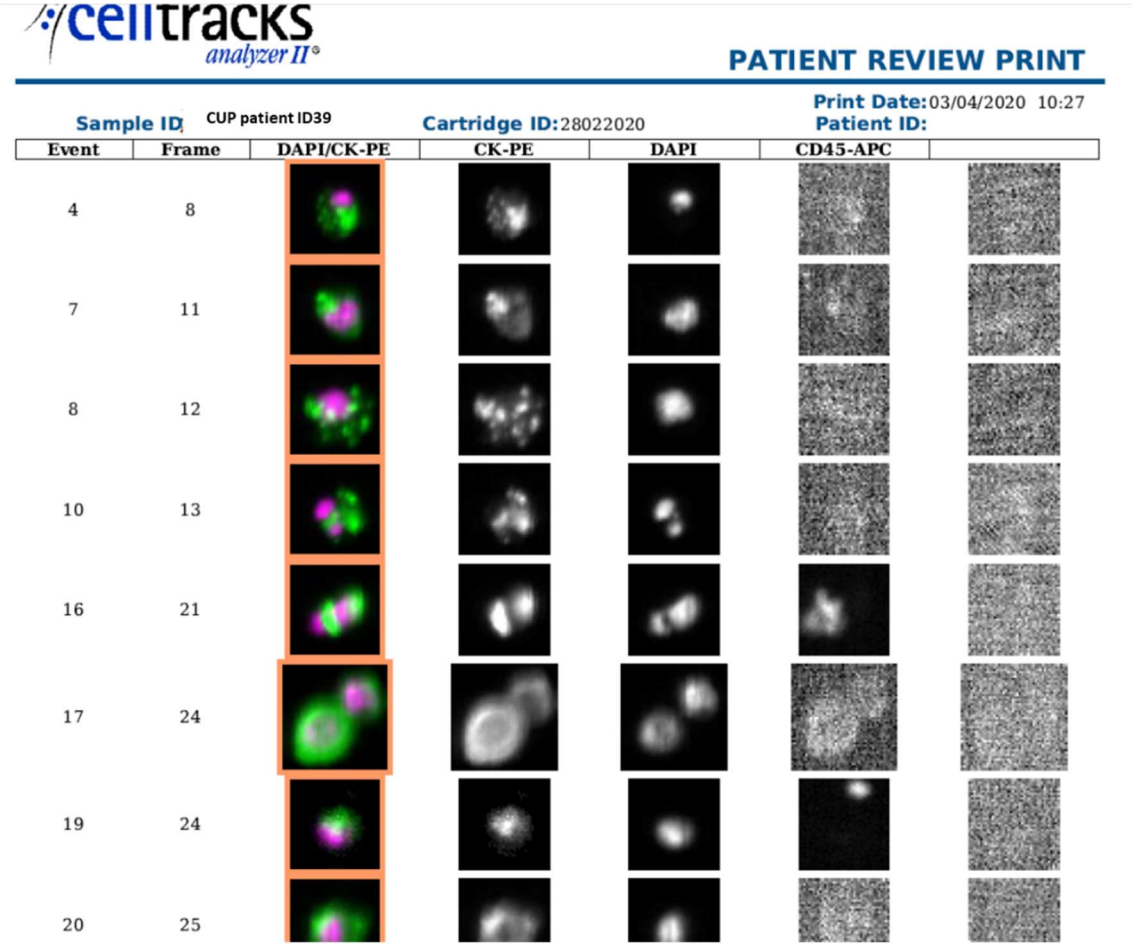

FigureA 64 Excerpt of the CellSearch Gallery patient ID39
Representative for the 70 disseminated cancer cells found in the cerebrospinal fluid (CSF) enrichment of cancer of unknown primary patient ID39 – CUP20-080. The first eight cells from the CellSearch Gallery. First the event number, the frame in which the cells can be found, a DAPI/CK overlay channel, the CK-PE channel, the DAPI and the CD45-APC channel.

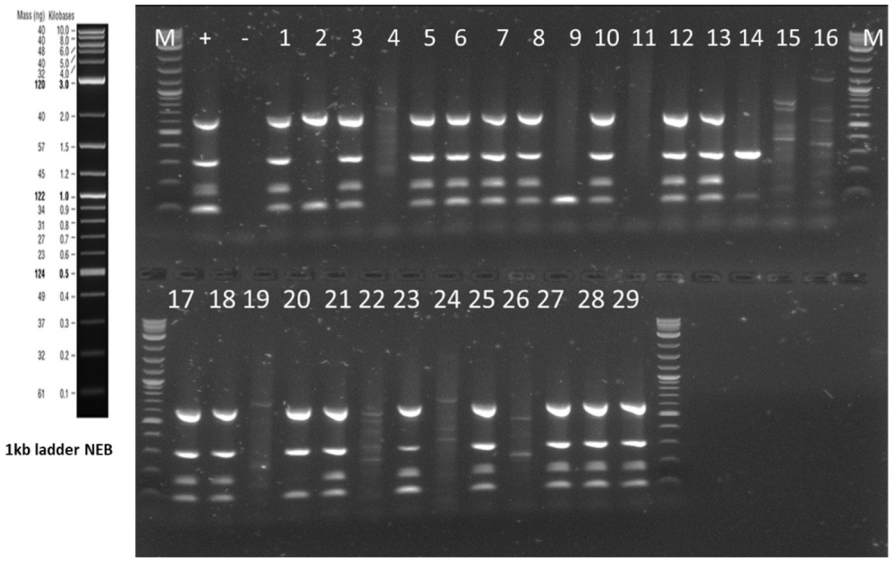

M	1 kb ladder NEB	GII
+	Positive control	4
-	Negative control	0
1	CUP20-080 TZ 01	4
2	CUP20-080 TZ 02	3
3	CUP20-080 TZ 03	4
4	CUP20-080 TZ 04	0
5	CUP20-080 TZ 05	4
6	CUP20-080 TZ 06	4
7	CUP20-080 TZ 07	4
8	CUP20-080 TZ 08	4
9	CUP20-080 TZ 09	1
10	CUP20-080 TZ 10	4
11	CUP20-080 TZ 11	0
12	CUP20-080 TZ 12	4
13	CUP20-080 TZ 13	4
14	CUP20-080 TZ 14	2
15	CUP20-080 TZ 15	0
16	CUP20-080 TZ 16	0
17	CUP20-080 TZ 17	4
18	CUP20-080 TZ 18	4
19	CUP20-080 TZ 19	0
20	CUP20-080 TZ Pool 01	3
21	CUP20-080 TZ Pool 02	4
22	CUP20-080 PK	0
23	CUP20-080 NZ 01	4
24	CUP20-080 NZ 02	0
25	CUP20-080 NZ 03	4
26	CUP20-080 NZ 04	0
27	CUP20-080 NZ 05	4
28	CUP20-080 NZ Pool 01	4
29	CUP20-080 NZ Pool 02	4
M	1 kb ladder NEB	-

FigureA 65 Agarosegel picture of quality control PCR patient ID39
Mulitplex (4x) of single disseminated cancer cells isolated from CSF of cancer of unknown primary patient ID39 CUP20-080, including the marker, a positive and a negative control and a sample list on the right. Cells were isolated manually by micromanipulation. Due to the bad genomic integrity index (GII) the cells were not analyzed by copy number variation experiment.

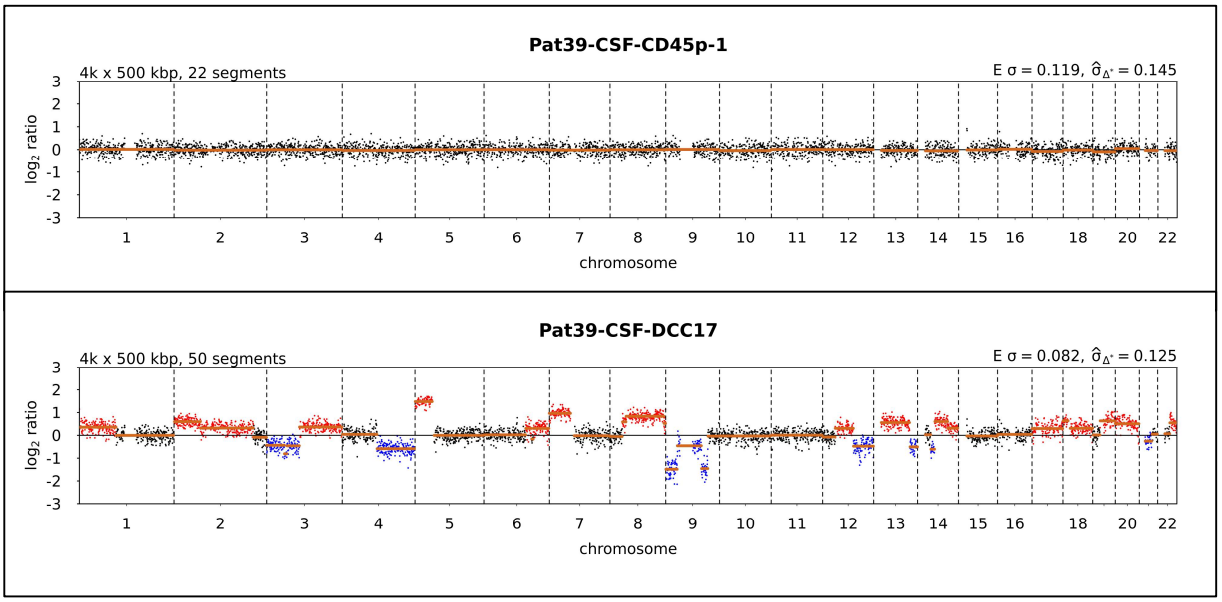

FigureA 66 Copy number variation profiles of cells from patient ID39
Above: Balanced copy number variation (CNV) profile of the isolated CD45 positive single cell1
Below: Aberrant CNV profile of disseminated cancer cell (DCC) 17. Cells are enriched with the CellSearch system and isolated manually by micromanipulation from CSF of cancer of unknown primary patient ID 39 – CUP20-080. Interpretation of profiles in 2.22.

Availble information from larynx cancer patient ID 44 – HN20-223 and ID45 – HN20-228 – represeting the same patient at two different timepoints (1 week in between)

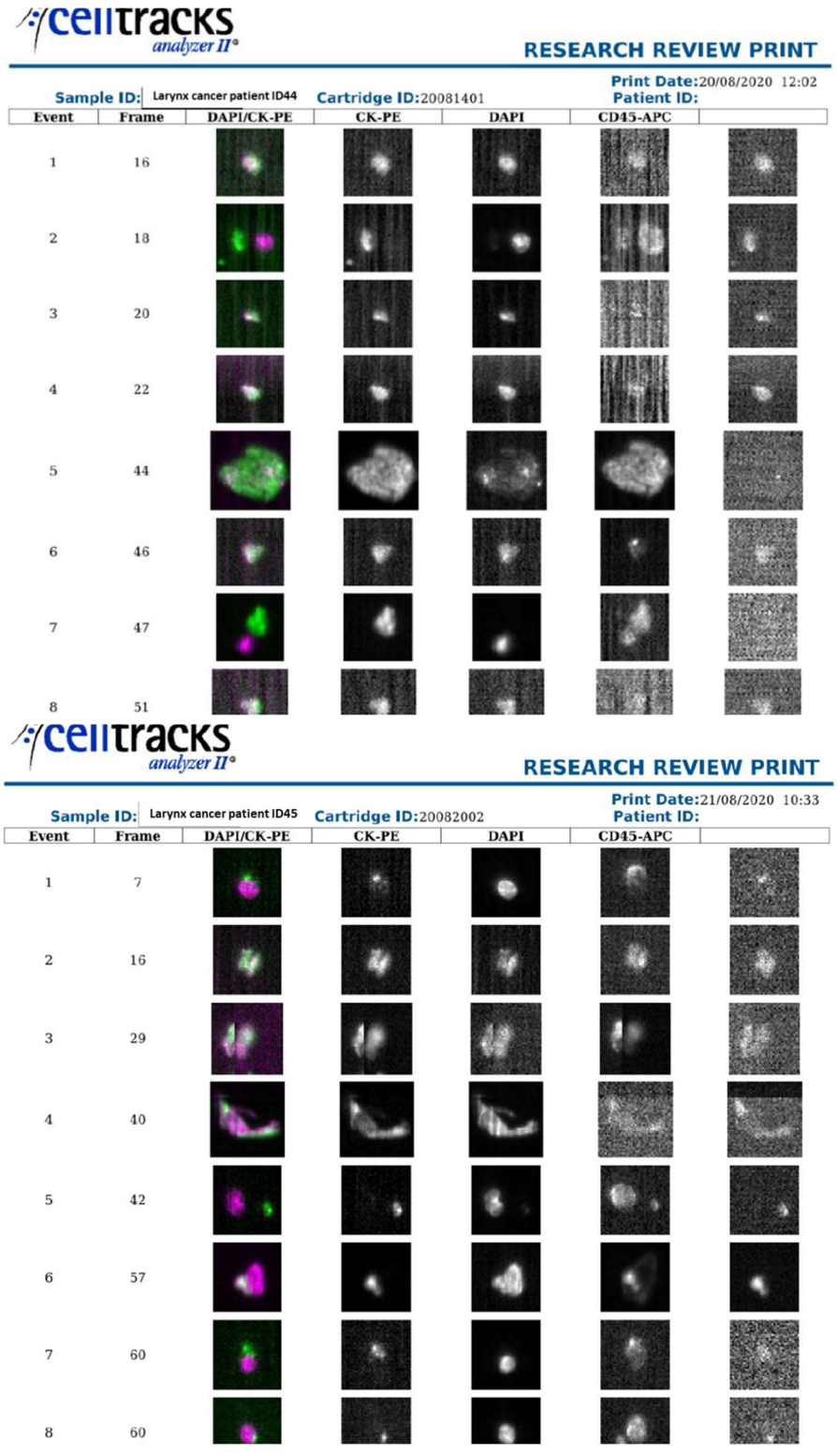

FigureA 67 Excerpt of the CellSearch Gallery patient ID44/45
No disseminated cancer cells found in the cerebrospinal fluid (CSF) enrichment of larynx patient ID44- HN20-223 (above) and ID45 HN20-228 (below). Representative for the cells the first part of the resp. gallery. First the event number, the frame in which the cells can be found, a DAPI/CK overlay channel, the CK-PE channel, the DAPI and the CD45-APC channel.

Availble information from breast cancer patient ID 46 – MC20-250

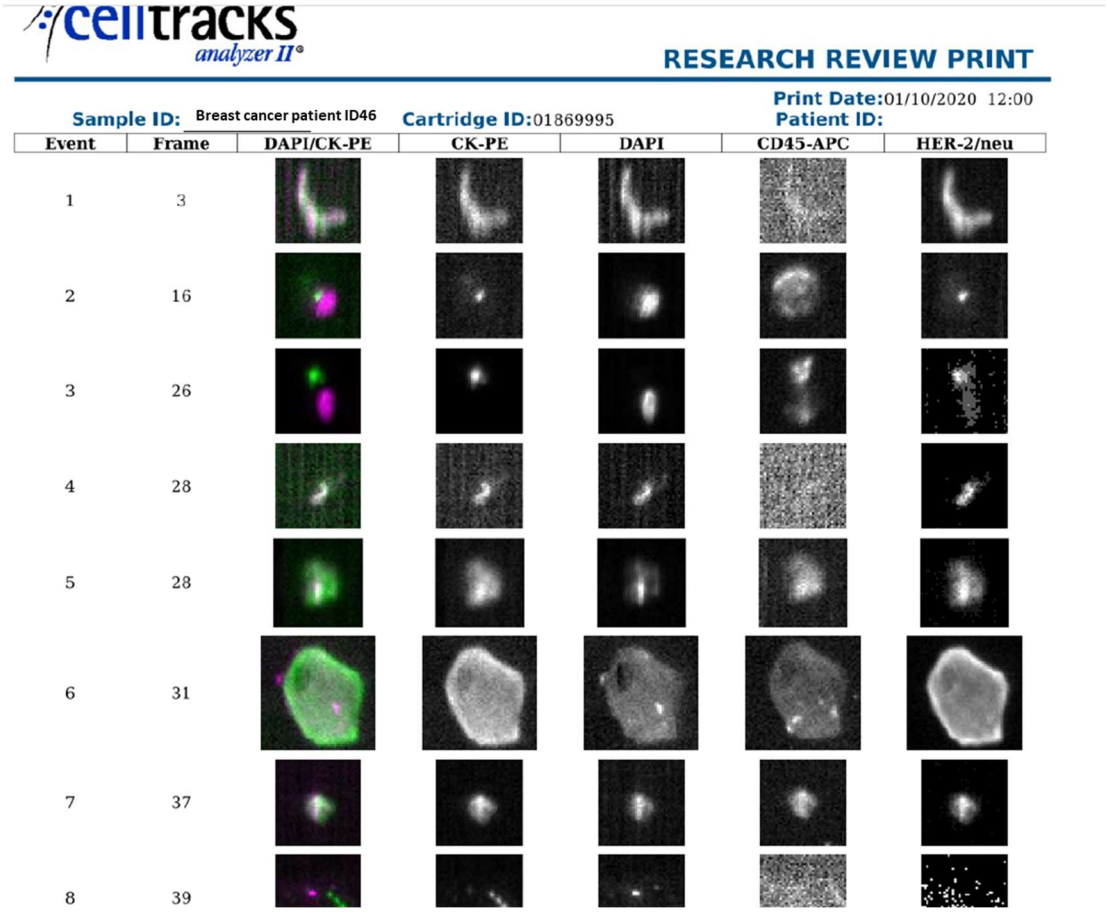

FigureA 68 Excerpt of the CellSearch Gallery patient ID46

No disseminated cancer cells found in the cerebrospinal fluid (CSF) enrichment of breast cancer patient ID46 – MC20-250. Representative for the cells the first eight cells are shown in this gallery. First the event number, the frame in which the cells can be found, a DAPI/CK overlay channel, the CK-PE channel, the DAPI and the CD45-APC channel.

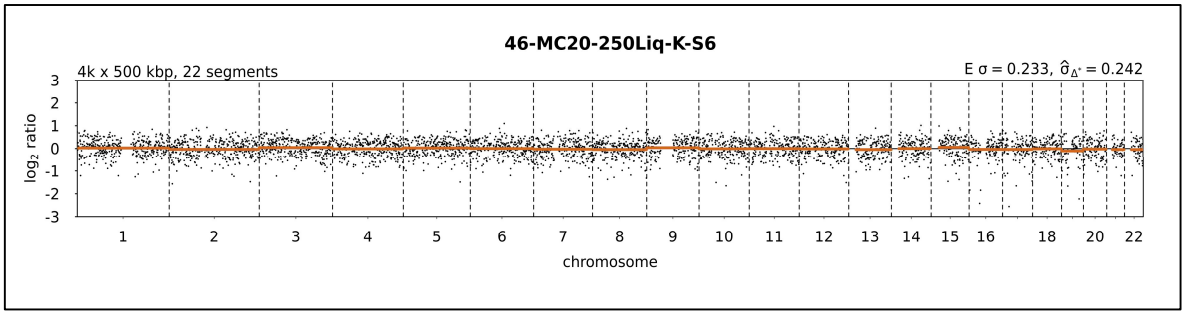

FigureA 69 Copy number variation profiles of cfDNA from patient ID46

Balanced CNV profile of circulating cell free tumor DNA (ctDNA) isolated from CSF from breast cancer patient 46 – MC20-250. Interpretation of profiles in 2.22.

Availble information from lung cancer patient ID 47 – BC20-273

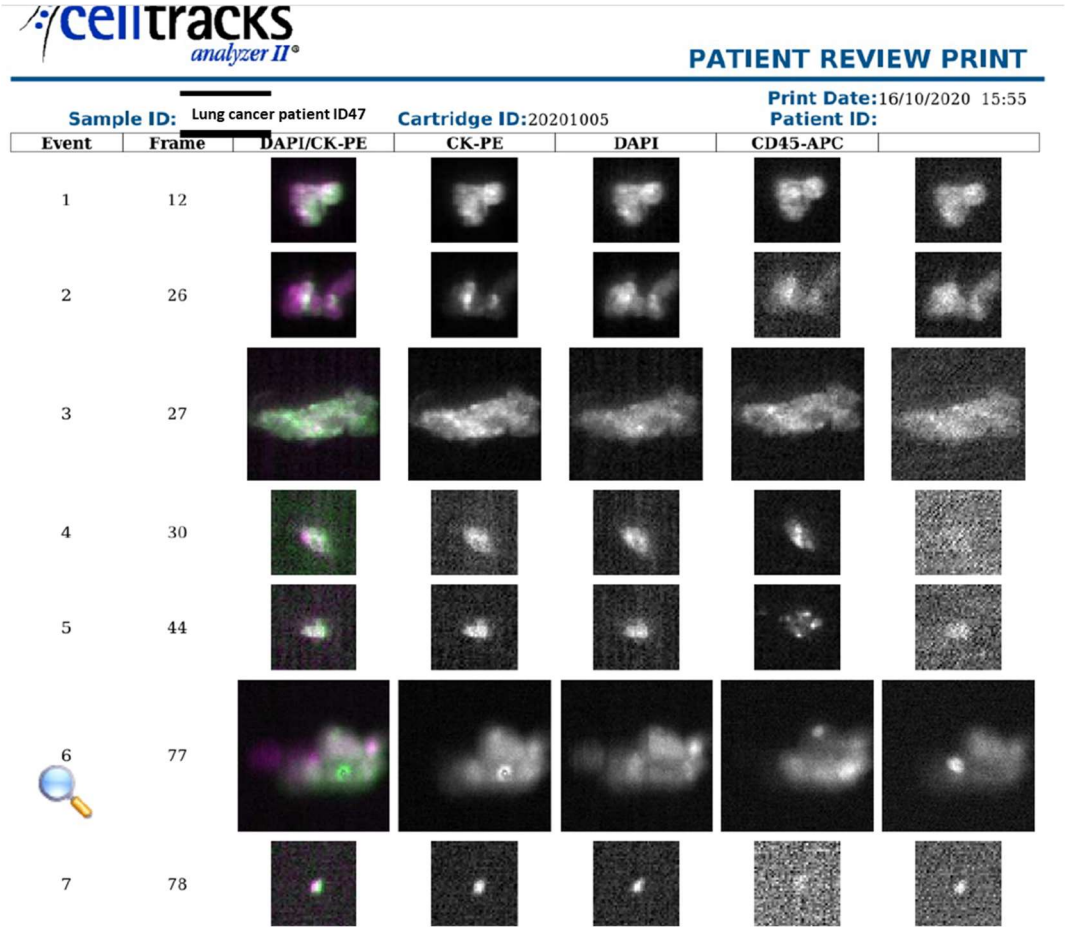

FigureA 70 Excerpt of the CellSearch Gallery patient ID47
No disseminated cancer cells found in the cerebrospinal fluid (CSF) enrichment of lung cancer patient ID47 – BC20-273. Representative for the cells the first seven cells are shown in this gallery. First the event number, the frame in which the cells can be found, a DAPI/CK overlay channel, the CK-PE channel, the DAPI and the CD45-APC channel.

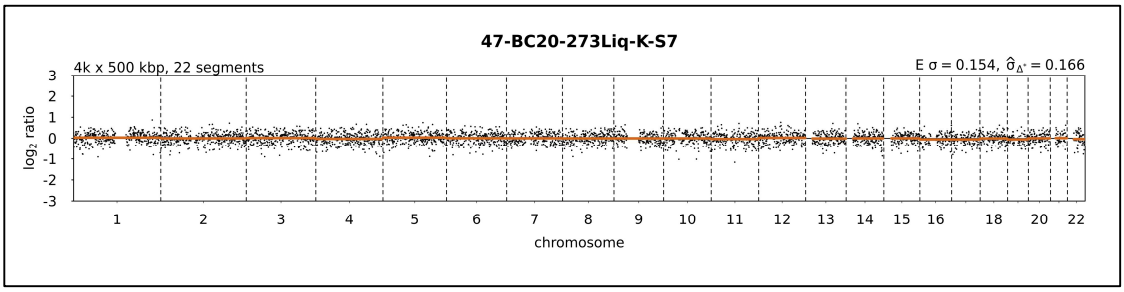

FigureA 71 Copy number variation profiles of cfDNA from patient ID47
Balanced CNV profile of circulating cell free tumor DNA (ctDNA) isolated from CSF from lung cancer patient 47 – BC20-273. Interpretation of profiles in 2.22.

Availble information from lung cancer patient ID 48 – BC20-279

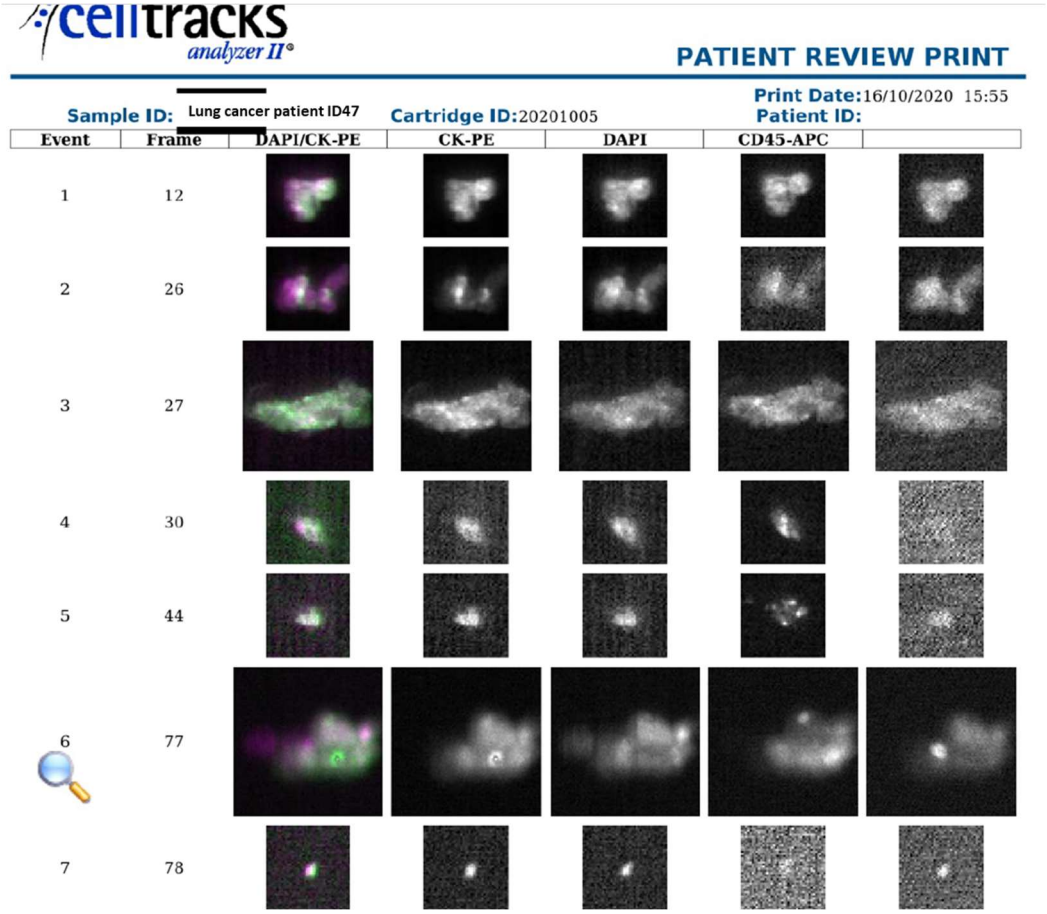

FigureA 72 Excerpt of the CellSearch Gallery patient ID48
No disseminated cancer cells found in the cerebrospinal fluid (CSF) enrichment of lung cancer patient ID48 – BC20-279. Representative for the cells the first seven cells are shown in this gallery. First the event number, the frame in which the cells can be found, a DAPI/CK overlay channel, the CK-PE channel, the DAPI and the CD45-APC channel.

Availble information from melanoma patient ID 49 – MM20-301

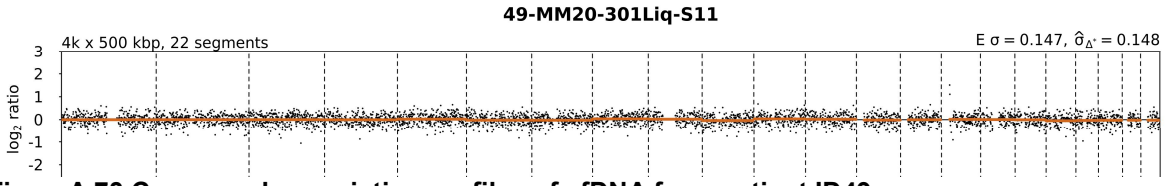

FigureA 73 Copy number variation profiles of cfDNA from patient ID49
Balanced CNV profile of circulating cell free tumor DNA (ctDNA) isolated from CSF from melanoma patient 49 – MM20-301. Interpretation of profiles in 2.22.

Availble information from melanoma patient ID 53 – MM20-327

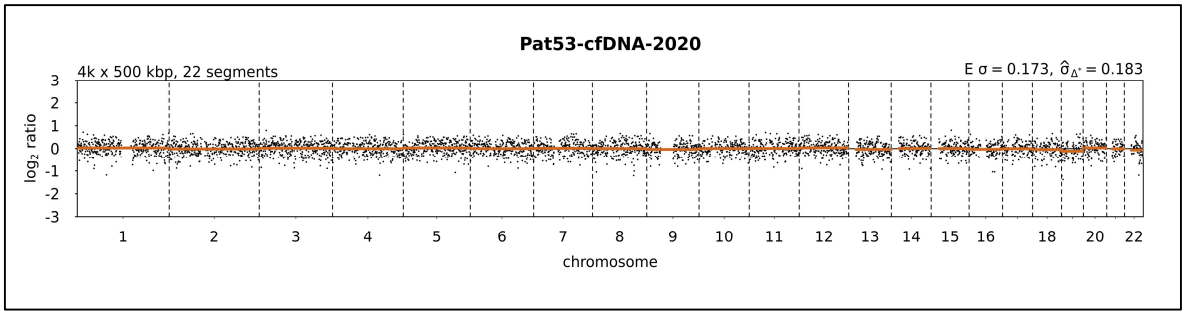

FigureA 74 Copy number variation profiles of cfDNA from patient ID53
Balanced CNV profile of circulating cell free tumor DNA (ctDNA) isolated from CSF from melanoma patient 53 – MM20-327. Interpretation of profiles in 2.22.

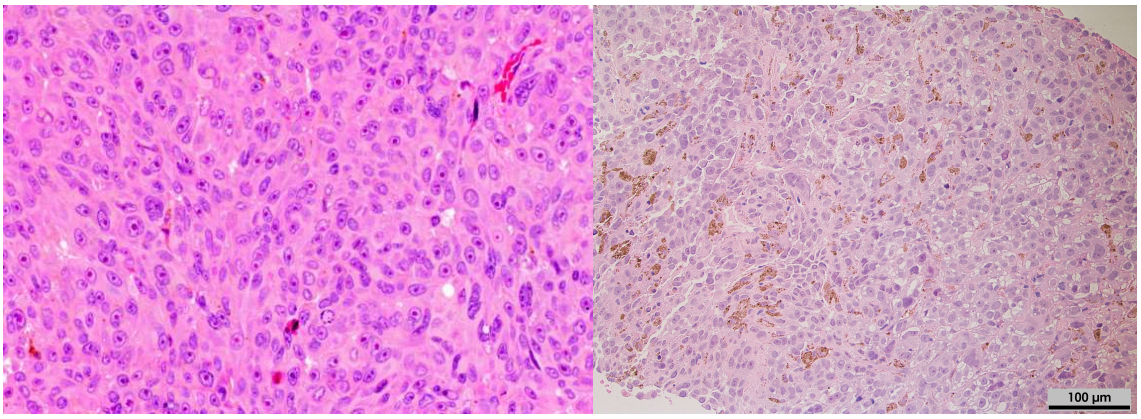

FigureA 75 Cytological staining of FFPE tissue from patient ID53
Left: Hematoxylin-Eosin staining of brain metastases 2018, **Right:** Hematoxylin-Eosin staining of lymph node metastases 2021.10 µm tissue slices stained by neuropathologists and pathologists of the University of Regensbug from tissue of melanoma patient ID53 – MM20-327 for defining the tumor content.Violet dots are representing tumor cells, scale bar 100 µm.

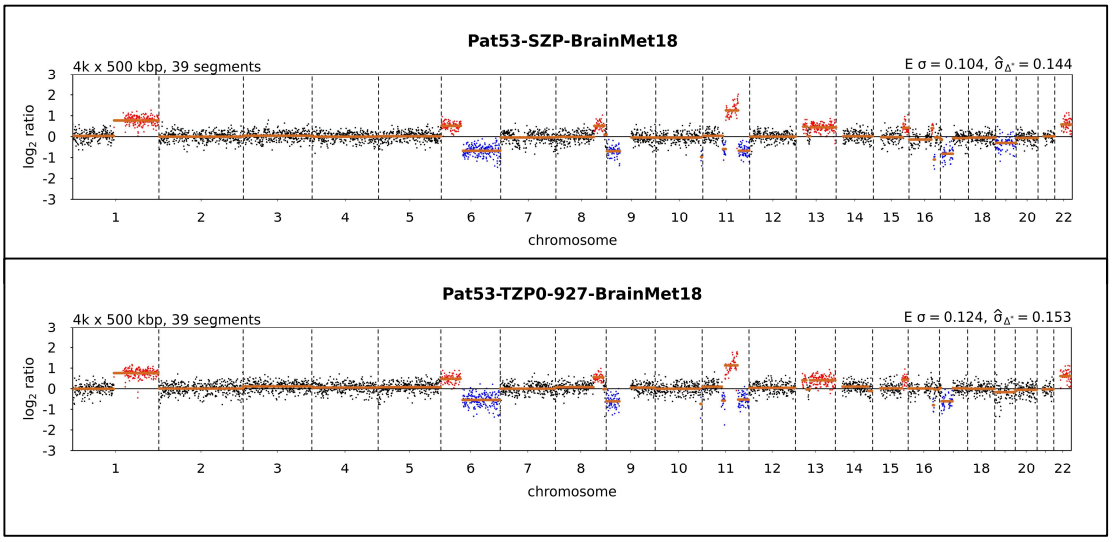

FigureA 76 Copy number variation profiles of tissue from patient ID53
Above: Aberrant copy number variation (CNV) profile of the isolated stromal cell pool from the brain metastases.**Below:** Aberrant CNV profile of the isolated tumor cell pool (TZP, DNAIndex 0.927) from brain metastases. Cell were isolated automatically with the DEPArray from a brain metastases detected in 2018 from melanoma patient ID53 – MM20-327. Interpretation of profiles in 2.22.

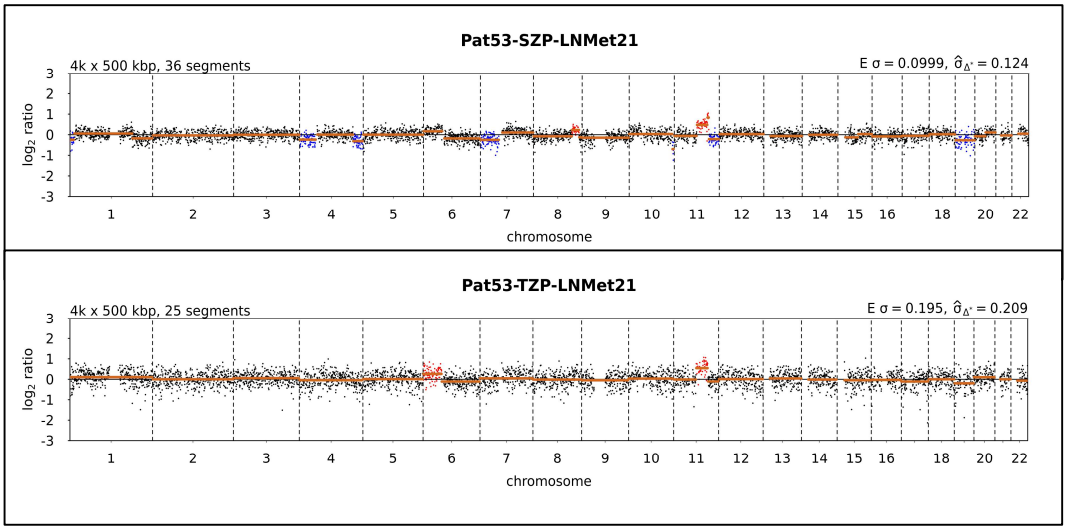

FigureA 77 Copy number variation profiles of tissue from patient ID53
Above: Aberrant copy number variation (CNV) profile of the isolated stromal cell pool from the lymph node metastases.**Below:** Aberrant CNV profile of the isolated tumor cell pool (TZP, DNAIndex n.a.) from lymph node metastases. Cell were isolated automatically with the DEPArray from a brain metastases detected in 2018 from melanoma patient ID53 – MM20-327. Interpretation of profiles in 2.22.

Availble information from breast cancer patient ID 55 – MC20-028

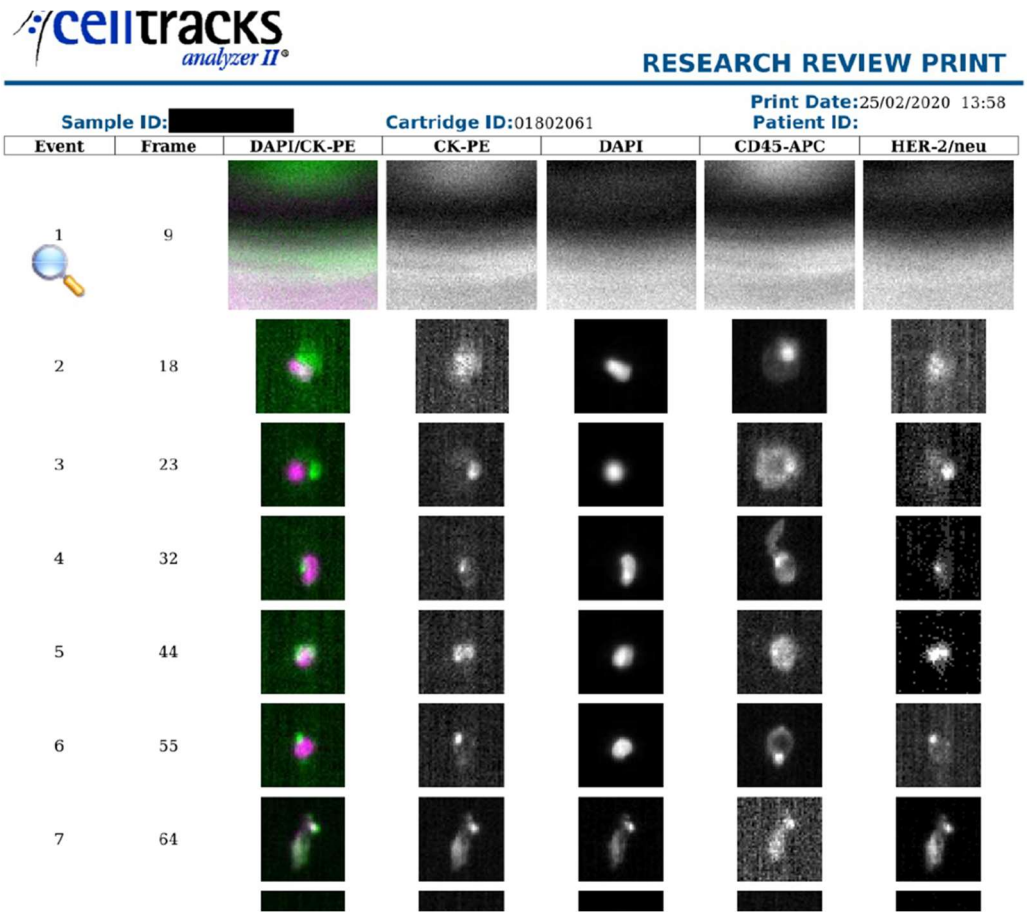

FigureA 78 Excerpt of the CellSearch Gallery patient ID55
No disseminated cancer cells found in the cerebrospinal fluid (CSF) enrichment of breast cancer patient ID55 – MC20-028. Representative for the cells the first seven cells are shown in this gallery. First the event number, the frame in which the cells can be found, a DAPI/CK overlay channel, the CK-PE channel, the DAPI and the CD45-APC channel.

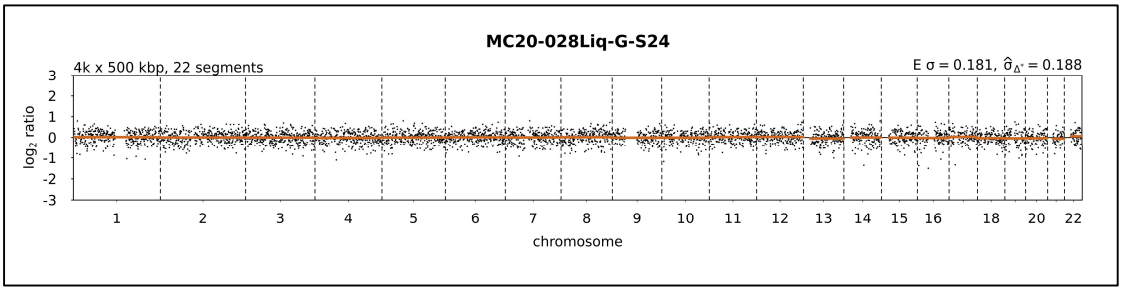

FigureA 79 Copy number variation profiles of cfDNA from patient ID55
Balanced CNV profile of circulating cell free tumor DNA (ctDNA) isolated from CSF from breast cancer patient 55 – MC20-028. Interpretation of profiles in 2.22.

Availble information from gastric cancer patient ID 56 – MA20-334

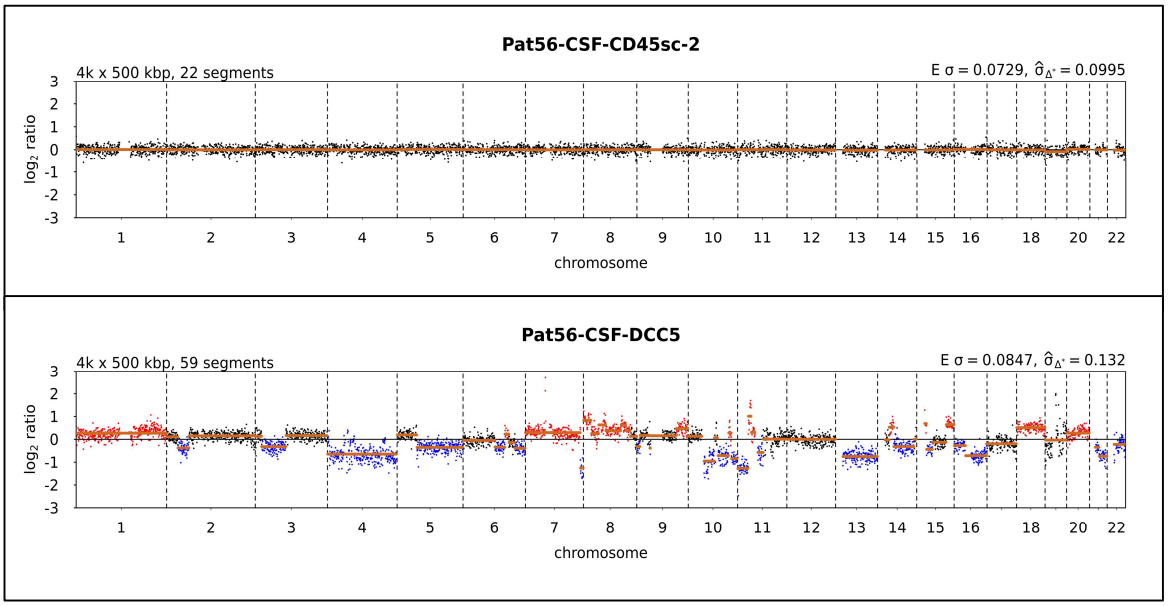

FigureA 80 Copy number variation profiles of cells from patient ID56
Above: Balanced copy number variation (CNV) profile of the isolated CD45 positive single cell2
Below: Aberrant CNV profile of disseminated cancer cell (DCC) 5. Cells are enriched with the CellSearch system and isolated manually by micromanipulation from CSF of larynx cancer patient ID 39 – CUP20-080. Interpretation of profiles in 2.22.

Available information from lung cancer patient ID 57 – BC20-335

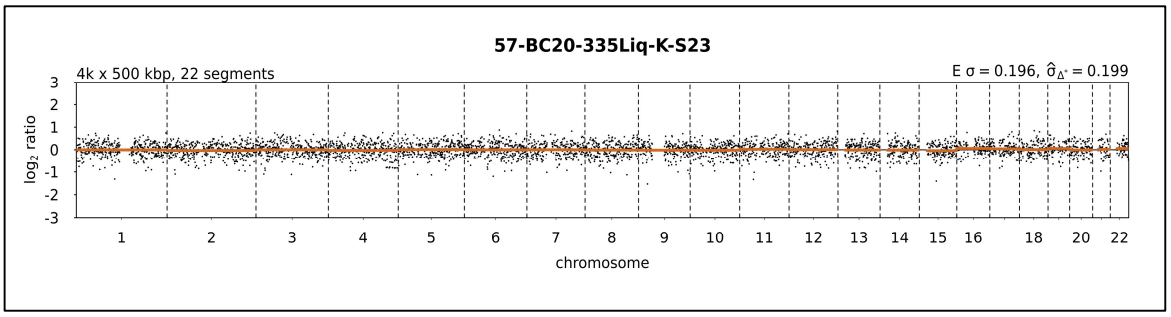

FigureA 81 Copy number variation profiles of cfDNA from patient ID57
Balanced CNV profile of circulating cell free tumor DNA (ctDNA) isolated from CSF from lung cancer patient 57 – BC20-335. Interpretation of profiles in 2.22.

Available information from lung cancer patient ID 62 – BC21-352

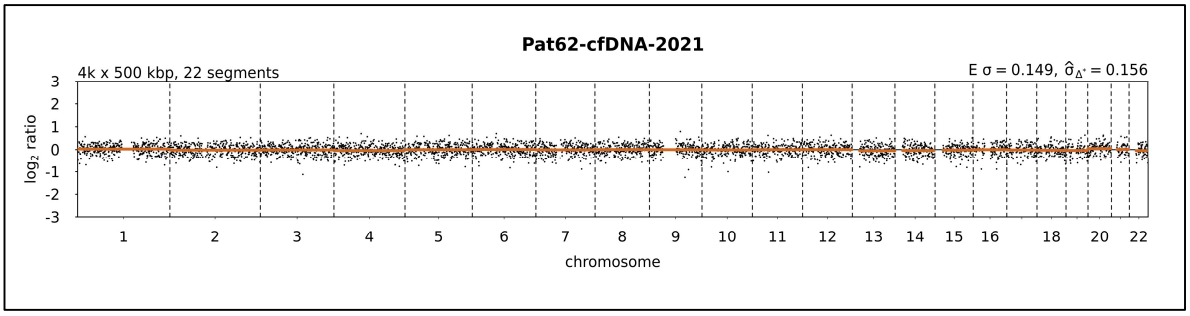

FigureA 82 Copy number variation profiles of cfDNA from patient ID62
Balanced CNV profile of circulating cell free tumor DNA (ctDNA) isolated from CSF from lung cancer patient 62 – BC21-352. Interpretation of profiles in 2.22.

Brain HE

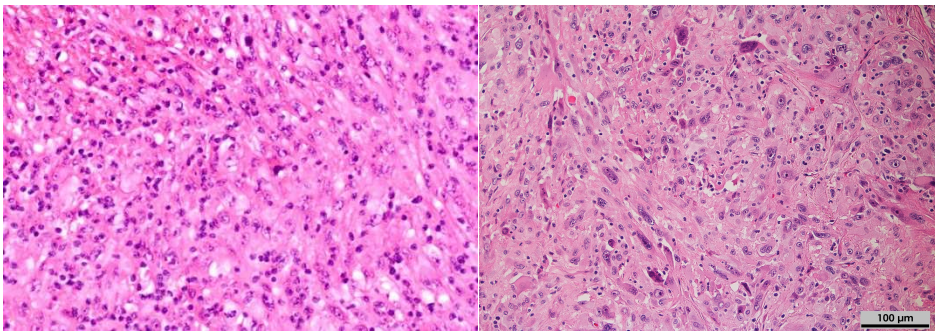

FigureA 83 Cytological staining of FFPE tissue from patient ID62
Left: Hematoxylin-Eosin staining of brain metastases 2018, **Right:** Hematoxylin-Eosin staining of primary tumor.10 µm tissue slices stained by neuropathologists and pathologists of the University of Regensbug from tissue of lung cancer patient ID62 – BC21-352 for defining the tumor content.Violet dots are representing tumor cells, scale bar 100 µm.

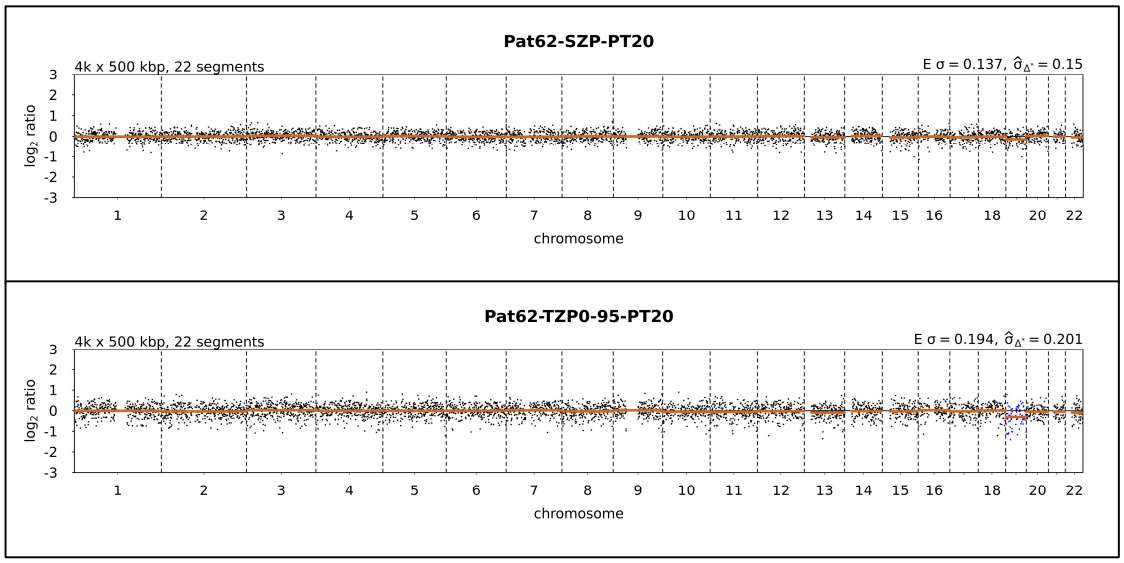

FigureA 84 Copy number variation profiles of tissue from patient ID62
Above: Balanced copy number variation (CNV) profile of the isolated stromal cell pool from the primary tumor.**Below:** Balanced CNV profile of the isolated tumor cell pool (TZP, DNAIndex 0.95) from primary tumor. Cell were isolated automatically with the DEPArray from the primary resected in 2020 from lung cancer patient ID62 – BC21-352. Interpretation of profiles in 2.22.

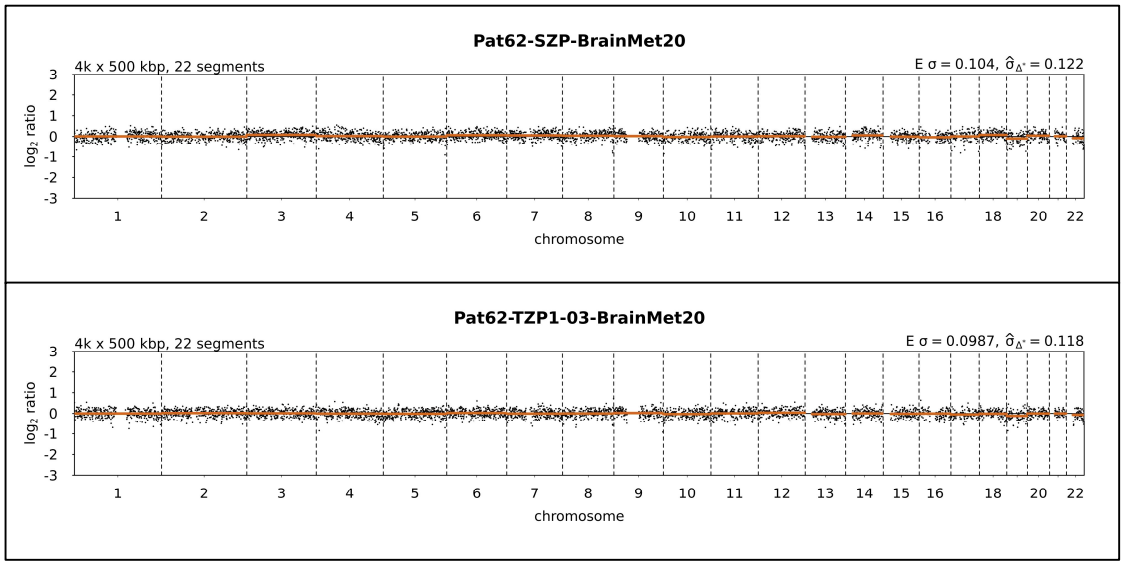

FigureA 85 Copy number variation profiles of tissue from patient ID62
Above: Balanced copy number variation (CNV) profile of the isolated stromal cell pool from the brain metastases.**Below:** Balanced CNV profile of the isolated tumor cell pool (TZP, DNAIndex 1.03) from brain metastases. Cell were isolated automatically with the DEPArray from a brain metastases detected in 2020 from lung cancer patient ID62 – BC21-352. Interpretation of profiles in 2.22.

Available information from breast cancer patient ID 64 – MC21-362

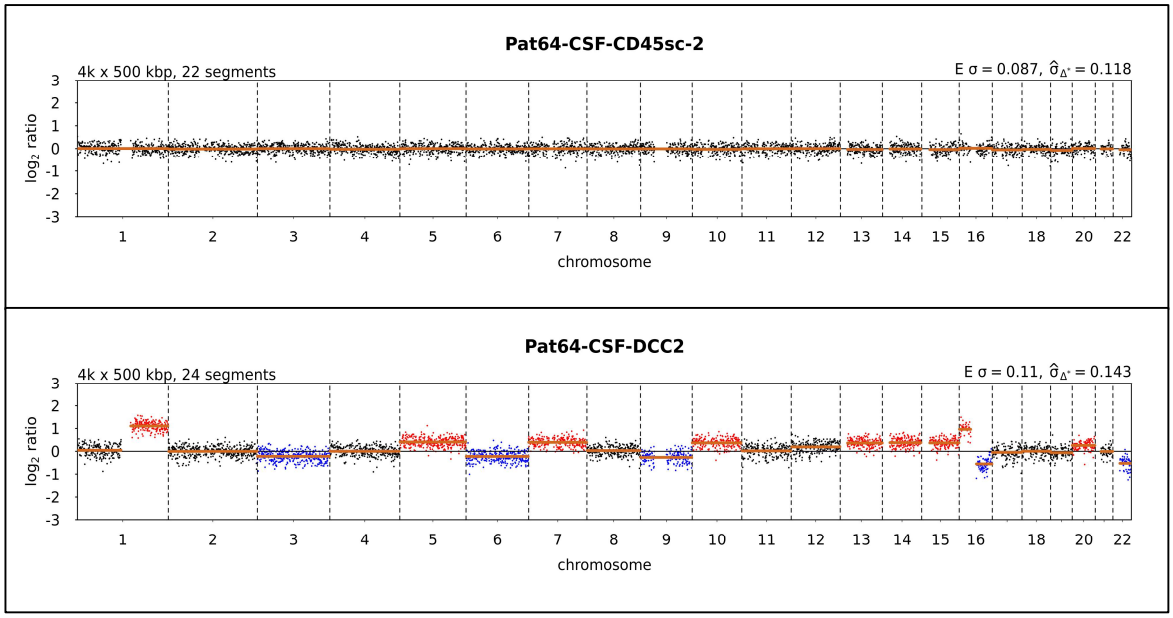

FigureA 86 Copy number variation profiles of cells from patient ID64
Above: Balanced copy number variation (CNV) profile of the isolated CD45 positive single cell2
Below: Aberrant CNV profile of disseminated cancer cell (DCC) 2. Cells are enriched with the CellSearch system and isolated manually by micromanipulation from CSF of breast cancer patient ID 64 – MC21-362. Interpretation of profiles in 2.22.

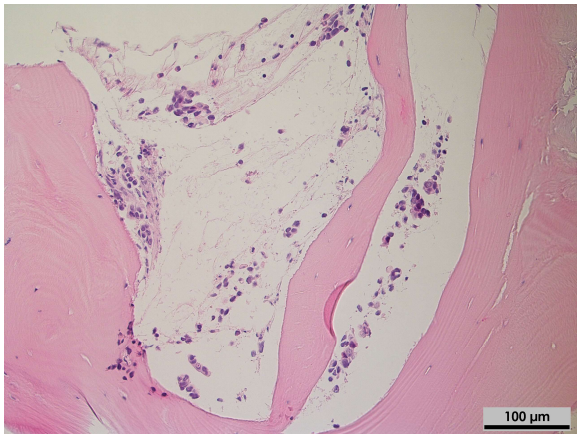

FigureA 87 Cytological staining of FFPE tissue from patient ID64
Hematoxylin-Eosin staining of bone metastases 201910 µm tissue slice stained by pathologists of the University of Regensbug from tissue of breast cancer patient ID64 – MC21-362 for defining the tumor content.Violet dots are representing tumor cells, scale bar 100 µm.

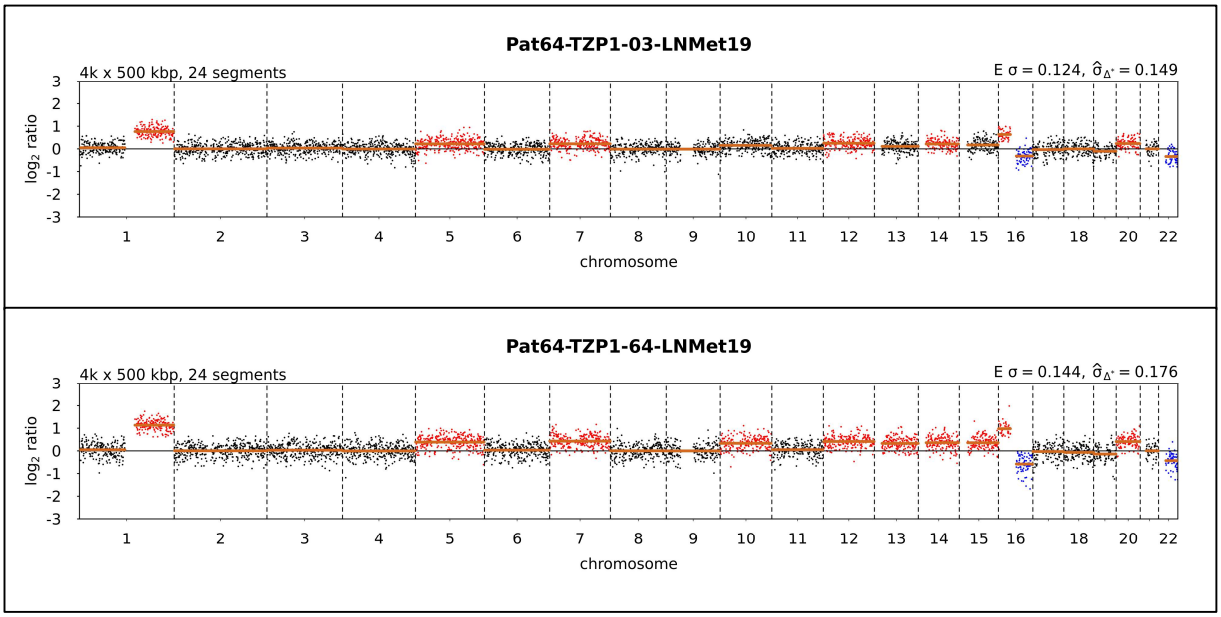

FigureA 88 Copy number variation profiles of tissue from patient ID64
Above: Aberrant copy number variation (CNV) profile of the isolated tumor cell pool (TZP, DNAIndex 1.03) from the bone metastases.**Below:** Aberrant CNV profile of the isolated tumor cell pool (TZP, DNAIndex 1.64) from bone metastases. Cells were isolated automatically with the DEPArray from a bone metastasis detected in 2019 from breast cancer patient ID64 – MC21-362. The stromal cell population could not be evaluated by CNV analysis. Interpretation of profiles in 2.22.

Available information from melanoma patient ID 65 – MM21-367

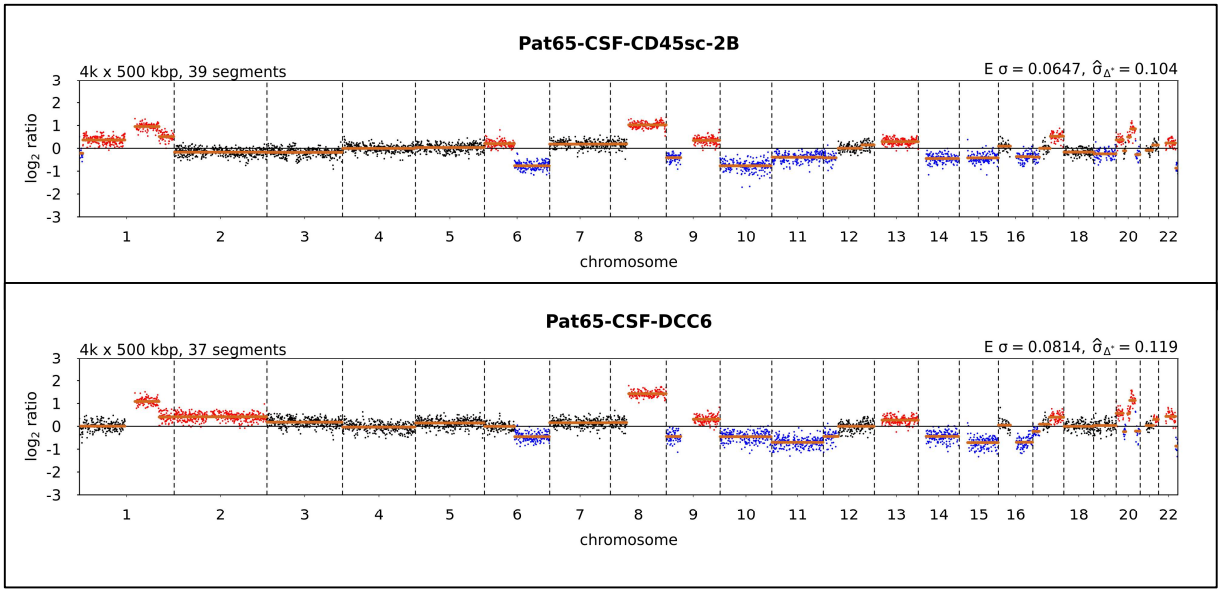

FigureA 89 Copy number variation profiles of cells from patient ID65
Above: Aberrant copy number variation (CNV) profile of the isolated CD45 positive single cell2B
Below: Aberrant CNV profile of disseminated cancer cell (DCC) 6. Cells are enriched with the CellSearch system and isolated manually by micromanipulation from CSF of melanoma patient ID 64 – MM21-367. Interpretation of profiles in 2.22.

Available information from lung cancer patient ID 66 – BC21-395

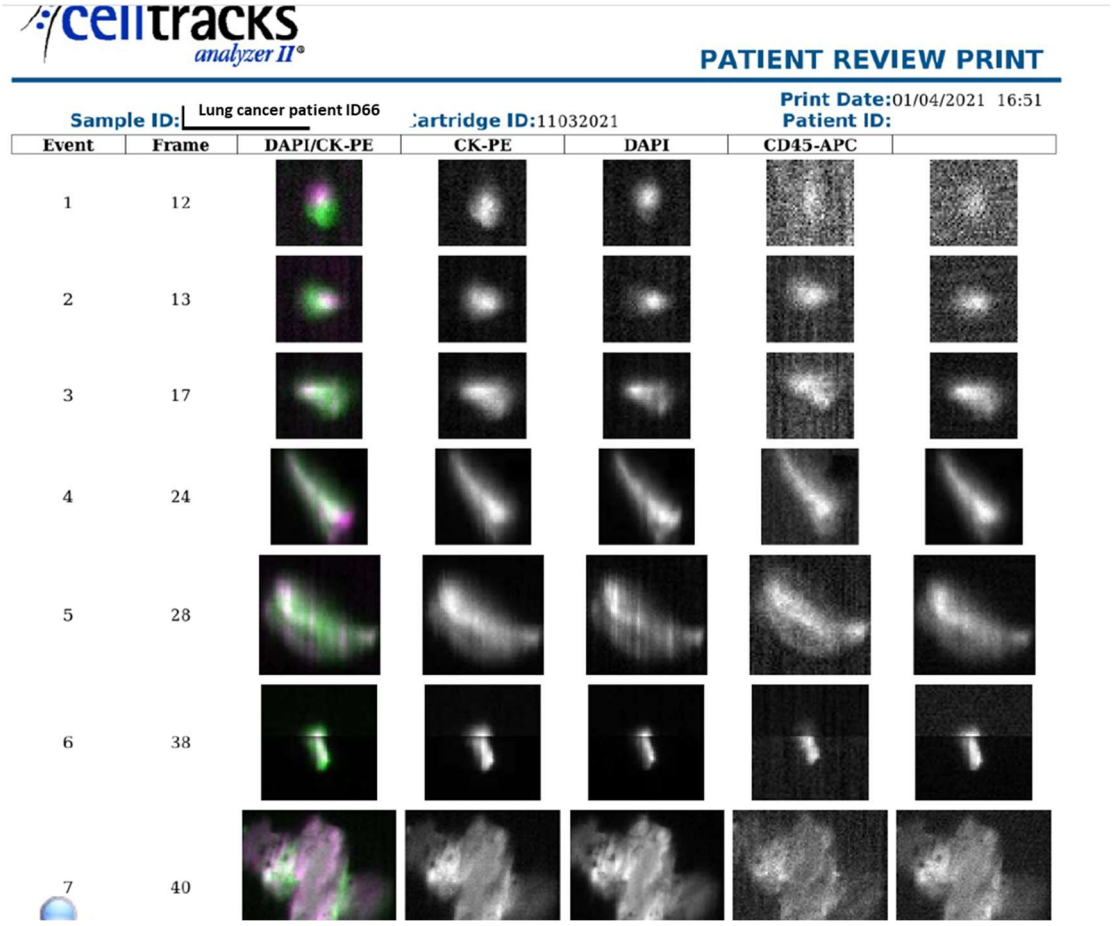

FigureA 90 Excerpt of the CellSearch Gallery patient ID66
No disseminated cancer cells found in the cerebrospinal fluid (CSF) enrichment of lung cancer patient ID66 – BC21-395. Representative for the cells the first seven cells are shown in this gallery. First the event number, the frame in which the cells can be found, a DAPI/CK overlay channel, the CK-PE channel, the DAPI and the CD45-APC channel.

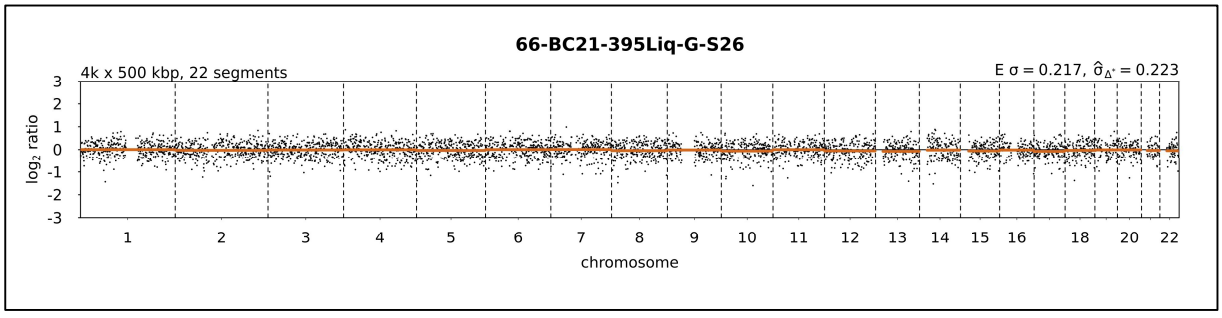

FigureA 91 Copy number variation profiles of cfDNA from patient ID66
Balanced CNV profile of circulating cell free tumor DNA (ctDNA) isolated from CSF from lung cancer patient 66 – BC21-395. Interpretation of profiles in 2.22.

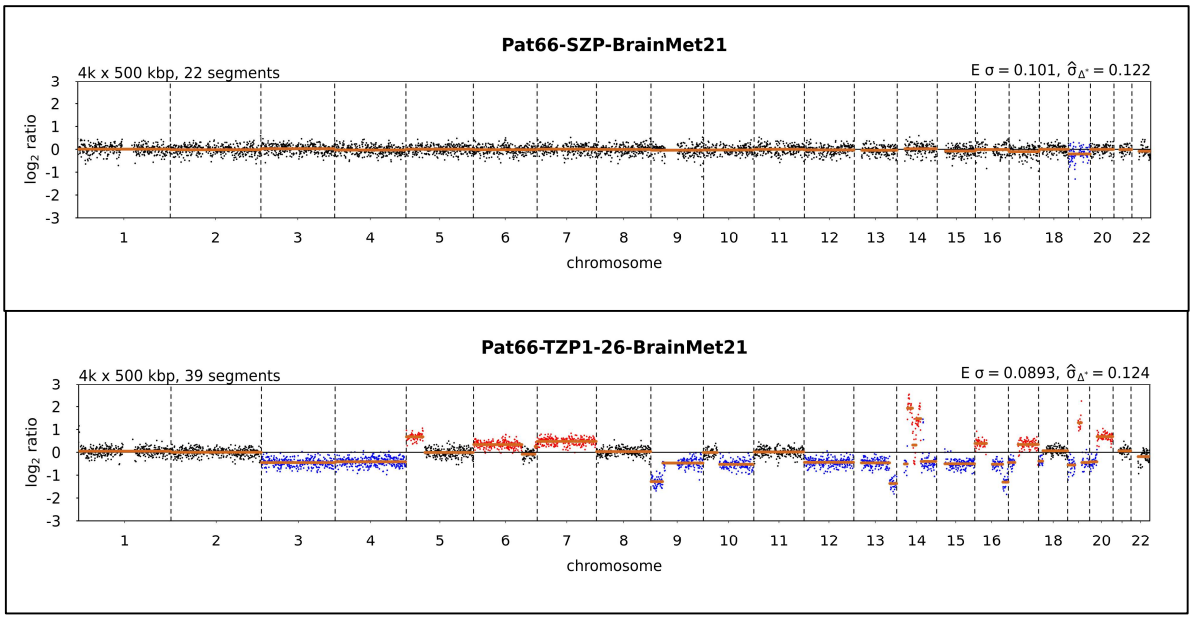

FigureA 92 Copy number variation profiles of tissue from patient ID66
Above: Balanced copy number variation (CNV) profile of the isolated stromal cell pool from the brain metastases.**Below:** Balanced CNV profile of the isolated tumor cell pool (TZP, DNAIndex 1.26) from brain metastases. Cell were isolated automatically with the DEPArray from a brain metastases detected in 2021 from lung cancer patient ID66 – BC21-359. Interpretation of profiles in 2.22.

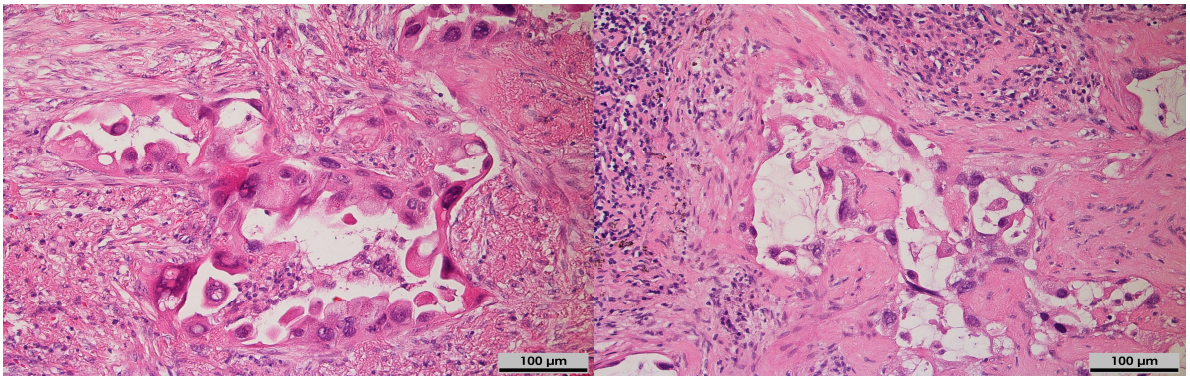

FigureA 93 Cytological staining of FFPE tissue from patient ID66
Left: Hematoxylin-Eosin staining of primary tumor 2021, **Right:** Hematoxylin-Eosin staining of lymph node metastases.10 µm tissue slices stained by pathologists of the University of Regensbug from tissue of lung cancer patient ID66 – BC21-35 for defining the tumor content.Violet dots are representing tumor cells, scale bar 100 µm.

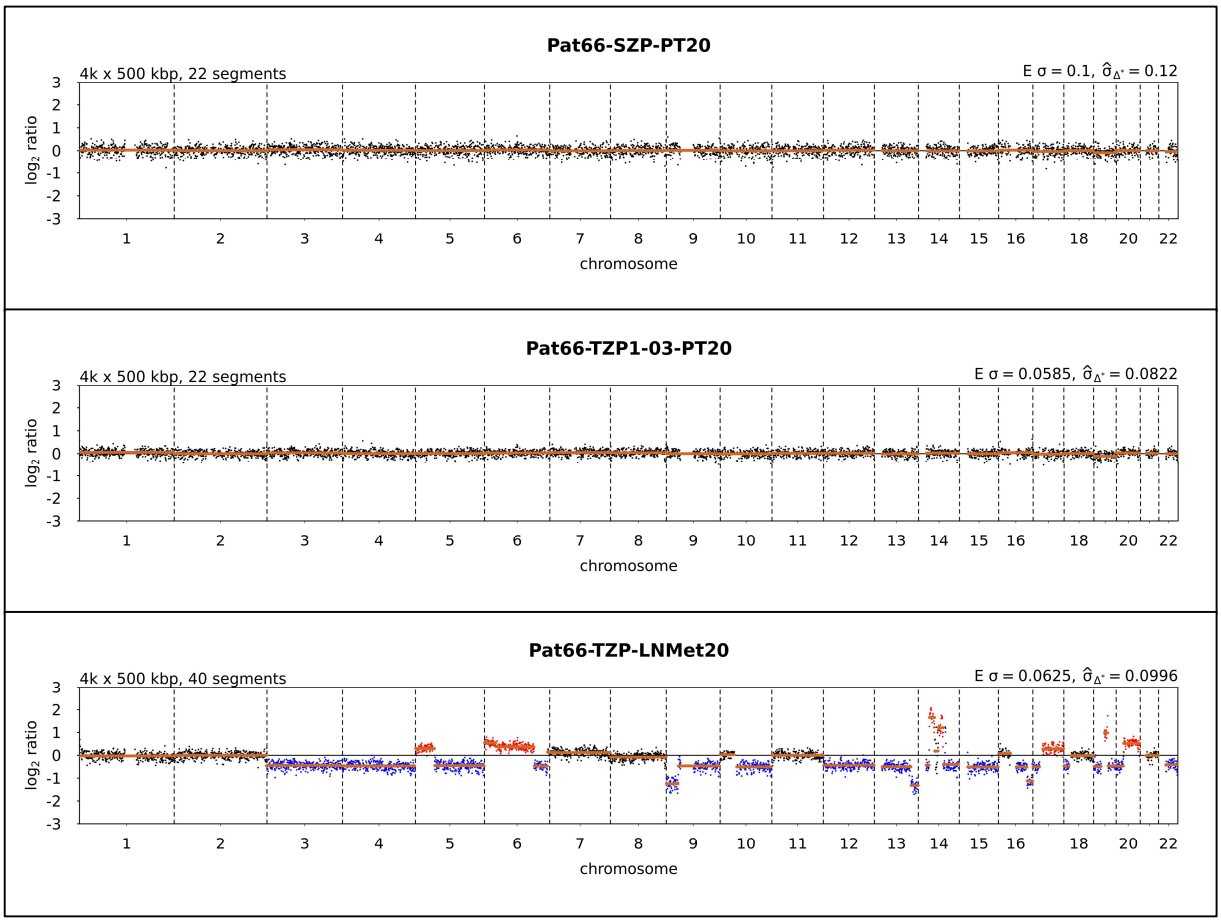

FigureA 94 Copy number variation profiles of tissue from patient ID66
Above: Balanced copy number variation (CNV) profile of the isolated stromal cell pool from the primary tumor.**Middle**: Balanced CNV profile of the isolated tumor cell pool (TZP, DNAIndex 1.03) from the primary tumor. **Below:** Aberrant CNV profile of the isolated tumor cell pool (TZP, DNAIndex n.a.) from lymph node metastases. Unfortunately the stromal cell population was not evaluable by CN analysis. Cell were isolated automatically with the DEPArray from the primary tumor or the lymph node metastases detected in 2020 from lung cancer patient ID66 – BC21-359. Interpretation of profiles in 2.22.

Available information from breast cancer patient ID 67 – MC21-414

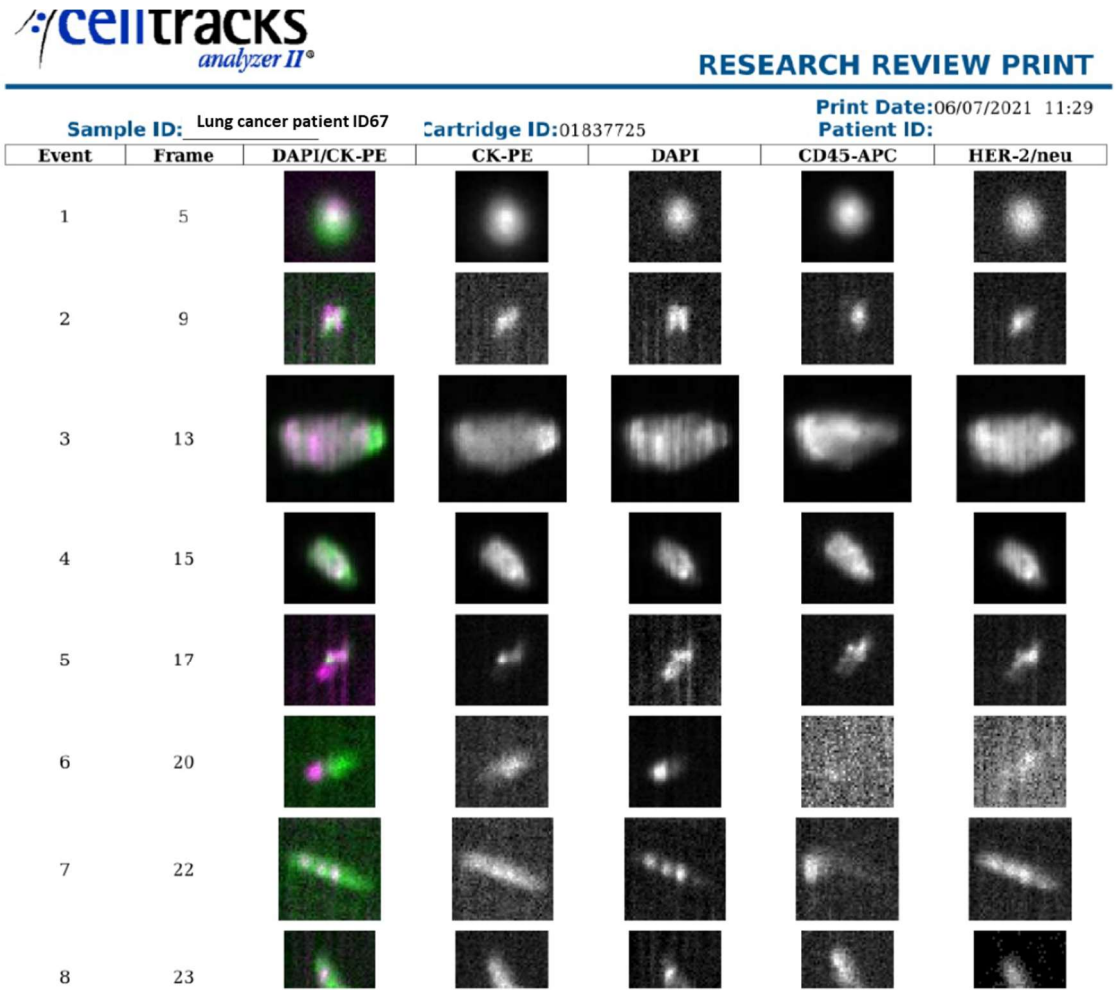

FigureA 95 Excerpt of the CellSearch Gallery patient ID67
No disseminated cancer cells found in the cerebrospinal fluid (CSF) enrichment of breat cancer patient ID67 – MC21-414. Representative for the cells the first seven cells are shown in this gallery. First the event number, the frame in which the cells can be found, a DAPI/CK overlay channel, the CK-PE channel, the DAPI and the CD45-APC channel.

6. References

1. van Horn A, Chamberlain MC. Neoplastic meningitis. J Support Oncol 2012;10(2):45–53. PubMed PMID: 22005214.
2. Le Rhun E, Taillibert S, Chamberlain MC. Carcinomatous meningitis: Leptomeningeal metastases in solid tumors. Surg Neurol Int 2013;4(Suppl 4):S265-88. PubMed PMID: 23717798; PubMed Central PMCID: PMC3656567.
3. Roth P, Weller M. Management of neoplastic meningitis. Chin Clin Oncol 2015;4(2):26. PubMed PMID: 26112812.
4. Graber JJ, Kesari S. Leptomeningeal Metastases. Curr Treat Options Oncol 2018;19(1):3. PubMed PMID: 29362920.
5. Le Rhun E, Weller M, Brandsma D, van den Bent M, Azambuja E de, Henriksson R, et al. EANO-ESMO Clinical Practice Guidelines for diagnosis, treatment and follow-up of patients with leptomeningeal metastasis from solid tumours. Ann Oncol 2017;28(suppl_4):iv84-iv99. PubMed PMID: 28881917.
6. Chamberlain MC. Leptomeningeal metastasis. Curr Opin Oncol 2010;22(6):627–35. PubMed PMID: 20689429.
7. Le Rhun E, Preusser M, van den Bent M, Andratschke N, Weller M. How we treat patients with leptomeningeal metastases. ESMO Open 2019;4(Suppl 2):e000507. PubMed PMID: 31231573; PubMed Central PMCID: PMC6555600.
8. van Bussel MTJ, Pluim D, Bol M, Beijnen JH, Schellens JHM, Brandsma D. EpCAM-based assays for epithelial tumor cell detection in cerebrospinal fluid. J Neurooncol 2018;137(1):1–10. PubMed PMID: 29192390.
9. Siegel RL, Miller KD, Wagle NS, Jemal A. Cancer statistics, 2023. CA Cancer J Clin 2023;73(1):17–48. PubMed PMID: 36633525.
10. Le Rhun E, Tu Q, Carvalho Bittencourt M de, Farre I, Mortier L, Cai H, et al. Detection and quantification of CSF malignant cells by the CellSearch technology in patients with melanoma leptomeningeal metastasis. Med Oncol 2013;30(2):538. PubMed PMID: 23504338.
11. Wang N, Bertalan MS, Brastianos PK. Leptomeningeal metastasis from systemic cancer: Review and update on management. Cancer 2018;124(1):21–35. PubMed PMID: 29165794; PubMed Central PMCID: PMC7418844.
12. Franzoi MA, Hortobagyi GN. Leptomeningeal carcinomatosis in patients with breast cancer. Crit Rev Oncol Hematol 2019;135:85–94. PubMed PMID: 30819451.
13. Hong Y, Duan P, He L, Li Q, Chen Y, Wang P, et al. Systematic Immunological Level Determined the Prognosis of Leptomeningeal Metastasis in Lung Cancer. Cancer Manag Res 2022;14:1153–64. PubMed PMID: 35321403; PubMed Central PMCID: PMC8934871.
14. Le Rhun E, Weller M, van den Bent M, Brandsma D, Furtner J, Rudà R, et al. Leptomeningeal metastasis from solid tumours: EANO-ESMO Clinical Practice Guideline for diagnosis, treatment and follow-up. ESMO Open 2023;8(5):101624. PubMed PMID: 37863528; PubMed Central PMCID: PMC10619142.
15. Le Rhun E, Guckenberger M, Smits M, Dummer R, Bachelot T, Sahm F, et al. EANO-ESMO Clinical Practice Guidelines for diagnosis, treatment and follow-up of patients with brain metastasis from solid tumours. Ann Oncol 2021;32(11):1332–47. PubMed PMID: 34364998.
16. Ignatiadis M, Sledge GW, Jeffrey SS. Liquid biopsy enters the clinic - implementation issues and future challenges. Nat Rev Clin Oncol 2021;18(5):297–312. PubMed PMID: 33473219.
17. Alimirzaie S, Bagherzadeh M, Akbari MR. Liquid biopsy in breast cancer: A comprehensive review. Clin Genet 2019;95(6):643–60. PubMed PMID: 30671931.
18. Nikanjam M, Kato S, Kurzrock R. Liquid biopsy: current technology and clinical applications. J Hematol Oncol 2022;15(1):131. PubMed PMID: 36096847; PubMed Central PMCID: PMC9465933.
19. Poulet G, Massias J, Taly V. Liquid Biopsy: General Concepts. Acta Cytol 2019;63(6):449–55. PubMed PMID: 31091522.
20. Oshi M, Murthy V, Takahashi H, Huyser M, Okano M, Tokumaru Y, et al. Urine as a Source of Liquid Biopsy for Cancer. Cancers (Basel) 2021;13(11). PubMed PMID: 34071230; PubMed Central PMCID: PMC8199052.
21. Baburaj G, Damerla RR, Udupa KS, Parida P, Munisamy M, Kolesar J, et al. Liquid biopsy approaches for pleural effusion in lung cancer patients. Mol Biol Rep 2020;47(10):8179–87. PubMed PMID: 33029702.
22. Fischer JC, Niederacher D, Topp SA, Honisch E, Schumacher S, Schmitz N, et al. Diagnostic leukapheresis enables reliable detection of circulating tumor cells of nonmetastatic cancer patients. Proc Natl Acad Sci U S A 2013;110(41):16580–5. PubMed PMID: 24065821; PubMed Central PMCID: PMC3799344.
23. Connal S, Cameron JM, Sala A, Brennan PM, Palmer DS, Palmer JD, et al. Liquid biopsies: the future of cancer early detection. J Transl Med 2023;21(1):118. PubMed PMID: 36774504; PubMed Central PMCID: PMC9922467.
24. Le Rhun E, Seoane J, Salzet M, Soffietti R, Weller M. Liquid biopsies for diagnosing and monitoring primary tumors of the central nervous system. Cancer Lett 2020;480:24–8. PubMed PMID: 32229189.

25. Malani R, Fleisher M, Kumthekar P, Lin X, Omuro A, Groves MD, et al. Cerebrospinal fluid circulating tumor cells as a quantifiable measurement of leptomeningeal metastases in patients with HER2 positive cancer. J Neurooncol 2020;148(3):599–606. PubMed PMID: 32506369; PubMed Central PMCID: PMC7438284.
26. Lüke F, Blazquez R, Yamaci RF, Lu X, Pregler B, Hannus S, et al. Isolated metastasis of an EGFR-L858R-mutated NSCLC of the meninges: the potential impact of CXCL12/CXCR4 axis in EGFRmut NSCLC in diagnosis, follow-up and treatment. Oncotarget 2018;9(27):18844–57. PubMed PMID: 29721166; PubMed Central PMCID: PMC5922360.
27. Telano LN, Baker S. StatPearls: Physiology, Cerebral Spinal Fluid. Treasure Island (FL); 2024.
28. Süssmuth SD, Brettschneider J, Spreer A, Wick M, Jesse S, Lewerenz J, et al. Aktuelle Liquordiagnostik bei erregerbedingten Krankheiten. Nervenarzt 2013;84(2):229–44. PubMed PMID: 23371378; PubMed Central PMCID: PMC7095826.
29. Cristofanilli M, Broglio KR, Guarneri V, Jackson S, Fritsche HA, Islam R, et al. Circulating tumor cells in metastatic breast cancer: biologic staging beyond tumor burden. Clin Breast Cancer 2007;7(6):471–9. PubMed PMID: 17386124.
30. Swaby RF, Cristofanilli M. Circulating tumor cells in breast cancer: a tool whose time has come of age. BMC Med 2011;9:43. PubMed PMID: 21510857; PubMed Central PMCID: PMC3107794.
31. Kagan M, Terstappen LW. A Sample Preparation and Analysis System for Identification of Circulating Tumorcells [Internet]. Journal of Clinical Ligand Assay: ; 2002.
32. Dawood S, Broglio K, Valero V, Reuben J, Handy B, Islam R, et al. Circulating tumor cells in metastatic breast cancer: from prognostic stratification to modification of the staging system? Cancer 2008;113(9):2422–30. PubMed PMID: 18785255.
33. Darlix A, Cayrefourcq L, Pouderoux S, Menjot de Champfleur N, Bievelez A, Jacot W, et al. Detection of Circulating Tumor Cells in Cerebrospinal Fluid of Patients with Suspected Breast Cancer Leptomeningeal Metastases: A Prospective Study. Clin Chem 2022;68(10):1311–22. PubMed PMID: 35953885.
34. Patel AS, Allen JE, Dicker DT, Peters KL, Sheehan JM, Glantz MJ, et al. Identification and enumeration of circulating tumor cells in the cerebrospinal fluid of breast cancer patients with central nervous system metastases. Oncotarget 2011;2(10):752–60. PubMed PMID: 21987585; PubMed Central PMCID: PMC3248154.
35. Diaz M, Singh P, Kotchetkov IS, Skakodub A, Meng A, Tamer C, et al. Quantitative assessment of circulating tumor cells in cerebrospinal fluid as a clinical tool to predict survival in leptomeningeal metastases. J Neurooncol 2022;157(1):81–90. PubMed PMID: 35113288; PubMed Central PMCID: PMC9119011.
36. Magbanua MJM, Melisko M, Roy R, Sosa EV, Hauranieh L, Kablanian A, et al. Molecular profiling of tumor cells in cerebrospinal fluid and matched primary tumors from metastatic breast cancer patients with leptomeningeal carcinomatosis. Cancer Res 2013;73(23):7134–43. PubMed PMID: 24142343.
37. Sundaresan TK, Sequist LV, Heymach JV, Riely GJ, Jänne PA, Koch WH, et al. Detection of T790M, the Acquired Resistance EGFR Mutation, by Tumor Biopsy versus Noninvasive Blood-Based Analyses. Clin Cancer Res 2016;22(5):1103–10. PubMed PMID: 26446944; PubMed Central PMCID: PMC4775471.
38. Dang DK, Park BH. Circulating tumor DNA: current challenges for clinical utility. J Clin Invest 2022;132(12). PubMed PMID: 35703177; PubMed Central PMCID: PMC9197509.
39. Leers MPG. Circulating tumor DNA and their added value in molecular oncology. Clin Chem Lab Med 2020;58(2):152–61. PubMed PMID: 31490771.
40. Cheng F, Su L, Qian C. Circulating tumor DNA: a promising biomarker in the liquid biopsy of cancer. Oncotarget 2016;7(30):48832–41. PubMed PMID: 27223063; PubMed Central PMCID: PMC5217053.
41. Metzenmacher M, Hegedüs B, Forster J, Schramm A, Horn PA, Klein CA, et al. The clinical utility of cfRNA for disease detection and surveillance: A proof of concept study in non-small cell lung cancer. Thorac Cancer 2022;13(15):2180–91. PubMed PMID: 35708207; PubMed Central PMCID: PMC9346179.
42. Bulbul A, Leal A, Husain H. Applications of cell-free circulating tumor DNA detection in EGFR mutant lung cancer. J Thorac Dis 2020;12(5):2877–82. PubMed PMID: 32642200; PubMed Central PMCID: PMC7330324.
43. Normanno N, Maiello MR, Chicchinelli N, Iannaccone A, Esposito C, Cecio R de, et al. Targeting the EGFR T790M mutation in non-small-cell lung cancer. Expert Opin Ther Targets 2017;21(2):159–65. PubMed PMID: 28002980.
44. Min S, Shin S, Chung Y-J. Detection of KRAS mutations in plasma cell-free DNA of colorectal cancer patients and comparison with cancer panel data for tissue samples of the same cancers. Genomics Inform 2019;17(4):e42. PubMed PMID: 31896242; PubMed Central PMCID: PMC6944046.
45. Kujala J, Hartikainen JM, Tengström M, Sironen R, Kosma V-M, Mannermaa A. High mutation burden of circulating cell-free DNA in early-stage breast cancer patients is associated with a poor relapse-free survival. Cancer Med 2020;9(16):5922–31. PubMed PMID: 32602248; PubMed Central PMCID: PMC7433819.
46. Sanne de Wit, Guus van Dalum, and Leon W.M.M Terstappen. Detection of Circulating Tumor Cells: Review Article. Scientifica 2014;2014. PubMed PMID: 25133014.
47. Tu Q, Wu X, Le Rhun E, Blonski M, Wittwer B, Taillandier L, et al. CellSearch technology applied to the detection and quantification of tumor cells in CSF of patients with lung cancer leptomeningeal metastasis. Lung Cancer 2015;90(2):352–7. PubMed PMID: 26386833.

48. Stevens M, Mentink A, Nanou A, Coumans FAW, Isebia KT, Kraan J, et al. Improved enrichment of circulating tumor cells from diagnostic leukapheresis product. Cytometry A 2023;103(11):881–8. PubMed PMID: 37461156.
49. Menarini Silicon Biosystems Inc. CellSearch® CirculatingTumorCellKit (Epithelial); 2017.
50. Köstler C, Polzer B, Alberter B. Circulating Tumor Cell Enrichment and Single-Cell Isolation Combining the CellSearch® and DEPArray™ Systems. Methods Mol Biol 2024;2752:11–42. PubMed PMID: 38194025.
51. Menarini Silicon Biosystems Inc. CELLTRACKS® AUTOPREP®System - User´s Guide; 2019.
52. Menarini Silicon Biosystems Inc. CELLTRACKS ANALYZER II® User´s Guide; 2019.
53. Le Rhun E, Massin F, Tu Q, Bonneterre J, Bittencourt MDC, Faure GC. Development of a new method for identification and quantification in cerebrospinal fluid of malignant cells from breast carcinoma leptomeningeal metastasis. BMC Clin Pathol 2012;12:21. PubMed PMID: 23145812; PubMed Central PMCID: PMC3539901.
54. Menarini Silicon Biosystems Inc. TRA_TUX_127-R3-DEPArray PLUS Sample Extraction from CELLSEARCH Cartridge. 7 p.
55. Bolognesi C, Forcato C, Buson G, Fontana F, Mangano C, Doffini A, et al. Digital Sorting of Pure Cell Populations Enables Unambiguous Genetic Analysis of Heterogeneous Formalin-Fixed Paraffin-Embedded Tumors by Next Generation Sequencing. Scientific Reports 2016;6(1):1–14.
56. Menarini Silicon Biosystems Inc. W_MKT_041_Semi-automatic cell counting with ImageJ_v1.0. 9 p.
57. Menarini Silicon Biosystems Inc. IFU_1007_R2.0 - Cartridge Plus -Instruction for Use. 5 p.
58. Di Trapani M, Manaresi N, Medoro G. DEPArray™ system: An automatic image-based sorter for isolation of pure circulating tumor cells. Cytometry A 2018;93(12):1260–6. PubMed PMID: 30551261; PubMed Central PMCID: PMC6590341.
59. Menarini Silicon Biosystems SpA. IFU_1011_DEPArrayPlusFFPEApplication. 58 p.
60. Klein CA, Schmidt-Kittler O, Schardt JA, Pantel K, Speicher MR, Riethmüller G. Comparative genomic hybridization, loss of heterozygosity, and DNA sequence analysis of single cells. Proc Natl Acad Sci U S A 1999;96(8):4494–9. PubMed PMID: 10200290; PubMed Central PMCID: PMC16360.
61. Polzer B, Medoro G, Pasch S, Fontana F, Zorzino L, Pestka A, et al. Molecular profiling of single circulating tumor cells with diagnostic intention. EMBO Mol Med 2014;6(11):1371–86. PubMed PMID: 25358515; PubMed Central PMCID: PMC4237466.
62. Menarini Silicon Biosystems SpA. M065_Ampli1 LowPass kit for Illumina_MSB_V3. 36 p.
63. Bushnel B. BBMap: BBTools - DOE Joint Genome Institute.
64. Chu J, Sadeghi S, Raymond A, Jackman SD, Nip KM, Mar R, et al. BioBloom tools: fast, accurate and memory-efficient host species sequence screening using bloom filters. Bioinformatics 2014;30(23):3402–4. PubMed PMID: 25143290; PubMed Central PMCID: PMC4816029.
65. Babraham Bioinformatics. FastQC A Quality Control tool for High Throughput Sequence Data.
66. Ewels P, Magnusson M, Lundin S, Käller M. MultiQC: summarize analysis results for multiple tools and samples in a single report. Bioinformatics 2016;32(19):3047–8. PubMed PMID: 27312411; PubMed Central PMCID: PMC5039924.
67. Li H. Aligning sequence reads, clone sequences and assembly contigs with BWA-MEM; 2013. Available from: http://arxiv.org/pdf/1303.3997v2.
68. Broad Institute. Picard Tools: Broad Institute.
69. Scheinin I, Sie D, Bengtsson H, van de Wiel MA, Olshen AB, van Thuijl HF, et al. DNA copy number analysis of fresh and formalin-fixed specimens by shallow whole-genome sequencing with identification and exclusion of problematic regions in the genome assembly. Genome Res 2014;24(12):2022–32. PubMed PMID: 25236618; PubMed Central PMCID: PMC4248318.
70. Poell JB, Mendeville M, Sie D, Brink A, Brakenhoff RH, Ylstra B. ACE: absolute copy number estimation from low-coverage whole-genome sequencing data. Bioinformatics 2019;35(16):2847–9. PubMed PMID: 30596895.
71. Okonechnikov K, Conesa A, García-Alcalde F. Qualimap 2: advanced multi-sample quality control for high-throughput sequencing data. Bioinformatics 2016;32(2):292–4. PubMed PMID: 26428292; PubMed Central PMCID: PMC4708105.
72. Krzywinski M, Schein J, Birol I, Connors J, Gascoyne R, Horsman D, et al. Circos: an information aesthetic for comparative genomics. Genome Res 2009;19(9):1639–45. PubMed PMID: 19541911; PubMed Central PMCID: PMC2752132.
73. Nayak L, Fleisher M, Gonzalez-Espinoza R, Lin O, Panageas K, Reiner A, et al. Rare cell capture technology for the diagnosis of leptomeningeal metastasis in solid tumors. Neurology 2013;80(17):1598-605; discussion 1603. PubMed PMID: 23553479; PubMed Central PMCID: PMC3662321.
74. Polasik A, Schramm A, Friedl TWP, Rack BK, Trapp EK, Fasching PA, et al. The DETECT study concept: Individualized therapy of metastatic breast cancer. JCO 2016;34(15_suppl):TPS634-TPS634.
75. Silvestri M, Reduzzi C, Feliciello G, Vismara M, Schamberger T, Köstler C, et al. Detection of Genomically Aberrant Cells within Circulating Tumor Microemboli (CTMs) Isolated from Early-Stage Breast Cancer Patients. Cancers (Basel) 2021;13(6). PubMed PMID: 33808748; PubMed Central PMCID: PMC8003526.
76. Le Rhun E, Galanis E. Leptomeningeal metastases of solid cancer. Curr Opin Neurol 2016;29(6):797–805. PubMed PMID: 27661208.

77. Subirá D, Simó M, Illán J, Serrano C, Castañón S, Gonzalo R, et al. Diagnostic and prognostic significance of flow cytometry immunophenotyping in patients with leptomeningeal carcinomatosis. Clinical & Experimental Metastasis 2015;32(4):383–91. PubMed PMID: 25795393.
78. Sener U, Kumthekar P, Boire A. Advances in the diagnosis, evaluation, and management of leptomeningeal disease. Neurooncol Adv 2021;3(Suppl 5):v86-v95. PubMed PMID: 34859236; PubMed Central PMCID: PMC8633748.
79. Bruna J, Simó M, Velasco R. Leptomeningeal metastases. Curr Treat Options Neurol 2012;14(4):402–15. PubMed PMID: 22736147.
80. Schwab M. Oncogene amplification in solid tumors. Semin Cancer Biol 1999;9(4):319–25. PubMed PMID: 10448118.
81. Shlien A, Tabori U, Marshall CR, Pienkowska M, Feuk L, Novokmet A, et al. Excessive genomic DNA copy number variation in the Li-Fraumeni cancer predisposition syndrome. Proc Natl Acad Sci U S A 2008;105(32):11264–9. PubMed PMID: 18685109; PubMed Central PMCID: PMC2516272.
82. Tonon G, Brennan C, Protopopov A, Maulik G, Feng B, Zhang Y, et al. Common and contrasting genomic profiles among the major human lung cancer subtypes. Cold Spring Harb Symp Quant Biol 2005;70:11–24. PubMed PMID: 16869734.
83. Andre F, Job B, Dessen P, Tordai A, Michiels S, Liedtke C, et al. Molecular characterization of breast cancer with high-resolution oligonucleotide comparative genomic hybridization array. Clin Cancer Res 2009;15(2):441–51. PubMed PMID: 19147748.
84. Hazra A, O'Hara A, Polyak K, Nakhlis F, Harrison BT, Giordano A, et al. Copy Number Variation in Inflammatory Breast Cancer. Cells 2023;12(7). PubMed PMID: 37048158; PubMed Central PMCID: PMC10093603.
85. Matsui A, Ihara T, Suda H, Mikami H, Semba K. Gene amplification: mechanisms and involvement in cancer. Biomol Concepts 2013;4(6):567–82. PubMed PMID: 25436757.
86. Kraehn GM, Utikal J, Udart M, Greulich KM, Bezold G, Kaskel P, et al. Extra c-myc oncogene copies in high risk cutaneous malignant melanoma and melanoma metastases. British Journal of Cancer 2001;84(1):72–9. PubMed PMID: 11139316; PubMed Central PMCID: PMC2363612.
87. Pouryazdanparast P, Brenner A, Haghighat Z, Guitart J, Rademaker A, Gerami P. The role of 8q24 copy number gains and c-MYC expression in amelanotic cutaneous melanoma. Mod Pathol 2012;25(9):1221–6. PubMed PMID: 22555175.
88. Comprehensive molecular portraits of human breast tumours. Nature 2012;490(7418):61–70. PubMed PMID: 23000897; PubMed Central PMCID: PMC3465532.
89. Bergamaschi A, Kim YH, Wang P, Sørlie T, Hernandez-Boussard T, Lonning PE, et al. Distinct patterns of DNA copy number alteration are associated with different clinicopathological features and gene-expression subtypes of breast cancer. Genes Chromosomes Cancer 2006;45(11):1033–40. PubMed PMID: 16897746.
90. Chin K, DeVries S, Fridlyand J, Spellman PT, Roydasgupta R, Kuo W-L, et al. Genomic and transcriptional aberrations linked to breast cancer pathophysiologies. Cancer Cell 2006;10(6):529–41. PubMed PMID: 17157792.
91. Scotto L, Narayan G, Nandula SV, Subramaniyam S, Kaufmann AM, Wright JD, et al. Integrative genomics analysis of chromosome 5p gain in cervical cancer reveals target over-expressed genes, including Drosha. Mol Cancer 2008;7:58. PubMed PMID: 18559093; PubMed Central PMCID: PMC2440550.
92. Kang JU, Koo SH, Kwon KC, Park JW, Kim JM. Gain at chromosomal region 5p15.33, containing TERT, is the most frequent genetic event in early stages of non-small cell lung cancer. Cancer Genet Cytogenet 2008;182(1):1–11. PubMed PMID: 18328944.
93. Venugopal S, Mascarenhas J, Steensma DP. Loss of 5q in myeloid malignancies - A gain in understanding of biological and clinical consequences. Blood Rev 2021;46:100735. PubMed PMID: 32736878.
94. Pan W, Gu W, Nagpal S, Gephart MH, Quake SR. Brain tumor mutations detected in cerebral spinal fluid. Clin Chem 2015;61(3):514–22. PubMed PMID: 25605683; PubMed Central PMCID: PMC5412506.
95. Kapeleris J, Kulasinghe A, Warkiani ME, Vela I, Kenny L, O'Byrne K, et al. The Prognostic Role of Circulating Tumor Cells (CTCs) in Lung Cancer. Front Oncol 2018;8:311. PubMed PMID: 30155443; PubMed Central PMCID: PMC6102369.
96. Kummar S, Fogarasi M, Canova A, Mota A, Ciesielski T. Cytokeratin 7 and 20 staining for the diagnosis of lung and colorectal adenocarcinoma. British Journal of Cancer 2002;86(12):1884–7. PubMed PMID: 12085180; PubMed Central PMCID: PMC2375436.
97. Chen Y, Cui T, Yang L, Mireskandari M, Knoesel T, Zhang Q, et al. The diagnostic value of cytokeratin 5/6, 14, 17, and 18 expression in human non-small cell lung cancer. Oncology 2011;80(5-6):333–40. PubMed PMID: 21791943.
98. Nassar A, Radhakrishnan A, Cabrero IA, Cotsonis GA, Cohen C. Intratumoral heterogeneity of immunohistochemical marker expression in breast carcinoma: a tissue microarray-based study. Appl Immunohistochem Mol Morphol 2010;18(5):433–41. PubMed PMID: 20485156.
99. Grzywa TM, Paskal W, Włodarski PK. Intratumor and Intertumor Heterogeneity in Melanoma. Transl Oncol 2017;10(6):956–75. PubMed PMID: 29078205; PubMed Central PMCID: PMC5671412.

100. Ulmer A, Schmidt-Kittler O, Fischer J, Ellwanger U, Rassner G, Riethmüller G, et al. Immunomagnetic enrichment, genomic characterization, and prognostic impact of circulating melanoma cells. Clin Cancer Res 2004;10(2):531–7. PubMed PMID: 14760074.
101. Rapanotti MC, Cugini E, Nuccetelli M, Terrinoni A, Di Raimondo C, Lombardo P, et al. MCAM/MUC18/CD146 as a Multifaceted Warning Marker of Melanoma Progression in Liquid Biopsy. Int J Mol Sci 2021;22(22). PubMed PMID: 34830300; PubMed Central PMCID: PMC8623757.
102. Rao C, Bui T, Connelly M, Doyle G, Karydis I, Middleton MR, et al. Circulating melanoma cells and survival in metastatic melanoma. Int J Oncol 2011;38(3):755–60. PubMed PMID: 21206975.
103. Deacon DC, Smith EA, Judson-Torres RL. Molecular Biomarkers for Melanoma Screening, Diagnosis and Prognosis: Current State and Future Prospects. Front Med (Lausanne) 2021;8:642380. PubMed PMID: 33937286; PubMed Central PMCID: PMC8085270.
104. Davis LE, Shalin SC, Tackett AJ. Current state of melanoma diagnosis and treatment. Cancer Biol Ther 2019;20(11):1366–79. PubMed PMID: 31366280; PubMed Central PMCID: PMC6804807.
105. Pawlik L, Morgenroth S, Dummer R. Recent Progress in the Diagnosis and Treatment of Melanoma and Other Skin Cancers. Cancers (Basel) 2023;15(6). PubMed PMID: 36980709; PubMed Central PMCID: PMC10046835.
106. Freeman JB, Gray ES, Millward M, Pearce R, Ziman M. Evaluation of a multi-marker immunomagnetic enrichment assay for the quantification of circulating melanoma cells. J Transl Med 2012;10:192. PubMed PMID: 22978632; PubMed Central PMCID: PMC3480925.
107. Gray ES, Reid AL, Bowyer S, Calapre L, Siew K, Pearce R, et al. Circulating Melanoma Cell Subpopulations: Their Heterogeneity and Differential Responses to Treatment. J Invest Dermatol 2015;135(8):2040–8. PubMed PMID: 25830652; PubMed Central PMCID: PMC4504811.
108. Bande MF, Santiago M, Muinelo-Romay L, Blanco MJ, Mera P, Capeans C, et al. Detection of circulating melanoma cells in choroidal melanocytic lesions. BMC Res Notes 2015;8(1).
109. Steen S, Nemunaitis J, Fisher T, Kuhn J. Circulating Tumor Cells in Melanoma: A Review of the Literature and Description of a Novel Technique. Proc (Bayl Univ Med Cent) 2008;21(2):127–32. PubMed PMID: 18382750; PubMed Central PMCID: PMC2277345.
110. Roland CL, Ross MI, Hall CS, Laubacher B, Upshaw J, Anderson AE, et al. Detection of circulating melanoma cells in the blood of melanoma patients: a preliminary study. Melanoma Res 2015;25(4):335–41. PubMed PMID: 26011119; PubMed Central PMCID: PMC5642955.
111. Hrishi AP, Sethuraman M. Cerebrospinal Fluid (CSF) Analysis and Interpretation in Neurocritical Care for Acute Neurological Conditions. Indian J Crit Care Med 2019;23(Suppl 2):S115-S119. PubMed PMID: 31485118; PubMed Central PMCID: PMC6707491.
112. Rack B, Schindlbeck C, Jückstock J, Andergassen U, Hepp P, Zwingers T, et al. Circulating tumor cells predict survival in early average-to-high risk breast cancer patients. J Natl Cancer Inst 2014;106(5). PubMed PMID: 24832787; PubMed Central PMCID: PMC4112925.
113. Capuozzo M, Ferrara F, Santorsola M, Zovi A, Ottaiano A. Circulating Tumor Cells as Predictive and Prognostic Biomarkers in Solid Tumors. Cells 2023;12(22). PubMed PMID: 37998325; PubMed Central PMCID: PMC10670669.
114. Cristofanilli M, Budd GT, Ellis MJ, Stopeck A, Matera J, Miller MC, et al. Circulating Tumor Cells, Disease Progression, and Survival in Metastatic Breast Cancer. N Engl J Med 2004;351(8):781–91.
115. Cohen SJ, Punt CJA, Iannotti N, Saidman BH, Sabbath KD, Gabrail NY, et al. Prognostic significance of circulating tumor cells in patients with metastatic colorectal cancer. Ann Oncol 2009;20(7):1223–9. PubMed PMID: 19282466.
116. Jesenko T, Modic Z, Kuhar CG, Cemazar M, Matkovic U, Miceska S, et al. Morphological features of breast cancer circulating tumor cells in blood after physical and biological type of isolation. Radiol Oncol 2021;55(3):292–304. PubMed PMID: 34384011; PubMed Central PMCID: PMC8366726.
117. Park S, Ang RR, Duffy SP, Bazov J, Chi KN, Black PC, et al. Morphological differences between circulating tumor cells from prostate cancer patients and cultured prostate cancer cells. PLoS One 2014;9(1):e85264. PubMed PMID: 24416373; PubMed Central PMCID: PMC3885705.
118. Asante D-B, Mohan GRKA, Acheampong E, Ziman M, Calapre L, Meniawy TM, et al. Genetic analysis of heterogeneous subsets of circulating tumour cells from high grade serous ovarian carcinoma patients. Scientific Reports 2023;13(1):2552. PubMed PMID: 36781954; PubMed Central PMCID: PMC9925814.
119. Hamid FB, Gopalan V, Matos M, Lu C-T, Lam AK-Y. Genetic Heterogeneity of Single Circulating Tumour Cells in Colorectal Carcinoma. Int J Mol Sci 2020;21(20). PubMed PMID: 33092235; PubMed Central PMCID: PMC7589365.
120. Menyailo ME, Tretyakova MS, Denisov EV. Heterogeneity of Circulating Tumor Cells in Breast Cancer: Identifying Metastatic Seeds. Int J Mol Sci 2020;21(5). PubMed PMID: 32121639; PubMed Central PMCID: PMC7084665.
121. Agnoletto C, Corrà F, Minotti L, Baldassari F, Crudele F, Cook WJJ, et al. Heterogeneity in Circulating Tumor Cells: The Relevance of the Stem-Cell Subset. Cancers (Basel) 2019;11(4). PubMed PMID: 30959764; PubMed Central PMCID: PMC6521045.

122. Miyamoto DT, Ting DT, Toner M, Maheswaran S, Haber DA. Single-Cell Analysis of Circulating Tumor Cells as a Window into Tumor Heterogeneity. Cold Spring Harb Symp Quant Biol 2016;81:269–74. PubMed PMID: 28389596; PubMed Central PMCID: PMC5501288.
123. Wang C, Mu Z, Ye Z, Zhang Z, Abu-Khalaf MM, Silver DP, et al. Prognostic value of HER2 status on circulating tumor cells in advanced-stage breast cancer patients with HER2-negative tumors. Breast Cancer Research and Treatment 2020;181(3):679–89. PubMed PMID: 32367460; PubMed Central PMCID: PMC7299127.
124. Kiniwa Y, Nakamura K, Mikoshiba A, Ashida A, Akiyama Y, Morimoto A, et al. Usefulness of monitoring circulating tumor cells as a therapeutic biomarker in melanoma with BRAF mutation. BMC Cancer 2021;21(1):287. PubMed PMID: 33731038; PubMed Central PMCID: PMC7968258.
125. Takayama Y, Suzuki K, Muto Y, Ichida K, Fukui T, Kakizawa N, et al. Monitoring circulating tumor DNA revealed dynamic changes in KRAS status in patients with metastatic colorectal cancer. Oncotarget 2018;9(36):24398–413. PubMed PMID: 29849949; PubMed Central PMCID: PMC5966256.
126. Orrapin S, Thongkumkoon P, Udomruk S, Moonmuang S, Sutthitthasakul S, Yongpitakwattana P, et al. Deciphering the Biology of Circulating Tumor Cells through Single-Cell RNA Sequencing: Implications for Precision Medicine in Cancer. Int J Mol Sci 2023;24(15). PubMed PMID: 37569711; PubMed Central PMCID: PMC10418766.
127. Hücker SM, Fehlmann T, Werno C, Weidele K, Lüke F, Schlenska-Lange A, et al. Single-cell microRNA sequencing method comparison and application to cell lines and circulating lung tumor cells. Nat Commun 2021;12(1):4316. PubMed PMID: 34262050; PubMed Central PMCID: PMC8280203.
128. Zhang L, Ridgway LD, Wetzel MD, Ngo J, Yin W, Kumar D, et al. The identification and characterization of breast cancer CTCs competent for brain metastasis. Sci Transl Med 2013;5(180):180ra48. PubMed PMID: 23576814; PubMed Central PMCID: PMC3863909.
129. Werno C, Honarnejad K, Polzer B. Predicting therapy response by analysis of metastasis founder cells: emerging perspectives for personalized tumor therapy. Expert Review of Precision Medicine and Drug Development 2020;5(6):413–20.
130. Baccelli I, Schneeweiss A, Riethdorf S, Stenzinger A, Schillert A, Vogel V, et al. Identification of a population of blood circulating tumor cells from breast cancer patients that initiates metastasis in a xenograft assay. Nat Biotechnol 2013;31(6):539–44. PubMed PMID: 23609047.
131. Yu M, Bardia A, Aceto N, Bersani F, Madden MW, Donaldson MC, et al. Cancer therapy. Ex vivo culture of circulating breast tumor cells for individualized testing of drug susceptibility. Science 2014;345(6193):216–20. PubMed PMID: 25013076; PubMed Central PMCID: PMC4358808.
132. Girotti MR, Gremel G, Lee R, Galvani E, Rothwell D, Viros A, et al. Application of Sequencing, Liquid Biopsies, and Patient-Derived Xenografts for Personalized Medicine in Melanoma. Cancer Discov 2016;6(3):286–99. PubMed PMID: 26715644.
133. McEwen AE, Leary SES, Lockwood CM. Beyond the Blood: CSF-Derived cfDNA for Diagnosis and Characterization of CNS Tumors. Front Cell Dev Biol 2020;8:45. PubMed PMID: 32133357; PubMed Central PMCID: PMC7039816.
134. Ranucci R. Cell-Free DNA: Applications in Different Diseases. Methods Mol Biol 2019;1909:3–12. PubMed PMID: 30580419.
135. Volckmar A-L, Sültmann H, Riediger A, Fioretos T, Schirmacher P, Endris V, et al. A field guide for cancer diagnostics using cell-free DNA: From principles to practice and clinical applications. Genes Chromosomes Cancer 2018;57(3):123–39. PubMed PMID: 29205637.
136. Diehl F, Li M, Dressman D, He Y, Shen D, Szabo S, et al. Detection and quantification of mutations in the plasma of patients with colorectal tumors. Proc Natl Acad Sci U S A 2005;102(45):16368–73. PubMed PMID: 16258065; PubMed Central PMCID: PMC1283450.
137. Schwarzenbach H, Alix-Panabières C, Müller I, Letang N, Vendrell J-P, Rebillard X, et al. Cell-free tumor DNA in blood plasma as a marker for circulating tumor cells in prostate cancer. Clin Cancer Res 2009;15(3):1032–8. PubMed PMID: 19188176.
138. Liu APY, Smith KS, Kumar R, Paul L, Bihannic L, Lin T, et al. Serial assessment of measurable residual disease in medulloblastoma liquid biopsies. Cancer Cell 2021;39(11):1519-1530.e4. PubMed PMID: 34678152; PubMed Central PMCID: PMC9620970.
139. Bale TA, Yang S-R, Solomon JP, Nafa K, Middha S, Casanova J, et al. Clinical experience of cerebrospinal fluid-based liquid biopsy demonstrates superiority of cell free DNA over cell pellet genomic DNA for molecular profiling. J Mol Diagn 2021. PubMed PMID: 33781965.
140. Song P, Wu LR, Yan YH, Zhang JX, Chu T, Kwong LN, et al. Limitations and opportunities of technologies for the analysis of cell-free DNA in cancer diagnostics. Nat Biomed Eng 2022;6(3):232–45. PubMed PMID: 35102279; PubMed Central PMCID: PMC9336539.
141. Dawson S-J, Tsui DWY, Murtaza M, Biggs H, Rueda OM, Chin S-F, et al. Analysis of circulating tumor DNA to monitor metastatic breast cancer. N Engl J Med 2013;368(13):1199–209. PubMed PMID: 23484797.
142. Olsson E, Winter C, George A, Chen Y, Howlin J, Tang M-HE, et al. Serial monitoring of circulating tumor DNA in patients with primary breast cancer for detection of occult metastatic disease. EMBO Mol Med 2015;7(8):1034–47. PubMed PMID: 25987569; PubMed Central PMCID: PMC4551342.

143. Kirchweger P, Kupferthaler A, Burghofer J, Webersinke G, Jukic E, Schwendinger S, et al. Circulating tumor DNA correlates with tumor burden and predicts outcome in pancreatic cancer irrespective of tumor stage. Eur J Surg Oncol 2022;48(5):1046–53. PubMed PMID: 34876329.
144. Aceto N, Bardia A, Miyamoto DT, Donaldson MC, Wittner BS, Spencer JA, et al. Circulating tumor cell clusters are oligoclonal precursors of breast cancer metastasis. Cell 2014;158(5):1110–22. PubMed PMID: 25171411; PubMed Central PMCID: PMC4149753.
145. Jahr S, Hentze H, Englisch S, Hardt D, Fackelmayer FO, Hesch RD, et al. DNA fragments in the blood plasma of cancer patients: quantitations and evidence for their origin from apoptotic and necrotic cells. Cancer Res 2001;61(4):1659–65. PubMed PMID: 11245480.
146. Heitzer E, Auinger L, Speicher MR. Cell-Free DNA and Apoptosis: How Dead Cells Inform About the Living. Trends Mol Med 2020;26(5):519–28. PubMed PMID: 32359482.
147. Stejskal P, Goodarzi H, Srovnal J, Hajdúch M, van 't Veer LJ, Magbanua MJM. Circulating tumor nucleic acids: biology, release mechanisms, and clinical relevance. Mol Cancer 2023;22(1):15. PubMed PMID: 36681803; PubMed Central PMCID: PMC9862574.
148. Cohnheim J. Congenitales, quergestreiftes Muskelsarkom der Nieren. Archiv f. pathol. Anat. 1875;65(1):64–9.
149. Zhang A, Miao K, Sun H, Deng C-X. Tumor heterogeneity reshapes the tumor microenvironment to influence drug resistance. Int J Biol Sci 2022;18(7):3019–33. PubMed PMID: 35541919; PubMed Central PMCID: PMC9066118.
150. Zheng X, Lu T, Wu S, Peng W, Miao Q, Jiang K, et al. Tumour response heterogeneity as a powerful independent predictor of treatment outcome in advanced lung adenocarcinoma: a retrospective analysis. The Lancet Oncology 2022;23:S13.
151. Strati A, Markou A, Kyriakopoulou E, Lianidou E. Detection and Molecular Characterization of Circulating Tumour Cells: Challenges for the Clinical Setting. Cancers (Basel) 2023;15(7). PubMed PMID: 37046848; PubMed Central PMCID: PMC10092977.
152. Lawrence R, Watters M, Davies CR, Pantel K, Lu Y-J. Circulating tumour cells for early detection of clinically relevant cancer. Nat Rev Clin Oncol 2023;20(7):487–500. PubMed PMID: 37268719; PubMed Central PMCID: PMC10237083.
153. Lin D, Shen L, Luo M, Zhang K, Li J, Yang Q, et al. Circulating tumor cells: biology and clinical significance. Signal Transduct Target Ther 2021;6(1):404. PubMed PMID: 34803167; PubMed Central PMCID: PMC8606574.
154. Munoz-Arcos LS, Nicolò E, Serafini MS, Gerratana L, Reduzzi C, Cristofanilli M. Latest advances in clinical studies of circulating tumor cells in early and metastatic breast cancer. Int Rev Cell Mol Biol 2023;381:1–21. PubMed PMID: 37739480.
155. Stoecklein NH, Oles J, Franken A, Neubauer H, Terstappen LW, Neves RP. Clinical application of circulating tumor cells. Medizinische Genetik 2023;35(4):237–50.
156. Vasseur A, Kiavue N, Bidard F-C, Pierga J-Y, Cabel L. Clinical utility of circulating tumor cells: an update. Mol Oncol 2021;15(6):1647–66. PubMed PMID: 33289351; PubMed Central PMCID: PMC8169442.
157. Müller V, Banys-Paluchowski M, Friedl TWP, Fasching PA, Schneeweiss A, Hartkopf A, et al. Prognostic relevance of the HER2 status of circulating tumor cells in metastatic breast cancer patients screened for participation in the DETECT study program. ESMO Open 2021;6(6):100299. PubMed PMID: 34839105; PubMed Central PMCID: PMC8637493.
158. Smalley I, Chen Z, Phadke M, Li J, Yu X, Wyatt C, et al. Single-Cell Characterization of the Immune Microenvironment of Melanoma Brain and Leptomeningeal Metastases. Clin Cancer Res 2021;27(14):4109–25. PubMed PMID: 34035069; PubMed Central PMCID: PMC8282775.
159. Brastianos PK, Carter SL, Santagata S, Cahill DP, Taylor-Weiner A, Jones RT, et al. Genomic Characterization of Brain Metastases Reveals Branched Evolution and Potential Therapeutic Targets. Cancer Discov 2015;5(11):1164–77. PubMed PMID: 26410082; PubMed Central PMCID: PMC4916970.

7. Acknowledgements

Am Ende meiner Doktorarbeit möchte ich mich bei allen Menschen bedanken, die es möglich gemacht haben, dass ich an diesem Punkt stehen kann!

Vielen Dank Dir, lieber Christoph, dass Du mir als mein Doktorvater das Vertrauen entgegengebracht hast, dieses Projekt zu meistern. Damit hatte ich nicht nur die Möglichkeit, meine fachliche Expertise in unserem Forschungsbereich auszubauen, sondern auch den Mut zu „wachsen“. Unterstützt durch Dein Feedback, den wissenschaftlichen Input, die Übergabe von Verantwortung, aber auch durch Deine Geduld und Dein offenes Ohr für meine Themen während der „Untiefen dieser Doktorarbeit“ bin ich nun an diesem Punkt angelangt. Dankeschön!

Danke auch an Dich, Bernhard. Begonnen bei der anfänglich noch praktischen Unterstützung und Anleitung im Labor, über die Themenfindung, Deine Ideen, die Möglichkeit der Präsentation meiner Daten auf internationalen Tagungen, die zahlreichen Diskussionen, bis hin zu den finalen Korrekturen – vielen Dank für Deine Geduld und das Zutrauen, dass ich das schaffen kann.

Dank gilt meinem Mentorat Prof. Dr. T. Pukrop, Prof. Dr. M.J. Riemenschneider und Prof. Dr. M. Rehli, das mich mit wissenschaftlichem Input, konstruktivem Feedback und seiner Bereitschaft, mich durch diese Arbeit zu führen, in den letzten Jahren unterstützt hat. Vielen Dank auch für die Organisation der Proben, die zu einem Großteil aus diesen Arbeitsgruppen gekommen sind. Vielen Dank auch an meine Prüfungskommission Prof. Dr. P. Hau, Prof. Dr. Nikolas Stoecklein und PD Dr. K. Evert.

Ein besonderer Dank gilt Dir, lieber Gianni. Durch Deine fachliche Expertise, die wissenschaftlichen Diskussionen, die Korrekturen, das Teilen von Büro, Freud, Leid, Kaffee, Aperol Sprizz und das Erlernen der „typisch italienischen Handbewegung“, die auf so sehr viele Situationen in den letzten Jahren gepasst hat, hast Du meinen Arbeitsalltag wahnsinnig bereichert. Non riesco a immaginare come sarebbe stato senza di te.

Weiterhin gilt besonderer Dank Dir, lieber Tom, für Deine Unterstützung im Labor vom ersten Tag an! Für die gemeinsamen Arbeiten am Projekt, die technische Unterstützung, Deine Bereitschaft, etwas zu Ende zu bringen, auch, wenn schon Feierabend war, das Korrekturlesen und natürlich die unvergessenen Dultabende – die sich hoffentlich bald wiederholen.

Vielen herzlichen Dank an alle meine Kolleginnen und Kollegen der AG Klein für ihre Unterstützung und die entspannte Arbeitsatmosphäre. Namentlich hier zu erwähnen seid Ihr, Karola, Judith und Dagmar als „LowPass Analyseheldinnen“, Irina als „WGA- und Pickkönigin“ und Kathrin und Steffi T., die Ihr mich mit Proben aus Euren Projekten für meine Publikation unterstützt habt. Nicht zu vergessen das SCP-Labor am LEX, besonders Anthea, Justin und Nathalie, für die superschnelle Umsetzung aller Datenanfragen, das aufwändige Probensuchen, -zuordnen und -finden und die Lösung für alle anderen Probleme, mit denen ich jemals ans LEX gekommen bin.

Vielen Dank Dir, liebe Marion, für Dein offenes Ohr, viele lustige und ernste Gespräche, die Beautytipps, die Organisation zahlreicher Reisen, Abrechnungen, Meetings, und Dein Mantra „Think big – be big“.

Ich möchte mich auch bei allen Patientinnen und Patienten bedanken, ohne die meine Arbeit nicht möglich gewesen wäre. Danke auch allen klinischen Partnerinnen und Partnern, die Proben zur Verfügung gestellt bzw. parallele Analysen oder Informationen durchgeführt oder zugänglich gemacht haben, insbesondere bei Dr. Saida Zoubaa, Dr. Florian Lüke, Dr. Florian Weber, Dr. Elisabeth Bumes, Prof. Dr. Peter Hau und Prof. Dr. Christina Wendl.

Vielen Dank an Heidi und Bernd aus Schwabach, die mich, während meiner intensiven Schreibphase, über mehrere Wochen beherbergt haben. Es war eine unglaublich schöne Zeit, die sich neben selbstgebackenem Brot, täglich frischem Gemüse, selbstgemachtem „Heidi-Tee“ und der Nähe zu den „Nelias“ (alias Ina, Nelia, Kaja, Mila und Joscha) einfach wie Familie angefühlt hat. Das seid Ihr auch!

Zu meiner psychischen Stabilität – nicht nur während dieser Arbeit - haben sehr liebe Menschen beigetragen, die mir zugehört, mich in den Arm genommen haben und immer für mich da (gewesen) sind. Zu diesen lieben Menschen (Reihenfolge hat keine Bedeutung) gehörst Du, liebe Sandra, Du, lieber Petar, Du, liebe Marie, Du, liebe Luc, Du, lieber Christoph (Danke fürs Korrekturlesen an dieser Stelle) und Du, liebe Kathi. Hier ist auch meine Chor-Partygang zu erwähnen, die mich über die letzten Jahre durch sämtliche Tanzeskapaden geleitet und begleitet hat. Nie wieder ohne Euch!

Vielen Dank an Dich, liebe Lydia, die Du uns, zusammen mit meinem lieben Schwiegerpapa Hermann, immer unterstützt hast, wenn es „gebrannt“ hat. Du bist unsere Nähkönigin, kennst Dich auf Regensburgs Straßen fast besser aus, als wir, warst oft bereit auf unsere Kinder aufzupassen und kochst das beste „Oma-Lydia-Geschnetzelte“ der Welt mit den besten Spätzle der Welt.

Herzlichen Dank, liebe Mutti und lieber Vati, für Alles! Dafür, dass Ihr mich so bildungsnah und musisch erzogen habt, mir die zwei besten Geschwister der Welt, Katha und Gregi, geschenkt habt und mich immer und immer wieder unterstützt habt, ohne eine einzige Pause. Danke für Eure Bereitschaft, von der Nordoberpfalz teilweise mehrmals wöchentlich zu uns zu fahren, um auf Eure Enkel aufzupassen, zu lernen, zu spielen, Orgafahrten zu übernehmen etc. Ohne Euch wären wir vermutlich verhungert und hätten niemals die ganzen Ferientage überbrückt bekommen.

Lieber Johann, lieber Ludwig und liebe Emma – Ihr seid so wahnsinnig geduldig und ausdauernd mit mir gewesen. Immer und immer wieder habt Ihr meine Launen, Erschöpfungszustände und meinen Zeitmangel ertragen und mir nie einen Vorwurf gemacht, auch, wenn ich mich um mich kümmern musste. Jetzt habt Ihr es geschafft – danke, dass Ihr so an mich geglaubt habt. Ihr habt den besten Papa der Welt!

Und das bist Du, lieber Michi - ohne Dich wäre das alles unmöglich gewesen. Danke, dass Du Du bist und mir alle Freiheiten gibst, die sich ein Mensch wünschen kann. Alles aufzuzählen, was uns verbindet, würde den Rahmen sprengen bzw. würde wohl einer weiteren Doktorarbeit entsprechen. Ich bin unendlich dankbar dafür, dass Du nie – wirklich nie – aufgehört hast, an mich zu glauben.

8. DECLARATION OF INDEPENDENT WORK

I, Köstler, Cäcilia Anita Rosa, born [redacted] in Tirschenreuth, hereby declare that I have written this thesis without unauthorized aid and without using sources other than those listed.

Data and concepts that have been taken directly or indirectly from other sources have been marked as such, citing the source. In particular, I have not used paid agency or advisory services (commercial advisers for doctoral degrees or others).

This thesis has so far never been submitted to another examination authority in Germany or abroad, neither in this form nor in a similar form.

Ich, Köstler, Cäcilia Anita Rosa, geboren [redacted] in Tirschenreuth, erkläre hiermit, dass ich die vorliegende Arbeit ohne unerlaubte Hilfe und ohne Benutzung anderer als der angegebenen Quellen verfasst habe.

Daten und Begriffe, die direkt oder indirekt aus anderen Quellen entnommen wurden, sind unter Angabe der Quelle als solche gekennzeichnet. Insbesondere habe ich keine bezahlten Vermittlungs- oder Beratungsdienste (kommerzielle Promotionsberater oder andere) in Anspruch genommen.

Diese Arbeit wurde bisher weder in dieser noch in einer ähnlichen Form einer anderen Prüfungsbehörde im In- oder Ausland vorgelegt.

Regensburg, 8. April 2024

9. CURRICULUM VITAE

Cäcilia Köstler
[redacted]

[redacted]	**Date of birth**
Tirschenreuth/Germany	**Place of birth**
Dipl. Biology	**Background**
Single cell enrichment/isolation, CellSearch® user (cert.), DEPArrayTM user (cert.), CellSorting, Liquid Biopsy technologies, FFPE processing, Immunostaining, NGS	**Expertise**
Project coordination, QM, Mentoring, Delegate for biological safety, Woman in charge for gender equal opportunities	

Professional Experience

PhD “Identification of molecular characteristics of CNS-seeking cancer cells”	12/2020 – to date
Scientist and project leader at the Faculty of Experimental Medicine and Therapy, University of Regensburg	01 / 2023 – to date
Parental leave	01 / 2016 – 08 / 2016
Scientist and project leader at the Fraunhofer Institute for Toxicology and experimental medicine Dept. “Personalized Tumortherapy”, Regensburg	06 / 2013 – to date
Parental leave	12 / 2011 – 02 / 2013
Scientist at the “Friedrich-Baur-Research Institute”, University of Bayreuth	06 / 2010 – 11 / 2011
Parental leave	12 / 2008 – 05 / 2010
Awardee/Student at the Max-Planck-Institute of Biochemistry, Martinsried	08 / 2007 – 11 / 2008

Education

Study of Biology (Dipl.) Julius-Maximilians-University of Würzburg	10 / 2003 – 07 / 2007

Publications/Conferences

“Circulating Tumor Cell Enrichment & Single-Cell Isolation Combining the CellSearch® and DEPArray™ Systems” **Methods in molecular biology, Koestler et al.**	2024
“Liquid Biopsy of CSF in a comparative study on patients with suspeceted leptomeningeal metastases” **Poster presentation EACR Sevilla, Koestler et al.**	2022
“ViBiBa: Virtual BioBanking for the DETECT multicenter trial program - decentralized storage and processing” **Translational Oncology, Asperger et al.**	2021
“Detection of Genomically Aberrant Cells within Circulating Tumor Microemboli (CTMs) Isolated from Early-Stage Breast Cancer Patients **Cancers, Silvestri&Reduzzi et al.**	
“Interleukin-6 trans-signaling is a candidate mechanism to drive progression of human DCCs during clinical latency” **Nat Commun. 2020, Werner-Klein M, et al.**	2020

„53BP1 Accumulation in Circulating Tumor Cells Identifies Chemotherapy-Responsive Metastatic Breast Cancer Patients”
Cancers 2020, Schochter et al.

„Development of a semi-automated Breast Cancer profiling workflow for Ampli1™ amplified DNA from CTCs of metastatic breast cancer patients” 2019
Poster Spotlight Presentation, Winner of the Poster Prize, EACR Liquid Biopsy, Bergamo, Koestler et al.

Regensburg | 08.04.2024